Cape Peninsula University of Technology

PERFORMANCE AND OPTIMISATION OF A JET LOOP REACTOR'S PILOT PLANT FOR THE TREATMENT OF ACID MINE WATER USING SOUTH AFRICAN COAL FLY ASH

By

Vinny Ndjate Katambwe

A thesis submitted in fulfilment of the requirements for the degree of

Master of Engineering: Chemical Engineering

In the Faculty of Engineering and the Build Environment

At Cape Peninsula University of Technology

Supervisor: Prof. Tunde, V. Ojumu

Co-supervisor: Prof. Leslie, F. Petrik

Bellville, Cape Town

July 2022

DECLARATION

I, Vinny Ndjate Katambwe declare that the contents of this thesis represent my own unaided work, and that the thesis has not previously been submitted for academic examination towards any qualification. Furthermore, it represents my own opinions and not necessarily those of Cape Peninsula University of Technology.

Signed

28/07/2022

Date

ABSTRACT

South Africa's freshwater resources are constantly under threat due to the pollution of surface and ground water as a result of different mining activities. Acid Mine Drainage (AMD) which is formed through pyrite oxidation and Coal Fly Ash (CFA) a by-product from coal burning process in thermal power stations, are both environmental pollutants that occur as a result of mining activities; and are causing long-term damage to waterways and biodiversity.

Many technologies for treating mine water have been developed in order to generate water appropriate for domestic, industrial, and irrigation purposes. This study aim's at evaluating the performance of the hydrodynamic cavitation jet loop reactor pilot plant at 1000 L industrial capacity, for the treatment of mine water from Eyethu coalmine with CFA from Lethabo and Kendal power stations, and some chemical reagents (lime and aluminium hydroxide). Mine water is conventionally treated with chemical such CaO, $CaCO_3$, NH_3 and $Ca(OH)_2$ etc., however, the use of these chemicals makes the process expensive. Therefore, ways are sought to solve this problem, and CFA has been found to be of the alternative ways to address this problem.

Treatment of EAMD with Lethabo Fly Ash (LFA) or Kendal Fly Ash (KFA) using different AMD:FA ratios of 7:1, 6:1 and 5:1 resulted in 46.11%, 48.16% and 45.25% of SO_4^{2-} removal respectively when using LFA, and 42.74%, 47.87% and 48.66% of SO_4^{2-} removal were observed when KFA was used. Using both LFA and KFA, the optimum amount of FA was obtained at an AMD: FA ratio of 6:1. To further improve the performance in cleaning up of the mine water with respect to SO_4^{2-} and heavy metals, lime (0.5, 1.0 or 1.5 kg) was added to the mixture of EAMD and FA (LFA or KFA). SO_4^{2-} % removal for the mixtures of EAMD and LFA containing 0.5 kg, 1.0 kg or 1.5 kg of lime was 74.63%, 73.54% and 74.64% respectively. In the case of EAMD and KFA mixtures, this was 73.82%, 73.97% and 74.58%. The concentration of elements such as Mg, Fe, Al and Mn was reduced to within the Target Water Quality Range (TWQR) required for domestic water in all the cases investigated. It was discovered that the removal of these elements was pH dependent. It was also observed that adding $Al(OH)_3$ to the solution (AMD+FA+lime) did not increase the performance in cleaning up of the mine water with respect to SO_4^{2-} removal. $Al(OH)_3$ addition was found to be an unnecessary expense, since SO_4^{2-} % removal was in the same range (73 – 75%) as when EAMD was neutralised with FA and lime. The success of FA treatment of mine water has been found to be site specific, i.e., the composition of the FA and the chemistry of the mine water to be treated will determine the efficacy of this treatment method.

After neutralisation of 1000 L of EAMD with 167 kg of FA (LFA or KFA) and 1.0 kg of lime, the treated water was separated from the solid residues (SR) by gravity settling for approximately 30 min. After separation by gravity settling, about 69.5% of treated water was recovered. The energy consumed during the entire process (from feeding the AMD to the slurry discharge) was found to be 9.674 kWh. The power needed to neutralise 1000 L of EAMD with 167.0 kg of FA and 1.0 kg of lime was found to be 7.284 kW after 138 min. The SR recovered after the treatment of EAMD with FA (LFA or KFA) was successfully synthesised into a geopolymer backfill material. The strength (0.68 MPa) developed by the material was within the acceptable range for mine backfill material strength requirement. The findings of this study demonstrated that this treatment procedure will lead to successful solutions to environmental challenges, including a process to fill (seal) mine voids and prevent the production of acid mine drainage utilising the SR recovered after AMD treatment.

ACKNOWLEDGWMENTS

Firstly, I would like to thank my LORD and SAVIOUR, The Almighty JESUS-CHRIST for His love, mercy and guidance throughout this journey. Your goodness and love will surely accompany me all the days of my life, and I will live in the LORD's house for all eternity. To HIM be the reign, the power and the glory forever and ever. Psalm 23:6.

I would like also to thank:

- Prof. T.V. Ojumu my supervisor, for giving me the opportunity to complete my master's degree under his supervision and guidance. Thank you for never saying no whenever I needed to consult with you.
- Prof. L.F. Petrik my co-supervisor, for having faith in me. I am grateful for everything that you have done for me throughout this journey. You have accepted and guided me by receiving me as a boy but leaving ENS as a man. Thank you for being an inspiration, a motivation last not least what a great mentor you have been. Whenever I needed you, you always make yourself available. Prof, I say thank you immensely for your advice, encouragement and mostly financial support you provided throughout my time at ENS. May the Almighty God, richly and abundantly bless you beyond measure.
- Eskom and TIA for supporting this project financially. Without your support, there is not this project. So, thank you very much for believing in this project.
- Mr. Ir. Rosicky Method Kalombe for always being there for me whenever I had a question to ask, you provided me with great insight throughout the duration of this project. Thank you for being a great mentor and friend.
- Mrs. Vanessa Kellerman, Mr. Denzel Bent and Mrs Ilse Wells for all your technical and administrative assistance and for making my research journey and time at ENS more comfortable and successful.
- Mr. Michael Nzadi for being part of the team. Thank you for your technical support.
- Ms. Kelley Reynolds-Clausen and Ms. Natasha Misheer from Eskom for making my time spent at their research and innovation centre so much comfortable.
- Mrs. Bulelwa Javu from Scientific Services (Athlone) for her help with the IC and ICP analyses. Thank you for taking your time and assisting me with these analyses. May God richly bless you.
- ROADLAB Civil Engineering Material Testing Laboratory, Stickland, Western Cape for opening their doors so that I could use their facilities without any constraints.

- Dr. Emile Massima, Dr. Jean Luc Kabal, Dr. Emmanuel Ameh and Dr. Cosmas Uche for their encouragement and technical support.
- Dr. Paul Eze and Dr. Fatoba for their insight throughout the duration of this project. Your support has been of great importance.
- Ms. Blessing Kwabene for being such a great and best friend. Thank you for your love, encouragement, support and prayers.
- Mr. Etienne Beya for being a great motivation and great friend. Thank you for your support and prayers. I am truly blessed to have met you.
- Mr. Evral Ntsa for being a great friend and thank you for your technical support and encouragement.
- Mrs. Astride Bupe, Mr. Hyacinth Imbi, Mrs. Rachel Bukasa, Mr. Einstein Kabamba, Mr. Patrick Zamba, and Mrs. Emilie Beya for their encouragement and prayers.
- Mr. Remy Bucher from iThembaLABS for helping with XRD analysis.
- Mr. Grant from Scientific Services (Athlone) for his help with the ICP analysis.
- Mrs. Kelly Moir from Scientific Services (Ndabeni) for her help with the ICP and XRF analyses.
- The Environmental and Nano-Sciences research group (ENS), and all my colleagues and seniors for welcoming and accepting me to be part of such a great team and family.
- Apostle Maurice Mushiba for his prayer and all the members of Divine Restoration Ministry.
- Auntie Alice Kabangu for her support and encouragement.
- Uncle Charles Okundji for his encouragement.
- To everyone who has supported or encouraged me both directly and indirectly, I say thank you very much.
- My beloved family, thank you very much, I could not ask more than being part of such an amazing family. Thank you for your love, support, encouragement, advice and prayers.

DEDICATION

I dedicate this thesis to **Jehovah** the highest **God** for giving me life. I also dedicate this thesis to Professor Leslie F. Petrik and my family for believing in me and being patient with me throughout the course of my studies:

- Gabriel Katambwe Ndjate (Beloved father)
- Doudou Muswamba Kabangu Katambwe my rock (Lovely mother)
- Prisca Kombe Katambwe (sister)
- Gaella N'sumpi Katambwe (sister)
- Israel Katambwe Ndjate Jr. (Brother)
- Jordy Muswamba Katambwe (Brother)

LISTE OF PRESENTATIONS AND PUBLICATIONS

The data generated during this experimental study were presented at international conferences and a paper has been published in an international journal. Another paper is in preparation for publication.

Oral presentations

Katambwe, V.N., Kalombe, R.M., Nzadi, M., Bent, D., Nieuwouldt, G., Misheer, N., Reynolds-Clausen, K., Kevern, J., Ojumu, T.V. and Petrik, L.F. 2019. Demonstration of 1000 L jet loop pilot plant reactor in the treatment of acid mine water using South African coal fly ash. World of coal ash. St Louis, MO, USA. May 13 – 16, 2019.

Katambwe, V.N., Ojumu T.V., Petrik F.L. and Kalombe, R.M. 2022. Performance of a jet loop reactor pilot plant for the treatment of acid mine water using South African coal fly ash. International Institute of Chemical, Biological and Environmental Engineering. Johannesburg, South Africa. March 17-18, 2022.

Paper published

Kalombe, R.M., Ojumu, T.V., Katambwe, V.N., Nzadi, M., Bent, D., Nieuwouldt, G., Madzivire, G., Kevern, J. and Petrik, L.F. 2020a. Treatment of acid mine drainage with coal fly ash in a jet loop reactor pilot plant. *Minerals Engineering*, *159*, 106611.

TABLE OF CONTENTS

LIST OF FIGURES

LISTE OF TABLES

LIST OF ABBREVIATION

AMD	Acid Mine Drainage
AMW	Acid Mine Water
ARD	Acid Rock Drainage
ASTM	American Society of Test Material
BFD	Block flow diagram
CFA	Coal fly ash
CMA	California mining association
DWAF	Department of Water Affairs and Forestry
EAMD	Eyethu Acid Mine Drainage
EMW	Eyethu Mine Water
EPA	Environmental Protection Agency
Eq.	Equation
FA	Fly ash
IAEA	International Atomic Energy Agency
IC	Ion chromatography
ICP-OES	Inductively couple plasma optical emission spectrometry
IDAWDPI	International Desalting Association World Desalting Plants Inventory
KFA	Kendal fly ash
LAMD	Lancaster Acid Mine Drainage
LFA	Lethabo fly ash
LOI	Loss of ignition
MFA	Malta fly ash
P&ID	Process and instrumentation diagram
PFD	Process flow diagram
RSA	Republic of South Africa
SA	South Africa
SR	Solid residues
TWQR	Target water quality range
US	United State
WEC	World Energy Council
WHO	World Health Organisation
XRD	X-ray diffraction
XRF	X-ray fluorescence

CHAPTER 1

INTRODUCTION

1.1. BACKGROUND

Urbanisation and industrialisation are two global trends that are, for the most part, inevitable because they are required by society. It is vital to consider their destructive effects on the environment and social life all around the world. The amounts of industrial wastes produced, as well as carbon dioxide (CO_2) emissions, and the issues associated with their safe management and disposal, are the health impacts of these global processes (Lokeshappa and Dikshit, 2011). Mining, as one of the most important activities on the planet, has had a positive and negative impact on many people's lives. On the one hand, it has aided in the growth of many nations' economies around the world, but on the other hand, it has wreaked havoc on various ecosystems. Mining activity in South Africa (SA) dates to the 1850s, when the first gold was found, and has been a turning point in the country's economic growth since then (Beavon, 2004). Gold discovery at Langlaagte Farm in mid-1886 earned Johannesburg the moniker of "City of Gold," and the mining of gold became the economic backbone of South Africa (Bobbins, 2015).

Mining operations have impacted negatively on the environment in a number of countries around the world, including South Africa. Water contamination is one of the most serious environmental consequences of mining. Acid drainage issues have been related to the mining of various commodities including nickel, gold, coal and copper, which can cause long-term damage to rivers and biodiversity. The existence of a high concentration of trace elements dissolved in ground and surface waters is one of the most serious issues connected with AMD formed in coal and associated sulphide-containing minerals (Taylor et al., 2005; Akcil and Koldas, 2006; Campaner et al., 2014).

AMD, also known as ARD (acid rock drainage), is generated when sulphides, most commonly pyrite, are oxidised (FeS_2). Sulphates (SO_4^{2-}) (1-20 g/L), iron (Fe), metalloids, higher acidity (pH 2-4), and toxic metals are all present in the water as this mineral interacts with water and oxygen (Akcil and Koldas, 2006; Campaner et al., 2014; Larsen and Mann, 2005; Vadapalli et al., 2008; Gilbert, 2015). AMD can be generated from abandoned mines and tailing ponds, but this is a natural process. Its output can be boosted by mining simply by increasing the amount of sulphides exposed, posing a serious threat to the equilibrium of various ecosystems, particularly if effective acidity mitigation measures are not taken (Johnson and Hallberg, 2005;

Moncur et al., 2005; Akcil and Koldas, 2006; Cravotta 2008). These actions may include the use of limestone, hydrated lime, ammonia, and fly ash to neutralise acid mine water (Akcil and Koldas, 2006; Campaner et al., 2014). However, if carbonate rocks in the surrounding stratigraphic sequence interact with AMD, attenuation of acidity can occur naturally in some cases (Campaner et al., 2014). In general, attenuation is caused by a rise in pH and a decrease in metal and metalloid solubility, which is heavily influenced by the presence and availability of neutralising agents (Cravotta et al., 1999; Campaner et al., 2014).

The Witwatersrand gold fields, the O'Kiep copper district, Mpumalanga and KwaZulu-Natal coalfields all contribute to the majority of AMD generated in South Africa. The Vaal and Olifants rivers freshwater supplies are threatened by the effects of coal mining in Mpumalanga coalfields (Coetzee et al., 2010). Water is a recognised issue in South Africa. The Western Cape capital, Cape Town, was facing a water shortage early in 2018, as the dams were drying up. Water scarcity and poor quality are major issues in the country. Water contamination in the Vaal and Olifants rivers needs immediate action (Coetzee et al., 2010). Various treatment options and methods have been identified and researched, including active, passive, and in-situ treatment methods (Taylor et al., 2005). Oxidation or reduction, pH control, chelation, biological mediation, electrochemistry, adsorption or absorption, sedimentation, filtration or settling, ion exchange, flocculation, and crystallisation are only a few of the chemical, physical, and biological processes used in AMD treatment (Taylor et al., 2005).

While renewable energy is gaining popularity, however, coal will keep on playing a significant role in meeting energy demands worldwide, South Africa included. Many countries around the world depend heavily on coal to generate electricity. Coal combustion processes currently meet about 42% of global energy demand, and this has a tendency to carry on for the next three to five decades (WEC, 2016; source: https://www.carbonbrief.org/mapped-worlds-coal-power-plants. Access on the 15th of February 2021). Unfortunately, coal mining has a significant negative impact on the environment (Ram and Masto, 2010). Coal mining creates unpleasant dumps and tailing dams, which, along with other mining operations, harm microbial ecosystems and affect the soil nutritional condition in mined areas through stockpiling and leaching (Corbett et al., 1996; Nyale, 2014). The burning of pulverised coal in thermal power plants produced approximately 70 - 80% of the total ash worldwide. The Republic of South Africa's energy demands are largely met by coal; approximately 90% of total energy demand is met by coal-fired power plants, and this is likely to continue in the future, given the country's vast coal reserves and steadily increasing economy and population (Eskom, 2016). Eskom consumes approximately 120 million tons of coal per year and generate about 36 million tons of ash per year from its coal-fired power plants; fly ash or pulverised fuel ash accounts for

nearly 90% of the total ash produced (Nyale, 2014; Eskom, 2016). While coal combustion produces a lot of fly ash, its use is still limited or underutilised.

The mining of coal is identified as one of the causes of AMD production, but coal combustion for electricity generation also produces a lot of waste materials (by-products). One of these wastes being CFA. CFA has been discovered to be useful in several applications, including replacing cement partially in concrete production, cleaning of flue gas as an absorbent, removing pollutants from wastewater, zeolites and geopolymers syntheses, improving agriculture soil, and backfilling of mine voids, among others (Iyer and Scott, 2001; Ahmaruzzaman, 2010). FA was discovered to be effective in sulphates (SO_4^{2-}) removal from mine water (Petrik et al., 2005; Misheer et al., 2010). FA treatment of AMD from gold and coal mining resulted in significant inorganic pollutants being reduced to within water quality requirements and FA treatment could be used in passive or active systems (Gitari et al., 2006, 2008b, 2013). FA has been shown in these studies to be a promising treatment option for AMD. The partition of major and trace inorganic pollutants in the solid residues (SR) generated from FA-AMD treatment technology was investigated in a passive column study (Gitari et al., 2010). Furthermore, most mine waters are high in Ca and Mg but low in Al and Fe, despite having high sulphate content. Madzivire et al. (2010a) demonstrated the removal of SO_4^{2-} from circumneutral mine water (CMW) into gypsum and/or ettringite precipitates using FA, and the fate of removing SO_4^{2-} during AMD and CMW treatment with FA was demonstrated using a modelling and experimental method (Madzivire et al., 2011).

The use of FA to treat AMD and then using the SR in backfill operations has been demonstrated (Fester et al., 2008). The ability of FA to neutralise AMD and the strength formation of the resulting SR has also been demonstrated (Vadapalli et al., 2008), and the effect of FA size fraction on the ability to treat AMD and the rheological properties of the residual sludge has been investigated further (Vadapalli et al., 2014). The amount of dewatering and particle size could be used to monitor the rheological properties, allowing for the backfilling of underground voids. The residues remaining after AMD treatment were found to be suitable for backfilling mine voids and developed sufficient strength once placed, to prevent collapse of pillars and would seal the ingress of air and water, thus could prevent AMD formation (Vadapalli et al., 2008, 2012; Gitari et al., 2013). The chemistry and speciation of potentially radioactive and toxic elements during the treatment of AMD have shown that mine waters of varying quality can be successfully treated with FA, lime, and aluminium hydroxide ($Al(OH)_3$) to provide product water that meets TWQR requirements for irrigation or drinking water (Madzivire, 2012a). The application of a jet loop reactor was investigated for mine water treatment with FA, lime and $Al(OH)_3$ at an 80 L scale, this resulted in the quality of mine water

drastically improving (Madzivire et al., 2015). As a result, these studies have shown that South African FA is a low-cost and competitive alternative for the treatment of AMD, as well as a way to prevent AMD formation by backfilling mine voids. This current study would serve to demonstrate the effectiveness of the jet loop reactors for mine water treatment with FA at 1000 L industrial scale.

1.2. PROBLEM STATEMENT

Many technologies for treating mine water have been innovated in order to generate water appropriate for domestic, industrial, and irrigation purposes. Most of these techniques use chemical regents such CaO, $CaCO_3$, $Ca(OH)_2$, $MgCO_3$, Na_2CO_3, NH_3 etc. Using most of these chemicals result in the process being costly. To lower the cost of treatment, FA has been found to be one of the alternative ways. Mine water treatment by FA using a jet loop reactor pilot plant with an 80 L capacity has been demonstrated to be successful at laboratory scale. But for it to be expanded at an industrial scale it needs to be scaled up and it is important to ascertain the performance at an industrial scale to ensure that it is comparable to the performance at laboratory scale. To do so the parameters or best conditions optimised at laboratory scale will be used at industrial scale (1000 L capacity). However, this process results in the production of a significant amount of solid residues (SR). Therefore, the current study will also investigate the fate of the SR generated as by-product from this treatment process to be reused to backfill mine voids.

1.3. AIM AND OBJECTIVES

The main aim of this study is to evaluate the performance of a jet loop reactor pilot plant (1000 L capacity) for treating Eyethu mine water with Lethabo and Kendal FA in order to optimise the amount of FA, lime and $Al(OH)_3$ required to remove toxic metals and reduce SO_4^{2-} content. This will be achieved by different objectives, which include to:

a. understand the chemical, physical, mineralogical and other important characteristics of Lethabo and Kendal FA in order to establish its suitability for Eyethu mine water treatment.
b. determine the optimal conditions required for the treatment of Eyethu mine water using Lethabo and Kendal FA.
c. conduct material and energy balances around the 1000 L jet loop reactor pilot plant.
d. Determine whether the solid residues can develop adequate compressive strength to be used as backfill or synthesised into geopolymer; therefore, showing the possibility of achieving a zero effluent (waste) process.

1.4. RESEARCH QUESTIONS

The research study will attempt to answer questions such as:

a. What is the chemical, mineralogical and physical properties of FA from Kendal and Lethabo power plants, as well as mine water from Eyethu coalmine?
b. Can Eyethu mine water be treated effectively with FA (Lethabo and Kendal) and some chemical reagents using a jet loop reactor pilot plant at a 1000 L capacity?
c. How relevant is the addition of chemical reagents to AMD treatment with FA?
d. Can the treated water be suitable for domestic, agricultural or industrial application?
e. Can the solid residue (sludge) after mine water treatment be synthesised into a geopolymer or be suitable for backfilling mine voids?
f. What is the energy consumption of the pilot plant? How much treated water and waste can be recovered at the end of the treatment process?

1.5. RESEARCH APPROACH

A thorough review of the literature on mining practices, AMD, CFA, and wastewater treatment technologies, was conducted. The current study on AMD neutralisation with FA was inspired by laboratory-scale studies suggested by Petrik et al. (2003) and Gitari et al. (2006). They noticed that when mixing AMD and FA in a beaker, the pH of the AMD increased while metal and sulphate concentrations decreased. Madzivire et al. (2015) used a tank, a centrifugal pump, and a patented jet loop reactor to scale up the process to 80 L capacity. The process was scaled up to a 1000 L industrial capacity based on the findings of Madzivire et al. (2015). The efficiency of the 1000 L jet loop reactor pilot plant should now be investigated using various parameters. The chemistry involved in treating AMD with FA will be clarified by analysing the water fed and recovered with techniques such as IC and ICP-OES. The changes in mineral phases and elemental composition of fresh FA and SR generated after treatment will be compared using XRF, XRD and ICP-OES techniques. The unit production cost will also be determined at the current (investigation) production rate. The solid residues will be converted into geopolymer or backfill material, by mixing the SR with different amount of sodium silicate liquid, FA and cement, and the resultant paste cast into a 100 mm^3 plastic mould and cured under ambient conditions (room temperature). The properties of the synthesised geopolymer will be characterised by compressive strength.

1.6. DELIMITATIONS OF STUDY

Mine water can be treated using different types of technologies. Some are effective on cost and energy consumption compared to others. This study will be limited on the following:

- This study will consider the use of FA from two power stations namely Lethabo and Kendal.
- The source of mine water in this study originated from a coalmine, Eyethu coalmine.
- The major investigation to be done on the synthesised geopolymer from the SR to be recovered after treatment will be limited only on the compressive strength development of the synthesised geopolymer.
- This research is limited to the scale-up of mine water treatment in a jet loop reactor pilot plant with a capacity of 1000 L.

1.7. SIGNIFICANCE AND CONTRIBUTION OF THE RESEARCH

This study is investigating the performance of a 1000 L jet loop reactor pilot plant for treating AMD with South African FA. This study will show how two waste materials can be used for recovery of water and geopolymer backfill benefit, which is a way to safeguard the environment. Since preventing AMD generation is almost impossible, this alternative will allow a cradle-to-cradle solution to make AMD less harmful to the environment and human health. This study will also show how treatment of mine water with FA is a cost-effective process with respect to chemicals (lime, limestone etc.).

1.8. OUTLINE OF THE THESIS

The thesis is consisted of 6 chapters. Chapter 1 introduces the research and underlines the aim and objectives, the problem statement, how the research is approached, the significance and contribution of the research, and the questions to be answered. Chapter 2 provides a literature review on mining activities, water treatment technologies, acid mine water formation, FA generation and utilisation. Chapter 3 describes the materials and methodology used to conduct the experiments, as well as the characterisation techniques used to achieve the aim and objectives of this study. While chapter 4, discusses the results obtained after different analyses. Chapter 5 presents the overall mass balance, as well as the energy balance around the pilot plant, it also presents the economics of the treatment process (production cost at 1000 L capacity). Chapter 6 presents the conclusion by answering the research questions and lays out recommendations and suggestions for future work on the current investigation.

CHAPTER 2

LITERATURE REVIEW

2.1. INTRODUCTION

The current chapter will look at a variety of mining activities. This also presents literature on the impacts of mine water generation and CFA production on the environment and human health. It also presents different technologies for treating mine water, such as passive and active methods, as well as application of FA for treating mine water and the synthesis of geopolymeric material for backfilling purposes.

2.2. COAL FLY ASH

CFA simply called fly ash (FA) is a solid waste produced by thermal power plants when pulverised coal is burned at higher temperatures (1200 – 1700 ^{o}C). It is made up of all the inorganic components left behind during coal combustion (Chindaprasirt and Rattanasak, 2010). During coal combustion for power generation, four types of wastes are produced, which are bottom ash (BA), fluidised bed boiler (FBB), flue gas desulphurisation (FGD), and fly ash (FA) (Fatoba, 2008). FA is the finest and most abundant of all the four wastes (by-product), accounting for 75 – 80% of the total ash generated during coal burning processes in thermal power stations (Ahmaruzzaman, 2010; Nyale, 2014). FA is transported by FGD from the combustion chamber to the removal particle system. Before being disposed of, it is separated from the FGD by a dust collection device, which is either mechanical or uses electrostatic precipitators (Brahammaji and Muthyalu, 2015). Figure 2.1 illustrates how FA is produced in thermal power plants.

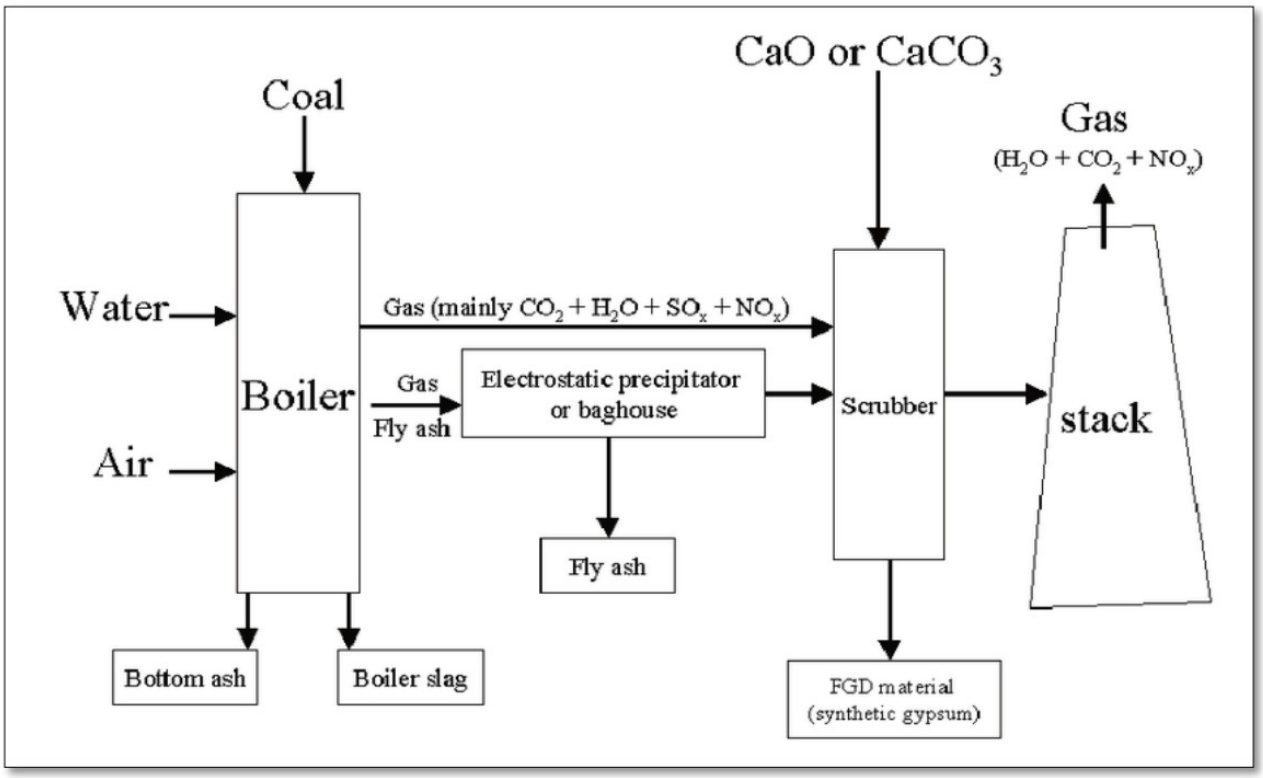

Figure 2.1: Flowchart of a coal-fired power station (Gitari et al., 2006).

Many elements are found in FA, including Si, Al, Fe, unburned carbon, and metals such as Ba, As, Co, Pb, Th, Sr, Ni, V, Zr, Cd, Cr, Cu, Hg, Se and Zn (EPA, 2009; Petrik et al., 2003; Vassilev & Vassileva, 2007).

2.2.1. Chemical composition of fly ash

Two key factors affect the chemical composition of FA: the type of coal utilised and the amount of non-combustible materials present (Madzivire et al., 2010). Different FAs have a broad variety of chemical compositions, meaning that the coal used in power facilities worldwide varies (Malhotra and Ramezanianpour, 1994; Hardjito, 2005). According to Brahammaji et al. (2015) oxides such as Fe_2O_3, SiO_2, CaO and Al_2O_3 make up most of the FA, while minor amount of MgO, K_2O, Na_2O, TiO_2, and SO_2 are also present. The chemical composition of various FA from different category of coal is shown Table 2.1. According to Ahmaruzzaman (2010), there is a small amount of anthracite FA because the combustion of anthracite coal over the world is small.

Table 2.1: Chemical composition of various FA derived from different types of coal (normal range) (ASTM, 2005; Ahmaruzzaman, 2010)

Components (wt.%)	Coal		
	Sub-bituminous	Bituminous	Lignite
SiO_2	40.0 – 60.0	20.0 – 60.0	15.0 – 45.0
Al_2O_3	20.0 – 30.0	5.0 – 35.0	10.0 – 25.0
Fe_2O_3	4.0 – 10.0	10.0 – 40.0	4.0 – 15.0
CaO	5.0 – 30.0	1.0 – 12.0	15.0 – 40.0
MgO	1.0 – 6.0	0.0 – 5.0	3.0 – 10.0
SO_3	0.0 – 2.0	0.0 – 4.0	0.0 – 10.0
Na_2O	0.0 – 2.0	0.0 – 4.0	0.0 – 6.0
K_2O	0.0 – 4.0	0.0 – 3.0	0.0 – 4.0
LOI	0.0 – 3.0	0.0 – 15.0	0.0 – 5.0

The main difference of the FA obtained from different type of coal shown in Table 2.1, can be observed by the amount of silica, alumina, iron and calcium present in the FA (ASTM C-618, 1993; Nyale, 2014). Other characteristics of FA to consider are loss of ignition (LOI), which is the measurement of unburnt carbon that remains in FA after combustion; fineness, which largely dependent on coal crusher operating conditions and coal grinding process; and homogeneity.

2.2.2. Classification of fly ash

The FA classification followed worldwide is the one proposed by the American Society for Testing Material (ASTM). The two main classes of FA are Class C and F. According to ASTM C-618 (1993), the difference between these two categories, is based on the total amount of SiO_2, Al_2O_3 and Fe_2O_3 present in FA. If the sum of these oxides is at least 50% by weight the ash is classified as Class C FA and, if this is 70% or more the ash is classified as Class F FA. According to Koukouzas et al. (2007) and Ahmaruzzaman (2010), CaO content in Class F FA is between 5 - 10% while in Class C FA this is between 15 – 35%. The classification of FA by ASTM standards is illustrated in Table 2.2.

Table 2.2: FA Classification by ASTM standards (ASTM C-618, 1993)

Element	Class F	Class C
$SiO_2 + Al_2O_3 + Fe_2O_3$, min %	70	50
CaO	<10	>15
LOI, max %	6	6
SO_3, max %	5	5
Moisture content, max %	3	3
Available alkalis, as Na_2O, max %	1.5	1.5

Note: min stands for minimum and max for maximum

Based on the classification both ashes can be labelled as pozzolanic. Pozzolans are siliceous or siliceous and aluminous materials that produce cementitious products when mixed with water and $Ca(OH)_2$ at room temperature (Wang and Wu, 2006; Ahmaruzzaman, 2010). Class C FA is more cementitious (self-hardening upon reaction with water) than Class F FA, due to its high CaO content (ASTM C-618, 1993). The ASTM C-618 classification was prompted using FA as a pozzolan or additive in concrete (Wang and Wu, 2006). Therefore, it may not be necessary for all the fly ashes to comply with ASTM C-618 standards if they are intended for other purposes than being used as pozzolan or admixtures in concrete. These standards are limited only to the pozzolanic properties of the FA.

2.2.3. Physical, mineralogical, and morphological characteristics of fly ash

The physical properties of FA are influenced by a variety of parameters, including the combustion process, coal source, boiler type and particle size (Malhotra and Ramezanianpour, 1994; Basu et al., 2009). Ahmaruzzaman (2010) stated that, FA is mostly alkaline, abrasive in texture, refractory in nature and grey in colour. FA is spherical is shape with the particle size ranging from 0.01 - 100 µm, specific gravity from 1.6 – 3.1, specific surface area from 170 – 1000 m^2/kg, and bulk density from 1.01 – 1.43 g/cm^3 (Adriano et al., 1980; Young, 1993; Gitari et al., 2006; Ayanda et al., 2012).

Different mineral phases occurred in FA during combustion and these phases are associated with high toxic elements. The mineralogy of FA consists of amorphous and crystalline phases combined with other mineral fractions (Saikia et al., 2006). Different crystalline minerals are present in FA, including quartz (SiO_2), mullite ($3Al_2O_3.2SiO_2$), hematite (Fe_2O_3), magnetite (Fe_3O_4), kaolinite, anhydrite, lime, calcite ($CaCO_3$) etc. (Adriano et al., 1980; Petrik et al., 2003). The mineral phases present in FA are formed in coal strata or are incorporated into coal during the process of converting peat to coal. Coal is divided into two main fractions: organic and inorganic. The organic fraction is the most valuable because it produces energy during coal combustion, while the inorganic fraction is the least valuable because it is non-

combustible and generates solid waste (ashes) during coal combustion (Huggins, 2002). During the combustion process, inorganic materials are transformed; carbonates are calcined, clay minerals are dehydrated and decomposed, and sulphides are oxidised (Mattigod et al., 1990; Steenari et al., 1999; Fatoba, 2008; Muriithi et al., 2014). Mattigod et al. (1990) stated that minerals in coal such as phyllosilicates are transformed into glass, quartz and mullite respectively; pyrite minerals into hematite and magnetite; quartz minerals into glass and quartz; and calcite minerals are transformed into lime after combustion process in thermal power plants.

According to Warren and Dudas (1984), lime is formed by the decarbonation of limestone and/or dolomitic impurities in coal and occurs on the surface of spherules (Fatoba, 2008). Liberation of inorganic species is part of the transformation process. Trace metals concentrate in FA because they are liberated in volatile form during combustion. These elements are more likely to be found on the surface of FA particles than in the glassy particles that result from combustion (Steenari et al., 1999; Fatoba, 2008).

The morphology of FA has been studied over numerous years. According to reports, FA is mostly made up of fine spherical alumino-silicate glass particles generated by the melting of silicate minerals during combustion (Ghosal and Self, 1995; Ahmaruzzaman, 2010; Nyale, 2014). Spherical particles in FA can be hollow (cenospheres) or densely filled with smaller crystals and amorphous particles (plerospheres) (Adriano et al., 1980; Fatoba, 2008). The existence of an alumino-silicate glass phase, which was formed by high temperatures during coal combustion, gives FA particles a smooth surface (Campbell, 1999).

2.2.4. Impacts of FA on the environment

FA is an alkaline material formed during coal combustion in thermal power plants (Akinyemi et al., 2011; Luis et al., 2014). It contains higher concentrations of trace elements including Sr, As, B, Zn, Ni, Se, Hg, V and Pb than in coal and soil (Madzivire, 2010). Eskom produces about 36 million tonnes of FA annually (Madzivire et al., 2010; Eskom, 2016), however, only a small amount of FA is beneficially used in South Africa (SA), the remainder is disposed of in ash ponds, dumps or landfills. The disposal of FA has caused significant environmental issues due to the risk of toxic elements leaching from the FA, which could have harmful consequences for the ecosystem (Adriano et al., 1980; Woolard et al., 2002; Akinyemi et al., 2011). According to Gonzalez et al. (2009), hazardous metal mobility in FA was maximum at pH <4 and pH >9. Because of the leaching of harmful components inherent in FA from disposal sites, inappropriate disposal and storage of FA results in contamination of ground and surface water, as a result, the ecological and environmental equilibrium is disrupted (Adriano et al.,

1980; Akinyemi et al., 2011). FA is disposed at one of Eskom's dumping sites in the Mpumalanga province, as seen in Figure 2.2.

Figure 2.2: FA disposal site near one of Eskom power plant in the Mpumalanga province.

2.2.5. Uses of fly ash

FA was previously thought to be a complete waste and a hazardous material in the environment, so its use was restricted, and its advantage were unknown. Fortunately, according to many studies, FA can no longer be considered a waste material, but rather a raw material, because its useful properties have led to various applications in a variety of fields. According to Gonzalez et al. (2009), knowing the chemical and physical properties of FA, as well as the mineralogy, is critical because these properties affect the possibilities for its application (Sakorafa et al., 1996). As illustrated in Figure 2.3, Wang and Wu (2006) summarised the uses of FA in various sectors of industries based on its physical and chemical characteristics.

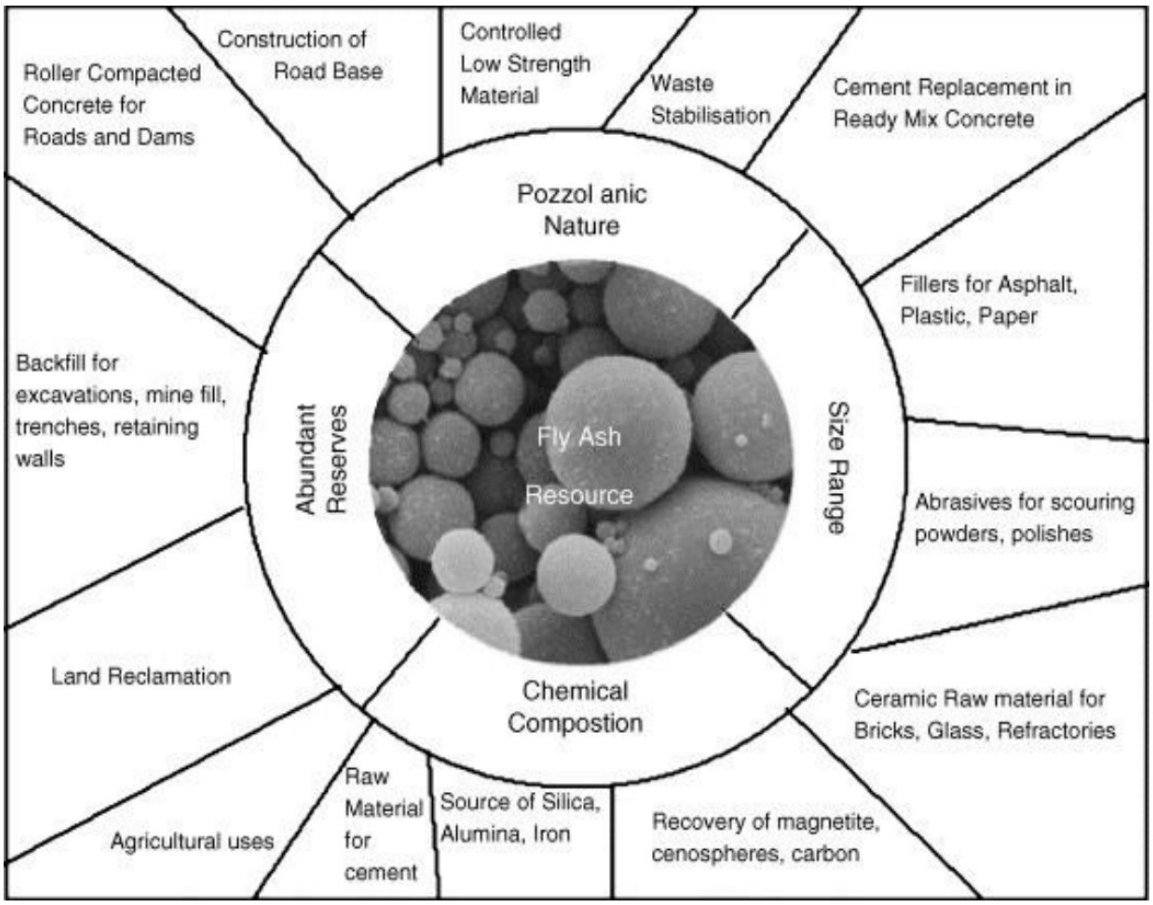

Figure 2.3: Possible uses of FA in various industrial sectors (Wang and Wu, 2006).

A huge amount of FA is produced every year, but only a small percentage of it is used. New innovative ways to recycle and re-use FA have been sought. This includes the treatment of mine water (Petrik et al., 2003; Klink, 2003; Gitari et al., 2006, 2008a, 2008b; Surender, 2009; Madzivire et al., 2010b, 2011, 2015, Nkongolo, 2020; Kalombe et al., 2020a), the synthesis of zeolite (Moreno et al., 2001; Somerset et., 2008; Musyoka et al., 2012a), backfill material (Vadapalli et at., 2008; Gitari et al., 2013) and the synthesis of geopolymer (Hardjito and Rangan, 2005c; Hardjito, 2005b; Hardjito et al., 2005a; Temuujin et al., 2009; Van Dam, 2010; Nyale et al., 2013; Kalombe et al., 2020b).

2.2.5.1. Cement and concrete manufacturing

For generations, the main binder used in the manufacture of concrete has been ordinary Portland cement (OPC) (Hardjito, 2005b). The release of CO_2 from the calcination of limestone and the burning of fossil fuels is a significant environmental effect associated with cement production (Kong and Sanjayan, 2008, Al Bakri et al., 2012; Hardjito and Rangan, 2005c). According to Davidovits (1994), approximately one ton of CO_2 is produced for every ton of OPC manufactured. Furthermore, this process consumes a lot of energy, second only to steel

and aluminium in term of energy consumption (Hardjito and Rangan, 2005c; Hardjito, 2005b). As a result, the cement and concrete industries have discovered a new way to lower raw material and energy costs by partly substituting FA for cement. The FA produced in thermal power stations can either be pozzolanic (Class F FA) or cementitious (Class C FA) (Kruger, 1997; Scheetz and Earle, 1998). Research studies show how cement can be completely replaced in concrete with FA. The pozzolanic properties of FA have made it possible to use it as an additive to OPC and admixture for concrete (Hardjito et al., 2005a; Chindaprasirt and Rattanasak, 2010). Using FA in cement production is an effective method to make concrete more sustainable, as it reduces the amount of water used during mixing, improves the settling time, increases the durability, and reduces the heat of hydration in concrete (Campbell, 1999; Tkaczewska et al., 2012; Nyale, 2014). Furthermore, Maslehuddin et al. (1989) observed that incorporating FA into concrete improves its compressive strength as well as its long-term resistance to corrosion (Ahmaruzzaman, 2010). According to numerous authors (Langley et al., 1989; Maslehuddin et al., 1989; Malhotra, 1990; Alasali and Malhotra, 1991; Bilodeau and Malhotra, 1992; Bilodeau et al., 1994), large volume of Class F FA addition into concrete displayed outstanding mechanical properties, excellent thawing and freezing stability, low permeability and no detrimental expansion by adding reactive aggregates to concrete.

2.2.5.2. Soil amelioration

The beneficial properties found in FA have made it useful as soil ameliorant (Al Bakri et al., 2012). FA added to soil as an ameliorant agent has shown a considerable increase in crop yield (Kruger and Krueger, 2005). Class F and C fly ashes have different advantages and disadvantages when it comes to various applications of FA in different industrial fields. For soil amelioration Class C FA, is preferred over Class F FA. Because of its high CaO content (>15%) and application rate, Class C FA has been used in many studies to show the ability of FA to increase the pH of soil that is acidic (Pandey and Singh, 2010). Class F FA, which has a low CaO content (<10%) has been reported to have a limited potential to ameliorate soil acidity compared to Class C FA (Manoharan, 2010). FA may be used as metal stabiliser in soil contaminated with Pb and Cu. Kumpiene et al. (2007) reported that approximately 98 % mobility of Pb and Cu was reduced by adding FA to soil contaminated with Pb and Cu respectively. Stevens and Dunn (2004) studied the nutritional characteristics of FA in plant growth. They observed a 28 % increase in cotton-produced lint when 3.5 t/ha of fly ash was applied. FA application to soil systems has a number of beneficial effects, including improved soil texture, reduced soil density, improved soil aeration, reduced crust formation, reduced consumption of other soil ameliorants such as fertilizers or lime, served as an insecticide, and reduced the availability and mobility of metals soil (Pandey and Singh, 2010; Blissett and

Rowson, 2012). Some negative effects of FA application to soil have been identified, such as reduced bioavailability of some nutrients when alkaline FA was applied. Excessive salinity, high levels of phytotoxic elements and elevated concentration of boron are some of the toxic side effects that have been identified (Blissett and Rowson, 2012).

2.2.5.3. Fly ash for wastewater treatment

Several researches have investigated the use of FA as an absorbent to remove a variety of metal ions and heavy metals from industrial wastewaters (Blissett and Rowson, 2012). Cr, Pb, Cu, Zn, Ni, Cd and Mn were all removed from wastewaters using FA with various chemical compositions (Cho et al., 2005; Alinnor, 2007; Mohan and Gandhimathi, 2009; Itskos et al., 2010; Ahmaruzzaman, 2010). The use of FA instead of activated carbon for phenol adsorption was explored by Aksu and Yener (1999), who discovered that FA had adsorption capacity of 2709.0 mg/g while activated carbon had adsorption capacity of 108.0 mg/g. PCBs (polychlorinated biphenyls) were removed from wastewater in a study by Nollet et al. (2003). FA was found to be effective in removing two types of PCBs: 2.3,4-trichlorobiphenyl (PCB No. 21; TCB) and 2.2′,3.3′,4.5,6-heptachlorobiphenyl (PCB No. 173; HeCB). FA is a less effective adsorbent than activated carbon, but it is a cost-effective alternative for removing organics from wastewater (Blissett and Rowson, 2012).

2.2.5.4. Synthesis of zeolites

Zeolites are extremely porous crystalline aluminosilicate materials with a tetrahedral matrix arrangement of aluminate (AlO_4) and silicate (SiO_4) bound together by their shared oxygen atoms (Weitkamp, 2000; Blissett and Rowson, 2012). The tetrahedral structure results in a three-dimensional network with numerous open channels and voids. These voids are responsible for many of zeolites' properties, such as molecule adsorption in the large internal channels, which leads to a fast diffusion rate, making zeolites good materials for adsorption processes (Ahmaruzzaman, 2010). Zeolites are composed of Si and Al ions and are produced in an alkaline environment at high temperatures. Because of its high Si and Al content, as well as its large specific surface area and alkalinity (pH >11), FA has been recognised as a good starting material for the production of zeolite. Höller and Wirsching (1985) developed a hydrothermal zeolite synthesis method using FA as a Si and Al ion source material. The hydrothermal method of Höller and Wirsching has been used several times for zeolites synthesis from FA (Hollman et al., 1999; Querol et al., 2001; Murayama et al., 2002; Moriyama et al., 2005; Walek et al., 2008; Blissett and Rowson, 2012). Mordenite, chabazite, clinoptilolite, laumontite, ferrierite, erionite, and phillipsite are examples of zeolites that occur naturally and are commercially exploited (Hanson, 1995). Natural zeolites are rarely pure

because they are created when volcanic rocks and ash deposits interact with an alkaline solution (Querol et al., 2001; Ahmaruzzaman, 2010). In laboratories across the world, synthetic or artificial zeolites have been synthesised. The synthesis of numerous types of zeolites from FA has been published in the literature including Zeolite-P (Musyoka et al, 2012b, 2013) and Zeolite-X (Musyoka et al, 2012b, 2014). Ion exchange, water adsorption and gas adsorption are only a few of the uses that zeolites have found in a variety of industries (Breck, 1984).

2.2.5.5. Mine backfill

The utilisation of FA as a backfill material to fill voids in mine has been tested under regulated conditions as well as in real-world situations. Mine voids are filled for a variety of purposes, including (1) AMD control at the intersection of the groundwater table and the mining waste. (2) Injections of FA paste or mortar help control AMD by filling voids in the mine and provide support where standing coal pillars are collapsing and causing soil subsidence at the surface. (3) FA is injected for mine fire control (Ahmaruzzaman, 2010).

Ahmaruzzaman (2010) stated that two methods could be used to inject FA to fill mine voids, dry FA and wet slurry. Drilling boreholes with a diameter of 152.4 mm into the mine void and putting steel casing down to that level are the methods used for dry FA injections. Injection of dry FA to mine void is at relatively low pressure (82.7 – 89.6 kPa). The FA slurry injection is similar to the dry injection except that it requires a higher injection pressure (up to 689.5 kPa) and a slightly wider diameter (254 mm) borehole. The possibility of using CFA to reclaim an abandoned mine is extremely practical. The commercial usage of a considerable volume of FA as a mine filler material is still under investigation.

2.2.5.6. Geopolymer and backfill material

Geopolymers can be developed using FA as a starting material. The synthesis of geopolymer using FA has gained popularity in recent years, owing to its low cost and low energy of formation, as well as the highly chemically stable products with good mechanical properties that may be generated from an industrial solid waste (Takeda et al., 2010; Kalombe et al., 2020b).

Geopolymers should not be seen as a competitor to Ordinary Portland Cement (OPC), but rather as an innovation that cement manufacturers may use to provide a wider range of cementitious products to consumers. Geopolymers are related to organic polymer. The geopolymer is chemically identical to natural zeolite, although it is amorphous rather than

crystalline in microstructure (Hardjito and Rangan, 2005c). The two most important components of geopolymers are base materials and alkaline solutions (Davidovits, 2008). Starting materials for geopolymers based on alumina-silicate should have a high Si and Al content (Srinivasan and Manoj, 2017).

Polymerisation is a three-dimensional polymeric chain and ring structure made up of Si-O-Al-O bonds that occurs in a very rapid chemical reaction on Si-Al minerals under highly alkaline conditions (Davidovits, 1999, 2008):

$$Mn\ [-(SiO_2)\ z–AlO_2]\ n.\ w\ H_2O \qquad (2.1)$$

Where M denotes a basic cation such as K, Na, or Ca; the symbol (–) denotes the presence of a bond; n denotes the polymerisation or polycondensation degree; and z is 1, 2, 3, or higher, up to 32. The actual mechanisms of geopolymer setting and hardening, as well as its reaction kinetics, are unknown. However, the majority of suggested mechanisms (Davidovits, 1999; Xu and Van Deventer, 2000) include the following:

- Si and Al atoms in the starting material are dissolved by hydroxide ions.
- Monomers are formed by transporting, orienting, or condensing precursor ions.
- Monomers are polymerised into polymeric structures.

However, because these three stages might overlap and occur virtually simultaneously, it is impossible to isolate and analyse each one separately (Palomo et al., 1999).

The three basic forms of a geopolymer (Davidovits1999) are:

- Poly(sialate), whose repeating unit is (-Si-O-Al-O-).
- Poly(sialate-siloxo), with the repeating unit (-Si-O-Al-O-Si-O-).
- Poly(sialate-disiloxo), which has (-Si-O-Al-O-Si-O-Si-O-) as the repeating unit.

Silicon-Oxo-aluminate is referred to as sialate.

The dissolution of Si and Al species from the surfaces of the raw materials, as well as the surface hydration of raw material particles that did not dissolve, results in the creation of a gel and, subsequently, a solidified geopolymer shape (Van Jaarsveld et al., 1997, Nyale et al., 2013).

Geopolymers synthesised from clays are used as fireproof building materials and heat insulators due to their ability to withstand high temperatures. These inorganic geopolymers can also be used as sound insulators and for encapsulating hazardous waste prior to storage

or disposal (Barbosa & Mackenzie, 2003). Van Jaarsveld et al. (1997) looked at the physical and chemical properties of geopolymeric matrices and suggested the possible application of geopolymeric materials for the immobilization of toxic materials, specifically toxic metals. Izquierdo et al. (2009) synthesized a FA-based geopolymer in an alkaline condition and found that the leaching of heavy metals and trace contaminants including Ba, Cu, Bi, Cd, Co, Pb, Be, Zr, Ni, Cr, Sr, Sn, Th, U, Y, and Nb is prevented. High pH, on the other hand, causes elements in their oxyanionic form, such as B, V, Mo, Se, As, and W, to leach from geopolymer matrices. The authors hypothesised that the oxyanionic components were physically contained rather than chemically incorporated into the geopolymer framework. Geopolymers' characteristics and, as a result, their industrial applications are influenced by their Si:Al molar ratio (Giannopoulos and Panias, 2007). Table 2.3 shows the various applications of the geopolymer material based on Davidovits (1999) suggested Si:Al molar ratio.

Table 2.3: Application of geopolymer materials (Davidovits, 1999)

Si/Al	Application
1	Ceramics, bricks, fire protection
2	Concrete, low CO_2 cement, radioactive and toxic waste encapsulation
3	Heat resistance composites, fibre glass
	Composites, foundry equipment
>3	Sealants for industry
20<Si/Al<35	Fire resistance and heat resistance fibre composites

As compared to Portland cement, the use of FA in geopolymer synthesis has the potential to offer environmental benefits such as reduced natural resource consumption and net carbon dioxide (CO_2) emissions. The production of geopolymer cement, for example, is projected to produce 5 to 6 times less CO_2 (Izquierdo et al., 2009).

In the construction and building industry, cement and clay are commonly utilised for making building and construction materials. Studies have shown that FA may not only partially replace cement but can totally replace it in the manufacturing of construction products (Ahmaruzzaman, 2010). Numerous studies reported on different methods by which construction materials can be produced using FA as feedstock. Li and Lin (2002) studied the making of FA bricks using FA with high content calcium oxide and water. Lingling et al. (2005) developed fired brick by combining FA and clay; Ferone et al. (2011) investigated the manufacturing of FA based geopolymer using Class F FA with the mixing of NaOH and Na_2SiO_3 solutions as activators.

Several studies on the synthesis of geopolymer materials from FA have been conducted (Hardjito and Rangan, 2005c; Nyale, et al., 2013; Nyale, 2014; Kalombe et al., 2020b). Chindaprasirt and Rattanasak (2010) showed that it is possible to prepare high compressive strength geopolymers (35 - 44 MPa). Which can sustain high temperatures (up to 1300-1400 °C) and are freeze-thaw resistant, by introducing a mixture of pulverized coal combustion FA, bottom ash and fluidized bed combustion (FBC) ash into high alkaline NaOH solution and Na_2SiO_3 solution and curing the resulting mixture at 65 °C for 48 hours. According to Izquierdo et al. (2009), these high compressive strength FA-based geopolymers exhibit long-term durability, good physical performance, and in certain cases acid resistance, and could be utilised to stabilise some metallic and radioactive wastes as well as industrial effluent. Hu et al., (2009) synthesised geopolymers by activating FA with NaOH and CaO while using zeolite or bentonite as supplementary ingredients. According to the authors, the concentrations of NaOH and CaO had a considerable impact on the strength of the synthesised geopolymer products.

For the current study, FA was used to neutralise mine water. However, this process results in a significant amount of solid residue (SR) generation after treatment. This study will investigate the possibilities to transform the resulting SR into a valuable material such as geopolymer, thus reducing the cost on the disposal and handling of the produced sludge. If it does not develop sufficient strength to be used as a construction material, it can be used as backfill material to fill the void formed at the mine, hence preventing AMD formation at the source.

According to Vadapalli et al. (2008), numerous authors have explored the suitability of FA as a backfill material; however, no studies relating to the suitability of solid residue (SR) recovered from mine water treatment using FA as a possible backfill material were found. Previous study by Gitari et al. (2006) showed that SR recovered after AMD treatment with FA still strongly alkaline after active treatment of AMD and possessed pozzolanic properties based on XRF analysis results. Filling mine voids with FA paste had the primary benefit of slowing or stopping AMD formation, preventing subsidence, providing protection for pillars and walls, and reducing void volume in underground coalmines (Vadapalli et al., 2008). Benzaazoua et al. (2002) reported that typical binder proportion additions are 3% and 7% by weight into paste fill, with the targeted strength for backfill in the range of 0.7 to 2 MPa (Vadapalli et al., 2008). However, for the current study to enhance the strength of the solid residue, Na_2SiO_3 and NaOH solutions will also be used. The neutralisation of AMD with FA generates SR that is less reactive and requires disposal. The proposed technique of using this as backfill in mine voids is of great benefit. On the other hand, this may be used to make geopolymer as building and construction material, for example, paving bricks. According to Gitari et al. (2013), the most major problem

in using SR as backfill is the degradation of the SR matrix and admixed precipitates as they come into contact with draining AMD, resulting in the release of pollutants into ground water. The impact of the SR over time was determined using a column leaching analysis based on pH and inorganic contaminants (Gitari et al., 2008a). According to the findings of Gitari et al. (2013), backfilling voids in coal mines with SR is a potential strategy for large-scale disposal of SR and in-situ treatment of AMD flows.

The experimental procedure used to achieve the study's goal and objectives will be discussed in the next chapter. In the following chapter, all of the analytical methods used are explained, as well as a description of the process is presented.

2.3. MINING ACTIVITIES

Mining activities, as previously reported, enhance the exposure of sulphide-bearing minerals like pyrite or pyrrhotite to the impact of oxygenated water (derived from rainfall), results in the formation of sulphuric acid. This mechanism manifests itself in a number of ways in gold and coal mining (McCarthy, 2011).

2.3.1. Coal mining

Mine water containing H_2SO_4 can be formed as a result of coal mining, which causes chemical weathering of rocks, culminating in heavy metal leaching into surface or ground water (Nyale, 2014). Although the resulting water is not usually acidic, this can be circumneutral, however containing higher concentration of sulphate and heavy metals. AMD and chemical contamination arising from the mining operations of coal may compromise the quality of potable water. The presence of hazardous materials including heavy metals and phenolic compounds in polluted water may have an effect on consumers (Madzivire et al., 2011; Nyale, 2014).

Coal can be extracted in two methods, either by underground or by opencast methods. About 51 % of coal extraction is by underground mining and about 49 % is extracted by opencast methods in SA (Munnik et al., 2010). In contrast to gold mining, coal is extracted on-site with minimum surface disposal. Pyrite can be found in both coal and host rock; however, a higher concentration is found in the coal strata. Underground mining causes the rock strata above to crumble, and once mining stops, voids in the fissured rock fill with water, causing settling from the lowest opening. Water becomes acidic when reacting with pyrite in unmined coal and host rock (McCarthy, 2011).

Blasting and excavating the rocks above the coal strata, which are then completely removed, is the process of opencast mining. The landscape is repaired after the coal is extracted by replacing the shattered cover rock (backfilling) and covering it with soil. Rainfall that penetrates the soil and enters the backfill material becomes acidic by interacting with pyrite and eventually decants on the surface. Decanting usually starts a decade or more after mining has become unprofitable. Opencast mining changes the pattern of ground-surface water interactions, destroying the natural groundwater regime (McCarthy, 2011).

Mining of coal in the Witbank/Middelburg (Mpumalanga province, SA) region began in 1894 to supply coal to the expanding gold and diamond mining industries, and this region offers insight into the long-term repercussions of the mining of coal. Many mines in the area have been abandoned; others have caught fire since coal is a fuel, a source of heat and energy; others have crumbled; and the rest are decanting acidic water. Dilution and numerous biological and chemical reactions gradually neutralise this water as it enters local systems (Olifants River tributaries). The salinity of the water, on the other hand, is high, and the sulphate concentration is high, above the recommended sulphate concentration for domestic use, which is about 200 mg/L (Munnik et al., 2010; McCarthy, 2011).

2.3.2. Gold mining

Following the discovery of gold in the 1886s, it has contributed to the economic expansion of South Africa. The extraction of the gold-bearing conglomerate deposit and transporting it to the surface where it is crushed, and the gold recovered is the process of gold mining. The crushed rock is put on tailings dumps once the metal is extracted (McCarthy, 2011). Since the commencement of gold mining, tailings dumps have been a part of the landscape of major gold mining areas (McCarthy, 2011). The amount of pyrite in the conglomerate is normally around 3%, and it winds up on the dumps. Water falls on the dumps, oxidising the pyrite and producing H_2SO_4, which runs down the landfill, dissolving toxic metals (uranium included) and emerging as a waste plume from the dump's base, mixing with local groundwater. The polluted water ultimately comes to the surface in the streams that empty the dump's surroundings. As a result, streams emptying tailings ponds are often acidic, with high levels of SO_4^{2-} ions and toxic metals.

Several gold mines on the Witwatersrand (Johannesburg) shut down many years ago, and as the mines closed and the water pumping stopped, water started to pool in the void, and this began to flow into neighbouring mines due to the high degree of connection of the mining area (McCarthy, 2011). Pumping halted after the last mine in a goldfield shut, and the voids began to fill. The Western Basin eventually reached capacity in 2002 and began to decant. Pumping

in the central basin stopped in 2008 and the water level in the void was rising at a rate of about 12 meters per month at the time. Pumping in the Eastern Basin became intermittent near the end of 2010, and it was eventually stopped in early 2011. The water decanting from the mine void is exceedingly poor in quality, as evidenced by the water discharged from the Western Basin (McCarthy, 2011). SO_4^{2-} ions concentrations are typically around 3500 mg/L, with a pH ranging from 2 to 3. The water contains high concentrations of iron and other heavy metals. When the iron comes into contact with air, it oxidises and precipitates along the flow path, leaving a bright orange trail on riverbeds and banks (McCarthy, 2011).

2.4. MINE WATER

Mine water has turned into a significant environmental problem for the mining industry. The chemical additives used during hydrometallurgical and mineral processing, as well as the ore being extracted, affect the composition of mine water (Madzivire, 2010). As a result, there is no uniform composition for mine waters, rendering categorising mine water based on its composition difficult. However, using some water parameters like pH, major cations and anions, and alkalinity vs acidity of mine water, certain classification methods for mine water have been developed (Lottermoser, 2010; Madzivire, 2010a).

- pH

This parameter indicates whether the wastewater is acidic, alkaline or circumneutral (Morin and Hutt, 2001). When the pH of the water falls below 6, it is considered acidic; when the pH falls between 6 and 7, it is considered circumneutral; and when the pH falls above 7, it is considered alkaline.

- Major cations and anions

The categorisation of mine waters with respect to their major cations (Mg^{2+}, K^{+}, Ca^{2+}, Na^{+}) and anions (Cl^{-}, SO_4^{2-}, CO_3^{2-}, HCO^{3-}) includes plotting the major cations and anions on piper plots (trilinear diagrams). Then, the plots are used to classify mine waters based on their cations and anions abundances (Madzivire, 2010). Figure 2.4 shows the representation diagram of a piper plot (Golden Software, 2018).

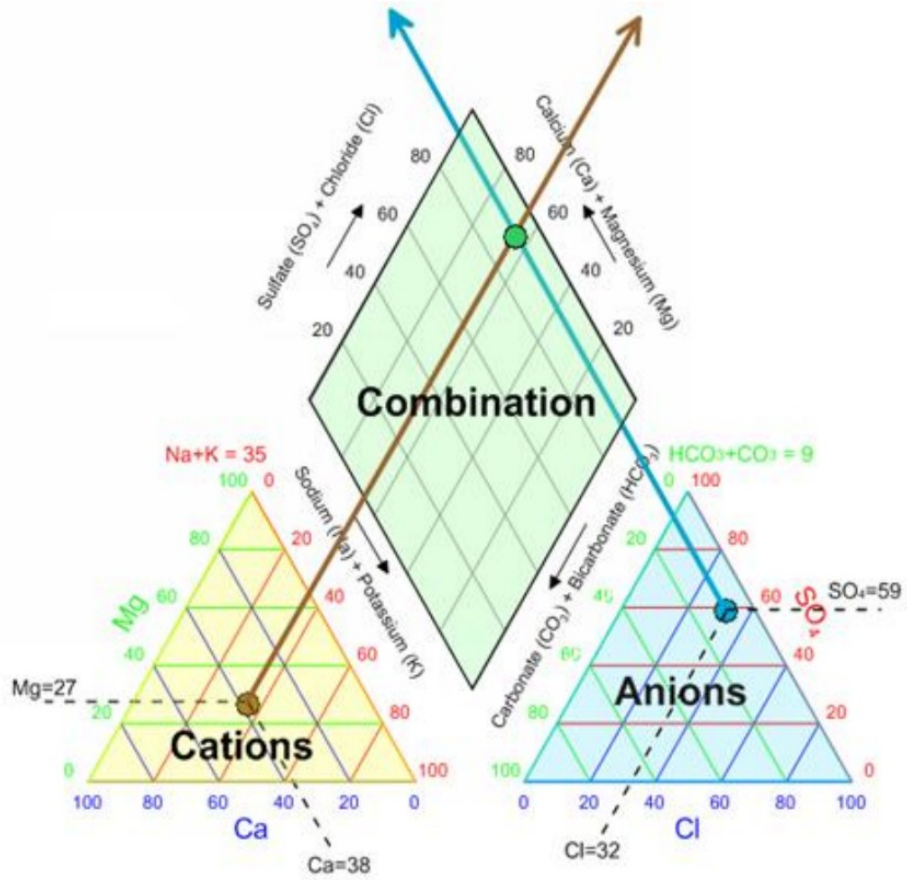

Figure 2.4: Piper plot representation (Golden Software, 2018).

In the disciplines of hydrogeology and groundwater analysis, this is a particularly powerful tool for visualizing the relative abundance of common ions in water samples. This type of plot makes it easier to determine the suitability of the water for human utilisation. The full interpretation of the diamond plot is shown in Figure 2.5 (Golden Software, 2018). It has to be noted that the unit in Figure 2.4 and 2.5 is in percent concentration in mg/L.

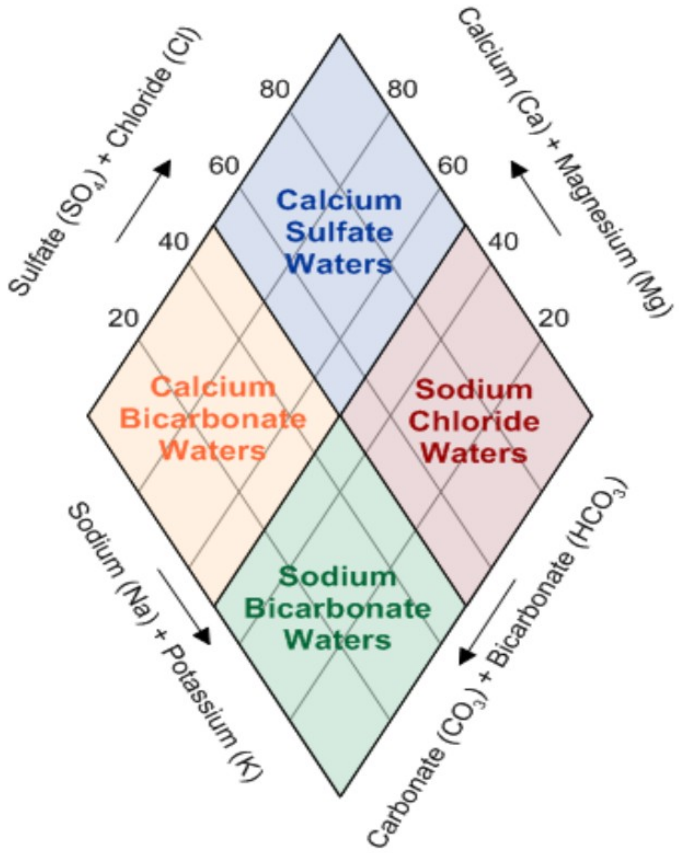

Figure 2.5: Diamond plot interpretation after combination of ions (Golden Software, 2018).

Figure 2.5 shows what type of groundwater one is looking at. The top quadrant shows that the water is calcium sulphate rich, which is typical of gypsum groundwater and mine drainage; the Left quadrant shows that the water is calcium carbonate rich, which is typical of shallow fresh ground water; the right quadrant shows that the water is sodium chloride rich water, which is typical of marine water and deep ancient ground water; and the bottom quadrant shows that the water is sodium bicarbonate water, which is typical of deep ground water influenced by ion exchange (Golden Software, 2018).

- Alkalinity vs acidity

Another technique for distinguishing mine water types is to examine how effectively they can be treated using anaerobic or aerobic passive method. Mine water that is alkaline undergoes aerobic treatment, while acidic mine water undergoes anaerobic treatment (Jennings et al., 2008; Madzivire, 2010a). Acidic mine water has a low pH, sometimes below 3, and is often toxic metal laden and high in SO_4^{2-}, while alkaline and circumneutral mine waters have a higher pH, contain fewer toxic metals, and have a moderate SO_4^{2-} concentration (Madzivire et al., 2009).

2.4.1. Acid mine drainage

2.4.1.1. Origin and generation of acid mine drainage

AMD is one of the most important major challenges facing the mining sector worldwide (Kuyucak, 2002). Long after mining operations have ended, the history of mining activities continues to have an impact on surface and ground water resources (Coetzee et al., 2010). AMD is a problem that occurs at both active and closed mines around the world (Kuyucak, 2002; Gilbert, 2015). Mine waste, such as rock dumps, heap leach pads, mine adits, open-cuts, pit walls, and mine tailings can all be the source of AMD production (Kuyucak, 2002). Sulphide minerals, such as pyrite (FeS_2), are abundant in many metallic ores. Pyrite and other sulphide minerals are frequently exposed to the effects of oxygen and water when waste rock and tailings are dumped (Taylor et al., 2005). Sulphides are exposed in the walls of opencast and underground mines, disrupting the host rock and hydrological regimes and allowing water and oxygen to enter (Akcil and Koldas, 2006; Coetzee et al., 2010; Feris and Kotze, 2015). Because of the exposure of ore in an underground environment and the conveyance of blasted and/or crushed waste rock and tailings to the surface, the disruption of ore bodies and the movement of significant volumes of pyritic material to the surface are extremely favourable to the formation of AMD (Coetzee et al., 2010). AMD can occur anywhere sulphide minerals are exposed, such as in highway and tunnel building, as well as other deep digging (Simate and Ndlovu, 2014).

AMD does not have to form while the mine is operational; it frequently causes problems when it is closed or abandoned. Some of the sulphide minerals found in the mining regions are pyrite, pyrrhotite, chalcocite, chalcopyrite, galena, etc. The most predominant acid generators are pyrite and marcasite (Skousen et al., 1998). According to Johnson and Hallberg (2005), pyrite is the most abundant sulphide mineral on the planet.

There are various processes involved in the oxidation of sulphide-rich materials. The rate of oxidation differs for each sulphide mineral. For example, marcasite and framboidal pyrite oxidise at a rapid rate, whereas crystalline pyrite oxidises at a slow rate. Several authors (Ford, 2003; Taylor et al., 2005; Johnson and Hallberg, 2005; Coetzee et al., 2007; Neculita et al., 2007; Kefeni et al., 2017) have defined the oxidation of pyrite (FeS_2) as follows:

Pyrite oxidises to a ferrous iron-sulphate acidic solution:

$$FeS_{2(s)} + 3½O_{2(g)} + H_2O \rightarrow Fe^{2+}{}_{(aq)} + 2SO_4{}^{2-}{}_{(aq)} + 2H^{+}{}_{(aq)} \quad (2.2)$$

The dissolved ferrous iron, sulphate ion, and hydrogen ion raise the total dissolved solids and acidity of the water, causing a pH decrease unless neutralised. A large amount of Fe^{2+} can oxidise to Fe^{3+} if the surrounding environment is adequately oxidising, which is determined by oxygen concentration, pH, and bacterial activity.

At lower pH values, Fe^{2+} oxidation to Fe^{3+} occurs more slowly:

$$Fe^{2+}_{(aq)} + ¼O_{2(g)} + H^{+}_{(aq)} \rightarrow Fe^{3+}_{(aq)} + ½H_2O_{(l)} \quad (2.3)$$

According to Fripp et al. (2000), at lower oxygen content, Eq. (2.4) would not occur before the pH reaches 8.5. Fe^{3+} precipitates as $Fe(OH)_3$ and jarosite $[H_3OFe_3(SO_4)_2(OH)_6]$ at pH values of 2.3 – 3.5, leaving little Fe^{3+} in the solution and reducing pH, as shown in Eq. (2.4) (Blowes et al., 2003; Akcil and Koldas, 2006). Eq. (2.3) is widely regarded as the limiting step in the pyrite oxidation phase under a variety of conditions due to the slow conversion of Fe2+ to Fe3+ that happens under abiotic conditions at pH values < 5 (Skousen et al., 1998).

Fe^{3+} dissolves in water (H_2O) to form $Fe(OH)_3$, which produces more acid:

$$Fe^{3+}_{(aq)} + 3H_2O_{(l)} \rightarrow Fe(OH)_{3(s)} + 3H^{+}_{(l)} \quad (2.4)$$

Any ferric iron (Eq. 2.3) that did not precipitate into $Fe(OH)_3$ from the solution by Eq. (2.4) can be used to oxidise more pyrite (Akcil and Koldas, 2006):

$$FeS_2 + 14Fe^{3+} + 8H_2O \rightarrow 15Fe^{2+} + 2SO_4^{2-} + 16H^{+} \quad (2.5)$$

Despite the fact that oxygen (O_2) is known as the primary oxidant, Fe^{3+} functions as the oxidant in Eq. (2.5) even at neutral pH values. Eq. (2.5) is known as a more rapid reaction than Eq. (2.2) (Pierre Louis et al., 2015). When the water pH is below 3, pyrite oxidation by Fe^{3+} is 10–100 times faster than pyrite oxidation by O_2, making pyrite oxidation by Fe^{3+} the dominant reaction. The production of iron by acid, which ultimately precipitates as $Fe(OH)_3$, can be represented by combining Eqs. 2.2 to 2.4, with the overall equation being:

$$FeS_{2(s)} + 15/4O_{2(g)} + 7/2H_2O \rightarrow Fe(OH)_{3(s)} + 2SO_4^{2-}{}_{(aq)} + 4H^{+}_{(aq)} \quad (2.6)$$

Amorphous, yellow, orange, or red deposits of ferric hydroxide [Fe(OH)3] on streambeds (yellow boy) are easily recognizable (Figure 2.6). AMD production slows or stops when one or both of the processes described by the above equations is slowed or stopped (Coetzee et al., 2010). Akcil and Kolas (2006) reported that the chemical composition of AMD depends on the ore extracted; therefore, the damage that it creates in the environment will vary from one area

to another. The sedimentation processes, metal toxicity, acidity and salinisation influence AMD impacts on water sources near mine sites; thus, waters that have these properties when released into rivers, lakes or coastal waters kill most aquatic organisms and affect human health (Gray, 1998). It is relevant to establish prevention plans, disposal or treatment methods before the mining projects start on a specific mine area in order to remediate the problems AMD may cause (Johnson and Hallberg, 2005).

AMD may have a variety of negative effects on the environment, such as lowering the pH of water to the point that it is unfit for drinking or other uses (Coetzee et al., 2010). The pH of AMD entering streams in the Western Basin of the Witwatersrand Goldfields in Johannesburg (Gauteng province, SA) is frequently at or slightly below 3 (Tutu et al., 2008). While not as corrosive as concentrated acid, this pH is similar to lemon juice in that it will have long-term impacts on material with which it comes into contact and will not support normal aquatic life. The processes that trigger AMD generation result in a high SO_4^{2-} content in the ensuing water, which persists long after the acidity is neutralised (Coetzee et al., 2010; McCarthy, 2011).

This makes the water unsuitable for domestic use, makes it potentially unsuitable for agriculture and some industrial purposes, and increases the salinity of the receiving aquatic ecosystem (Coetzee et al., 2010; McCarthy, 2011).

Figure 2.6: AMD environmental impact in the West Rand (Coetzee et al., 2010)

The acidity of the water releases metals from the rocks it comes into contact with, including toxic metals and radionuclides. This has the potential to cause acute and chronic toxicity in humans and the environment, rendering water unsuitable for most purposes (Wade et al.,

2002; Coetzee et al., 2006). As a result, AMD should not be allowed to enter surface waterways or aquifers unless it is well monitored and treated.

2.4.1.2. Impacts of AMD

AMD is a global phenomenon, which leads to ecological damages, to watersheds and human resources pollution. Once pyrite has been exposed to the impact of water and oxygen, the process of AMD production become difficult to stop (Gilbert, 2015). Gilbert (2015) stated that, AMD run-off could continue for many years (1000 of years) until the sulphide mineral in the mine is completely drained out. One of the major issues resulting from AMD is the contamination of freshwater resources. Because it contains high concentration of heavy metals, AMD is harmful to aquatic life, damages ecosystems, and corrodes infrastructure such as bridges, dams, wells, and even docks (Simate and Ndlovu, 2014; Gilbert, 2015).

2.4.2. Prevention and remediation methods of AMD

According to the adage "prevention is better than cure," it is usually best, though not always possible, to prevent AMD from forming in the first place. These approaches are commonly referred to as "source control and migration control" techniques (Johnson and Hallberg, 2005). AMD has a long-term detrimental impact on the environment. The aim of source control techniques is to prevent AMD from forming at the source. They are focused with isolating sulphide minerals from waste or preventing water and/or oxygen from interacting with sulphide-bearing material (Kuyucak, 2002; Johnson and Hallberg, 2005). According to Kuyucak (2002), developing and implementing source control techniques is particularly critical for new operating mines because it may prevent acid generation before it occurs. Several source control strategies have been studied in order to prevent or limit AMD formation. Controlling water migration, separating and mixing wastes with alkaline products, and using dry and water covers are some of the AMD control and prevention techniques (Kuyucak, 2002). Some of AMD control measures are presented below and a short description is given for each (Kuyucak, 2002; Johnson and Hallberg, 2005; Kumari et al., 2010; Simate and Ndlovu, 2014):

- **Water migration control:** Water is intercepted and redirected away from the waste materials to prevent it from mixing with them and forming AMD, as well as being polluted by the release of metals and acidity.
- **Flooding or sealing of underground mines:** Mines are being sealed to prevent oxygenated water from infiltrating. This should prevent or reduce the occurrence of AMD.

- **Mine tailings underwater storage:** Due to lower solubility of oxygen in water and a rate of diffusion in the order of four magnitudes lower in water than in air, reactive wastes oxidation can be minimised by submerging and storing the wastes containing sulphide minerals.
- **Land-based storage in sealed waste heaps:** Caps, dry coverings, and seals (with an organic coating) are used to separate or contain sulphide minerals, thus, preventing water or oxygen, or both, from entering.
- **Minerals wastes blending:** Creating environmentally sustainable composites by mixing acid-forming and acid-consuming materials.
- **Anionic surfactants application:** Anionic surfactants are used as bactericides to avoid bacteria from catalysing the conversion of ferrous iron and, as a result, preventing formation AMD.
- **Mine wastes coating:** Coating is the application of a PO_4^{3-} solution containing H_2O_2 to waste. PO_4^{3-} precipitation creates a passive surface layer when H_2O_2 oxidises the surface component of the pyrite and releases iron oxides.

The prevention of AMD generation at source has proven to be a difficult task despite many attempts. Due to these difficulties, research has pushes towards migration control techniques, which is treating the generated mine water. The active and passive treatment methods are the two main categories of these techniques. A more practical distinction can be made between remediation techniques that depend on biological activity and those that do not. There are processes that can be classified as either passive or active under these major categories (Figure 2.7) (Johnson and Hallberg, 2005). These techniques are elaborated under section 2.5.

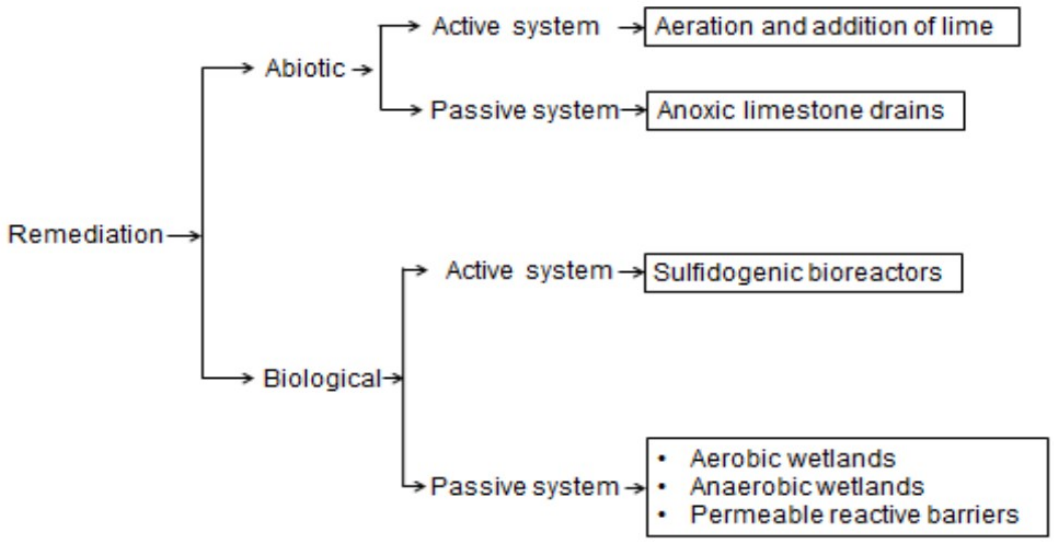

Figure 2.7: Remediation techniques of AMD (Biological and abiotic) (Johnson and Hallberg, 2005).

2.4.3. Circumneutral mine water

Mine water is not universally characterised by a low pH. For example, circumneutral mine waters (CMW) are formed from rocks containing high level of neutralising minerals than sulphide minerals. CMW is characterised by high calcium and magnesium concentrations, moderate sulphate concentrations, and very low Fe, Al, and Mn concentrations (White, 2000; Madzivire et al., 2009).

Mine water is generated by a variety of mining activities, including mineral processing, mine tailings, and metal extraction. As a result, the effluent may have an acidic, neutral, or alkaline pH. Madzivire (2010a) and Madzivire et al. (2014) proved that naturally occurring carbonates and silicates can neutralise the acidity created by the oxidation of sulphide minerals. $CaCO_3$, $CaMg(CO_3)_2$, $Ca_2MgFe(CO_3)_4$, NaOH and $MgCO_3$ are some of the carbonate mineral deposits that are involved in neutralising the acidity formed during the oxidation of sulphide minerals as shown in the chemical equations, (Eqs 2.7 – 2.9) below:

$$FeS_2 + CaMg(CO_3)_2 + 1.5H_2O + 3.5O_2 \rightarrow Fe(OH)_3 + Ca^{2+} + Mg^{2+} + 2CO_2 + 2SO_4^{2-} \quad (2.7)$$

$$FeS_2 + CaCO_3 + 1.5H_2O + 3.5O_2 \rightarrow Fe(OH)_3 + 2Ca^{2+} + 2CO_2 + 2SO_4^{2-} \quad (2.8)$$

$$4FeS_2 + NaOH + 15O_2 \rightarrow 4Fe(OH)_3 + 16Na^{+} + 8SO_4^{2-} \quad (2.9)$$

Calcite ($CaCO_3$) is the most reactive carbonate, and its solubility is determined by proton concentration as shown in the equation (2.10).

$$CaCO_3 + H^+ \leftrightarrow Ca^{2+} + HCO_3^{2-} \quad (2.10)$$

Eq. (2.10) will buffer at pH between 6.5 and 7, whereas in more acidic condition the same Eq. (2.10) can be written as:

$$CaCO_3 + 3H^+ \leftrightarrow Ca^{2+} + CO_2 + H_2O \quad (2.11)$$

Silicate minerals act as neutralising reagents as well. To achieve stability and electrical neutrality, the silicate [$(SiO4)^{4-}$] unit has four residual negative charges that are balanced either by appropriate cations such as Fe^{2+}, Mg^{2+}, Na^+, K^+, Al^{3+}, hydroxyl anions, and water, or by sharing one or more oxygen atoms with other silicate units. Silicate minerals include olivine, epidote, cordierite, pyroxenes, quartz, micas, clays, amphiboles and feldspar. The most common mineral group in the crust is feldspar; it is a group of chemically similar minerals made up of Si, O, Al, and either Na, K, or Ca. The mineral feldspar was used as a neutralising agent in acid mine water, resulting in the formation of kaolinite and gibbsite, according to Eq. (2.12) (Madzivire, 2010a).

$$\underset{\text{K-feldspar}}{2KAlSiO_3O_8} + 9H_2O + 2H^+ \text{ <-> } \underset{\text{kaolinite}}{Al_2Si_2O_5(OH)_4} + 2K + 4H_4SiO_4 \quad (2.12)$$

As shown in Eq. (2.13) below, the kaolinite formed by Eq. (2.12) can be hydrolysed to produce gibbsite without involving any acidity.

$$Al_2Si_2O_5(OH)_4 + 5H_2O \leftrightarrow \underset{\text{Gibbsite}}{2Al(OH)_3} + 2H_4SiO_4 \quad (2.13)$$

As previously stated, several alkaline reagents are involved in the neutralisation of acid mine waters. CMW can be formed because of the partial neutralisation of AMD by contact with dolomite minerals. Dolomite weathering results in Al and Fe precipitating into their respective hydroxides at pH greater than 3.5, as well as the precipitation of sulphate as gypsum and an increase in Ca and Mg concentrations (Madzivire et al., 2010b). In anoxic AMD, Fe and Mn are typically present in reduced ionic states (Fe^{2+} and Mn^{2+}), which are substantially more stable at higher pH than fully oxidised ions (Fe^{3+} and Mn^{4+}) (Johnson and Hallberg, 2005; Madzivire, 2010a). Some AMD channels remain neutral to alkaline whereas others undergo a considerable reduction in pH when they oxygenate, according to Johnson and Hallberg (2005). This is because both proton acidity, such as hydrogen ion concentration and mineral acidity result in net acidity. The net acidity in AMD must be balanced against any alkalinity present;

this is mainly in the form of bicarbonate resulting from the dissolution of basic minerals, in particular $CaCO_3$; however, biological processes can also produce alkalinity in AMD streams.

2.4.4. Mine water type prediction

Mine water is formed as a result of various mining activities. Predictive testing aims to identify whether a certain amount of mining waste will produce acid and to forecast the quality of the outflow depending on the acid formation rate detected (California Mining Association, 1991). A mine's potential to create acid and release pollutants is determined by a variety of elements and site conditions (US EPA, 1994). Water contamination at mine sites is caused by a variety of factors. Ferguson and Erickson reported three of them in 1988. The first element is the acid's formation, which involves oxidation reactions. The second factor concerns the oxidation reaction's products (for example, reactions with other minerals that consume acid), which may neutralise acid or react with other minerals (US EPA, 1994). The third factor concerns the waste management unit's physical characteristics, such as waste rock dumps, tailings impoundments, or pit walls, which initiate the oxidation reaction, acid migration, and consumption (Ferguson and Erickson 1988; US EPA, 1994). Table 2.4 lists some of the factors that affect the overall measurement and rate of acid formation.

Table 2.4: Elements influencing total measurement and rate of acid generation (US EPA, 1994)

Total measurement of acid generation	Rate of acid generation
• The presence of acid-producing (sulphide) minerals (assuming total reaction of sulphide minerals) • Acid-neutralising mineral concentration • The number and type of possible pollutants that are present	• Type of sulphide mineral present including crystal form • The type of carbonate mineral present, as well as any other neutralizing minerals • Surface area of the mineral that can be reacted • Available oxygen and water • Bacteria.

In nature, static and kinetic analytical tests are used to determine a material's ability to produce acid, according to the US EPA (1994). A static test is used to assess a material's total acid output and total acid neutralisation, while a kinetic test is used to characterise processes found at mine sites.

2.5. TREATMENT TECHNOLOGIES OF MINE WATER

Mining wastewaters contain high levels of sulphates and metals and must be treated before being released into rivers or the environment (Zagury et al., 2007). Various methods for handling mine water have been developed and are used based on the quantity of the effluent as well as the type and the pollutants concentration. The aim of an effective treatment method is to produce water with a low acidity and neutral pH, as well as to decrease the concentrations of elements such as Fe, SO_4^{2-}, Mg, Ca, Al, Mn, B, As, Zn etc. in the water to levels that are safe for consumption. To be appealing, a method must be cost-effective, simple to install, inexpensive to operate, and generate little to no waste (Duarte and Ladeira, 2011). According to Kalin et al. (2006), a long-term solution to any industrial issue must be cost-effective, produce small or zero waste, be energy efficient and not be a source of pollution in itself.

To purify mine waters for drinking and industrial use, a variety of treatment technologies have been developed. There are two main types of treatment approaches: passive and active (Bosman et al., 1990; Taylor et al., 2005; Annandale et al., 2006). Mine water is permitted to move through a system that is not monitored on a regular basis in passive treatment methods, while active treatment uses equipment (e.g., pumps, mixers, tanks, etc.) that is monitored and maintained by a responsible workforce. Neutralisation, oxidation, adsorption, and absorption processes are used in both passive and active treatment techniques to remove pollutants from mine water (Taylor et al., 2005; Madzivire, 2010a). The main goals of both methods are to lower sulphate ion concentrations and salinity, increase pH and, in most cases, lower acidity, and remove toxic metals from the water (Taylor et al., 2005).

Alkaline chemicals, as well as ion exchange, adsorption, and membrane separation, are used to precipitate metals. Different neutralising agents such as CaO, $CaCO_3$, $Ca(OH)_2$, $MgCO_3$, NH_3, NaOH, $BaCO_3$ etc. are used to neutralise AMD, thus raising the pH of the water (Taylor et al., 2005). Alkaline chemicals such as $Ca(OH)_2$ or $CaCO_3$ are commonly used to treat AMD by removing metals as metal hydroxide precipitates and SO_4^{2-} as $CaSO_4.2H_2O$ (gypsum) sludge (Madzivire, 2010; Olds et al., 2013; Tolonen et al., 2014). Eq. (2.14) is given to explain how $Ca(OH)_2$ neutralises acidity.

$$Zn^{2+} + Ca(OH)_2 \leftrightarrow Zn(OH)_2 + Ca^{2+} \quad (2.14)$$

Passive treatment techniques started gaining momentum in the 1990s for treating AMD (Yadav and Jamal, 2015). This includes biological treatment in the form of constructed wetlands, chemical treatment in the form of limestone drains, and sulphate-reduction bioreactors (Zipper and Skousen, 2014; Kefeni et al., 2017). One of the most widely used

passive approaches is the permeable reactive barrier (PRB), which employs biological or chemical processes, or a mix of both. (Neculita et al., 2007). Because of some of its advantages, such as low operating and maintenance costs, the passive treatment method is best suited for use at abandoned mines (Lukacs and Ortolano, 2015; Song and Chio, 2015; Kefeni et al., 2017).

Chemical and physical properties are very critical when selecting the most appropriate and efficient chemical for the desired treatment outcomes, according to Taylor et al. (2005).

If some metals need a pH of 10 to precipitate, for example, limestone would be ineffective because it only increases the pH to about 8 (refer to Table 2.5). Cd, Pb, Zn, Ni, Cu, Fe, Mn, Al, Cr-III, Sb, Ag, Se, Th, and Be can all be precipitated by pH control (Taylor et al., 2005). However, most metals' minimum solubility happens at various pH values, so the optimal treatment pH is site and AMD specific.

Table 2.5: Solubility and pH of some AMD neutralising chemicals (Taylor et al., 2005)

Neutralising chemicals	solubility (mg/L in cold water)	Saturation pH
$CaCO_3$	14.0	8.0 - 9.4
$MgCO_3$	60.0 - 100.0	9.5 - 10.0
CaO	1300.0 - 1850.0	12.4
$Ca(OH)_2$	1300.0 - 1850.0	12.4
Na_2CO_3	75 000.0	11.6
NaOH	450 000.0	14.0
NH_3	900 000.0	9.2

When comparing these two treatment methods, passive treatment has been regarded as a cost-effective alternative to active treatment since no chemical inputs are needed on a continuous basis; however, it is susceptible to high sludge disposal costs (Johnson and Hallberg, 2005). Economic factors (operating and capital costs) are critical in assessing the feasibility of active treatment techniques (Taylor et al., 2005). The capabilities of these two techniques are shown in Table 2.6.

Table 2.6: Broad guideline for determining the applicability of passive and active treatment methods based on influent water properties (Taylor et al., 2005)

Treatment Method	Av. Acidity load (kg $CaCO_3$/day)	Av. Acidity range (mg $CaCO_3$/L)	Typical pH range	Max pH attainable	Av. Flow rate (L/s)
Passive	1.0 - 150.0	1.0 - 800.0	>2	7.5 - 8.0	<50
Active	1.0 - 50 000.0	1.0 - 10 000.0	No limit	14.0	No limit

Different factors influence the choice of AMD treatment options, including environmental, AMD composition, pH and economic. Kefeni et al. (2017) stated that in general there is no global technology to treat AMD, because the composition of AMD differs from one site to another, and this leads to the difference in AMD treatment choices and the waste generated during the treatment process of AMD. Many studies are ongoing around the globe, and the motivation behind this is based on the cost reduction of treatment and sought for low-cost treatment options (Kefeni et al., 2017).

2.5.1. Active treatment technologies

Active water treatment technologies are highly engineered treatment processes that require continuous chemical inputs, operations and maintenance personnel, electrical power, and frequent monitoring in order to meet the water quality standards set forth in a discharge permit (Jennings et al., 2008; Trumm, 2010). Aeration, neutralisation (which includes metal precipitation and removal), ion exchange, membrane processes, and biological sulphate removal are some of the technologies used (Jennings et al., 2008).

Active treatment entails the construction of a treatment plant that includes agitator reactors, precipitators, clarifiers, and thickeners, among other reactor systems. The majority of AMD treatment plants begin by neutralising acid mine water with lime or limestone, often a mixture of the two chemicals, and then passing it through settling tanks to remove sediments and particulate content (Madzivire, 2010a; Madzivire et al., 2010b). The sulphate concentration in the water provided by these neutralisation processes is often higher than the normal limit for discharge to the environment. Furthermore, the cost of lime alone will cost a medium-sized mining operation thousands of Rand per year. Many mining companies may not be able to afford this costly treatment process (Madzivire et al., 2010b).

Since the chemistry of mine water varies, predicting a suitable technique of treatment should be dependent on the quality and quantity of mine water, the quality of the treated water, and, most significantly, treatment process cost (Madzivire, 2010a).

2.5.1.1. Chemical treatment

The treatment of mine water using chemicals consists of using conventional alkaline reagents such as $CaCO_3$, CaO, NaOH, Na_2CO_3, MgO, and NH_3. $CaCO_3$ is the most alkaline reagent use, because it is economical and less expensive compared to the other chemicals (Kumari et al., 2010). Alkali is used to rise the pH of water and cause the dissolution of metals into hydroxides or oxyhydroxides precipitates (Madzivire, 2010a).

- **Lime or limestone**

The precipitation of SO_4^{2-} into gypsum, as well as co-precipitation with or adsorption on metal hydroxides, is necessary for mine water neutralization using lime and/or limestone (Madzivire, 2010a).

$$Ca(OH)_{2\,(s)} + H_2SO_4 \rightarrow CaSO_4.2H_2O_{\,(s)} \quad (2.15)$$

$$CaCO_{3\,(s)} + H_2SO_4 \rightarrow CaSO_4.2H_2O_{\,(s)} + CO_{2\,(g)} \quad (2.16)$$

$$Me^{2+} + 2OH^- \rightarrow Me(OH)_{2\,(s)} \quad (2.17)$$

According to Madzivire (2010a), most metals are reduced to levels below the effluent limit, however due to gypsum's partial solubility in water, SO_4^{2-} is typically above the statutory Department of Water Affairs and Forestry (DWAF) standard of 500 mg/L. Gypsum solubility varies in the range of 1500 - 2000 mg/L, relying on water's composition and ionic strength. Madzivire (2010a) also reported that the presence of ions such Mg^{2+}, Na^+ and K^+ reduce gypsum precipitation. A mixed lime/limestone process was designed to reduce $SO_4^{2-}$to less than 1200 mg/L as a countermeasure. This process includes adding lime to raise the pH above 11, which causes $Mg(OH)_2$ to precipitate, increasing the formation of gypsum. The limestone/lime combined process involves several stages:

Stage 1

The mine water is neutralised with limestone, which raises the pH to circumneutral or no higher than 8. This process causes gypsum to precipitate, heavy metals to be removed, and CO_2 to be released.

Stage 2

Lime is added to the process, which raises the pH of the water to 12 or greater, thus removing $Mg(OH)_2$ and further precipitates gypsum.

Stage 3

The water pH has to be adjusted. This is done by using the CO_2 that was generated in stage 1. The addition of CO_2 results in the formation of higher-purity $CaCO_3$, which is recycled and used in stage 1 for the neutralisation of mine water. Figure 2.8 describes the all process.

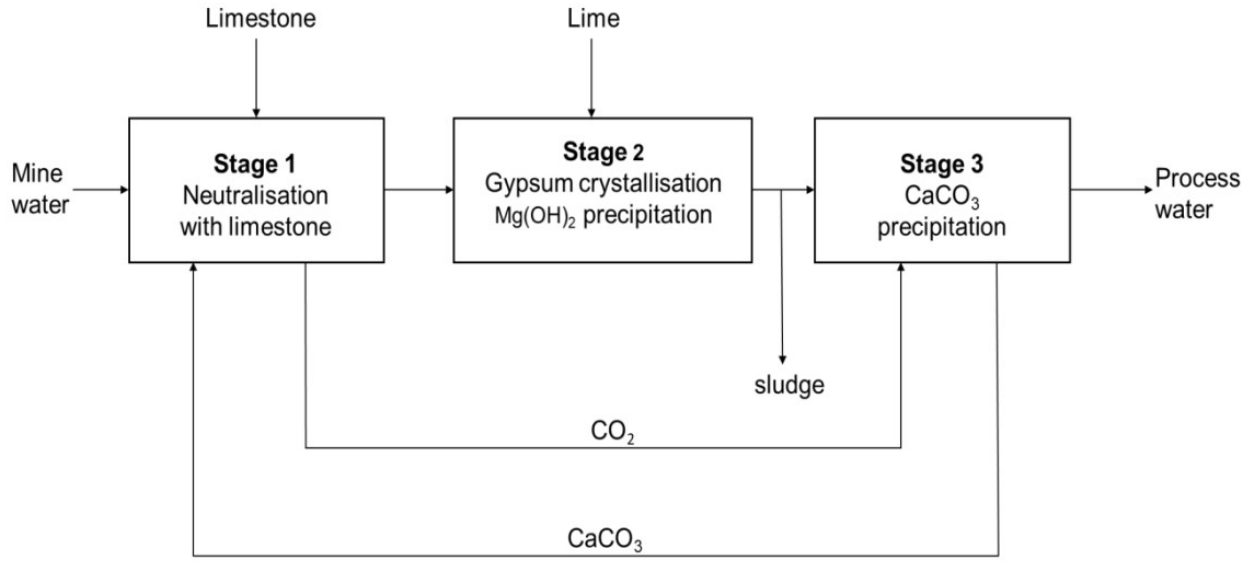

Figure 2.8: Block flow diagram of the integrated limestone/lime mine water treatment (Geldenhuys et al., 2003; Madzivire, 2010a).

This process has an advantage of lowering SO_4^{2-} concentrations under gypsum saturation level of 1200 mg/L. The acidity load is neutralised, and metals removal reached the effluent limits recommended by DWAF (Madzivire, 2010a), making the water produced suitable for irrigation purpose. The major disadvantage of this process is the iron-rich sludge generated, which is highly voluminous, containing only 2 - 5% solids and the rest being water, and this is difficult and costly to handle. The process is improved by partially recycling of the low-density sludge (LDS) back into the neutralisation tank, thus completing the first neutralisation phase (Figure 2.9). This step has a positive effect by increasing the sludge density, which now containing 20% solids, hence producing a high-density sludge (HDS) process (Johnson and Hallberg, 2005; Taylor et al., 2005; Madzivire, 2010a). According to Taylor et al. (2005), the sludge density might be increased up to 40% solids before dewatering. The solids content is improved to 50% after the dewatering process. The major advantage of HDS process is that the cost reduces on the disposal and handling of the sludge as well as the chemical reagent cost is reduced (Johnson and Hallberg, 2005; Taylor et al., 2005).

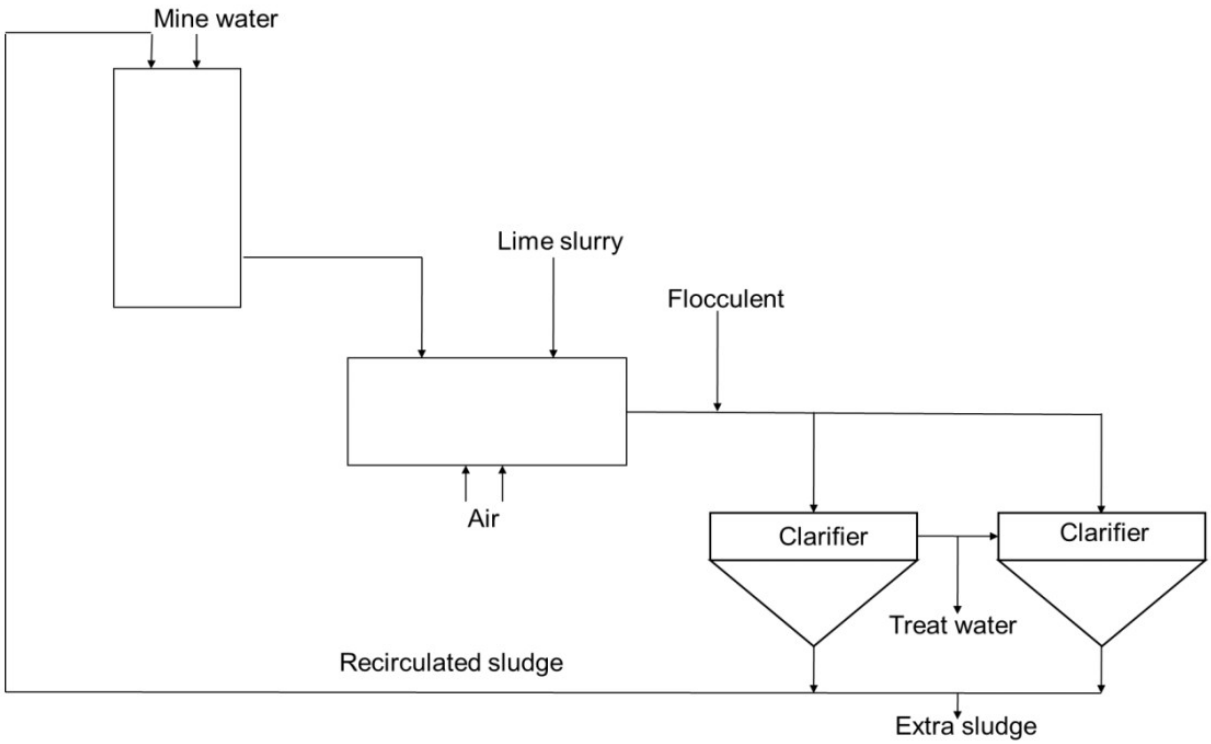

Figure 2.9: Block flow diagram of HDS mine water treatment plant (Coulton et al., 2003; Madzivire, 2010a).

- **SAVMIN Process**

Mintek (SA) created this process for mine water treatment according to Simate and Ndlovu (2015). As shown in Figure 2.10, this process has several stages.

Stage 1

The mine water is neutralised with lime by raising the pH to between 12 and 12.3, causing metals to precipitate as hydroxides.

Stage 2

In terms of gypsum, the water is still supersaturated at this stage. Gypsum is precipitated and separated from the water using gypsum seed crystals, but the water is still saturated with gypsum, and the concentration of SO_4^{2-} was found to be above the DWAF requirement level of 500 mg/L.

Stage 3

At this stage, $Al(OH)_3$ is added to the water, removing dissolved Ca and SO_4^{2-} from the water via precipitation as ettringite (a calcium-aluminium sulphate material) with a chemical formula of ($3CaO.3CaSO_4.Al_2O_3.31H_2O$).

Stage 4

The water from the previous stage still has a pH of 12 although dissolved SO_4^{2-} is less than 200 mg/L. CO_2 is introduced to lower the pH, which decreases in the range of 6 - 9. The introduction of CO_2 results in the precipitation of pure $CaCO_3$.

Stage 5

H_2SO_4 is used to decompose ettringite, resulting in the regeneration of $Al(OH)_3$, which is then recycled and used in stage three. After $Al(OH)_3$ has been removed from water, the gypsum-supersaturated water is reacted with seed crystals (stage 2), which causes the precipitation and removal of gypsum. The gypsum-saturated water is recycled to stage 3 for ettringite precipitation. This method produces potable water as well as a variety of useful by-products such as metal hydroxides, gypsum, and calcite. One of the most significant benefits of this method is that the products are of higher quality. The main disadvantage of this method is the high cost of disposing of the large amount of sludge generated (Madzivire, 2010a; Simate and Ndlovu, 2014).

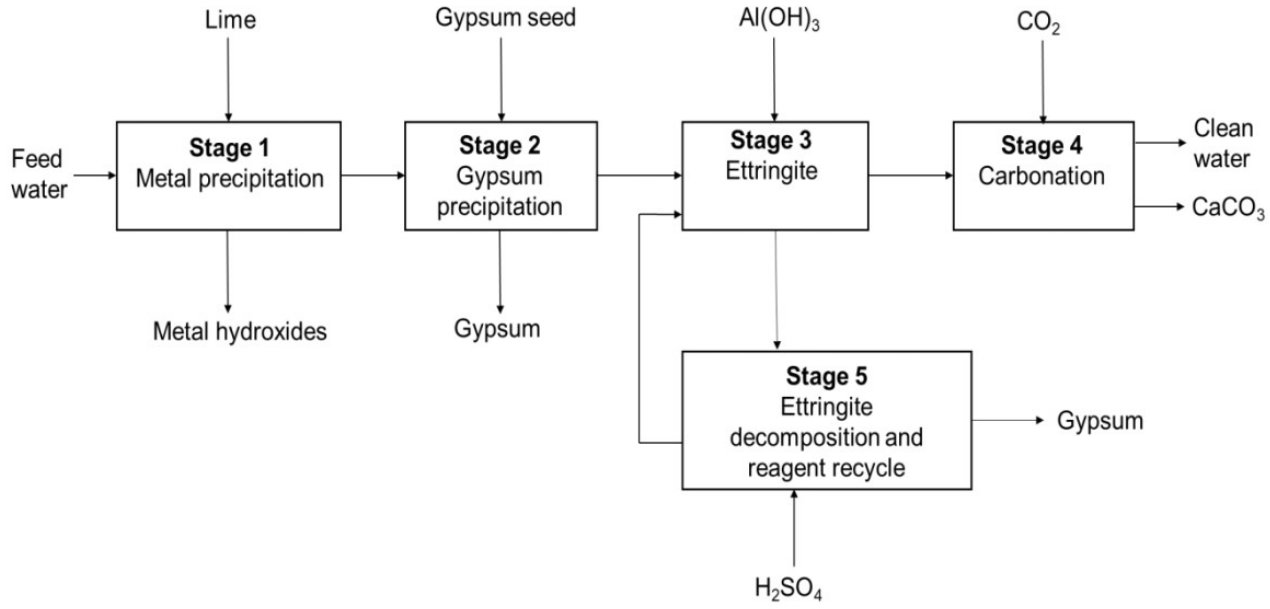

Figure 2.10: Block flow diagram of SAVMIN process (Smit, 1999; Madzivire, 2010a; Simate and Ndlovu, 2014).

2.5.1.2. Membrane technology

Membrane technology has been developed since the 1960s for dialysis and the 1970s for pressure driven or asymmetric techniques. By dialysis, is meant the operation of passing liquid through a membrane by diffusion in order to separate the constituents therefrom. The pressure

driven operation, on the other hand, involves passing liquid through semi-permeable membranes, by forced convection, in order to purify the solvent (Berland and Juery, 2002).

Dialysis was one of the techniques that first allowed separation of dissolved compounds. It was then thought to be more judicious to let a small amount of solutes pass through the membrane rather than the large mass of the solvent (Berland and Juery, 2002). Electro dialysis (ED) is one of the dialysis techniques that consist of a membrane separation using a succession of membranes alternately exchanging anions and cations, often used for desalination of brackish water.

The ED process, as shown in Figure 2.11, uses direct current (DC) power to transport salts and other ionised species to a concentrate collecting stream via cation and anion selective membranes. Membranes are made up of ion exchange resins cast as sheets. Selectivity for cations or anions is created by applying a negative or positive charge to the resin's ion exchange sites. (Allison, 2005). Oztekin and Altin (2016) reported that regardless of many applications of ED, the used of this system is limited by membrane fouling. Fouling results from the accumulation of big particles inside the membrane or on the membrane surface. Particles larger than the membrane pore size are unable to move through the membrane, resulting in accumulation on the membrane surface. The ED absorbs a lot of energy as fouling forms on the membrane, and the separation is inefficient. Pre-treatment of the feed solution, turbulence in the compartments, zeta potential regulation, flow rate optimisation, adjustment of the membrane properties, and pulsed voltage are all recommended to avoid these problems (Oztekin and Altin, 2016).

The early 1970s saw the invention of electro dialysis reversal (EDR) (Allison, 2005). The EDR process is a mechanical enhancement on the ED process that reverses the polarity of the applied DC power on a regular basis. As shown in Figure 2.12, the reversal phase alternatively opens the membrane surfaces and flow chambers to the concentrate and desalting streams. Since water recovery capabilities increased and continual chemical input to the concentrate stream for scaling control was no longer necessary for most systems, it quickly became the most popular type of electro dialysis. According to the International Desalting Association's World Desalting Plants Inventory (IDAWDPI), ED and EDR (All Desalting Plants) account for 13.7% of global brackish water desalting capability (Allison, 2005).

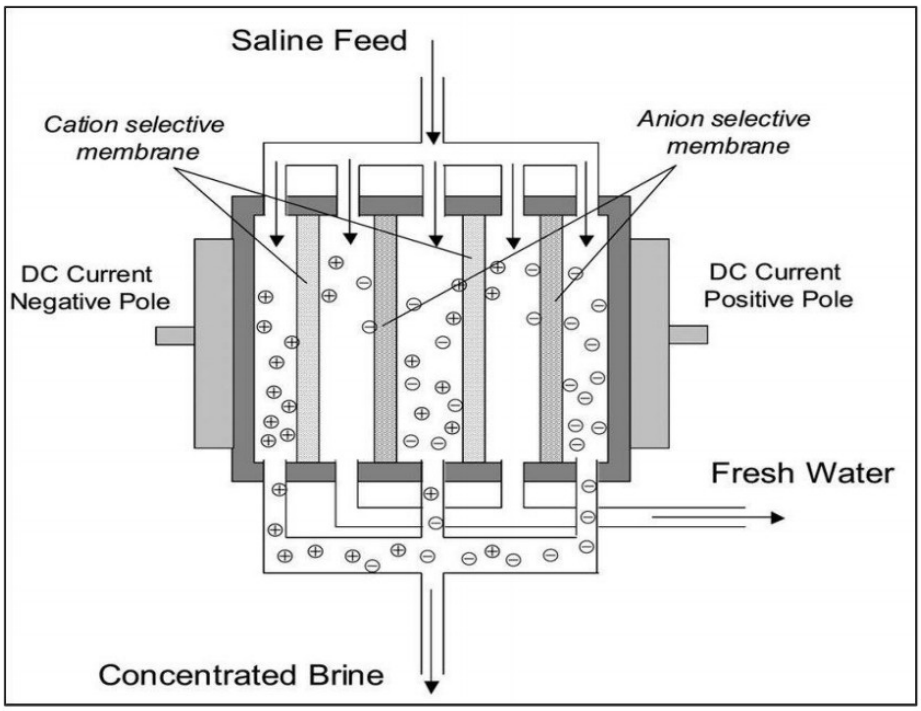

Figure 2.11: Schematic diagram of ED process (Saadat et al., 2018).

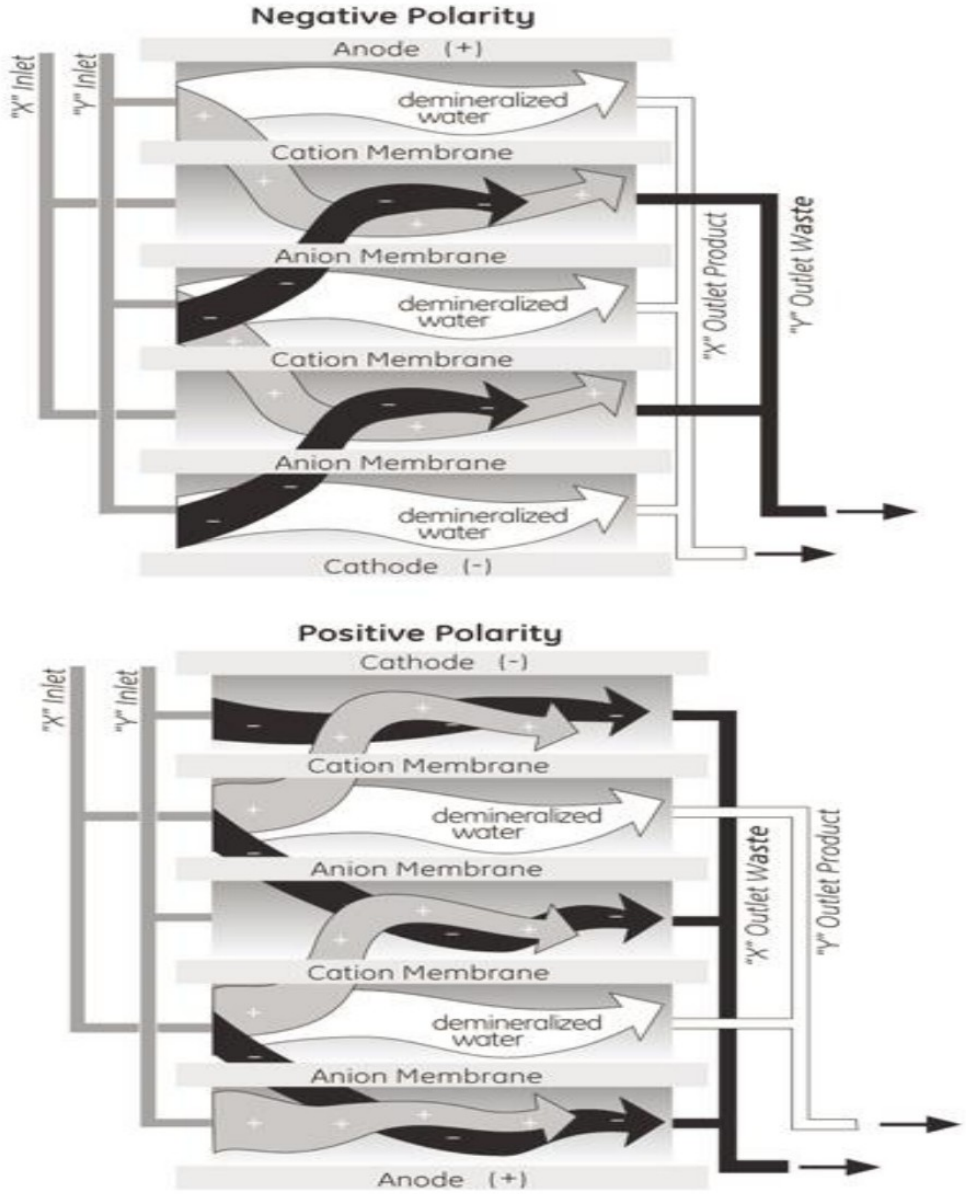

Figure 2.12: EDR Operation in Negative and Positive Polarities (Allison, 2005).

Reverse osmosis, microfiltration, ultrafiltration, and nanofiltration became possible after the appearance and growth of asymmetric (pressure-driven) membranes; dialysis methods could not keep up with the development of these membranes. Asymmetric membranes are made up of a sequence of material layers that have an asymmetric structure, with a thin layer of about 50 µm thickness protected by a thicker layer of more than 100 µm thickness (Berland and Juery, 2002). The four types of pressure-driven techniques are described as follows (Trussell-tech, 2021; source: https://emis.vito.be/en/bat/tools-overview/wass/techniques, Access on 25 March 2021):

- **Microfiltration (MF) membranes** are used to reduce turbidity and remove suspended solids, parasites, bacteria, and viruses from water. These membranes have the largest

pore size rankings, ranging from 0.1 to 3 µm, and require low transmembrane pressures ranging from 0.1 to 3 bar.

- **Ultrafiltration (UF) membranes** are effective at removing viruses, as well as certain colour, odour, and organic contaminants, in addition to all that MF can remove. As compared to MF membranes, these membranes have a narrower range of pore sizes (0.01 - 0.1 µm) and require low transmembrane pressure (2 – 10 bar).
- **Nanofiltration (NF) membranes** are primarily used to remove natural organic material for the purpose of controlling disinfection by-product precursors, water softening, and sulphate removal. NF membranes, which have a pore size of less than 0.002 µm, need a moderate transmembrane pressure rating of 5 to 30 bar.
- **Reverse osmosis (RO) membranes** are essentially non-porous membranes that need a high transmembrane pressure ranging from 10 to 100 bar and are used to remove monovalent salts.

In the salt removal process, MF and UF membranes are used to protect ED, NF, and RO membranes from suspended solids and larger colloidal particles that can degrade their efficiency. To put it another way, the MF and UF membranes are not capable of salt rejection, so they are only useful as a pre-treatment method in desalination membrane systems (Trussell-tech, 2021). NF membranes are close to UF membranes that reject bacteria, colloidal particles, and suspended solids based on size exclusion, but also exclude hardness, such as multivalent ions, based on a charge repulsion mechanism. Monovalent salts, on the other hand, have a hard time passing through NF membranes. As a result, the majority of desalination is operated using non-porous RO membranes that provide a physical barrier to a variety of pollutants, including monovalent ions.

The Environmental Protection Agency (EPA) has designated RO as a best available technology (BAT) for removing a variety of inorganic pollutants, including Sb, As, B, Ba, F, NO_3^-, NO_2^-, Se, emerging pollutants and radionuclides, such as endocrine disrupting compounds and a number of pharmaceutical compounds (Trussell-tech, 2021).

2.5.1.3. Ion exchange

Ion exchangers are synthetic polymers. Ion exchange is the process of removing unwanted ions and replacing them with less aggressive ones by passing water through a layer of ion exchange material, and demineralisation is the process of converting all anions to OH^- and all cations to H^+. While sorption occurs when a solute is taken up by another species without, being replaced (Madzivire, 2010a). Ion exchangers are utilised as storage batteries, and they must be recharged on a regular basis in order to maintain their power. These systems can

virtually completely remove specified ions if they are correctly designed and operated. It has been discovered that ion exchange is a cost-effective and efficient wastewater treatment method. Some of the adsorbent materials that can be used to remove metal ions in the ion exchange treatment process include peat, alumina, silica, activated carbons and bentonite (Gaikwad et al., 2010). Non-specific adsorbents can be outperformed by ion exchange resins with higher sorption capacities (Kim et al., 2002).

When an exchanger comes into contact with an ion-exchanging solution, the following three stages can be used to control the rate of exchange (Kentish and Stevens, 2001):

- **Film diffusion** is governed by the rate at which an ion passes through a film of water molecules, which can be considered stagnant due to the surface charge on the exchanger.
- **Particle diffusion** is governed by the movement of ions within the exchanger.
- **Chemical reaction** is governed by the formation of bonds.

Ion exchange process requires less energy, inexpensive regenerants, and well-maintained resin beds that can last several years before needing to be replaced. (New Zealand Institute of Chemistry, 2002). Although several ion exchange processes are theoretically effective in achieving water quality objectives, only a handful have shown to be economically sustainable (Taylor et al., 2005).

2.5.2. Passive treatment technologies

Mine water treatment through passive methods involves the use of naturally available resources to facilitate biological and chemical processes for the removal of toxins from mine water in systems that are designed to require little monitoring (Alhamed, 2016). When acidic water combines with alkaline water or comes into contact with carbonate minerals, the pH of the water is elevated. Hydroxides, sulphides and oxyhydroxides precipitate and remove metals. (Gazea et al., 1996). Local factors including water, oxygen concentration, and soil chemistry dictate whether these reactions occur in aerobic or anaerobic environments (Hedin and Watzlaf, 1994b; Sheoran and Sheoran, 2006).

Aggregate-carbonate-based passive treatment systems, with or without organic matter, are commonly used, though not exclusively. Passive systems must be designed to tolerate slow reaction rates and minimise armouring, such as covering neutralising materials with metal precipitates or gypsum. Because slow reaction kinetics, such as slow limestone dissolution, necessitate long water retention time, the size of the systems is important to their performance.

Organic materials can be used to assess the system's redox condition while also lowering armouring (Taylor et al., 2005). Passive treatment systems provide low cost. These processes cannot be considered "one-and-done" remedies. A passive systems life span can be extended if it is properly installed. Instead of active mine sites, the majority passive treatment methods are used for post-closure, low-acidity-load treatment conditions. Furthermore, while several passive methods are carbonate-based, not all elements are removed from AMD due to maximum pH constraints; for example, Mn is not totally removed (Taylor et al., 2005).

Passive methods for treating mine water may be classified as either chemical or biological. The AMD is put in close contact with alkalinity-producing materials such as limestone in chemical passive methods. Biological systems depend on bacterial activity for the most part, and organic matter may be used to boost microbial sulphate reduction and adsorb pollutants (Skousen et al., 2017). Table 2.7 list some passive treatment methods.

Table 2.7: Mine water passive treatment techniques

Chemical	Biological	Biochemical
Anoxic limestone drains (ALD)	Constructed wetlands	Permeable reactive barriers
Open limestone drains (OLD)	Sulphate reducing passive	
Successive alkalinity	bioreactors (SRPBR)	

The efficiency and practicability of wastewater treatment are highly dependent on the treatments used and the particular characteristics of each site. Most of these processes involve various techniques, typically in series, to enhance acid neutralisation, oxidation, and precipitation of the resultant metal flocs. Furthermore, alkalinity, acidity, flow, metal, and dissolved oxygen concentrations are critical for the proper sizing and performance of passive treatment technologies (Skousen et al., 2017).

2.5.2.1. Permeable reactive barriers

Permeable reactive barriers (PRBs) are buried layers of reactive material including organic material, limestone, or zero valent iron that are engineered to prevent acidic groundwater plumes and promote in-situ remediation (Taylor et al., 2005). PRBs, which operate under the same principles as anaerobic wetlands, are often used to treat large volumes of contaminated groundwater (Johnson and Hallberg, 2005). Because PRBs are in-situ processes, they entail digging a trench in the direction of contaminated groundwater flow, filling the void with reactive material made up of organic materials and limestone aggregate that is porous enough to allow unrestricted groundwater flow, and landscaping the disturbed area (Johnson and Hallberg, 2005). The organic material may increase bacterial-mediated sulphate reduction, which

causes aqueous H_2S and HS^- to react with dissolved metals in the AMD, forming sulphide precipitates with Cu, Pb, As, Fe, Ni, Cd and Zn. Bacteria absorb organic material, leaving void spaces that are gradually filled by metal sulphide precipitates (Taylor et al., 2005). During microbial digestion of organic matter, alkalinity is generated, which reduces acidity and increases metal precipitation in the permeable barrier. PRBs' lifespan is limited by two key factors: the mass of available reactive matter and the volume of available pore spaces in the barrier. Substrate compaction and metal precipitation will cause the barrier's porosity and permeability to decrease. Low soil temperatures of less than 5°C inhibit bacterial development, so PRBs are better suited to cold climates (Taylor et al., 2005).

2.5.2.2. Open limestone drains

Open limestone drains (OLD) are the most basic type of passive treatment system. OLDs are open channels that contain coarse limestone aggregates (Taylor et al., 2005), and the water is diverted through (Seervi et al., 2017). OLDs can be constructed in a variety of sizes depending on the available area and influents; however, for successful OLD operation, large areas can be needed. Most OLD ponds have 0.3 to 1 m of limestone at the bottom, and they should retain 1 to 3 m of water to keep the seep and limestone submerged (Johnson and Hallberg, 2005). The acidic water flows through layers of limestone of varying sizes that are positioned along the drain's bottom and sides. In an OLD system, the contact of limestone and AMD increases the pH to about 6 - 8 (Seervi et al., 2017). Since OLDs techniques do not reject oxygen or reduce precipitation, they can have a short operating life if built in the wrong location. Armoured limestone (limestone covered with Al or Fe hydroxides) was once thought to stop dissolving, but studies have shown that it tends to dissolve at a slower rate, about 20 to 50% slower than uncoated limestone (Ziemkiewicz et al., 2003). OLD processes require constant maintenance to ensure maximum life and effectiveness. The length of the channel and the gradient of the channel, both of which influence turbulence and coating build-up, are design variables that can be changed. On slopes greater than 12%, where flow velocities hold precipitates in suspension and aid in the cleaning of precipitates from limestone surfaces, optimal performance is achieved (Ziemkiewicz et al., 2003). OLD can be newly constructed channels, or they can be connected to an existing passive treatment system (Taylor et al., 2005). Although residence time is critical to OLD's performance, water velocity must be maintained at a high level. OLDs systems are suitable to treat acidic water with the properties depicted in Table 2.8.

Table 2.8: Properties influents AMD requires for passive treatment method using open limestone drains (Taylor et al., 2005)

Av. Acidity Range (mg $CaCO_3$/L)	Av. Acidity Load (Kg $CaCO_3$/day)	Av. Flow Rate (L/s)	Oxygen Concentration	Typical pH range	Max pH Attainable
< 500	< 150	< 20	Ambient	> 2	6 – 8

According to Skousen et al. (2002), OLDs are capable of removing Fe (70%), Al (40 – 50%), and Mn (10 – 20%) from solution. This shows that not all metals precipitate out of solution in all limestone-based treatment methods. Figure 2.13 depicts a typical cross section of an open limestone channel system.

Figure 2.13: Cross section of an open limestone channel (Seervi et al., 2017).

2.5.2.3. Anoxic limestone drains

Anoxic limestone drains (ALDs) are one of the passive treatment methods for AMD's environmental effects. ALDs are found beneath the ground's surface. Along lightly graded slopes, limestone aggregate beds are coated with an impervious liner or plastic, and then capped with compacted soil or clay (Seervi et al., 2017). According to Taylor et al. (2005), special care needs to be taken during the process to avoid coating limestone with organic material or clay, as well as to guarantee that only a small volume of air is entrained into the drain. The lack of oxygen keeps metals from oxidising and the system from becoming clogged. ALDs are trenches that are typically 1 m deep, 1 - 7 m wide, and 25 - 100 m long. The pH of ALD's effluent varies between 6 and 7. The process could take up to 15 hours to complete (Seervi et al., 2017). AMD effluent is stored in a settling pond before being discharged into streams and lakes to improve pH and metal precipitation. The ALD system is depicted in Figure 2.14.

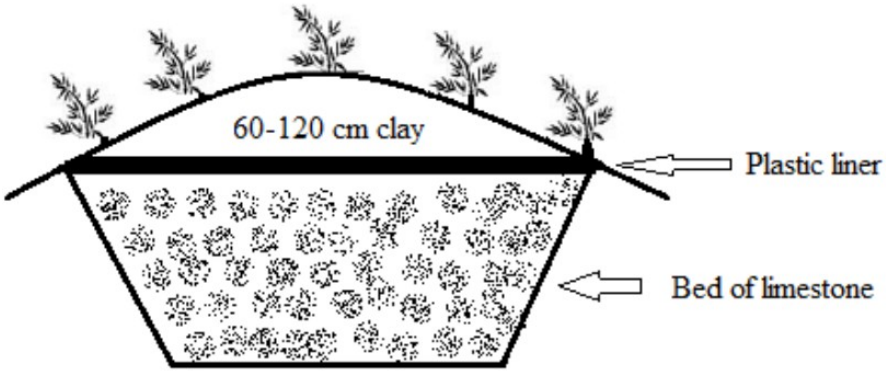

Figure 2.14: Anoxic limestone drains system (Seervi et al., 2017).

Equation (2.18) shows how $CaCO_3$ dissolves and releases bicarbonate alkalinity,

$$CaCO_3 + H^+ \rightarrow Ca^{2+} + HCO_3^- \quad (2.18)$$

The main goal of an ALD is to make bicarbonate alkalinity available through the dissolution of $CaCO_3$ and to increase the pH of the AMD in the range of 6 - 8, while preserving the Fe in its reduced state to avoid oxidation of Fe^{2+} and the precipitation of $Fe(OH)_3$ on the $CaCO_3$, both of which would significantly decrease the alkaline material's effectiveness. When compared to an open system containing 50 to 60 mg alkalinity/L in equilibrium, the drain increases the partial pressure of CO_2, speeding up $CaCO_3$ dissolution and, as a result, elevating the alkalinity concentration reaching up to 275 mg/L (Johnson and Hallberg, 2005; Seervi et al., 2017).

ALD systems are more suited for treating AMD from coal mines than AMD from metal mines because coal mines are usually linked with reduced water, minimising the precipitation of Fe (Taylor et al., 2005). Table 2.9 summarizes the characteristics of the AMD types that ADL can handle.

Table 2.9: Characterization of influent AMD require for successful passive treatment using ALDs (Taylor et al., 2005)

Av. Acidity Range (mg $CaCO_3$/L)	Av. Acidity Load (Kg $CaCO_3$/day)	Av. Flow Rate (L/s)	Typical pH range	Max pH attainable	Dissolved Oxygen (mg/L)
< 500	< 150	< 20	> 2	6 – 8	< 1

ALD systems are not suitable for the treatment of all acidic waters; this includes AMD that contains a high concentration of aluminium and ferric iron. The short-term operation of ALD may be good. However, in the long-term operation of ALD, all the aluminium and ferric iron will precipitate as the hydroxide hydrate once in contact with limestone and hold back the movement of water through the system. The prediction of ALD's design life has not been

achieved due to the variation in aluminium and ferric iron concentration in AMD; as a consequence, void spaces in the drain become plugged. As a result, a better design should include enough porosity to prevent the ALD from failing during its design life due to plugging. Problems may emerge when ALDs are used to treat aerated mine waters; it may be necessary to feed AMD via an anoxic pond before the ALD to reduce dissolved oxygen content to the levels needed to prevent Fe oxidation. Another disadvantage is that the formation of $FeCO_3$ and $MnCO_3$ gels within ALDs can result in the limestone aggregate dissolving in different ways (Johnson and Hallberg, 2005; Taylor et al., 2005).

ALD is a low-cost AMD neutraliser; this system does not need to be maintained on a regular basis, but it does benefit from frequent inspection of the ALD and maintenance of the vegetation cover. Because of the system's buried trench, however, maintaining the limestone layer can be difficult (Taylor et al., 2005). The addition of ALDs to poorly performing constructed wetlands, according to Kleinmann et al. (1998) findings, resulted in significant changes in the water quality draining from these systems.

2.5.2.4. Sulphate reducing passive bioreactors

Sulphate reducing passive bioreactors (SRPB), also called bioreactors, are a type of passive treatment that does not require as much water diversion as other passive methods. This process is commonly used to backfill spoils in mining sites, where AMD is a common occurrence (Jennings et al., 2008). Bioreactors are similar to vertical flow wetlands (VFW) but the principal reagent is organic material, usually, the organic matter (mostly organic carbon source) is fully combined with limestone. The primary type of treatment is microbial sulphate removal (Rose, 2004; Neculita et al., 2007). Bioreactors can handle highly acidic, metal-rich water, as well as mine water containing transition and heavy metals (Skousen et al., 2017).

The advantages of using SRPB systems include cheap running costs, stable sludge, high metal removal at low pH and lower energy consumption. Furthermore, building materials are cheap and readily available (Zaluski et al., 1999). According to Zagury et al. (2007), SRPB systems depend on sulphate reducing bacteria (SRB), which can be found in nature in anoxic environments. Under anaerobic conditions, SBR oxidise organic material to produce bicarbonates, which increase water alkalinity and pH, and decrease sulphates in AMD to sulphides. As a result, sulphides react with metals to form metal sulphides that are insoluble. SRPB processes, however, have slow flow rates, so they're best suited for small flows or conditions where multiple units can operate in parallel (Skousen et al., 2017).

2.5.2.5. Successive alkalinity producing systems

Successive alkalinity producing systems (SAPS) are aerobic ponds that are connected to vertical-flow wetlands. The performance of these systems is dependent on the production of alkalinity in wetlands cells via bacterial sulphate reduction and mineral (for example, $CaCO_3$) dissolution, followed by the removal of metals in aerobic ponds through settling, precipitation, hydrolysis and oxidation, according to several authors (Nairn and Mercer, 2000; Skousen and Ziemkiewicz, 2005).

SAPS systems are special in that they allow for conservative wetland treatment sizing measurements based on alkalinity values and pH, as well as related contaminant loadings, to be calculated as a rate function. SAPS processes can reduce treatment area requirements while still producing alkalinity in excess of acidity, regardless of acidic concentrations (Skousen et al., 2000). Figure 2.15 shows a diagram of the SAPS process.

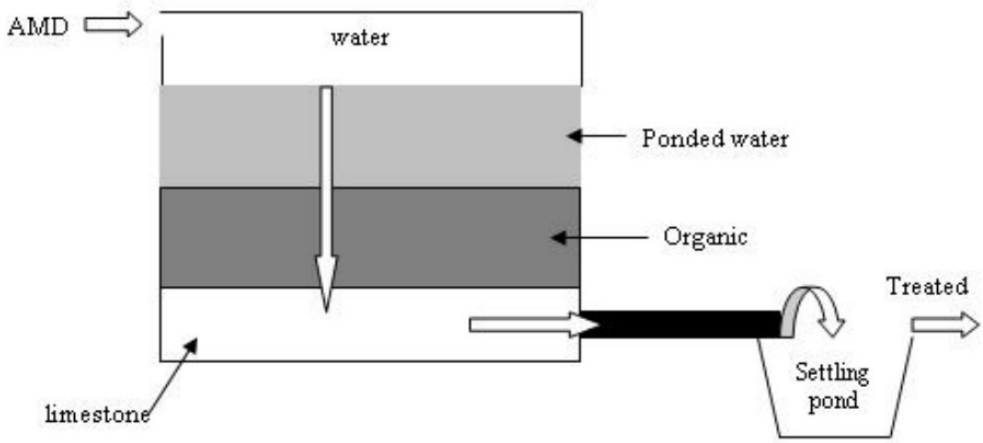

Figure 2.15: Schematic diagram of SAPS (Kalin et al., 2006).

As shown in Figure 2.15, the AMD will pass through several stages until water reaches a good quality. According to Nairn and Mercer (2000), proton acidity produced by aerobic metal removal mechanism in ponds can be mitigated by establishing enough alkalinity in vertical-flow wetlands, and waters can be released into the environment. If appropriate buffering capacity is not established, AMD might be channelled through a separate set of vertical-flow wetlands and aerobic ponds. As a result, this cycle continues until the water satisfies the requirements for release into the environment.

2.5.2.6. Constructed wetlands

One of the most common passive treatment methods is wetlands. Natural wetlands, according to Taylor et al. (2005), are complex ecosystems made up of water-saturated soil and

sediments with supporting vegetation which can naturally enhance water quality through processes such as physical, microbial, chemical and plant-mediated. These incorporate precipitation, oxidation, reduction, filtration, sedimentation, adsorption, complexation, and chelation, active metal uptake by plants, microbial conversion and immobilisation mechanisms (Taylor et al., 2005). Critical factors that influence the choice of the size, type and cost of a suitable wetland process are (1) the acidity loads, pH, and redox condition of the influent water, (2) water flow rates and retention time, and (3) the area of land available for a wetland (Taylor et al., 2005). Based on these parameters, wetlands can be defined as aerobic or anaerobic.

- **Aerobic wetlands**

Aerobic wetlands (AeWLs) are shallow wetlands with depths of somewhere around 30 cm, consisting of Typha and other wetland plants planted in clay, soil or mine spoil sediments (Ziemkiewicz et al., 2003). These processes are commonly used when the influent water is net alkaline. If the water is not net-alkaline, limestone must be added to make it so; otherwise, the AeWLs long-term efficiency and effectiveness would be compromised (Skousen et al., 2017). Their primary function is to aerate and precipitate metals from alkaline mine water (Skousen and Ziemkiewicz, 2005). This type of wetlands, as indicated in Eqs (2.19 – 2.22) below, favours metal oxidation and hydrolysis, resulting in Mn, Al, and Fe hydroxides precipitation and physical retention (Skousen et al., 2017). Effective metal removal is influenced by the existence of active microbial biomass, concentration of dissolved metals, dissolved oxygen (DO) content, pH and net acidity of mine water, and water detention period in the wetland. The pH of the water, as well as its total acidity or alkalinity, are crucial because pH impacts the solubility of metal hydroxide precipitates as well as the kinetics of metal oxidation and hydrolysis. As a result, to neutralise metal acidity, aerobic wetlands should be used in combination with water that contains net alkalinity (Skousen et al., 2017).

$$Fe^{3+} + 3H_2O \rightarrow Fe(OH)_3 + 3H^+ \quad (2.19)$$

$$Al^{3+} + 3H_2O \rightarrow Al(OH)_3 + 3H^+ \quad (2.20)$$

$$Fe^{2+} + 1/4O_2 + 5/2H_2O \rightarrow Fe(OH)_3 + 2H^+ \quad (2.21)$$

$$Mn^{2+} + ¼O_2 + 3/2H_2O \rightarrow MnOOH + 2H^+ \quad (2.22)$$

Equations (2.19 and 2.20) represent hydrolysis reactions, which need only water and enough alkalinity to neutralise the hydrogen ions generated. To oxidise the metal before hydrolysis, equations (2.21 and 2.22) need the presence of oxygen. Acidity is generated by all four equations (Madzivire, 2012a). However, while AeWLs have been shown to be successful in

reducing Fe (60–95%) from solution under a variety of conditions, they have shown some limitations in removing Mn. Because of insufficient alkalinity levels and the system's inability to achieve pH levels greater than 8, Mn precipitation is often in the 10% or less range (Taylor et al., 2005; Zipper et al., 2018). According to Skousen et al. (2017), Mn oxidation is slower than Fe oxidation and is affected by Fe^{2+}, which can slow or reverse Mn oxidation. After all of the Fe has been depleted, Mn precipitation occurs mostly in the system's later stages. AeWLs are often used as the final treatment step, similar to settling ponds, and to catch any fine suspended precipitates that remain (Taylor et al., 2005; Skousen et al., 2017).

- **Anaerobic wetlands**

Anaerobic wetlands, also known as compost wetlands, are the most commonly used passive technique for net acidic mine waters today. Alkalinity is created in anaerobic wetlands in order to neutralise the acidity in the influent waters. Mine water with high content of Fe, Al, DO, and acidity greater than 300 $CaCO_3$ mg/L will benefit from these processes (Hedin and Nairn 1992; and Hedin et al., 1994a). Via natural interaction between bacterial activity and dissolved limestone, this mechanism produces alkalinity. The sulphate-reducing bacteria require a rich organic substrate in order to generate anoxic conditions (such as carbon source and sulphate as an electron acceptor for development, as shown in Eq. 2.23), limestone dissolution can also occur in this anoxic condition (Gazea et al, 1996). Limestone dissolution and the metabolic products of sulphate-reducing bacterial increase pH and precipitate metals as hydroxides, sulphides and carbonates (Skousen et al., 2000).

$$2H_2O + SO_4^{2-} + C \leftrightarrow H_2S + 2HCO_3^- \quad (2.23)$$

The lifespan of most anaerobic wetland processes is limited by the fact that they require large areas for their implementation, and they should be only used to treat small flows of acidic water. High acidity levels can create treatment precipitates that armour limestone particles, exhaust sorption sites on organic material, and block pore spaces within the limestone and organic matter layers (Taylor et al., 2005). Because of the organic material and mass of limestone in the wetland, as well as the available porosity within the limestone or organic material, the lifespan of anaerobic wetlands is shortened in general. The volume available for storing treatment precipitates is determined by porosity, which has an effect on the wetland's treatment efficiency as well as water retention time (Taylor et al., 2005). Gazea et al. (1996) stated that vegetation that grows on the surface of anaerobic cells should be stopped in order to avoid plant roots invading the cell surface and eventual inoculation of excess oxygen into the substrate, which would negatively affect the output of the sulphate reducing bacteria.

2.5.2.7. Selection of passive treatment technique

The chemistry of water, topography, flow rate and site factors all play a role in determining which passive system is appropriate (Ziemkiewicz et al., 2003; Skousen and Ziemkiewicz, 2005; Skousen et al., 2017). Figure 2.16 depicts a method for determining which type of passive system is most suitable. Metal precipitates from net-alkaline mine drainage are often removed effectively by aerobic wetlands. ALDs can treat acidic water with low content of Al, Fe^{3+}, and DO; and vertical flow wetlands, anaerobic wetlands; OLDs can treat net acidic water with higher concentration of Al, Fe^{3+} and DO. Passive systems are becoming more scientifically and technologically advanced. As a result, their ability to handle more challenging waters with suitable designs and sizes is increasing (Ziemkiewicz et al., 2003; Skousen et al., 2017).

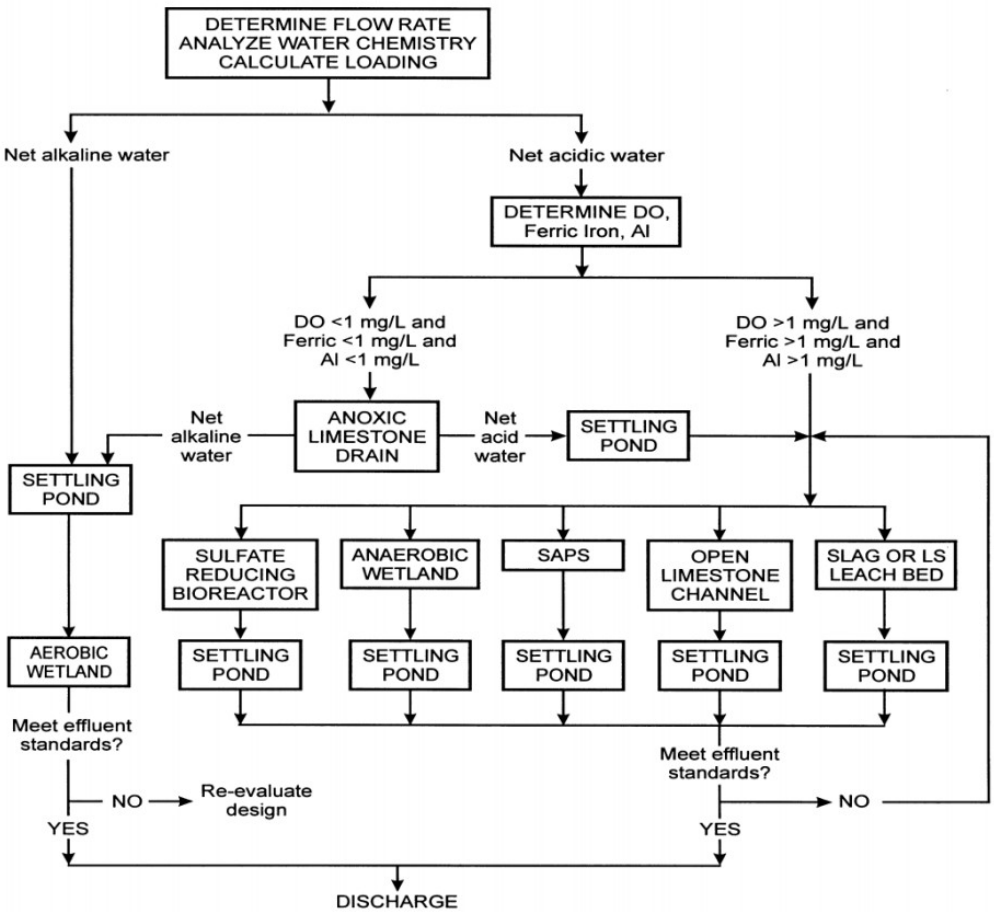

Figure 2.16: Flow diagram for selection of passive system based of flow rate and water chemistry (Ziemkiewicz et al., 2003; Skousen and Ziemkiewicz, 2005).

However, passive treatment has a number of drawbacks. It's good for treating mine water with low acidity (800 mg $CaCO_3$/L), low flow rates (50 L/s), and thus low acidity loads, with a pH near to neutral and low metal concentrations as the main chemical result (Taylor et al., 2005;

Kefeni et al., 2017). The amount of limestone and organic matter in a passive treatment system determines how long it will last (Taylor et al., 2005). Because porosity determines the volume required to retain treatment precipitates, the quantity of available porosity within the $CaCO_3$ and organic matter can also influence the lifespan. The performance of a passive treatment system can become unproductive if it becomes clogged with precipitates due to a lack of porosity in the $CaCO_3$ or organic material layers (Taylor et al., 2005). Almost any acidity, flow rate, or acidity load can be accommodated with active treatment techniques. And, unlike passive treatment systems, they are not constrained by strict operating parameters. However, active treatment systems chemical flexibility comes at a cost.

2.5.3. Treatment of mine water with Fly ash

AMD is caused by the oxidation of sulphur-bearing minerals in the presence of water and oxygen (Gilbert, 2015). FA has been shown to be effective in the remediation of AMD (Petrik et al., 2003; Klink, 2003; Gitari et al., 2006; Gitari et al., 2008a, 2008b; Madzivire et al., 2010b). Most metals present in the water precipitate in their respective hydroxides or oxyhydroxides, sulphate concentration reduces as gypsum precipitation, and the pH of the water raises from 2 - 4 to neutral or higher value (Petrik et al., 2003; Klink, 2003; Gitari et al., 2006; Surender, 2009; Madzivire, 2010a; Kalombe et al., 2020a). While neutralising AMD with FA using a jet loop reactor, Madzivire et al. (2015) reported that sulphate ions concentration was reduced by 70 - 90%, heavy metals such as Fe, Al and Mn were significantly removed, thus meeting the TWQR for drinking water.

Active treatments of acid mine drainage are expensive operations, these systems involve the use of different types of equipment, addition of chemical reagents, disposal of the produced metal laden sludge, and regular maintenance. Acid mine water is usually treated with lime to raise the pH while also precipitating heavy metals (Gazea et al., 1996; Potgieter et al., 2006). Most of mining companies are not capable of purchasing tons of lime in order to neutralise the huge volume of acid mine water produced from their activities and also cannot dispose of the more slimes than residues which need impoundment in hazardous lined ponds produced during the treatment of AMD with lime or limestone. Therefore, other alternatives for alkaline reagents have been or are being investigated to remediate to the problems experienced by previous treatment systems. Low-cost liming material alternatives are being pursued as an option to minimise treatment costs. Such alternatives should be readily available, cost-effective, and produce less sludge that can easily be handled or disposed.

The use of FA to treat mine water takes advantage of the CaO in the FA, which leaches out as it comes into contact with the mine water, neutralising AMD by raising the pH, precipitating

metals as hydroxides, and reducing SO_4^{2-} in the form of gypsum (Gitari et al., 2006; Madzivire, 2010a; Madzivire et al., 2010b).

$$CaO + H_2O \rightarrow Ca^{2+} + 2OH^- \quad (2.24)$$

$$Ca^{2+} + SO_4^{2+} + 2H_2O \leftrightarrow CaSO_4.2H_2O \quad (2.25)$$

$$Me^{n+} + nOH^- \rightarrow Me(OH)_n \quad (2.26)$$

Where, Me^{n+} stands for metal pollutants in the AMD, and n for any number (1, 2, 3, etc.).

2.6. CHAPTER SUMMARY

The literature previously done on mining activities, mine water treatment technologies, mine water production as well as FA generation, was reviewed in this chapter. Mine water is conventionally treated with lime and/or limestone, the only limitation to this technology is the cost associated with these chemicals, which is quite high and cannot be afford by many small mining houses. Therefore, alternatives liming agents are being sought to curb this problem. Several researchers have found that FA can be used as an alternative liming agent for the remediation of mine water. Mine water treatment with FA is not new. This has been investigated by several authors, both in active treatment methods and in passive treatment methods as well. In both cases the capability of neutralising mine water using FA as the primary source of alkali was successfully demonstrated in term of SO_4^{2-} attenuation as well as heavy metals removal. It was also found that there is not a one fit all technology when it comes to mine water treatment.

Prior to the current study mine water was successfully treated using a combination of FA and chemical reagents (lime and $Al(OH)_3$) at an 80 L jet loop reactor pilot plant at laboratory scale. Based on the results obtained at 80 L capacity, the current study will show how mine water can be treated at an industrial scale using FA and minimum amount of chemical reagents. Therefore, minimising the cost with respect to chemical reagents that is crippling many mining houses.

CHAPTER 3

EXPERIMENTAL AND ANALYTICAL TECHNIQUES

3.1. INTRODUCTION

This chapter describes the sampling and analytical techniques used in this study. It outlines the experimental procedure used to achieve the aim and objectives of the study. The chemicals used in this study are also mentioned here. Furthermore, this chapter illustrates the block flow diagram (BFD), the process flow diagram (PFD) and the process and instrumentation diagram (P&ID).

3.2. EXPERIMENTAL OUTLINE

In order to achieve the aim and the objectives of this study, a schematic diagram was designed to summarise the research approach that was used to answer the research questions, as shown in Figure 3.1.

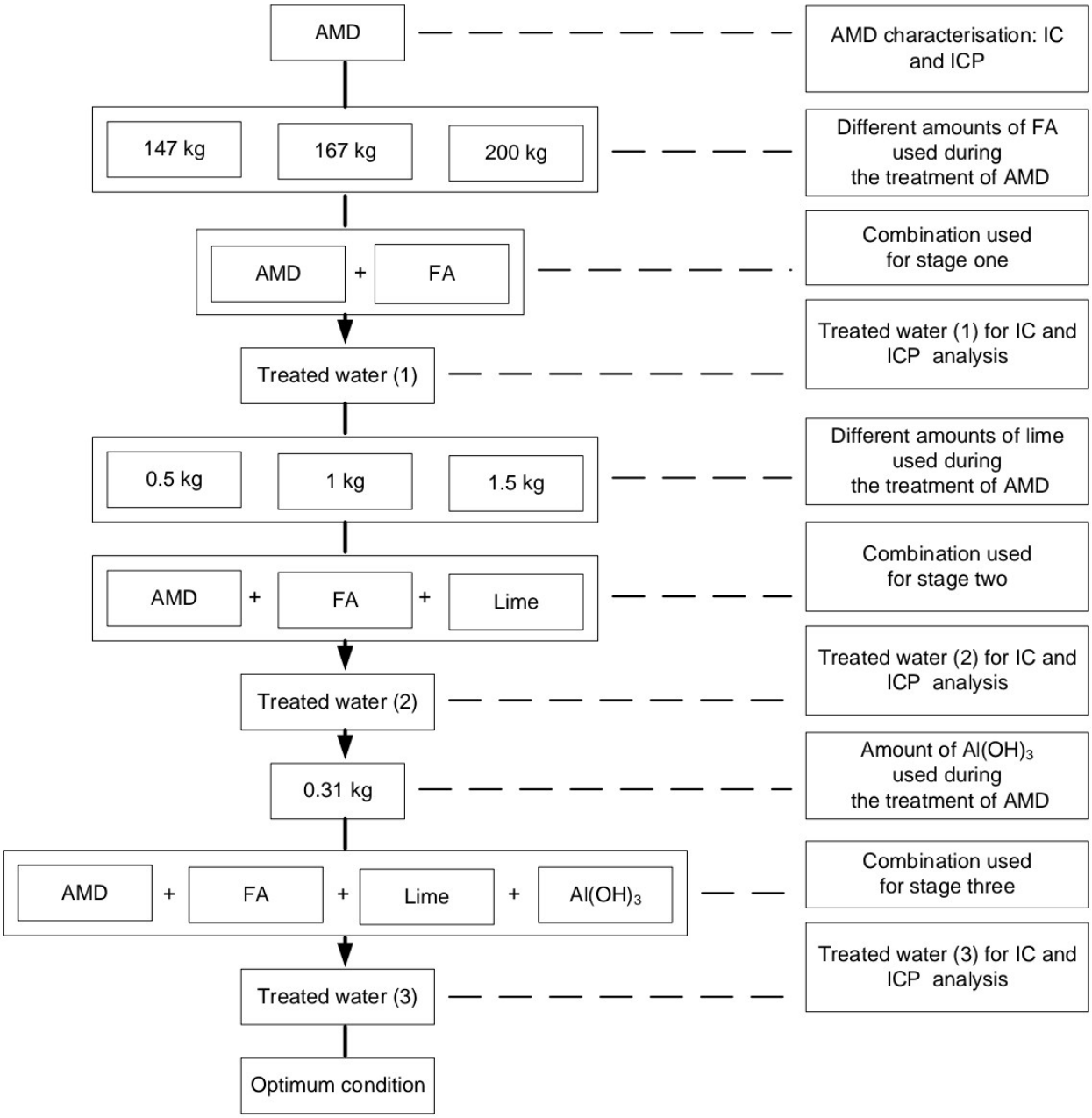

Figure 3.1: Schematic diagram of the research approach summary.

3.3. MATERIALS AND CHEMICALS

3.3.1. Sampling

The FA used in this study was collected from ash dumps at Lethabo and Kendal power stations, and the mine water was obtained from Eyethu coalmine. The fly ash was sampled in sealed plastic bags and kept at room temperature in a dry cool place. The AMD was sampled in 1000 L storage tanks and sealed. Figure 3.2 shows of how FA was sampled.

Figure 3.2: Sample of Lethabo (a) and Kendal (b) fly ash in sealed plastic bags.

3.3.2. Chemicals use

The chemicals used in this experimental study are tabulated in Table 3.1.

Table 3.1: List of chemical reagents used for the current study

Chemical name	Chemical formula	Purity (%)	Supplier
Lime	CaO	95.00	Ace chemical
Sodium hydroxide	NaOH	98.87	Kimix
Aluminium hydroxide	$Al(OH)_3$	98.00	Ace chemical
Carbon dioxide	CO_2	99.99	Air liquid
Hydrochloric acid	HCl	32.00	Ace chemical

3.4. AREA OF STUDY

Eskom Lethabo and Kendal power stations, located respectively in the Free State and Mpumalanga province of the Republic of South Africa (RSA) as well as Eyethu coalmine in the Mpumalanga province were chosen as the area of this research study.

3.5. EXPERIMENTAL PROCEDURE AND PROCESS DESCRIPTION

The procedure and the description of the process are presented under this section.

3.5.1. Process description

The pilot plant was designed to treat AMD and circumneutral mine water (CMW). Two sources of mine water were considered while designing this plant, which were from gold or coal mines.

The purpose behind the plant is the removal of trace elements and sulphate reduction from mine water to the standard required by the DWAF guidelines. The description of the process is based on the block flow diagram (BFD) (Figure 3.3). Mine water treatment was carried out in a semi batch process consisting of two major cycles:

- Cycle 1: Neutralisation and clarification (refer to red and green lines on the BFD)
- Cycle 2: Carbonation (refer to blue and green lines on the BFD)

During cycle 1, 1000 L of mine water is neutralised by adding a certain amount of fly ash, lime and $Al(OH)_3$. The mixture is circulated through the jet loop reactors for a certain period; and this is allowed to settle for about 30 - 40 minutes for clarification. After settling, the clarified water is decanted to the clear water tank. During cycle 2, the clarified water is circulated through the jet loop reactors and dosed with CO_2, while monitoring the pH. This is a pH control system, for each cycle there is a targeted pH to be reached or achieved; this is further elaborated in section (3.5.3.1). After carbonation, the water is pumped to the recovered water storage tank. The slurry that remained in the clarifier is pumped to the slurry storage tank.

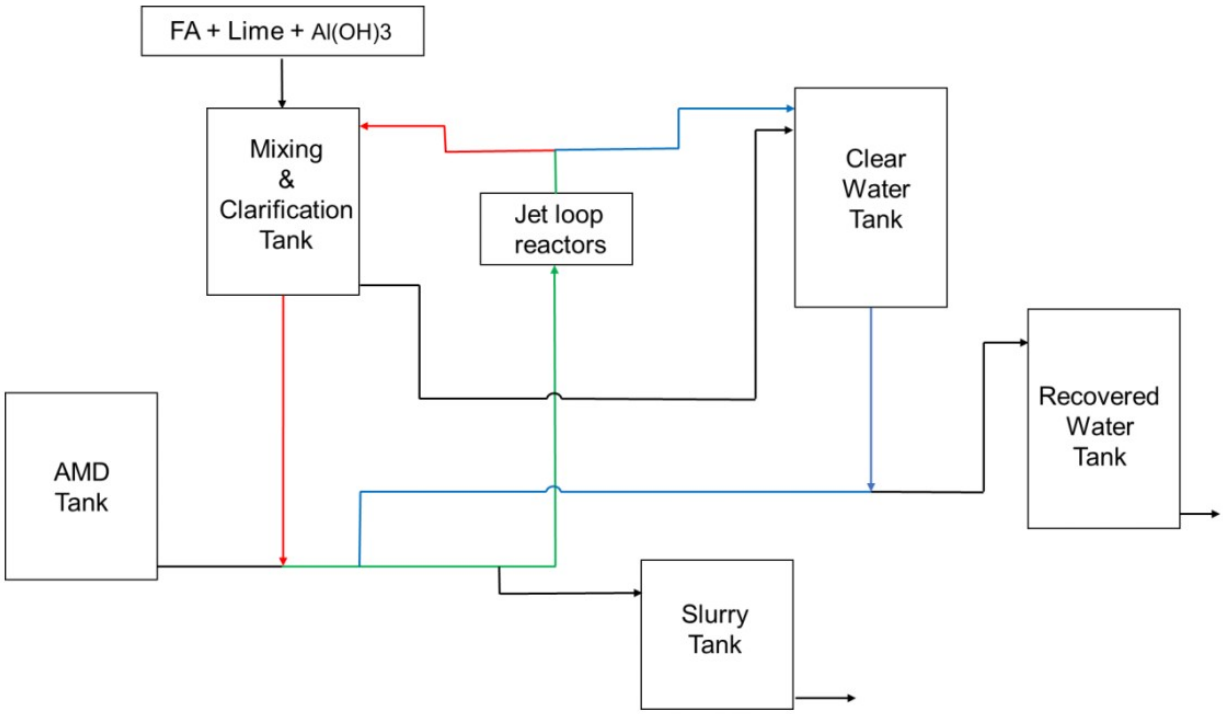

Figure 3.3: Block flow diagram of the pilot plant describing the two major cycles of the process.

3.5.2. Description of the jet loop reactor

The jet loop reactor (JLR) role is to provide intense mixing based on cavitation and impingement principle. The compartment of the reactor consists of two adjustable orifices through which the mixture flows. While flowing through the orifices the mixture's kinetic energy

decreased and the pressure increases. When this come out of the orifices the pressure decreased and the kinetic energy increases. This drop and increased in kinetic energy and pressure caused hydrodynamic cavitation in the mixture of AMD and FA as the low pressure caused bubble to form, grow and collapse. The movement of water in the JLR is shown in Figure 3.4.

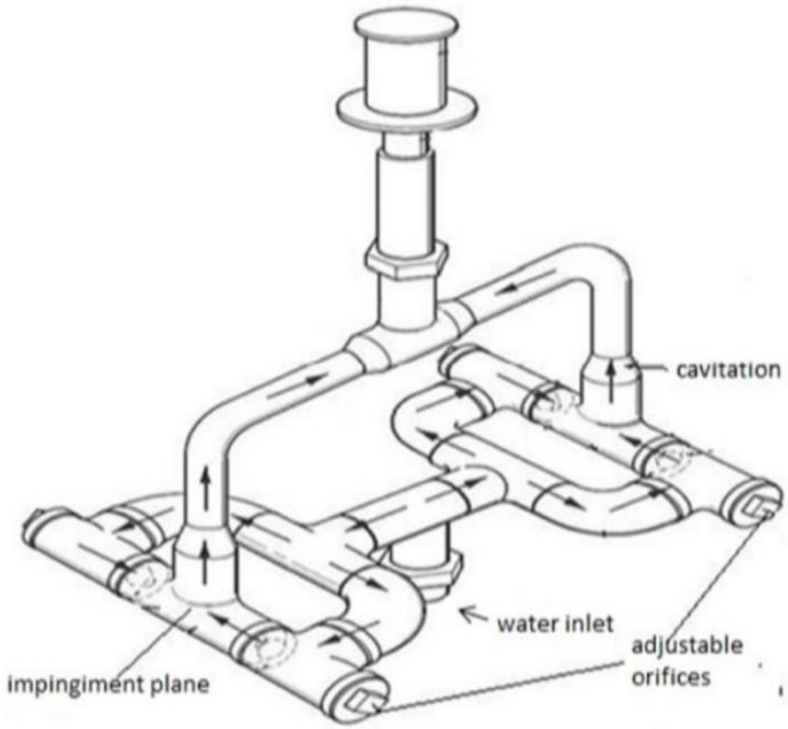

Figure 3.4: Water's movement in the jet loop reactor shown by arrows (Madzivire et al., 2012b).

The mixture flows in opposing directions from the two orifices, clashing with high kinetic energy inside the JLR. Impingement is the collision of two jet streams with high kinetic energy (Nyale, 2014). Figure 3.5 shows how this operates.

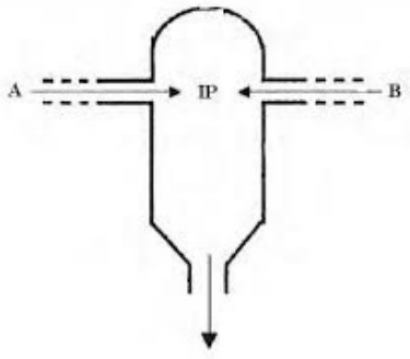

Figure 3.5: Impingement presentation inside the jet loop reactor (Madzivire et al., 2012b).

3.5.3. Monitoring and controlling

Monitoring and controlling are valuable tools in chemical industrial processes to ensure reliability in product quality. The process is monitored through a supervisory control and data acquisition (SCADA) software. This software was chosen because of its primary drivers, which can increase efficiency, reduced costs, enhanced decision-making and simplification of operations.

The process is operated from a control room; operators from one or more human-machine interface (HMI) workstations engage the system. Sensors are installed to measure the changes at the field level, when equipment starts or stops, these transmit a signal to the programmable logic controllers (PLC), which then communicate the information to the HMI system, where the graphical elements change colour to reflect the current conditions. In anomaly occurrence, the same procedure is repeated, and the HMI system alerts the operators.

3.5.4. Procedure and plant start up

This describes how the pilot plant is operating. The process flow diagram (PFD) of the pilot plant is illustrated in Figure 3.6. This shows the different equipment that consist the pilot plant, it’s also indicate the general flow of plant processes. It's used to highlight the relationship between a plant's main components, but it doesn't reveal minor details like piping details or designations. The P&ID in the other hand (Figure 3.7), includes more details than a PFD. It includes both major and minor details of the chemical process, in short P&ID is a detail form of PFD.

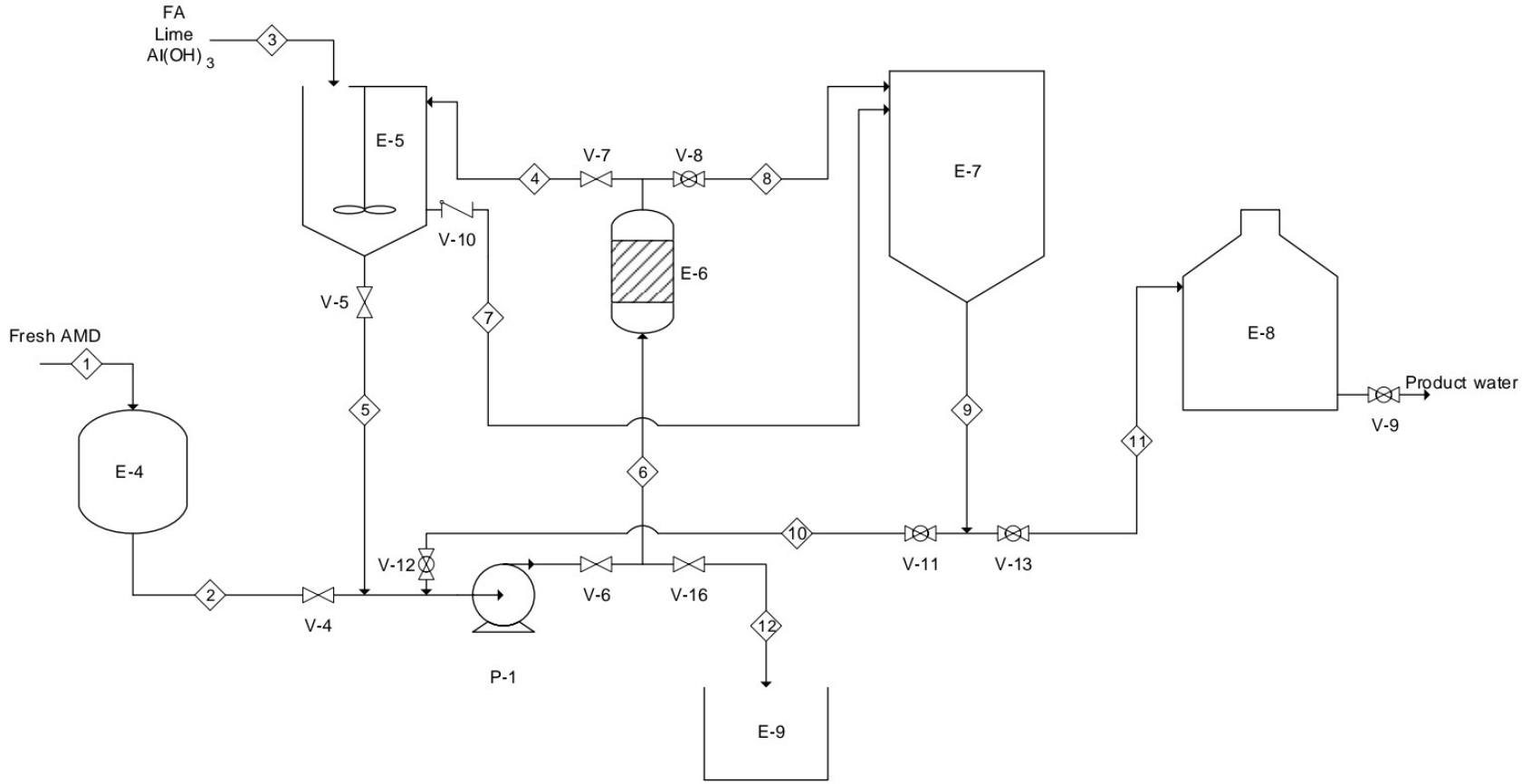

Figure 3.6: Jet loop reactor 1000 L capacity pilot plant PFD.

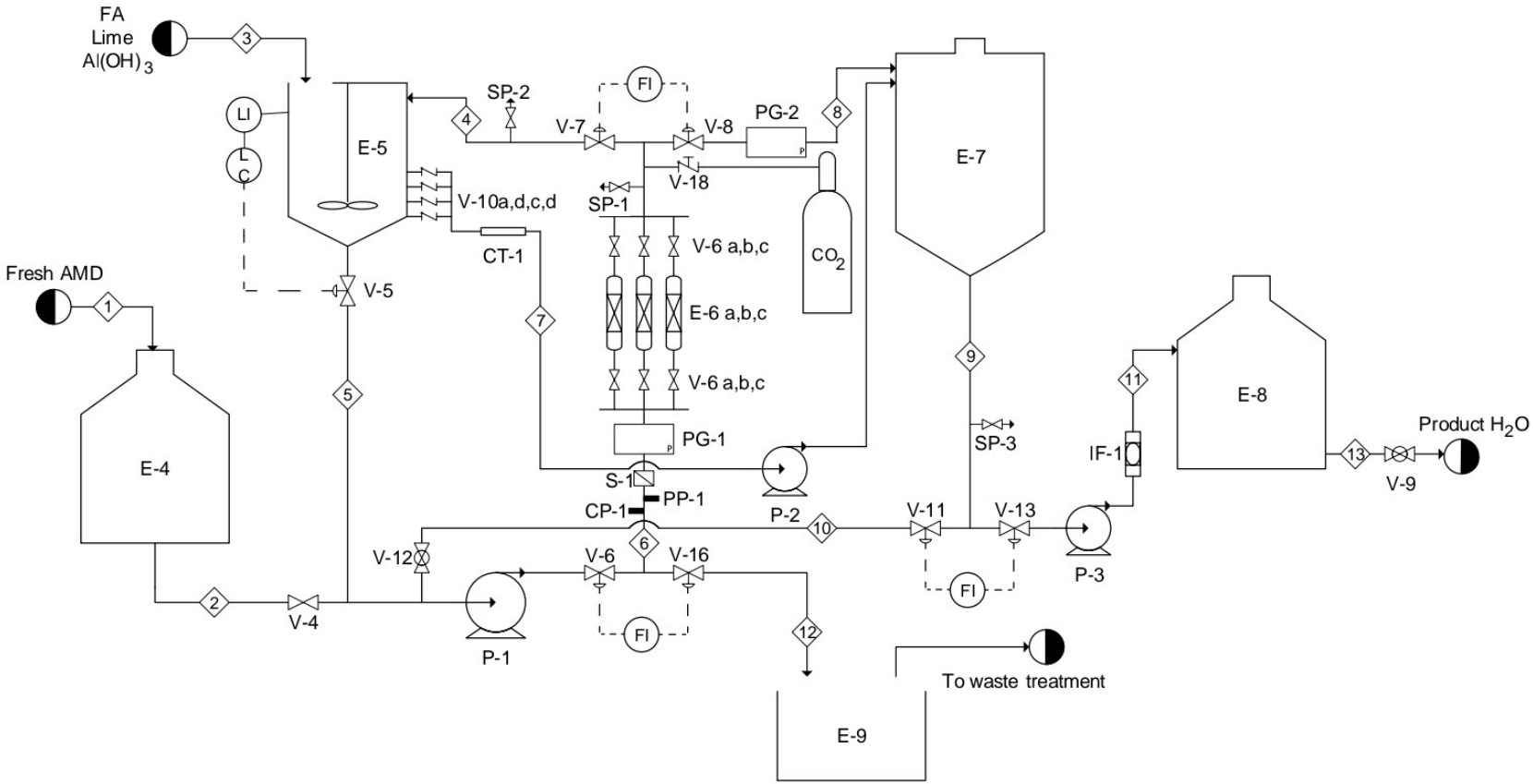

Figure 3.7: P&ID of the 1000 L jet loop reactor pilot plant for the treatment of AMD using fly ash.

The units illustrated on the PI&D are tabulated in Table 3.2 with each unit corresponding to equipment. The symbols used on the PI&D are listed in Table 3.3.

Table 3.2: Equipment constituting the pilot plant

Unit number	Equipment	Unit number	Equipment
E-1	FA storage	P-2	Discharge pump 1
E-2	Calibrated Bucket	P-3	Discharge pump 2
E-3	Crane & Hoist	IF-1	Inline Filter
E-4	AMD Tank (storage)	PG-1	Pressure gauge
E-5	Mixing and Clarification Tank	SP-1	Sampling point
E-6 (a,b,c)	Jet loop reactors	PP-1	pH probe
E-7	Carbonation Tank	S-1	Strainer
E-8	Treated or Product water Tank	CT-1	Glass tube
E-9	Slurry Tank	CP-1	Conductivity probe
P-1	Recirculation pump (main)	V	Valve

Table 3.3: PI&D symbols

Symbol	Description
FI	Flow indicator
LI	Level indicator
LC	Level controller

3.5.4.1. Pilot plant scale operating procedure

The treatment of AMD was performed in a semi batch process. The process consisted of two major cycles as described above under section (3.5.1). For a better and safer operation, the two major cycles were divided into 6 cycles, which are illustrated in Figure 3.6 (P&ID). To start any cycle one had to ensure that all the valves were closed, expect the jet loop reactors valves. The operating procedure is as follows:

- **Cycle 1: Filling up of the mixing tank**

Ensure that all the valves are closed and that valves (V-6 a-b-c) around the jet loop reactors are always open. Then open valve 4 (V-4), V-6 and V-7, to allow the AMD to flow within the system through the jet loop reactors, then press the main pump button on the control panel to start pump 1 (P-1) to fill the mixing tank (unit E-5) with 1000 L of AMD via streams (2.6 and 4). A level indicator is mounted on the tank, thus when the 1000 L mark is reached P-1 stops instantly, and then field operator closes V-4.

- **Cycle 2: Neutralisation and clarification**

At the neutralisation stage, pressure and temperature are also monitored. Because of the reaction in the jet loop reactors some changes in the temperature may occur. Fly ash is added at this stage, by filling up a calibrated bucket with the amount of fly ash needed for the neutralisation process to take place. The bucket is lifted using a crane to which a hoist is attached (unit E-3). A funnel is mounted on the bucket for channelling the fly ash into the mixing tank (unit E-5). Start stirring by pressing on the stirrer button on the control panel, and simultaneously start feeding FA by opening the valve fitted on the bucket. Since the bucket can only take up to 100 kg, the feeding of FA is done twice, while stirring. The time taken to feed FA into unit E-5 should be about 5 to 15 minutes. After all the required amount of FA is fed, the mixture of AMD and FA is further stirred for about 10 minutes to ensure thorough mixing, before the start of circulation through the jet loop reactors (unit E-6). Then V-5, V-6 and V-7 are opened, and then P-1 is started by pressing the start button on the control panel to allow the mixture of AMD and FA to circulate through the jet loop reactors. Following AMD and FA mixing, selected amounts of pre-weighted lime are added to elevate the pH of the mixture, since FA itself could raise the pH only to about 7 - 9. From the control panel the pH is monitored, when this is greater than 11.5, pre-weighted $Al(OH)_3$ is added, then mixed and the mixture of AMD + FA + lime + $Al(OH)_3$ is circulated for approximately 30 minutes. The neutralisation process takes about 2 - 3 hours depending on the pH variation. This time includes the addition of lime and $Al(OH)_3$. Throughout this process, pH was monitored. Within this period, the reaction was completed; then stop P-1 and the agitator then V-5, V-6 and V-7 were closed. The mixture was left to settle for clarification to take place. After about 30 - 40 minutes, clarification was completed, and then the clarified water was decanted.

- **Cycle 3: Clear water decanting**

To start this process, it was ensured that all the valves were closed. Then open V-10 (V-10a-b-c-d), then press on the start button to start P-2 on the control panel to decant the clarified water into the clear water or carbonation tank (unit E-7). To avoid any agitation, these valves (V-10a-b-c-d) were opened stepwise; starting with V-10a, after the water level down, the previous valve is closed and opens the next one and so on. The colour of the water was observed through a clear glass tube fitted on stream (7), so that there is not FA slurry pumped in unit E-7, this could change the colour of the water. Then closed V-10 after decanting is completed.

- **Cycle 4: Carbonation**

It was made sure that the cylinder contained enough CO_2 before starting the process. Check if the cylinder was well connected to the system. To start this cycle V-11, V12, V-6 and V-8 were opened, and then start P-1 on the control panel to allow the water in unit E-7 to circulate through unit E-6 (a, b, c). Open the cylinder valve, and then press the gas regulator button on the control panel to allow carbonation to take place, while monitoring the pH. A one-way valve (V-18) was installed to prevent water from flowing in the CO_2 stream. Carbonation is stopped when the pH falls in the range of 6 - 9, simultaneously stop P-1, then close V-11, V-12, V-6 and V-8. This process took about 10 - 20 minutes; depending on how, the system was responding.

- **Cycle 5: Treated water discharge**

The treated water was discharged to the treated or product water storage tank (unit E-8) by opening V-13 and starting the discharged pump (P-3) on control panel, to discharge the water from unit E-7 to E-8. An inline filter is fitted in this stream (11) to capture all calcium carbonate ($CaCO_3$) that may form during the carbonation cycle. Do not pump all the water in unit E-7, the remaining water will be used for rinsing the system after the last cycle. Stop P-3, and close V-13. The inline filter is cleaned manually after taking out all the $CaCO_3$ that may form, which is pure.

- **Cycle 6: slurry discharge and system cleaning**

Open V-5 and V-16 and start P-1 to discharge the slurry from unit E-5 to the slurry tank (unit E-9). The water in E-7 is pumped into E-5 by opening V-11, V-12, V-6 and V-7 and starting P-1. Then stop P-1 and close V-11 and V-12, open V-5 to circulate the water in E-5 through the Jet loop reactors by starting P-1. After circulation close V-6 and V7 then open V-16, then pumped the water from E-5 to E-9, so that this stream (12) also can be cleaned. Unit E-5 walls are cleaned by using a hosepipe to remove the solids attached to the walls of the tank.

3.6. TREATMENT OF EYETHU AMD WITH FLY ASH, LIME AND ALUMINIUM HYDROXIDE

A number of experiments were performed using Eyethu AMD at 1000 L capacity. The experiments can mainly be classified as, the optimisation of the amount of FA (Lethabo or Kendal), lime and $Al(OH)_3$ required and to investigate the performance of the jet loop reactors. Different parameters were investigated such as the amount of FA, lime, and $Al(OH)_3$ needed

to rise the pH of the AMD to pH above 11.0 in order to remove SO_4^{2-} as ettringite or gypsum and remove heavy metals, which precipitate to form amorphous hydroxides and oxyhydroxides. The procedure described in section (3.5.3.1) was applied. Three stages of experiments were carried out to optimise the process. At every stage a set of experiments was performed, while measuring pH and EC after every 10, 20 or 30 min, and samples collected for analysis after every 20 – 30 min. The samples of water collected were filtered through a 0.45 µm membrane filter and the filtrate analysed using IC and ICP.

- **Stage 1: Optimisation of the amount of fly ash**

1000 L of AMD was mixed with different amount of fly ash and circulated through the jet loop reactors. The mixing effect in the jet loop reactors is a combination of impingement and cavitation. The combinations are shown in Table 3.4.

Table 3.4: AMD neutralisation using FA

Run	Raw material	
	AMD (L)	FA (kg)
1	1000	143
2		167
3		200

The results obtained after this set of experiments are discussed in chapter 4. The amounts of FA in Table 3.4 were determined based on the work done at 80 L pilot plant laboratory scale by Madzivire et al. 2015.

- **Stage 2: Optimisation of the amount of lime**

The best combination obtained in stage 1 (optimised amount of FA), was used to optimise the amount of lime needed to elevate the pH of the solution, thus further reducing sulphate ions concentration and removing heavy metals. AMD was treated with FA, while monitoring the pH, when this was constant; the circulation was stopped by stopping P-1. Then lime was added to the mixture of AMD + FA, and stirred for about 20 min. After 20 min of stirring the mixture of AMD + FA + lime was circulated through unit E-6 (Jet loop reactors) by starting P-1, while monitoring the pH. The operation was stopped when no variation was observed in the pH value. The mixture was left to settle.

Table 3.5: AMD neutralisation using FA + lime (amount of lime optimisation)

Run	Raw Material		
	AMD (L)	FA (kg)	Lime (kg)
1	1000	Stage 1	0.5
2			1.0
3			1.5

The results obtained are discussed in chapter 4.

- **Stage 3: Amount of $Al(OH)_3$ determination**

The addition of $Al(OH)_3$ depended on the SO_4^{2-} ions concentration that remained in the water after lime optimisation, for further SO_4^{2-} precipitation by ettringite formation. This was done as describe below using Eq. (3.1), which shows how ettringite is formed.

$$6Ca^{2+} + 2Al(OH)_3 + 3SO_4^{2-} + 32H_2O \rightarrow 3CaO.3CaSO_4.Al_2O_3.32H_2O + 6H^+ \quad (3.1)$$

Now using the stoichiometry:

For every 2 moles of $Al(OH)_3$ there is 3 moles of SO_4^{2-} present:

$$2Al(OH)_3 \rightarrow 3SO_4^{2-}$$

$$X \rightarrow [SO_4^{2-}]\ g/L$$

using the mathematical formula of the rule of three, the mass of $Al(OH)_3$ will be determined using the following Eq. (3.2) below.

$$X = \frac{2*[SO_4^{2-}]*A*1000}{3*B} \quad (3.2)$$

Where,

The […] symbol represents the concentration of a species and 1000 is for the volume of the AMD in L

X: stands for the mass of $Al(OH)_3$ to be determined in grams (g)

A: molar mass of $Al(OH)_3$, which is 78 g/mole

B: molar mass of SO_4^{2-}, which is 96.06 g/mole

3.7. EXPERIMENTAL PROCEDURE FOR THE SYNTHESIS OF GEOPOLYMER FROM SOLID RESIDUE

This section presents the procedure, the synthesis conditions and parameters varied, during the synthesis of geopolymer from the SR recovered after treatment of AMD with FA. The synthesised geopolymer is to be used as a backfill material.

The geopolymer was produced by mixing the SR or slurry with NaOH and/or Na_2SiO_3 solutions, FA and cement. Different parameters were investigated in order to determine the best synthesis conditions for producing geopolymer as a backfill material from SR, which were the amount of fresh FA, NaOH and Na_2SiO_3, and the amount of cement added. Most these parameters were investigated by trial and error as tabulated in Table 3.6. The synthesis method carried out in this researched was inspired by work done by Vadapalli et al. (2008) and Kalombe et al. (2020b).

Table 3.6: Parameters investigated during the synthesis of geopolymer-backfill material

		Parameters (kg)				
Exp.	**SR (kg)**	**Fly ash (wt.% of SR)**	**OPC (wt.% of SR)**	**NaOH**	**Na_2SiO_3**	**H_2O**
1	3.00	--	--	--	--	--
2	1.50	100.00	--	--	--	0.40
3	1.50	100.00	--	--	0.25	0.15
4	1.50	100.00	6.00	--	0.40	0.40
5	3.00	--	--	0.30	0.90	--
6	3.00	--	3.00	0.30	0.90	--
7	3.00	--	6.00	0.30	0.90	--
8	3.00	--	6.00	--	--	0.10
9	3.00	--	10.00	--	--	0.10
10	3.00	--	10.00	--	0.10	--
11	3.00	--	15.00	--	0.10	--
12	3.00	--	30.00	--	0.10	--

Exp. stands for experiment, OPC stands for ordinary Portland cement.

The addition of NaOH, Na_2SiO_3 and OPC to the SR was inspired by previous works done by Kalombe et al. (2020b) and Vadapalli et al. (2008). The results obtained after analysis are presented in Table 4.18 and discussed in chapter 4 (Section 4.5). The concentration of NaOH solution was 10M.

The mixing process took about 10±2 minutes using a mixer. The resulting paste was placed in a plastic mould (100 x 100 x 100 mm) and left to set a room temperature (≈25 ˚C) for 28 days until loading. It has to be noted after casting the samples were covered with a plastic to keep the humidity during curing. The full process in shown in Figure 3.8.

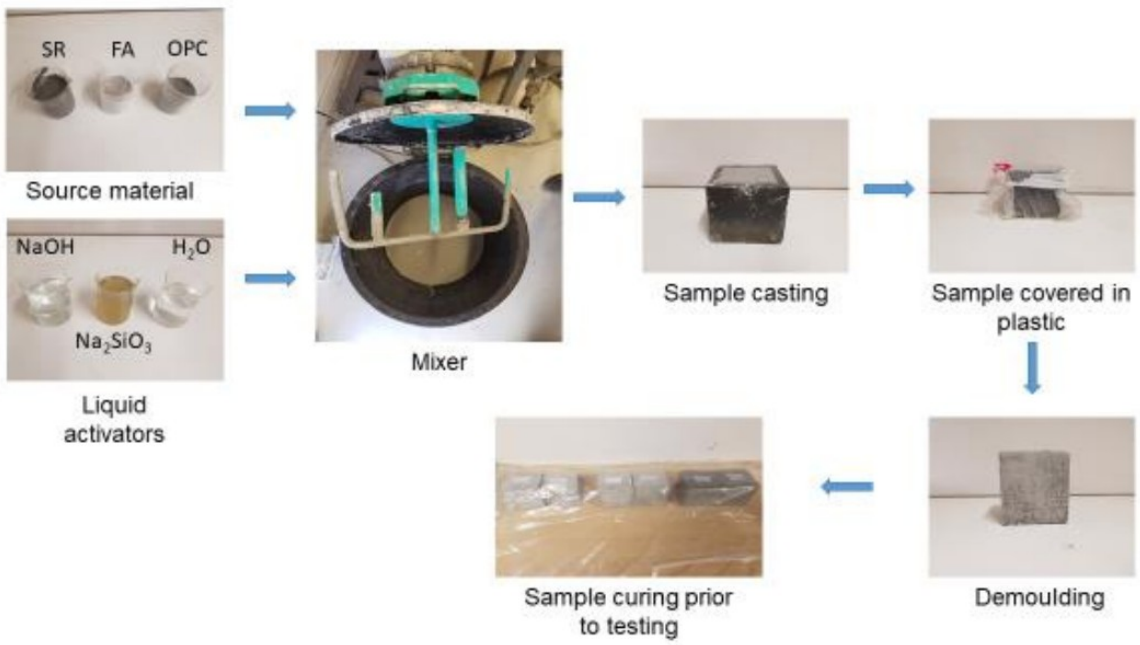

Figure 3.8: Flow diagram of the procedure during the synthesis of the SR based geopolymer backfill material.

3.8. CHARACTERISATION TECHNIQUES AND STANDARD EXPERIMENTAL METHODS

This section presents the different analytical techniques done during this study and it also describes the procedure of sample preparation prior to the analysis.

3.8.1. pH measurement and electrical conductivity (EC)

The determination of pH is one the most common analyses carried out in chemical process industries. pH is the measurement of the concentration of H^+ and OH^- ions in an aqueous solution. Electrode-based electrical measurements are used to determine the pH of a solution. An indicating electrode and a reference electrode make up the two half-cells of a pH electrode. Currently, the majority of applications use a combination electrode, which integrates both half cells into a single body. The vast majority of pH measurements are in the range of 0 to 14. An acidic solution has a higher H^+ concentration than water (pH less than 7), while an alkaline solution is characterised by a lower concentration of H^+ (pH greater than 7). In this study, a STARTER 300 portable pH/MTC/Temperature pH meter was used.

The pH meter was calibrated using buffer solutions of pH 4.01 and 7.0 before measurement. The instrument was set to pH Mode after calibration, and the temperature was set to 25°C. The electrode was inserted into the sample to be tested, and the pH of the solution appeared

on the display; it was then allowed to stabilize before the measurement was recorded. These readings were compared with the ones displayed on the control panel (system display). After taking the reading, the pH electrode was rinsed for the next measurement. Thereafter the electrode was rinsed and placed back in the storage solution at the end of the experiment. The pH, which is the logarithmic measure of the concentration of hydrogen ions in a solution, is defined as the negative log base 10 of the hydronium concentration as shown by Eq. (3.3).

$$pH = - \log [H^+] \quad (3.3)$$

3.8.2. X-ray diffraction (XRD)

XRD analysis was done on the fresh FA and SR recovered for the identification of mineral phases. Moreover, the mineralogical changes were evaluated between the fresh FA and the SR. A Philips PANalytical equipment with a pw3830 X-ray generator operating at 40 KV and 40 mA was used. Prior to analysis, the FA and SR samples were dried at a temperature of 105°C to remove any moisture. Before being placed into the XRD device, the samples were finely crushed and pressed into a rectangular sample holder. After step-scanning the samples at intervals of 0.02° 2θ between 5° and 90° with Highscore Xpert software, the mineral phases were detected. The resulting spectra were compared to standard line patterns from the International Centre for Diffraction Data's powder diffraction database (ICDD).

3.8.3. X-ray fluorescence (XRF)

Fresh FA and SR samples were analysed for major oxides using a Philips PW1480 X-ray spectrometer. A chromium tube and five analysing crystals (LIF 200, LIF 220, GE, PE, and PX) were included in the spectrometer, as well as a gas flow proportional counter and scintillating detectors. The P10 gas, which is 90% argon (Ar) and 10% methane (CH_4), was utilised in the gas flow proportional counter. Major elements were analysed on a fixed glass bead at 40 kV and 50 mA by drying the samples at 105 °C and prepared as follow: the mixture of 0.65 g of sample and 5.60 g of flux ($Li_2B_4O_7$ 66.67%, $LiBO_2$ 32.83%, and LiBr 0.50%) was combined and fused on a glass bead. Different oxides were identified, including SiO_2, Al_2O_3, Fe_2O_3, CaO, TiO_2, MgO, K_2O etc. About 2 g of each sample was heated in a furnace at 1000 oC for 4 hours to determine LOI.

3.8.4. Ion chromatography (IC)

IC was used to identify and quantify anion concentrations in mine water before and after treatment, revealing the various changes in anions concentration. The samples were filtered through a 0.45 µm membrane filter paper for the removal of any suspended particles. The

filtrate can be preserved in a refrigerator at 4 ˚C until the samples are analysed. A Dionex DX-120 Ion Chromatograph with an AS40 automated sampler, an ASRS-300 suppresser, an AS14 analytical column, an AG14 guard column, and a conductivity detector was used for the analysis. The eluent used was a mixture of 3.5 mM $NaHCO_3$ and 1.0 mM Na_2CO_3.

3.8.5. Inductively coupled plasma-optical emission spectroscopy (ICP-OES)

One of the major applications of ICP-OES is the multi-element analysis of water to determine major, minor and trace elements. This was performed on both the mine water, the product water, the FA and the SR produced after the treatment process. On the FA it was performed to determine trace elements such as Sb, As, S, Mo, Co, Ge, Mn, Th, Cd, Be, Bi, Cu, V, Zn, Pb etc. The instrument was calibrated in the first stage by introducing the first standard solution to the plasma and pushing a key on the computer, then adding other standards and a blank solution. For suspended solids removal, the samples were filtered through a 0.45 µm membrane filter. A Varian 710-ES ICP-OES instrument equipped with a PMT detector was used for this analysis.

3.8.6. Compressive strength test

This was done to determine the structural strength of the synthesised geopolymer prepared from SR. The test was performed using King test auto 2000 model Pat 2001 compression testing machine with a load capacity of 2000 kN and a load rate of 40 - 1000 kN/min. The test was done on samples of 100 mm^3; a Vernier calliper was used to determine the geometry of the sample. SANS method 5863:2006 was the standard considered. Between the compression plates of the testing machine, the specimen was put horizontally with the mortar-filled face facing upwards. The load was applied axially at a rate of 180 kN/min until it failed, and the maximum load at failure was recorded. The specimen had failed to produce any further increases in the indicator on the testing equipment at this point. To illustrate this scenario, Figure 3.9 is given.

Figure 3.9: Specimen testing for compressive strength.

3.9. CHAPTER SUMMARY

Under this chapter the procedure followed to achieve the research objectives was fully described. The area of research was defined and presented in this chapter. Different analytical techniques were presented as well, and a detail explanation was given for each technique. This chapter also outlined how the research was approach. The results obtained under this chapter are presented and discussed in the next chapter.

CHAPTER 4

RESULTS AND DISCUSSION

4.1. INTRODUCTION

This chapter presents the findings of the experimental work described in Chapter 3. This chapter will discuss the results from the investigation of various parameters, including the effect of FA addition, the effect of lime addition, and the effect of $Al(OH)_3$ on the removal of SO_4^{2-} from Eyethu mine water (EMW). This chapter will also explain the chemistry of the removal of some toxic metals such as Fe, Ca, Al, Na, Mn and Mg from EMW when neutralised with LFA and KFA, and some chemical reagents. The fate of the solid residue generated after mine water treatment will also be addressed.

4.2. CHARACTERISATION OF RAW MATERIAL

Different characterisation techniques were done on FA and mine water as described in section 3.9.

4.2.1. Characterisation of Lethabo and Kendal FA

The FA used in this experimental work was collected from two different power stations, which are Lethabo and Kendal power plants. The location of these two stations is given in section 3.4. The FA was name after the collection site. Figure 4.1 shows the characterisation of LFA and KFA using XRD for mineralogical determination as explained in section 3.9.1.

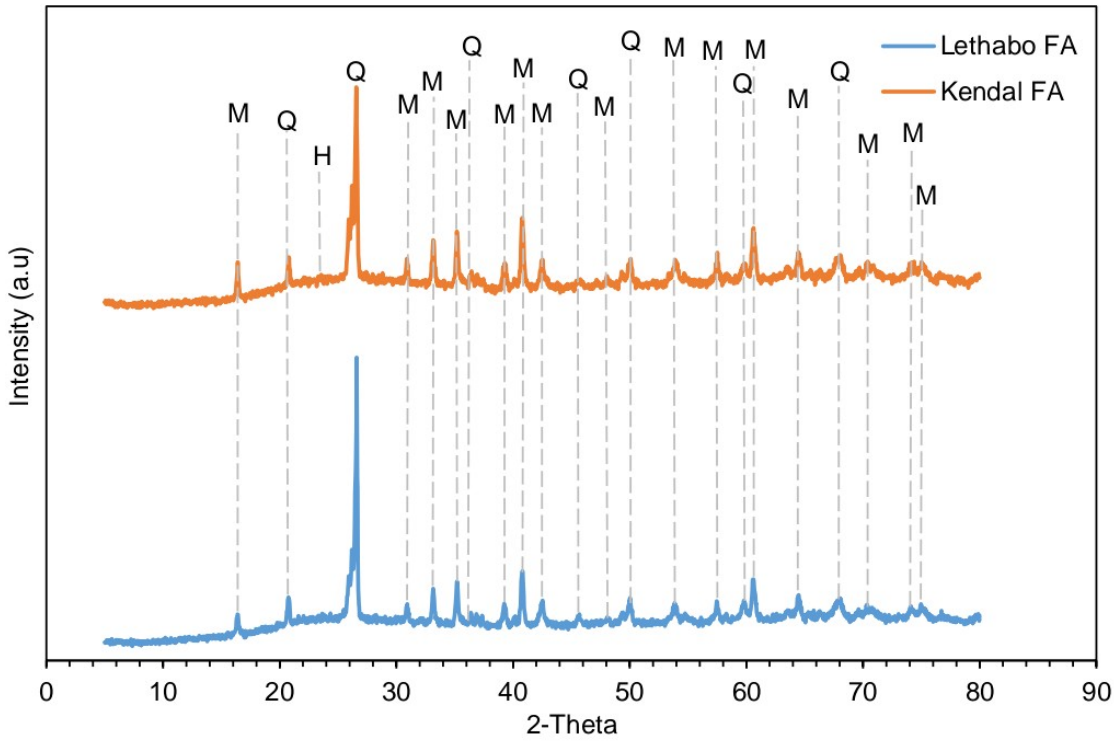

Figure 4.1: XRD spectrum depicting the mineralogical composition of Lethabo and Kendal FA (Q-quartz; M-mullite; H-hematite; Ma-maghemite).

According to the XRD data, both Lethabo FA (LFA) and Kendal FA (KFA) were mainly made up of quartz (SiO_2) and mullite ($Al_2Si_2O_{13}$) as major mineral phases. Low intensity peaks of hematite and maghemite were also visible in Kendal FA as shown in Figure A-1b in appendix A, but these elements were quite difficult to represent on the plotted graph.

XFR and ICP-OES results for elemental composition and traces elements are respectively presented in Table 4.1. Based on the classification by ASTM C618-12, the composition of both LFA and KFA after XRF analysis showed that both FAs were Class F with the sum of their major oxides (SiO_2 + Fe_2O_3 + Al_2O_3) being ≥70% (ASTM C618-12, 1993). Class F FA possesses pozzolanic properties, which means it hardens when reacting with $Ca(OH)_2$ and water (Wang and Wu, 2006; Gitari et al., 2008a; Ahmaruzzaman, 2010).

Table 4.1: Elemental composition of Lethabo FA (LFA) and Kendal FA (KFA) analysis by XRF and ICP-OES

Major oxide			Trace element		
% w/w	LFA	KFA	Element (mg/L)	LFA	KFA
SiO_2	56.71	53.06	Ag	ND	0.4
Al_2O_3	29.22	30.53	As	6.3	10.0
CaO	4.59	5.75	Be	1.5	6.8
Fe_2O_3	3.38	4.77	Bi	ND	10.3
TiO_2	1.54	1.63	Cd	1.3	10.3
MgO	1.17	1.55	Co	3.9	21.2
K_2O	0.78	0.69	Cu	13.9	39.0
Na_2O	0.33	0.16	Ge	ND	0.3
P_2O_5	0.35	0.48	Mn	92.4	313.0
MnO	0.03	0.04	Ni	9.8	50.0
Cr_2O_3	0.04	0.03	Pb	20.2	117.1
V_2O_5	0.02	0.01	Re	ND	0.1
LOI	0.86	1.33	S	1079.2	1177.0
Total	**99.02**	**100.05**	Sb	ND	9.1
			Sc	6.0	16,.6
			Se	5.0	6.0
			Sr	941.0	1486.0
			Th	29.0	34.2
			V	152.2	129.1
			Y	15.7	60.4
			Zn	9.7	26.2

ND stands for not detectable

Lethabo and Kendal FA were found to contain 4.59 % and 5.75 % of CaO respectively. Treatment of mine water using FA takes advantage of the lime presents in the FA. Lime is responsible for the alkaline property of FA. The total CaO content does not differentiate the free lime from the lime trapped within the glass matrix after the XRF analysis. Free CaO content is essential, according to Gitari et al. (2003), since it dissolves into the solution faster than CaO contained within the glass matrix, influencing the pH of the resulting process water (Gitari et al., 2006). Trace element analysis showed that Lethabo and Kendal FA contained 17 and 22 elements respectively. Different research have shown how FA can be useful for various applications such as bricks (Li and Lin, 2002), concrete (Tkaczewska et al., 2012), cement additive (Chindaprasirt and Rattanasak, 2010), geopolymer synthesis (Kalombe et al., 2020b), soil ameliorant (Al Bakri et al., 2012), and zeolite synthesis (Musyoka et al., 2012), etc. The presence of Th among the trace element may cause a problem in the reuse of the FA and to radioactive emissions from thoron gas. For the current study, FA was used to neutralise mine water. And the reuse of FA (SR) after treatment is mainly focused for backfill application.

4.2.2. Characterisation of Eyethu mine water

The IC and ICP-OES results of Eyethu mine water are tabulated in Table 4.2. The pH of Eyethu mine water was found to be around 2.0 as presented in Table 4.2. This means that mine water from Eyethu coalmine is acidic.

Table 4.2: Physicochemical parameters of Eyethu mine water

	Eyethu mine water			TWQR	
Parameter	**AMD 1**	**AMD 2**	**AMD 3**	**Domestic water limits**	**Irrigation water**
pH	2.00	2.00	2.10	6.0 - 9.0	6.5 - 8.4
EC (mS/cm)	4.92	4.94	5.97	0 - 0.7	0 - 0.4
TDS (mg/L of $CaCO_3$)	2460.0	2470.0	2980.0	0 - 600 (0 - 450)	0 - 2.6
Element (mg/L)					
Sulphate	2680.00	2006.28	2179.61	0 - 500.	NL
Al	120.00	132.25	165.88	0 - 0.2 (0 - 0.15)	0 - 5.0
As	2.41	0.09	0.02	0 - 0.001	0 - 0.1
Ba	0.20	0.03	0.05	0 - 0.7	NL
Ca	219.60	442.75	512.26	0 - 32	NL
Cd	< 0.005	0.06	0.01	0 -0.003 (0 - 0.005)	0 - 0.01
Chloride	15.38	21.44	16.90	0 - 250 (0 - 100)	0 – 100
Co	1.62	2.67	3.31	NA	0 - 0.05
Cr	< 0.005	0.03	0.32	0 - 0.05	0 - 0.1
Cu	0.05	0.03	0.83	0 - 2 (0 - 1)	0 - 0.2
Fe	209.81	216.07	236.70	0 - 0.3 (0 - 0.1)	0 - 5.0
K	11.14	12.65	13.87	0 - 50	NL
Mg	256.11	242.99	296.37	0 - 30	NL
Mn	62.84	65.59	80.56	0 - 0.1 (0 -0.05)	0 - 0.02
Mo	< 0.005	< 0.019	< -0.002	0 - 0.07	0 - 0.01
Na	44.62	53.93	68.65	0 - 200	0 - 70.0

Note: NA stands for "not available"; NL denotes for "no limits specified"; min: minutes. The unit for parameters is in mg/L, except pH, which is unit less and EC in mS/cm. The TWQR values in brackets are from the DWAF of South Africa if the values are different from those given by the World Health Organisation (DWAF, 1996a, 1996c; WHO, 2011).

When compared to AMD used in previous studies, the AMD provided for this study had a reduced Al and Fe concentration, as well as a lower SO_4^{2-} concentration (Gitari et al., 2003, 2006, 2008b; Vadapalli et al., 2008). The mine water has a high concentration of Ca and Mg, indicating that it was impacted by dolomitic mineralogy (Madzivire et al., 2009). Furthermore, seasonal and other fluctuations in the composition of AMD were detected every time a new batch of water was delivered on the treatment site (Table 4.2). The use of FA to treat AMD takes advantage of the CaO present in FA, which is required for the neutralisation to take

place, thus, removing SO_4^{2-} and other contaminants found in AMD. Results in Table 4.2 are duplicated results.

SO_4^{2-} concentration in Eyethu AMD (EAMD) was above the TWQR required for domestic water set by DWAF and WHO. According to Madzivire (2012a), when water contains a high concentration of SO_4^{2-} ions, it has a taste. This varies depending on the cation that is connected to SO_4^{2-} ions. It was reported that the taste threshold for water containing SO_4^{2-} coupled with Ca ions is around 1000 mg/L, as in the case of Eyethu AMD. The taste threshold is 250 mg/L if the water contains SO_4^{2-} that is associated with Na ions (WHO, 2011). The pH of Eyethu AMD was extremely low, making it unfit for agricultural, industrial, or domestic application.

4.3. TREATMENT OF EYETHU ACID MINE DRAINAGE

Eyethu AMD (EAMD), Lethabo FA (LFA) and Kendal FA (KFA) characterisation results are presented under section (4.2). High concentration of elements such as SO_4^{2-}, Ca, Mg, and Mn was reported in EAMD, the concentration of these elements was not within the required TWQR for domestic water as depicted in Table 4.2. It was observed that both LFA and KFA were mainly made up of mullite ($Al_6Si_2O_{13}$) and quartz (SiO_2) as shown in Figure 4.1.

Findings by Madzivire et al. (2015) recommended that treatment of mine water with FA combined with lime and $Al(OH)_3$ should be scaled up from 80 L pilot plant capacity to 1000 L pilot plant capacity using jet loop reactors. To generate more data and demonstrate the technology, EAMD, LFA and KFA were selected for the current study. It must be noted that the first experiment at 1000 L pilot plant capacity was done with Lancaster AMD and Malta FA (Kalombe et al., 2020a). For the current study, the first experiment conducted at 1000 L pilot plant capacity was carried out using the optimal conditions found at 80 L pilot plant capacity by Madzivire et al. (2015). These conditions included neutralising mine water with FA at a 5:1 liquid to solid ratio (L/S), then adding 0.25% lime (w/v %) and reacting for 150 minutes to raise the pH of the mixture above 11. After 150 min, 3.6 kg of $Al(OH)_3$ was added to the mixture, and this was mixed and circulated through the jet loop reactor up to 180 min. The results obtained are presented in Table 4.3. Data in Table 4.3 have been published by Kalombe et al. (2020a).

Table 4.3: pH, ICP-OES and IC results of AMD before and after treatment with FA, lime and $Al(OH)_3$ at 1000 L jet loop reactors pilot plant capacity (Kalombe et al., 2020a)

Parameter	Raw AMD	Treated AMD					
Time (min)	**0**	**30**	**60**	**90**	**120**	**150**	**180**
pH	2.26*	10.10*	9.90*	9.90*	9.70*	10.50*	8.80*
Element (mg/L)							
Sulphate	5680.33*	92.77*	90.99*	85.01*	92.28*	83.37*	87.27*
Al	1862.51*	26.07*	21.20*	10.18*	2.68*	1.30*	13.37*
As	ND*	0.36*	0.48*	1.41*	0.11*	0.93*	0.55*
Ca	1694.55*	305.13*	250.56*	228.48*	253.02*	248.77*	242.77*
Cd	1.50*	0.07*	0.06*	0.08*	0.04*	0.08*	0.03*
Co	30.55*	ND*	ND*	ND*	ND*	ND*	ND*
Cu	23.74*	ND*	ND*	ND*	ND*	ND*	ND*
Cr	1.03	1.01*	1.78*	0.98*	1.28*	1.12*	1.27*
Fe	1377.74*	1.38*	0.43*	0.77*	0.11*	0.08*	0.54*
K	51.27*	3.49*	ND*	ND*	ND*	ND*	ND*
Li	ND*	0.82*	0.61*	0.67*	0.69*	0.56*	ND*
Mg	765.62*	0.33*	0.04*	0.07*	0.07*	0.27*	0.05*
Mn	224.44*	0.01*	ND*	0.01*	0.06*	0.07*	0.05*
Mo	ND*	1.26*	0.35*	0.63*	1.31*	1.16*	0.84*
Na	463.35*	73.07*	70.02*	71.46*	71.94*	71.26*	86.46*
Ni	79.62*	0.64*	0.47*	0.48*	0.89*	0.39*	ND*
P	ND*	1.39*	1.16*	0.36*	0.46*	0.01*	0.66*
Pb	16.55	1.18*	0.70*	1.07*	0.34*	1.66*	1.49*
Se	ND*	ND*	ND*	ND*	ND*	0.80*	ND*
Si	482.22*	16.96*	17.03*	17.53*	17.54*	21.26*	16.60*
Sr	3.43*	4.90*	4.08*	6.33*	7.52*	9.04*	7.16*
Ti	4.80*	ND*	ND*	ND*	ND*	ND*	ND*
Zn	154.59*	0.57*	0.08*	0.18*	ND*	ND*	ND*

Note: ND: no detected, min: minutes. The unit for parameters is in mg/L, except pH, which is unit less. (*) indicates data published.

Results in Table 4.3 showed that although the pH of the mine water was not elevated to above pH 11; 98.5% removal in SO_4^{2-} was achieved. It has been reported that SO_4^{2-} concentration is controlled by gypsum precipitation at lower pH and ettringite precipitation at higher pH with other species present in the water (O'Brien, 2000; Surrender, 2009). The AMD (LAMD) was rich in Fe and Al. Addition of $Al(OH)_3$ after 150 min to the mixture did not enhance the removal of SO_4^{2-} and other species from the mine water. Most of the contaminants in the mine water were significantly reduced during treatment of AMD with FA and lime after the first 30 min. The formation of amorphous phases is responsible for aluminium concentration decreasing (Vadapalli et al., 2008). It was discovered that when the pH of the solution increased, the concentration of SO_4^{2-} decreased, indicating that SO_4^{2-} was removed due to the formation and/or precipitation of a secondary mineral phase such as gypsum. (Gitari et al., 2006;

Vadapalli et al., 2008). Many minerals are associated with this phenomenon, one of these being gypsum, which is reported to be formed through CaO dissolution, present in FA and the lime added. However, Fe^{2+} oxidation is optimum at pH >6 and the precipitation of iron hydroxides, with the hydrolysis of the Fe^{3+} which resulted in the formation of amorphous $Fe(OH)_3$ are known to adsorb high concentration of SO_4^{2-} due to their large surface area (Gitari et al., 2008a; Vadapalli et al., 2008). According to Vadapalli et al. (2008), the formation of minerals such as $BaSO_4$ and $SrSO_4$ which are caused by Ba and Sr salts dissolution from FA and their interaction with SO_4^{2-} is another cause of the reduction of SO_4^{2-} content.

4.3.1. Treatment of Eyethu AMD with Lethabo FA

This section will present the results obtain during treatment of EAMD with LFA. This consisted of the optimisation of LFA amount that is needed to elevate the pH of the water, so that the amount of lime and $Al(OH)_3$ required to further remove SO_4^{2-} could be kept at a minimum.

4.3.1.1. Effect of adding Lethabo FA only to Eyethu AMD

The first set of experiments consisted of neutralising EAMD using LFA only, so as the optimum amount of LFA could be determined. EAMD was reacted with different amount of LFA using a L/S ratio of 7:1 (1000 L of AMD and 143 kg of FA), 6:1 (1000 L of AMD and 167 kg of FA) and 5:1 (1000 L of AMD and 200 kg of FA) at 1000 L jet loop reactor pilot plant capacity as presented in section (3.6). The pH and electrical conductivity (EC) trends during neutralisation of EAMD with LFA (143 kg, 167 kg or 200 kg) are illustrated in Figure 4.2.

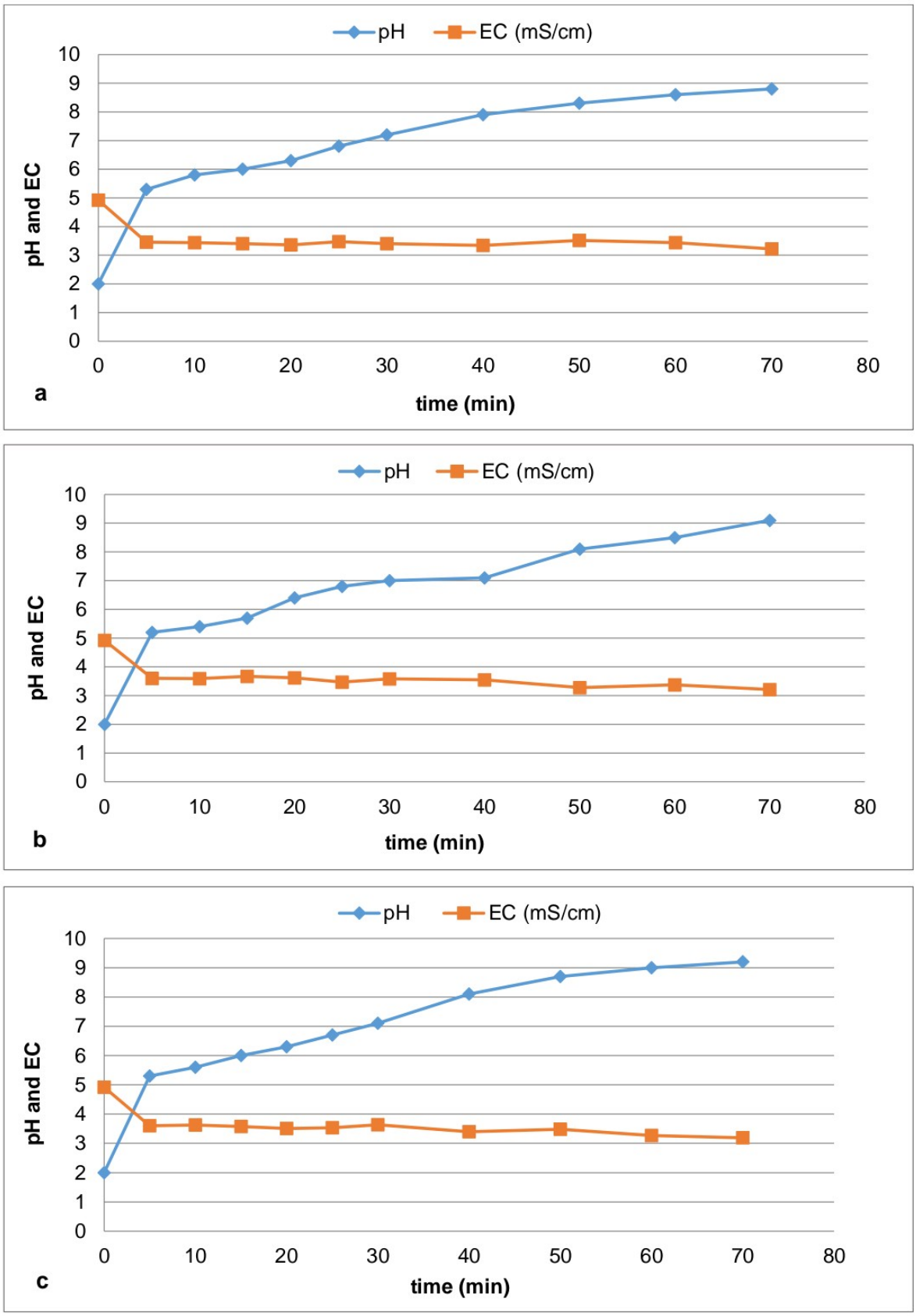

Figure 4.2: pH and EC profile during the treatment of 1000L Eyethu AMD with Lethabo FA (143 kg (a), 167kg (b) and 200 kg (c)).

When EAMD (1000 L) was treated with 143 kg, 167 kg or 200 kg of LFA, a rapid increase in pH was observed after the first 5 min, and then started to increase gradually (Figure 4.2). After 30 min of mixing EAMD with LFA, the water pH increased from 2.0 to 7.2, 7.0 and 7.1 for the mixture containing 143 kg, 167 kg or 200 kg of LFA respectively. The increase in pH during treatment of EAMD with LFA was due to the dissolution of CaO present in LFA as shown by Eq. (2.20). When using FA to treat AMD, the experiments were stop at 70 min in most cases, because the change in pH values of the solution was observed to be almost constant. In both cases EC slightly decreased first and then remain almost constant throughout the neutralisation period.

According to Gitari et al. (2008b), two factors are known to dictate the nature of the final solution during the treatment of mine water with FA, which are: (a) AMD: FA ratio and (b) contact time. For this study, the contact time was kept at the lowest for both ratios compared to previous studies by Petrik et al. (2003), Gitari et al. (2008b) and Madzivire et al. (2015). It was observed that the difference in pH values was not major even when more FA was added; since addition of more FA is synonymous with more CaO being made available for dissolution, the lower contact time could have altered the dissolution of more CaO as more FA was added. When 1000 L of EAMD was mixed with 143 kg of LFA, the pH increased from 2.0 to 8.8 after 70 min (Figure 4.2a). When the amount of FA was increased to 167 kg, a slight increase in pH was observed, after 70 min of mixing this reached a pH value of 9.1 (Figure 4.2b). As the amount of LFA was further increased to 200 kg, a pH of 9.2 was recorded after 70 min of mixing EAMD and LFA as shown in Figure 4.2c.

During treatment of 1000 L of EAMD with 143 kg, 167 kg or 200 kg of LFA, samples were collected after every 20 min. The collected samples were filtered using a 0.45 µm membrane filter paper prior to analysis using IC and ICP-OES for anions and cations respectively. The results of the analysed samples obtained are depicted in Figure 4.3.

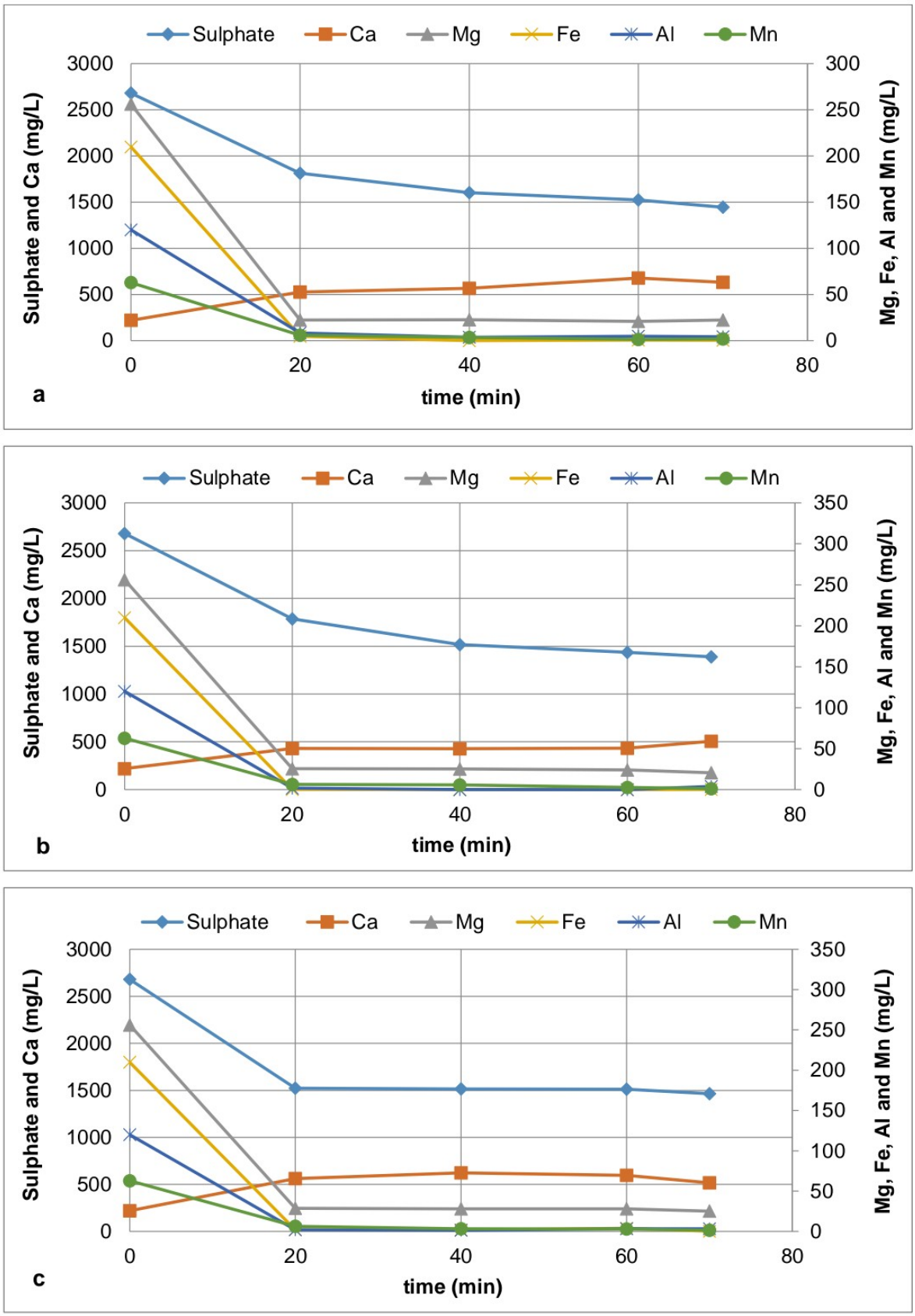

Figure 4.3: Sulphate, Ca, Mg, Fe, Al and Mn concentrations during neutralisation of EAMD (1000 L) with 143 kg (a), 167 kg (b) or 200 kg (c) of LFA.

The results in Figure 4.3a show that treatment of EAMD (1000 L) with LFA (143 kg) only resulted in SO_4^{2-} concentration decreasing from 2680.00 mg/L to 1813.23 mg/L after the first 20 min of mixing in the JLR. After 50 min of mixing (up to 70 min), the concentration of SO_4^{2-} further decreased to 1444.18 mg/L. Ca ion concentration during the first 20 min of treating EAMD with 143 kg of LFA increased from 219.60 mg/L to 527.00 mg/L as shown in Figure 4.3a. CaO dissolution in the mine water from LFA caused an increase in Ca content, which caused the pH of the water to increase. After 50 min of mixing (up to 70 min), the concentration of Ca increased to 631.10 mg/L in the solution.

When 1000 L of EAMD was reacted with 167 kg of LFA, it was observed that SO_4^{2-} concentration decreased from 2680.00 mg/L to 1785.74 mg/L after the first 20 min, whereas the Ca concentration increased from 219.60 mg/L to 430.44 mg/L. After 50 min of mixing (up to 70 min), the concentration of SO_4^{2-} further decreased to 1389.22 mg/L (Figure 4.3b), that of Ca increased to 505.71 mg/L. The addition of more FA resulted in more SO_4^{2-} being removed from the AMD compared to when 143 kg of LFA was used (Figure 4.3a).

Treatment of EAMD (1000 L) with 200 kg of LFA resulted in the concentration SO_4^{2-} decreasing from 2680.00 mg/L to 1523.94 mg/L after the first 20 min of mixing as shown in Figure 4.3c, this further decreased to 1464.54 mg/L after a further 50 min of mixing (up to 70 min). The kinetics of the removal of SO_4^{2-} should have increased with the addition of more FA, but this was not the case when more FA was added. Although the addition of more FA means that more CaO was made available for dissolution, this did not result in more SO_4^{2-} being removed from the mine water. This could be ascribed to the fact that the contact time was not enough for more CaO to dissolve, thus increasing the rate of SO_4^{2-} removal and elevating mine water pH. The dissolution of CaO from LFA resulted in Ca content increasing from 219.60 mg/L to 561.78 mg/L after the first 20 min of mixing in the JLR. Then, it decreased to 516.63 mg/L after a further mixing of about 50 min (up to 70 min on stream).

Treatment of EAMD with LFA only resulted in significant removal of heavy metals such as Mg, Fe, Al and Mn. The concentration of Mg was reduced to within the TWQR for potable after the first 20 min of mixing EAMD (1000 L) with 143 kg of LFA as this decreased from 256.11 mg/L to 22.25 mg/L. Then it remained more of the same at 22.34 mg/L after 50 min of mixing (Figure 4.3a). Fe was removed to zero after 40 min of mixing from an initial concentration of 209.81 mg/L, and then slightly increased to 0.52 mg/L after a further 30 min of mixing (up to 70 min). The concentration of Al and Mn decreased from 120.00 mg/L and 62.84 mg/L to 4.28 mg/L and 1.83 mg/L respectively after 70 min (Figure 4.3a). When EAMD (1000 L) was treated with LFA (167 kg), the concentration of Mg and Fe was within the TWQR required by WHO and

DWAF for domestic water use after the first 20 min of mixing. After a further 40 min (up to 60 min), the concentration of Fe and Al significantly decreased to 0.01 mg/L and 0.08 mg/L respectively when the pH of the water increased to ≥ 7. The concentration of Mn decreased from 62.84 mg/L to 1.1 mg/L after 70 min of mixing (Figure 4.3b). When 200 kg of LFA was used to neutralise EAMD (1000 L), it was observed that Mg and Fe concentrations were within the TWQR after 70 min of mixing at 25.08 mg/L and 0.22 mg/L down from 256.11 mg/L and 209.81 mg/L respectively. After the first 20 min, only Mg concentration (28 mg/L) was within the TWQR limits. The concentration Al and Mn was not within the TWQR for domestic water throughout the treatment of EAMD with 200 kg of LFA (Figure 4.3c). Madzivire (2012) and Gitari et al. (2008a) stated that toxic element such as Fe and Al are well known to precipitate out of the water around pH ≥3; while the optimum precipitation of Mg and Mn occurs around pH ≥10 and ≥9 respectively due to their respective hydroxides being formed according to Eqs (2.15 - 2.18). The precipitation of metal pollutants is generalised by Eq. (2.22).

Treatment of EAMD with 143 kg, 167 kg, or 200 kg of LFA has shown that toxic elements like Mg, Fe, Al, and Mn can be removed to the lowest concentration possible, with some of these metals being removed by nearly 100%. SO_4^{2-} content remaining in water was in the range of 1300 mg/L - 1500 mg/L. SO_4^{2-} removal from EAMD during the treatment with LFA (143 kg, 167 kg or 200 kg), could have been limited by gypsum solubility and low concentration of Al in EAMD to form ettringite. This can be explained by the pH of the water, which was below pH 11.5. SO_4^{2-} is reported to be stable at pH range of 11.5 – 12.5 (Mynemi et al., 1998; Madzivire et al., 2015). The addition of lime was thus deemed necessary, thus, increasing the pH of the water, and resulting in the removal of more SO_4^{2-} from the mine water, which will be addressed in the next section.

After treatment of EAMD with LFA using different L/S ratios (7:1, 6:1 and 5:1), the highest percentage in cleaning up of the mine water with respect to different elements (SO_4^{2-}, Fe, Mg, Al, and Mn) was observed at the AMD:FA ratio of 6:1. This ratio was selected as the optimum ratio and will be used in the next stage when investigating the addition of lime to the treatment process.

4.3.1.2. Effect of adding lime to the mixture of Eyethu AMD and Lethabo FA

The second set of experiments investigated the effect of lime addition to the treatment process involving EAMD and LFA. 1000 L of EAMD was treated with 167 kg of LFA for about 70 min. After 70 min, 0.5 kg, 1.0 kg or 1.5 kg of lime was added respectively to each mixture of AMD and FA, samples were collected after every 20 - 30 min and these were analysed using IC

and ICP-OES. During the treatment of EAMD with LFA and lime, the pH and EC of the mine water were recorded every 10 min; and results are illustrated in Figure 4.4.

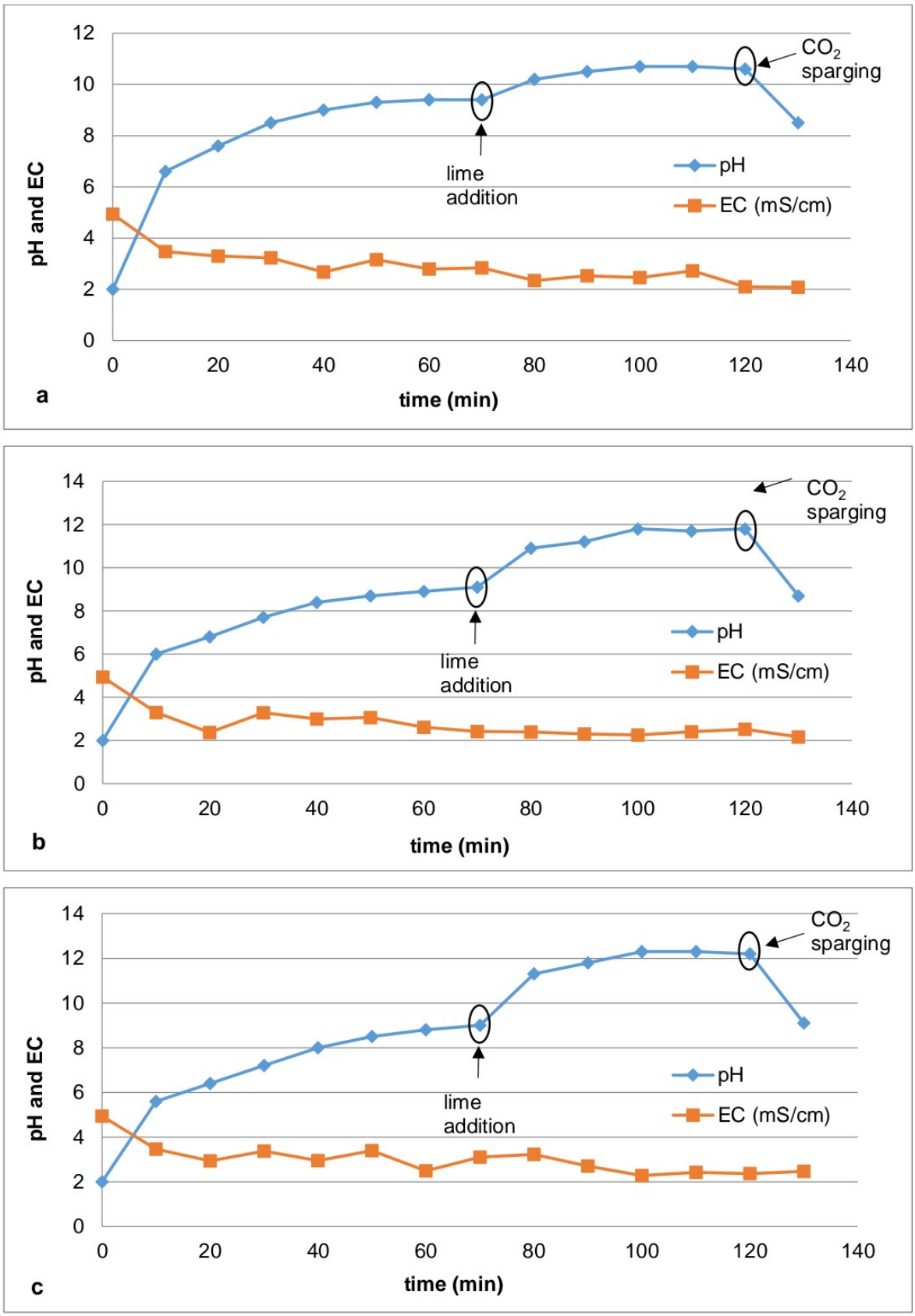

Figure 4.4: pH and EC profile during treatment of 1000 L of EAMD with 167 kg of LFA, and 0.5 kg (a), 1.0 kg (b) or 1.5 kg (c) of lime.

The results in Figure 4.4 show that the pH of AMD increased when lime was added to the mixture of EAMD and LFA. For all cases as shown in Figure 4.4, EAMD (1000 L) was first treated with LFA (167 kg) for about 70 min while monitoring the pH, since the process is a pH-controlled system. The addition of lime was retarded so that the behaviour of FA with the mine water could first be investigated to see how this would affect the change in pH. However, it was observed that the pH value did not change; it stayed at approximately pH 9, same as in Figure 4.2b.

Treatment of EAMD (1000 L) with LFA (167 kg) for about 70 min, resulted in the pH increasing from 2.0 to 9.4 (Figure 4.4a). After 70 min of stirring and circulating through the jet loop reactors, 0.5 kg of lime was added to the mixture of EAMD (1000 L) and LFA (167 kg). After adding lime, the new mixture of EAMD (1000 L), LFA (167 kg) and lime (0.5 kg) was first stirred using the agitator only for about 20 min (up to 90 min) at a speed of 50 rpm, without circulating it through the jet loop reactors. After 20 min of stirring (up to 90 min), the pH of the water increased to 10.5, and then the mixture was stirred and mixed through the jet loop reactors. After 10 min of mixing in the jet loop reactors, the pH of the water slightly increased to 10.7 (up to 100 min), and then remained constant after further mixing for about 20 min (up to 120 min) (Figure 4.4a). Treatment of EAMD (1000 L) with LFA (167 kg) and Lime (0.5 kg) resulted in the pH of water increasing from 2.0 to 10.7 after 120 min of mixing. As shown in Figure 4.4a, the EC of the water was fluctuating. EC decreased from 4.94 mS/cm to 2.10 mS/cm after 120 min. then slightly decrease to 2.08 mS/cm after 10 min of carbonation (up to 130 min).

When EAMD was mixed with LFA, the water pH increased from 2.0 to 9.1 and 9.0 before adding 1.0 kg or 1.5 kg of lime respectively. After 70 min, lime (1.0 kg or 1.5 kg) was added to the mixtures of EAMD (1000 L) and LFA (167 kg), and then these mixtures (AMD+FA+lime) were stirred for about 20 min (up to 90 min), this resulted in pH increasing to 11.2 and 11.8 respectively. After 10 min of stirring and mixing in the jet loop reactor, the pH further increased to 11.8 and 12.3 for the mixture containing 1.0 kg (Figure 4.4b) or 1.5 kg (Figure 4.4c) of lime respectively (up to 100 min). Further mixing of the solution up to 120 min did not result in elevating the pH, for the mixture containing 1.0 kg of lime the pH remained constant at 11.8 (Figure 4.4b) and for the mixture containing 1.5 kg of lime the pH slightly decreased to 12.2 (Figure 4.4c). It was observed that as more lime was added, it resulted in the pH of the solutions increasing, meaning that more CaO was made available for dissolution, thus, elevating the pH of the mixture to more alkaline regions. Figure 4.4b shows how the EC fluctuated during the first 60 min, then remained almost constant after adding 1.0 kg of lime. In Figure 4.6c, the EC fluctuated throughout the duration of the experiment. The EC decreased

from 4.94 to 2.10 mS/cm or 2.47 mS/cm for the mixtures containing 1.0 kg or 1.5 kg of lime respectively.

Treatment of EAMD (1000) with LFA (167 kg) and 0.5 kg, 1.0 kg, or 1.5 kg of lime, resulted in the pH of the mixtures increasing from 2.0 to 10.7, 11.8 or 12.3 respectively after 120 min of stirring and jet loop mixing. It was observed that the pH of the product water was above the TWQR required for domestic water as tabulated in Table 4.2. The pH of the water was reduced by sparging CO_2 into the recovered water. Sparging occurred after separating the recovered water from the solid residues (the separation process took about 14 min). After 10 min of carbonation (from 120 to 130 min as shown on Figure 4.4), the pH of the treated water recovered was reduced to 8.5, 8.7 and 9.1 respectively after treatment of EAMD (1000 L) with LFA (167 kg) and 0.5 kg, 1.0 kg or 1.5 kg of lime (Figure 4.4). As a result, the pH of the water recovered was within WHO and DWAF's TWQR standards for domestic water use.

Samples collected during treatment of EAMD (1000 L) with LFA (167 kg) and lime (0.5 kg, 1.0 kg or 1.5 kg) were filtered through a 0.45 µm filter paper and the filtrates were analysed using IC and ICP-OES. Figure 4.5 depicts the outcomes from the analyses.

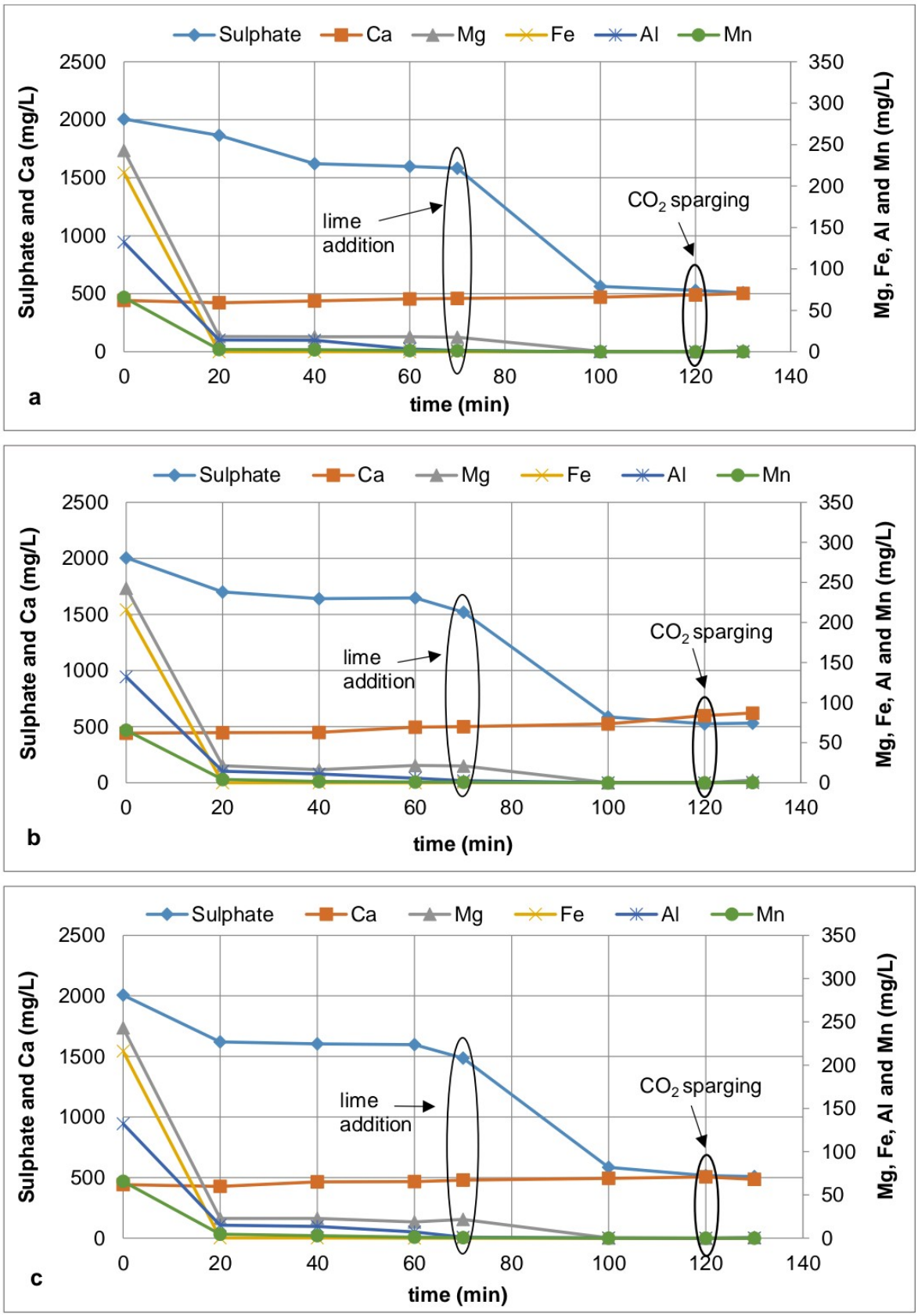

Figure 4.5: Sulphate, Ca, Mg, Fe, Al and Mn concentration during treatment of Eyethu AMD (1000 L) with 167 kg of Lethabo FA and 0.5 kg (a), 1.0 kg (b) or 1.5 kg (c) of lime.

Results in Figure 4.5 showed that, when EAMD (1000 L) was treated with 167 kg of LFA and lime (0.5 kg, 1.0 kg or 1.5 kg) the concentration of metals such as Mg, Fe, Al and Mn was significantly reduced, with some of them being removed by almost 100%. Treatment of EAMD (1000 L) with LFA (167 kg) and 0.5 kg of lime, resulted in the concentration of Mg, Fe, Al and Mn decreasing from 242.99 mg/L, 216.07 mg/L, 132.25 mg/L and 65.59 mg/L to 0.09 mg/L, 0.001 mg/L, 0.01 mg/L and 0.01 mg/L respectively up to 120 min. Therefore, the concentration of these elements was within the TWQR required for domestic water use. It was observed that, as the pH was increasing the concentration of these elements was decreasing, therefore confirming what is reported in literature (Gitari et al., 2006, 2008a, 2010; Madzivire et al., 2010b, 2015) that the removal of these elements is pH dependent. The concentration of Mg, Fe, Al and Mn increased slightly after 10 min (up to 130 min) of carbonation using CO_2 to lower water pH, the concentration of these elements was 1.17 mg/L, 0.09 mg/L, 0.34 mg/L and 0.07 mg/L respectively as shown in Figure 4.5a. Sparging of CO_2 in the recovered water resulted in most metals concentration slightly increasing, with that of Al rising above the TWQR limits required for domestic water use (Table 4.2); at 0.34 mg/L.

Mg, Fe, Al and Mn concentrations during the treatment of EAMD with LFA (167 kg) and 1.0 kg or 1.5 kg of lime was significantly reduced. These elements were reduced to 0.03 mg/L, 0.01 mg/L, 0.05 mg/L and 0.01 mg/L after adding 1.0 kg of lime (Figure 4.5b), and 0.01 mg/L, 0.001 mg/L, 0.02 mg/l and 0.01 mg/L after adding 1.5 kg of lime (Figure 4.5c) up to 120 min of stirring and jet loop mixing. As the pH of the mine water increased to above pH 10 the optimum removal of Mg was observed. After carbonation using CO_2, which consisted in decreasing the pH of the water to neutral pH (6 - 9), it was observed that the concentration of Mg, Fe, Al and Mn increased slightly for the mixture containing 1.0 kg or 1.5 kg of lime respectively (Figure 4.5b or 4.5c). After 10 min of carbonation, the concentration of these elements increased to 3.18 mg/L, 0.12 mg/L, 0.17 mg/L and 0.10 mg/L respectively for the mixture containing 1.0 kg of lime (Figure 4.5b). And for the mixture containing 1.5 kg of lime, as shown in Figure 4.5c; Mg, Fe, Al and Mn concentrations increased to 0.91 mg/L, 0.06 mg/L, 0.21 mg/L and 0.02 mg/L respectively. Although there was a slight increase in the concentration of Mg, Fe, Al and Mn for the mixture containing 1.0 kg (Figure 4.5b) or 1.5 kg (Figure 4.5c) of lime after carbonation, these elements were all within the TWQR for domestic water use.

Treatment of EAMD with LFA and different amount of lime has shown that initially Ca ions leached out into the water during the first 70 min of neutralisation with FA only. Then, after 70 min of treating AMD with FA, lime was added, which resulted in more Ca ions leaching out into the mine water. Therefore, causing Ca ions concentration and pH of the water to increase

as shown in Figures 4.5 and 4.4 respectively. For the mixture containing 0.5 kg of lime, Ca concentration increased from 442.76 mg/L to 489.28 mg/L after 120 min of stirring and jet loop mixing. The same trend was observed when 1.0 kg or 1.5 kg of lime was added. Ca concentration increased from 442.76 mg/L to 588.02 mg/L and 505.30 mg/L for the mixtures containing 1.0 kg or 1.5 kg of lime respectively. Before adding lime (0.5 kg, 1.0 kg or 1.5 kg), the concentration of SO_4^{2-} was in the range of 1450 mg/L – 1600 mg/L when EAMD (1000 L) was neutralised with LFA (167 kg) for about 70 min (Figure 4.5). After adding 0.5 kg, 1.0 kg or 1.5 kg of lime, stirred for about 20 min (up to 90 min), then stirred and mixed in jet loop for about 10 min (up to 100 min), the concentration of SO_4^{2-} decreased from 1581.48 mg/L, 1521.74 mg/L and 1486.23 mg/L to 564.45 mg/L (Figure 4.5a), 587.97 mg/L (Figure 4.5b) and 585.05 mg/L (Figure 4.5c) respectively. Further stirring and jet loop mixing for about 20 min (up to 120 min), resulted in the concentration of SO_4^{2-} decreasing to 528.95 mg/L, 525.21 mg/L and 515.92 mg/L respectively for the mixtures containing 0.5 kg of lime (Figure 4.5a), 1.0 kg (Figure 4.5b) or 1.5 kg (Figure 4.5c). The initial SO_4^{2-} concentration in EAMD (AMD 2, Table 4.2) was about 2006.28 mg/L. The decrease in SO_4^{2-} can be attributed to the formation of gypsum and/or ettringite. After 10 min of carbonation (up to 130 min), the concentration of SO_4^{2-} slightly decreased further to 508.9 mg/L and 508.8 mg/L for the mixtures containing 0.5 kg and 1.5 kg of lime as shown in Figures 4.5a and 4.5c respectively, however, for the mixture containing 1.0 kg of lime a slight increase in SO_4^{2-} concentration was observed as this increased to 530.82 mg/L. Lime addition to the mixture of EAMD and LFA enhance the removal of SO_4^{2-}. However, this was still above the TWQR limits for domestic water set by WHO and DWAF (Table 4.2).

The solid residue (SR) recovered after 120 min of treating EAMD (1000 L) with LFA (167 kg) and Lime (1.0 kg) was analysed using XRD by collecting a sample of this. The results obtained are shown in Figure 4.6.

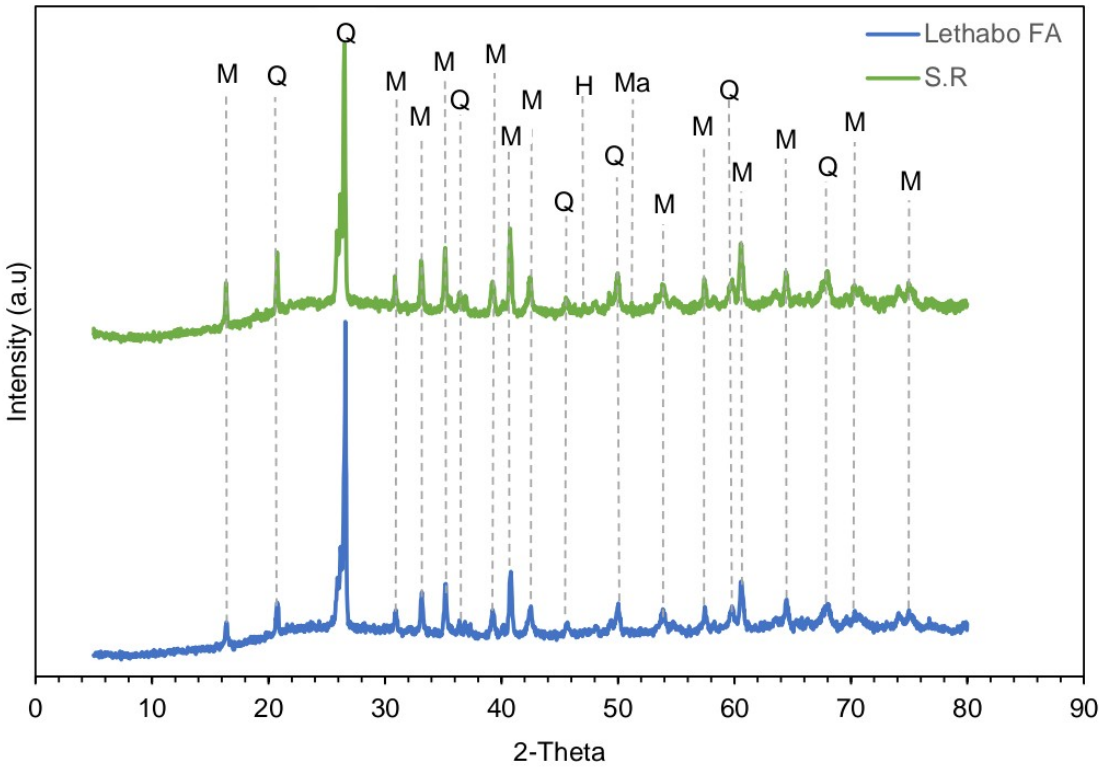

Figure 4.6: XRD spectra of SR recovered after treatment of Eyethu AMD (1000 L) with Lethabo FA (167 kg) and Lime (1.0 kg) compared to fresh Lethabo FA (Q-quartz; M-mullite; Ma-maghemite; H-hematite).

The XRD spectrum of the SR produced after neutralisation of EAMD (1000 L) with LFA (167 kg) and lime (1.0 kg) showed the appearance of maghemite and hematite peaks in the spectrum of the SR as the only new minerals formed. Nor maghemite neither hematite peaks were initially present in the spectrum of fresh Lethabo FA. These two mineral phases were quite difficult to represent on the plotted graph from data obtained. The presence of hematite and maghemite peaks in the SR is due to the precipitation of Fe. Figure A-2a (appendix A) shows maghemite and hematite peaks in the spectrum of the SR clearly. There was not any sign of gypsum or ettringite peaks being formed as new minerals although the decrease in SO_4^{2-} is attributed to those phases forming, however, it is not limited to the formation or precipitation of one or both phases (Gitari et al., 2006; 2008a; Vadapalli et al., 2008). Gitari et al. (2008b) reported that the oxidation of Fe^{2+} is at an optimum at pH >6, therefore, $Fe(OH)_2$ that precipitate out adsorb a high concentration of SO_4^{2-}. As the pH of the water is increasing, this provokes the precipitation of Fe^{3+}, forming amorphous $Fe(OH)_3$ and $FeHO_2$ which have a large surface area, thus, resulting in the adsorption of SO_4^{2-} (Vadapalli et al., 2008). During the neutralisation reaction consisting of AMD and FA, the precipitates formed are mainly amorphous and therefore cannot be detected by XRD (Gitari et al., 2008b).

After treatment of 1000 L of EAMD with 167 kg of LFA and 1.0 kg of lime, a sample of the solid residue generated was collected and analysed using XRF. The results obtained are tabulated in Table 4.4 and compared to the XRF results of fresh LFA.

Table 4.4: Elemental composition of Lethabo FA and SR recovered after treatment of Eyethu AMD (1000 L) with 167 kg of Lethabo FA and 1.0 kg of lime

	Major oxide	
% w/w	**LFA**	**S.R**
SiO_2	56.71	55.80
Al_2O_3	29.22	29.22
CaO	4.59	4.15
Fe_2O_3	3.38	3.47
TiO_2	1.54	1.53
MgO	1.17	1.35
K_2O	0.78	0.75
Na_2O	0.33	0.13
P_2O_5	0.35	0.35
MnO	0.03	0.06
Cr_2O_3	0.04	0.03
V_2O_5	0.02	0.03
LOI	0.86	2.19
Total	**99.02**	**99.07**

From the results obtained after XRF analysis, it was observed that the percentage of the oxides of Mg, Fe and Mn in the SR were higher than in fresh LFA but those of Si, Ca, Ti, K, and Na were slightly lower. The increase of Mg, Fe and Mn in the solid residue in comparison to fresh Lethabo FA was due to the precipitation of these elements from EAMD. This agreed well with the decrease in Mg, Fe and Mn concentrations when EAMD (1000 L) was treated with LFA (167 kg) and lime (1.0 kg) (Figure 4.5b). The decrease in Si, Ca, Ti, K and Na content in the SR was due to these elements leaching out from FA into the water. Al and P content remained constant.

The treatment of EAMD with LFA and various amount of lime has demonstrated that SO_4^{2-} removal from EAMD was dependent on the amount of lime added and the removal of heavy metals such Fe, Mg, Mn and Al was depending on pH. However, even when the amount of lime was increased to 1.5 kg for every 1000 L of AMD, the concentration of SO_4^{2-} in the water remained above the TWQR limits for potable water of 500 mg/L; this was 508.8 mg/L. Consequently, the effect of $Al(OH)_3$ on SO_4^{2+} removal as ettringite was investigated. This was done in order to keep the amount of lime added at a minimum; thus, reducing the concentration of SO_4^{2-} and cleaning up the water in term of toxic elements.

4.3.1.3. Effect of adding $Al(OH)_3$ to the mixture of Eyethu AMD, Lethabo FA and lime

This section deals with the addition of $Al(OH)_3$ to the mixture of EAMD (1000 L), LFA (167 kg) and lime (1.0 kg) in order to reduce SO_4^{2-} to within the TWQR for domestic water use. Eqs 3.1 and 3.2 were used to calculate the amount of $Al(OH)_3$ to be added (section 3.6). This was done based on the amount of SO_4^{2-} remaining in the water after treatment with lime, so that SO_4^{2-} could precipitate as ettringite as shown in Eq. (3.1) in section (3.6). The amount of $Al(OH)_3$ to be added was found to be 0.31 kg.

During treatment of 1000 L of EAMD with 167 kg of LFA, 1.0 kg of lime and 0.31 kg of $Al(OH)_3$, the pH and EC were recorded after every 10 min and the results obtained are depicted in Figure 4.7.

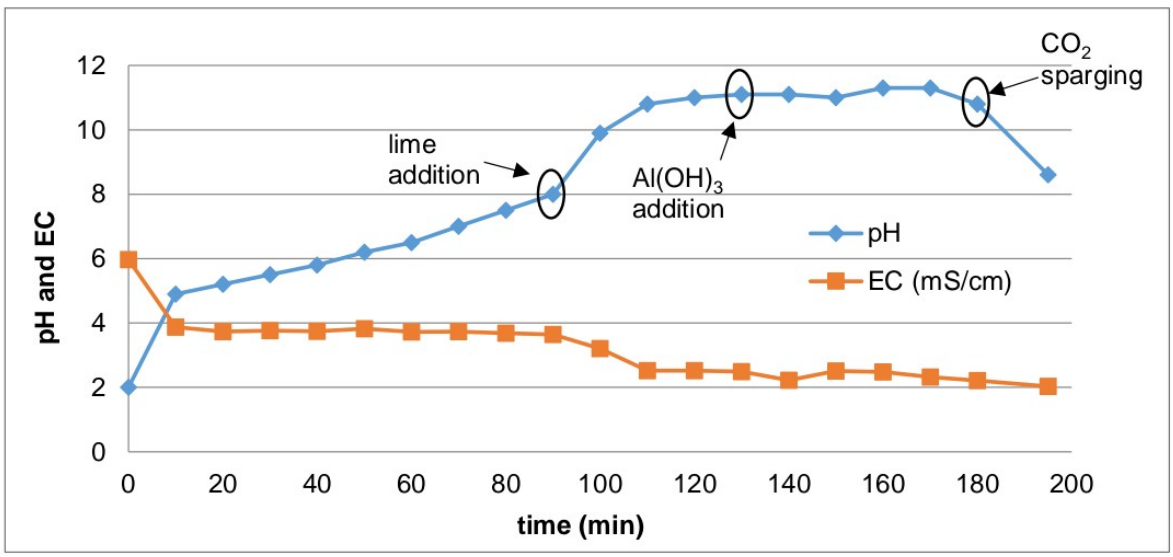

Figure 4.7: pH and EC trend of Eyethu AMD (1000 L) treated with 167 kg of Lethabo FA, 1.0 kg of lime and 0.31 kg of $Al(OH)_3$.

Results in Figure 4.7 show that treatment of EAMD (1000 L) with LFA (167 kg) for about 90 min resulted in the pH increasing from 2.1 to 8.0. After adding lime (1.0 kg), the pH of the mixture increased to 10.8 after 20 min of stirring (up to 110 min), and then the pH increased to 11.1 after a further 20 min of stirring and jet loop mixing (up to 130 min). After 130 min of stirring and jet loop mixing the solution, 0.31 kg of $Al(OH)_3$ was added to the mixture, after adding $Al(OH)_3$ the mixture was first stirred for about 20 min (up to 150 min on stream) this resulted in the pH slightly decreasing to 11.0. Then stirring and jet loop mixing of the mixture of EAMD, LFA, lime and $Al(OH)_3$ for a further 20 min (up to 170 min on stream) resulted in the pH slightly increasing to 11.3. After further mixing for about 10 min (up to 180 min on stream), the pH of the water decreased from 11.3 to 10.8, and then this decreased to 8.6 after 15 min of carbonation using CO_2. Prior to carbonation, the water was separated from the SR.

In the case of EC trends, it was observed that during the first starting 10 min of the treatment the EC decreased from 5.97 to 3.87 mS/cm and then remained almost constant after 80 min (up to 90 min). This slightly decreased, after adding lime, to 2.52 mS/cm. After adding $Al(OH)_3$ (at 130 min) to the mixture, the EC started to gradually decrease. After 195 min of treatment, the EC of the water decreased from 5.97 to 2.03 mS/cm. Although a decrease in the EC was observed, this value was still higher than the EC recommended by the WHO and DWAF for domestic water as given in Table 4.2.

During treatment of EAMD (1000 L) with LFA (167 kg), lime (167 kg) and $Al(OH)_3$ (0.31 kg), sample collection was done after every 20 min. The collected samples were filtered using a 0.45 µm membrane filter paper and analysed using IC and ICP-OES for anions and cations respectively. Figure 4.8 shows the results.

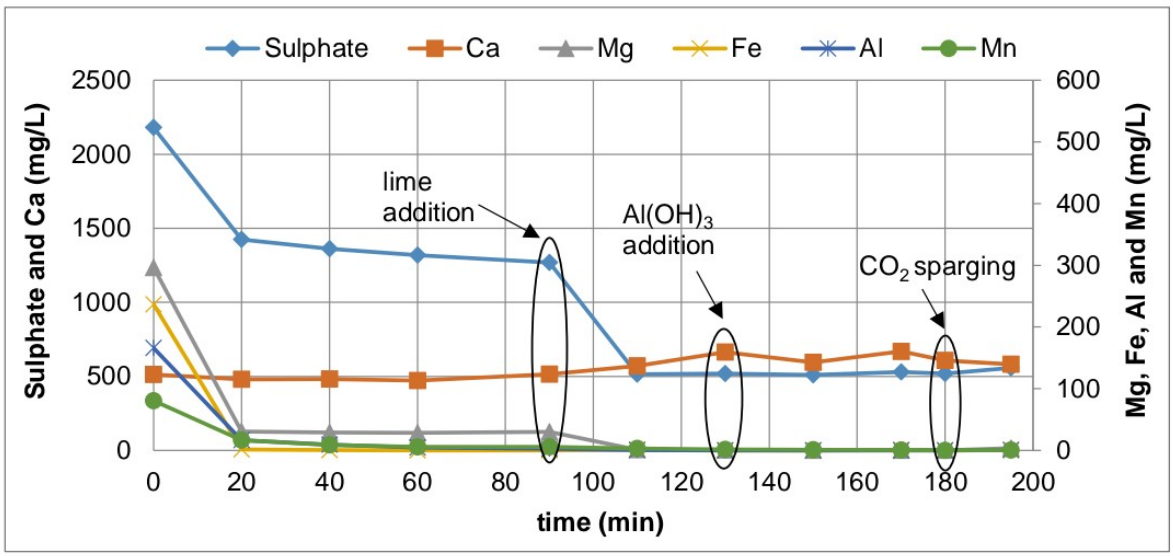

Figure 4.8: Sulphate, Ca, Mg, Fe, Al and Mn concentration during treatment of Eyethu AMD (1000 L) with Lethabo FA (167 kg), lime (1.0 kg) and 0.31 kg of $Al(OH)_3$.

Figure 4.8 showed that during neutralisation of EAMD with LFA (167 kg) for 90 min, SO_4^{2-} concentration decreased from 2179.61 mg/L to 1269.23 mg/L. After 90 min, 1.0 kg of lime was added, the concentration of SO_4^{2-} decreased to 515.33 mg/L after 20 min of stirring (up to 110 min), and then slightly increased to 519.17 mg/L after a further 20 min of stirring and jet loop mixing (up to 130 min). After 130 min of treating EAMD with LFA and lime, 0.31 kg of $Al(OH)_3$ was added to the mixture as the pH was above pH 11, this resulted in SO_4^{2-} concentration decreasing to 509.64 mg/L after 20 min (up to 150 min) of stirring. SO_4^{2-} concentration increased to 528.60 mg/L after a further 20 min of stirring and mixing in the jet loop reactors (up to 170 min). after a further 10 min (up to 180 min) of stirring and jet loop mixing, a slight reduction in SO_4^{2-} concentration was observed, this was reduced to 517.72 mg/L. Smit (1999)

stated that $Al(OH)_3$ addition to the solution causes an insoluble salt known as ettringite ($3CaO.3CaSO4.Al_2O_3.32H_2O$) to form, therefore resulting in the removal of both Ca and SO_4^{2-} from solution as shown in Eq. (3.1) (section 3.6).

The results showed that addition of $Al(OH)_3$ could not enhance the removal of SO_4^{2-} from the solution. SO_4^{2-} removal could have been limited by gypsum solubility (Madzivire et al., 2015). Ettringite formation could have also been limited by low Al concentration in EAMD, since ettringite formation occurs in association with gypsum and $Al(OH)_3$ (Germishuizen et al., 2018). According to Germishuizen et al. (2018), ettringite formation necessitates the presence of Al as the amphoteric species $Al(OH)_4^-$, whereas Al exists largely as amorphous aluminium hydroxide (gibbsite) at pH below 10.3, making ettringite formation pH dependent.

Treatment of EAMD with LFA, lime and $Al(OH)_3$ resulted in Ca concentration increasing from 512.26 mg/L to 608.24 mg/L after 180 min (Figure 4.9). When EAMD (1000 L) was neutralised with 167 kg of LFA, Ca content slightly increased from 512.26 mg/L to 514.68 mg/L after the first 90 min. After adding 1.0 kg of lime, Ca concentration further increased to 570.54 mg/L after 20 min of stirring (up to 110 min), and then increased to 663.07 mg/L after a further 20 min (up to 130 min on stream) of stirring and jet loop mixing. This was due to CaO dissolution after adding more lime to the mixture. Addition of 0.31 kg of $Al(OH)_3$ (at 130 min on stream) resulted in Ca concentration decreasing to 593.79 mg/L after 20 min of stirring (up to 150 min), and then increased to 668.87 mg/L after a further 20 min (up to 170 min on stream) of stirring and jet loop mixing. After a further 10 min (up to 180 min) of stirring and jet loop mixing, Ca concentration decreased to 608.24 mg/L. After 180 min carbonation was started using CO_2 to reduce to water pH, this resulted in a decrease of Ca concentration to 580.69 mg/L down from 608.24 mg/L after 15 min (up to 195 min on stream) of carbonation.

It was assumed that after 20 min (up to 150 min) of stirring when $Al(OH)_3$ was added (at 130 min) most of it was dissolved but it is evident the optimum removal of Al in EAMD already was reached before even extra Al was added to the solution, since this occurs at pH value of >5 (Surrender, 2009). This explained why there was not major or significant decrease in Ca and SO_4^{2-} concentrations. After adding $Al(OH)_3$ to the solution, there was a slight decrease in Ca concentration, the same thing was observed with SO_4^{2-} concentration. When Ca concentration started to increase, SO_4^{2-} concentration also started increasing. This showed that, SO_4^{2-} concentration was dependent on the concentration of Ca, since SO_4^{2-} removal can be a result of different mechanisms, such as initial dissolution of CaO from FA in the presence of AMD.

Results in Figure 4.8 showed that there was a significant decrease in the concentration of heavy metals such Mg, Fe, Al and Mn when EAMD was neutralised with a combination of LFA,

lime and $Al(OH)_3$. During neutralisation of EAMD with FA, only Fe (0.15 mg/L) and Mg (30.31 mg/L) were within the TWQR limits after 90 min. After adding lime (at 90 min), the pH of the solution increased to above 10, as the pH increased, the concentration of these elements was gradually decreasing as illustrated in Figure 4.7 and 4.8 respectively. Mg (0.29 mg/L), Fe (0.00 mg/L) and Al (0.17 mg/L) concentrations were within the TWQR after 130 min of stirring and jet loop mixing. When 0.31 kg of $Al(OH)_3$ was added (at 130 min), this resulted in Mg being removed by almost 100 %, while Fe first decreased and then increased, whereas Al and Mn slightly decreased. After 20 min (up to 170 min) of stirring and jet loop mixing, only Mg and Al were within the TWQR at 0.01 mg/L and 0.17 mg/L respectively. Treatment of EAMD (1000 L) with a combination of LFA (167 kg), lime (1.0 kg) and $Al(OH)_3$ (0.31 kg), resulted in the concentration of Mg, Fe, Al and Mn decreasing from 296.37 mg/L, 236.70 mg/L, 165.88 mg/L and 80.56 mg/L to 0.01 mg/L, 0.10 mg/L, 0.20 mg/L and 0.10 mg/L respectively up to 180 min. The concentration of these elements was within the TWQR required for domestic water use (Table 4.2). After carbonation using CO_2 (started at 180 min), Mg, Fe, Al and Mn concentrations slightly increased. Only Mg (3.80 mg/L) was still within the TWQR, both Fe (0.41 mg/L), Al (0.71 mg/L) and Mn (0.38 mg/L) were not within the TWQR for domestic water as the concentration of these elements increased after 15 min of carbonation.

After treatment of EAMD (1000 L) with LFA (167 kg), lime (1.0 kg) and 0.31 kg of $Al(OH)_3$, a sample of the SR recovered was collected. The sample was analysed using XRD to determine any mineral phase that could have appeared or disappeared during the neutralisation process. The XRD results are illustrated in Figure 4.9.

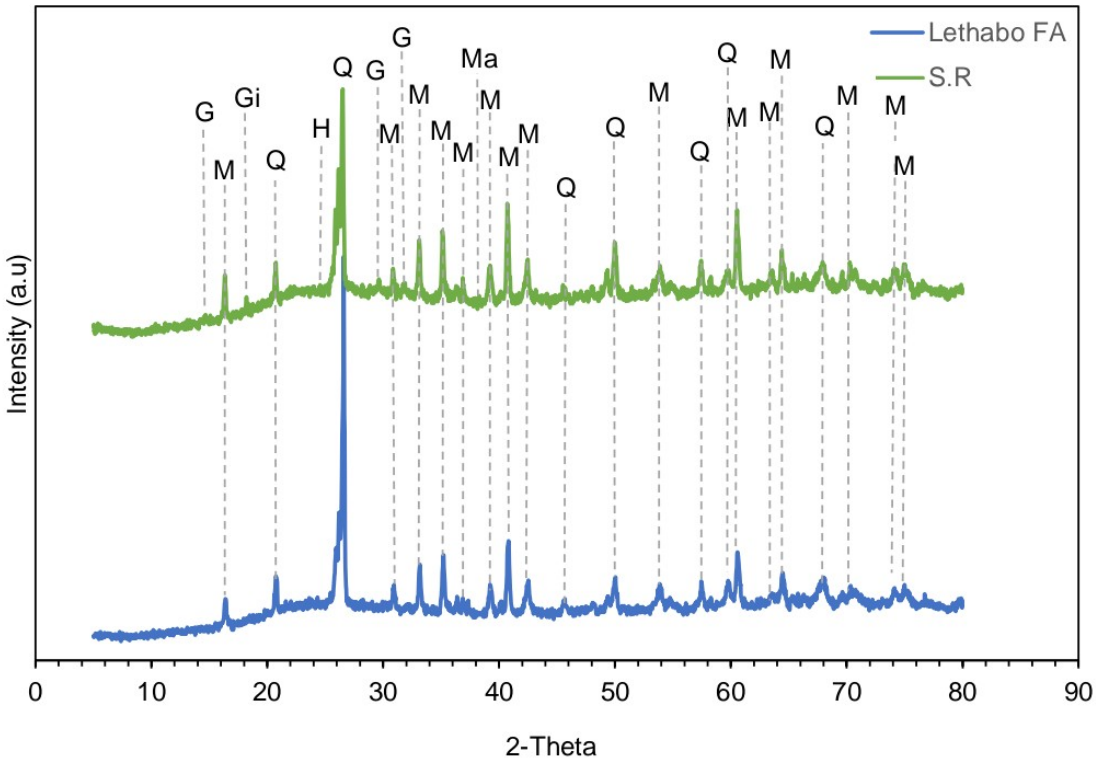

Figure 4.9: XRD spectra of the solid residue recovered after treatment of Eyethu AMD (1000 L), Lethabo FA (167 kg), lime (1.0 kg) and 0.31 kg of $Al(OH)_3$ compared to Lethabo FA (M-mullite; Gi-Gibbsite; Q-quartz; G-gypsum; H-hematite; Ma-maghemite).

Figure 4.9 shows the XRD spectra of the solid residue recovered after treatment of EAMD with LFA, lime and $Al(OH)_3$. The result obtained showed the appearance of new mineral peaks such as gypsum and gibbsite in the solid residue. In addition, hematite and maghemite peaks were visible in the SR XRD spectrum. The appearance of gypsum in the SR confirmed that the decrease in SO_4^{2-} concentration was due to gypsum precipitation. The formation of gibbsite as a secondary phase confirmed that Al removal was controlled by this phase in the presence of $Al(OH)_4^-$. At any pH, according to Gitari et al. (2008b), regulation of Al content cannot be attributed to a specific mineral phase.

The solid residue recovered after the treatment of 1000 L of EAMD with 167 kg of LFA, 1.0 kg of lime and 0.31 kg of $Al(OH)_3$ was analysed for major oxides using XRF. The results obtained were compared to that of fresh LFA and are tabulated in Table 4.5.

Table 4.5: Major oxides of Lethabo FA compared to that of the SR recovered after 180 min of treating 1000 L of Eyethu AMD with 167 kg of Lethabo FA, 1.0 kg of lime and 0.31 kg of Al(OH)3

	Major oxide	
% w/w	**LFA**	**S.R**
SiO_2	56.71	53.89
Al_2O_3	29.22	29.87
CaO	4.59	4.09
Fe_2O_3	3.38	3.57
TiO_2	1.54	1.54
MgO	1.17	1.34
K_2O	0.78	0.72
Na_2O	0.33	0.17
P_2O_5	0.35	0.42
MnO	0.03	0.07
Cr_2O_3	004	0.04
V_2O_2	0.01	0.03
LOI	0.86	3.57
Total	**99.02**	**99.33**

Results obtained from the XRF analysis showed that the amount of CaO in the SR decreased, this confirmed that indeed the increase in the value of pH was due to the dissolution of CaO in the solution. It was observed that even after the addition of $Al(OH)_3$ the concentration of Ca was still very high in the product water (Figure 4.8). The amount of Al_2O_3, Fe_2O_3, MgO, and MnO increased because of the precipitation of these elements from EAMD in their respective hydroxides or oxyhydroxides form. The amount of SiO_2, K_2O and Na_2O in LFA was a bit higher than in the SR, as these could have leached from LFA into the water. The amount of P_2O_5 increased in the SR. However, Cr_2O_3 and TiO_2 amount remained constant.

The treatment of 1000 L of EAMD with 167 kg of LFA, 1.0 kg of lime and 0.31 kg of $Al(OH)_3$ showed that most of the major elements were significantly removed with some of these elements being removed to within the TWQR required for potable water. It was observed that the addition $Al(OH)_3$ did not enhance SO_4^{2-} removal from the mine water. Bowell et al. (2004) reported that in SA, the maximum SO_4^{2-} effluent level recommended is 600 mg/L (DWAF, 1993). SO_4^{2-} is not toxic, however, it has been reported that when the concentration of this is above 600 mg/L in drinking water, this results in a purgation of the alimentary canal (Bowell et al., 2004). The addition of $Al(OH)_3$ was not necessary since the recommended effluent level of SO_4^{2-} by DWAF was already reached just by reacting EAMD with LFA and lime (DWAF, 1993; Bowell et al., 2004).

In this study, the effect of LFA, lime and $Al(OH)_3$ on the removal of SO_4^{2-} and heavy metals from EAMD were investigated using a jet loop reactor pilot plant at 1000 L capacity. After

treatment, it was found that LFA alone as the reactant could not reduce SO_4^{2-} concentration from EAMD to within the TWQR limits for domestic water use as recommended by WHO and DWAF, therefore, lime was added to the mixture of EAMD and KFA to further remove SO_4^{2-} from EAMD. After treatment of EAMD with LFA, the AMD:FA ratio of 6:1 was selected as the optimum ratio. This was followed by investigating the amount of lime (0.05%, 0.1% and 0.15%; w/v) to be added to the solution of EAMD and LFA as shown in Figure 4.5. After treatment of EAMD with LFA and different amount of lime, 0.1% (w/v %) of lime was selected as the optimum amount of lime; this was selected based on SO_4^{2-} removal percentage, pH level, and minimum amount of lime used. This was followed by the investigation of adding $Al(OH)_3$, and the amount of $Al(OH)_3$ was determined as described in section 3.6. The addition of $Al(OH)_3$ to the solution was found not to be necessary or economically viable as this did not improve the performance of the process in cleaning up of the water with respect to SO_4^{2-}.

The following section will investigate the performance of the jet loop reactors in cleaning up of EAMD using KFA, by keeping the same parameters as when this was treated with LFA.

4.3.2. Treatment of Eyethu AMD with Kendal FA

This section explains (elaborates) the chemistry of potentially toxic elements removal from Eyethu AMD (EAMD) when neutralised with Kendal FA (KFA), lime and $Al(OH)_3$.

4.3.2.1. Effect of Kendal FA addition to EAMD

A series of experiments were carried out in order to determine the optimum amount of KFA required to elevate the pH of EAMD, thus, reducing SO_4^{2-} concentration. EAMD and KFA were mixed using 3 different liquids to solid ratios of 7:1, 6:1 and 5:1 and circulated through the jet loop reactors as described in section 3.6. The same L/S ratio used when EAMD was treated with LFA was repeated with KFA. Figure 4.10 illustrates the trends of pH and EC during treatment of 1000 L of EAMD with 143 kg, 167 kg or 200 kg of KFA respectively.

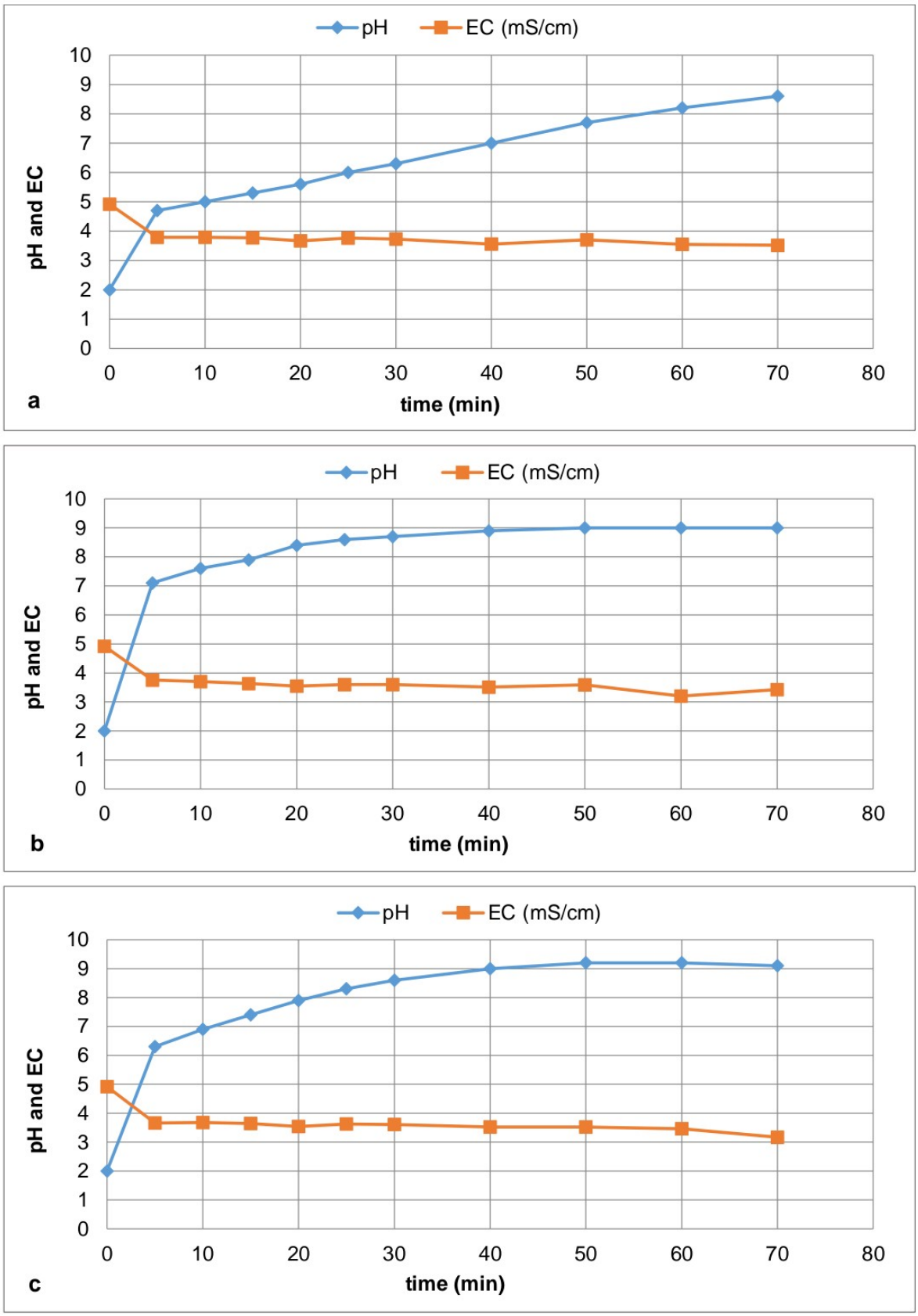

Figure 4.10: Trends of pH and EC during treatment of Eyethu AMD (1000 L) with 143 kg (a), 167 kg (b) or 200 kg (c) of Kendal FA.

Treatment of 1000 L of EAMD with KFA (143 kg, 167kg or 200 kg) showed an increase in pH value after the first 5 min of reaction, and then pH continued to increase gradually as the experiment proceeded (Figure 4.10). The pH of the mine water increased from 2.0 to 8.6 when EAMD was reacted with 143 kg of KFA after 70 min (Figure 4.10a). The increase in pH value was due to the dissolution of CaO present in KFA. When adding the FA amount of up to 167 kg to EAMD (1000 L), this resulted in the pH increasing from 2.0 to 9.0 after 70 min of reaction time. Comparing this to when 143 kg of FA was used to neutralise the mine water, there was a slight increase in the value of the pH, this is a result of more CaO being available for dissolution as more FA was added (Figure 4.10b). When EAMD (1000 L) was mixed with 200 kg of KFA, the pH of the mine water increased from 2.0 to 9.0 after the first 40 min (Figure 4.10c), and then slightly increased to 9.2 up to 60 min, thereafter, a slight decrease in pH value occurred (9.1) up to 70 min of mixing. Although, the addition of more FA is equivalent to more CaO being available for dissolution, it was observed that the contact time was not enough for more CaO to dissolve when 200 kg of FA was added. After the first 5 min a slight decrease in the value of EC was observed, then this remained almost constant during treatment of EAMD with KFA (143 kg, 167 kg or 200 kg) as shown in Figure 4.10.

When EAMD (1000 L) was treated with KFA (143 kg, 167 kg or 200 kg), samples were collected after every 20 min, and then filtered using a membrane filter with a pore size of 0.45 µm. The results are presented in Figure 4.11.

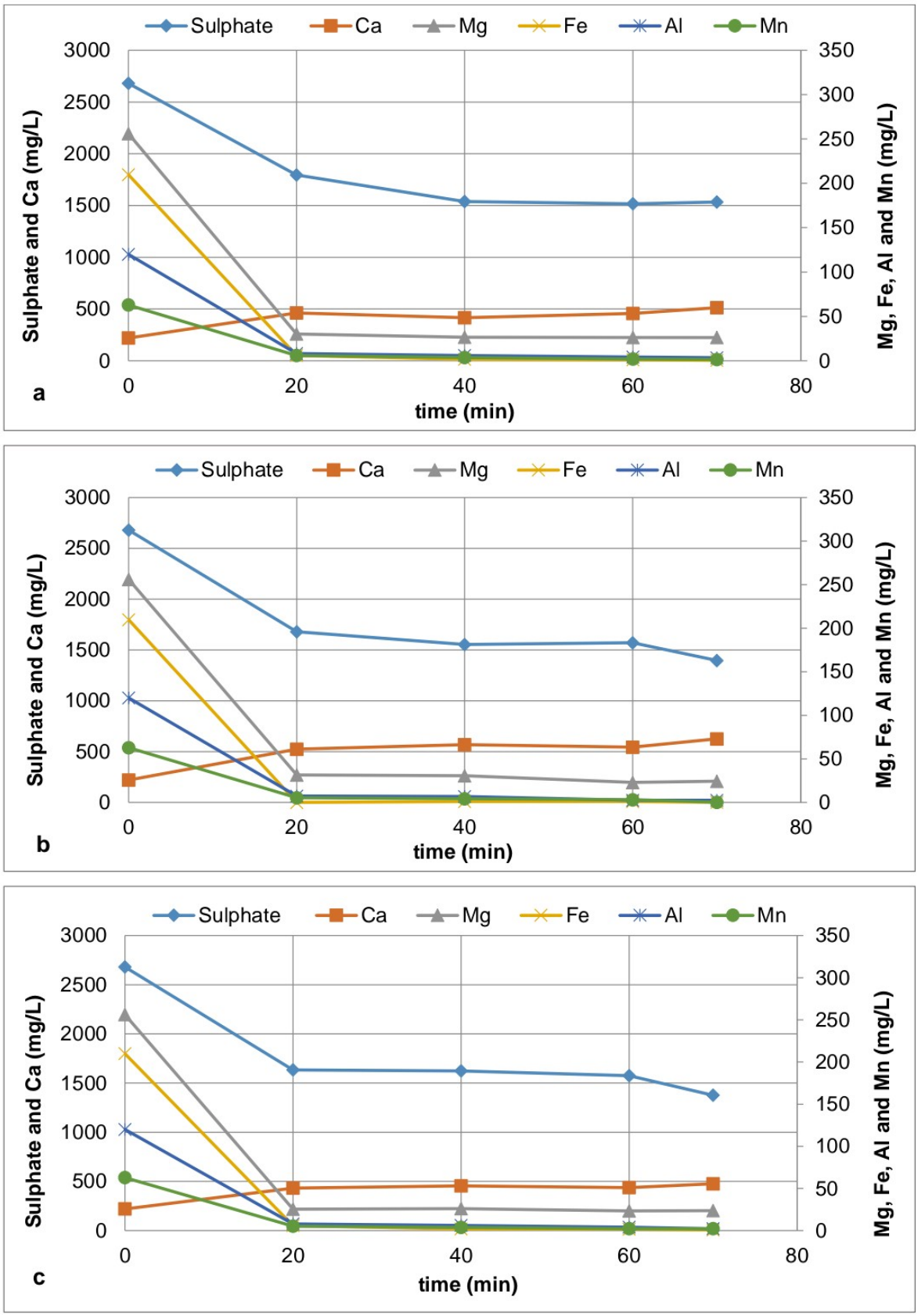

Figure 4.11: Sulphate, Ca, Mg, Fe, Al and Mn concentrations during treatment of Eyethu AMD (1000 L) with 143 kg (a), 167 kg (b) or 200 kg (c) of Kendal FA.

Figure 4.11 shows the IC and ICP-OES results obtained after treating EAMD with different amount of KFA in order to determine the optimal amount of KFA required to remove SO_4^{2-} and heavy metals. Treatment of EAMD (1000 L) with 143 kg of KFA resulted in SO_4^{2-} concentration decreasing from 2680.00 mg/L to 1534.62 mg/L after 70 min (Figure 4.11a). When the amount of FA was increased from 143 kg to 167 kg, this increased the performance in cleaning up of EAMD; the concentration of SO_4^{2-} was reduced from 2680.00 mg/L to 1397.00 mg/L after 70 min as shown in Figure 4.11b. A further increase in the performance of cleaning up of Eyethu mine water based on SO_4^{2-} removal was observed when the amount of FA was further increased up to 200 kg. As shown in Figure 4.11c, the concentration of SO_4^{2-}decreased from 2680.00 mg/L to 1375.83 mg/L.

After treatment of EAMD with different amounts of KFA, Ca concentration was increasing in the treated water; this was attributed to the dissolution of CaO from KFA into the water as described in Eq. (2.20). The results obtained when 1000 L of EAMD was reacted with 143 kg of KFA, show an increase in the concentration of Ca from 219.60 mg/L to 513.00 mg/L. When the FA amount was increased from 143 kg to 167 kg, this resulted in the availability of more CaO for dissolution; thus, resulting in Ca concentration to increase in the water from 219.60 mg/L to 625.43 mg/L (Figure 4.11b). A further increasing in the amount FA from 167 kg to 200 kg, resulted in the concentration of Ca to increase from 219.60 mg/L to 476.23 mg/L. However, this was lower compared to when EAMD was reacted with 167 kg of KFA.

The concentration of metals such as Mg, Fe, Al and Mn was significantly reduced, with some of these elements being removed to within the TWQR required for potable water set by WHO (2011) and DWAF (1996) when EAMD was neutralised with KFA for about 70 min. For example, when EAMD was treated with 143 kg of KFA, this resulted in Mg being removed to within the TWQR limits for potable water. The concentration of Mg, decreased from 256.11 mg/L to 30.22 after the first 20 min, and then further decreased to 26.16 mg/L up to 70 min. The concentration of Fe, Al and Mn decreased from 209.81 mg/L, 120.00 mg/L and 62.84 mg/L to 0.41 mg/L, 3.45 mg/L and 1.50 mg/L respectively after 70 min. Although, these elements concentrations significantly decreased, however their concentrations were still above the TWQR required for domestic water use (Figure 4.11a). Fe was removed to zero concentration when EAMD was reacted with 167 kg of KFA after the first 20 min of mixing. However, this increased to 1.09 mg/L up to 40 min. Up to 70 min of mixing, Fe concentration decreased to 0.14 mg/L, therefore, reaching the TWQR required for domestic water use. The concentrations of Mg, Al and Mn were 24.3 mg/L, 2.43 mg/L and 0.29 mg/L after 70 min (Figure 4.11b). Increasing the amount of FA up to 200 kg did not result in cleaning up the mine water

with respect to Fe (0.80 mg/L), Al (2.17 mg/L) and Mn (2.23 mg/L) to within the TWQR limits for domestic water but Mg (23.72 mg/L).

Experiments during treatment EAMD with different amount KFA resulted in 167 kg of FA being selected as the optimum amount. A higher percentage in cleaning up of EAMD with respect to different elements was achieved at this AMD:FA ratio of 6:1.

Treatment of EAMD (1000 L) with 143 kg, 167 kg or 200 kg of KFA could not raise the pH of the water to higher than 11, which was the targeted pH prior to $Al(OH)_3$ addition (Figure 4.10). For SO_4^{2-} to precipitate out as ettringite, a pH of at least 11 is needed before adding $Al(OH)_3$. Since mixing EAMD and KFA could not raise the pH of the mine water to around 11 or higher, lime addition to the mixture of EAMD (1000 L) and KFA (167 kg) was explored.

4.3.2.2. Effect of lime addition to Eyethu AMD and Kendal FA mixture

In order to further remove SO_4^{2-} and heavy metals from Eyethu mine water, a set of experiments was carried out by adding different amounts of lime to the mixture of EAMD and KFA. 1000 L of EAMD was neutralised with 167 kg of KFA and 0.5 kg, 1.0 kg or 1.5 kg of lime. During the treatment of EAMD with KFA and lime, the pH and EC were recorded from the display after every 10 min as the experiment proceeded; the trends of these are shown in Figure 4.12.

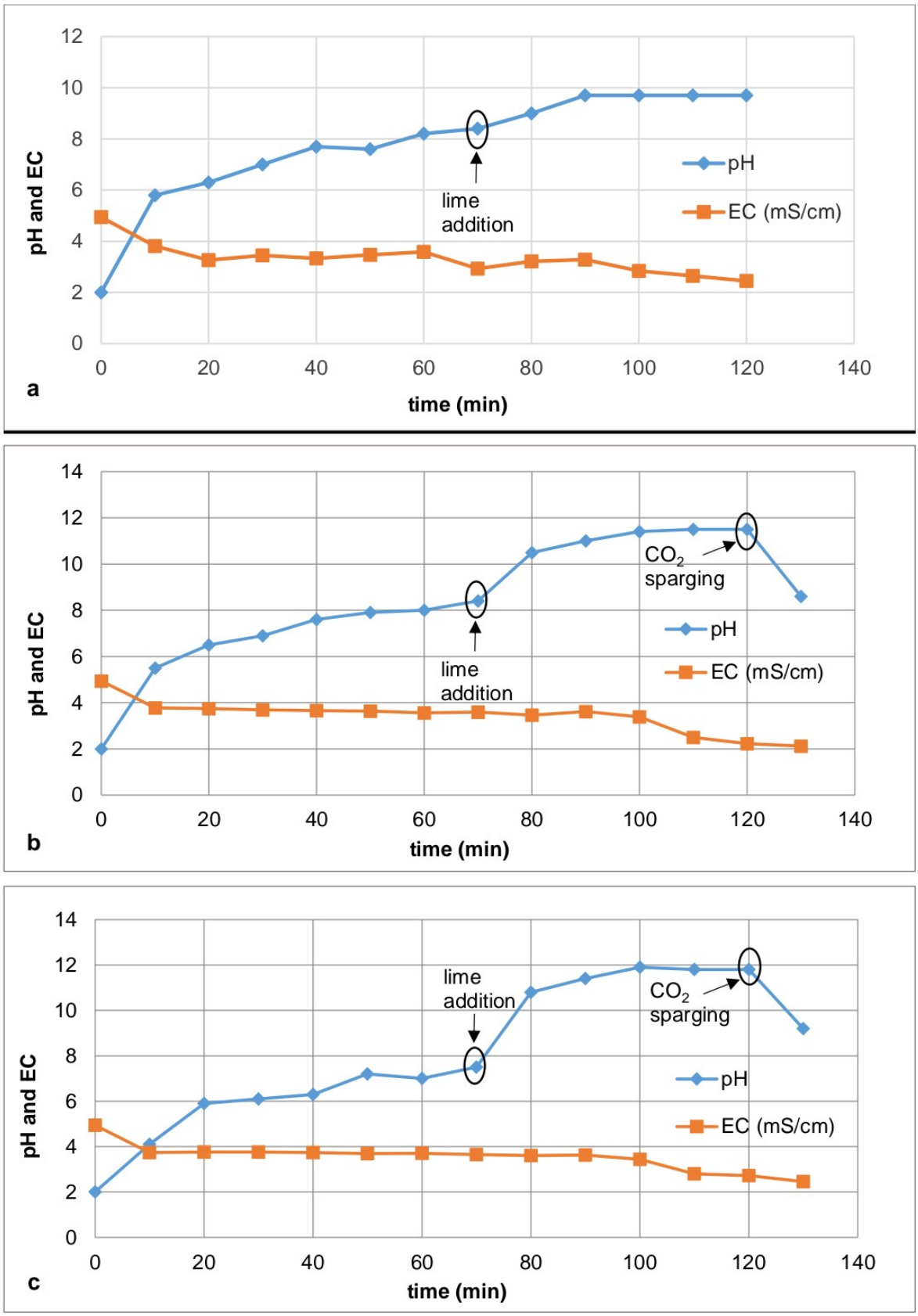

Figure 4.12: pH and EC recorded during the treatment of 1000 L of Eyethu AMD with 167 kg of Kendal FA and 0.5 kg (a), 1.0 kg (b) or 1.5 kg (c) of lime.

Treatment of 1000 L of EAMD with 167 kg of KFA for 70 min resulted in the mine water pH increasing from 2.0 to 8.4, 8.4 and 7.5 before adding 0.5 kg, 1.0 kg or 1.5 kg of lime respectively to the mixture of EAMD and KFA (Figure 4.12). A decrease in the values of pH was observed compared to previous experiment (section 4.3.2.1) when Eyethu mine water was reacted with 167 kg of KFA (Figure 4.10b). From the results obtained after adding lime, it was observed that the mixture pH was influenced by the addition of lime amount. After 70 min of starring and jet loop mixing, lime was added to the mixture of EAMD and KFA, the new mixture consisting of EAMD, KFA and lime was first stirred for about 20 min for homogeneous mixing (up to 90 min on stream) before jet loop mixing; this resulted in the pH of the mixtures increasing to 9.7, 11.0 or 11.4 after adding 0.5 kg (Figure 4.12a), 1.0 kg (Figure 4.12b) or 1.5 kg (Figure 4.12c) of lime respectively. After a further 20 min (up to 110 min on stream) of stirring and jet loop mixing, the mixture containing 0.5 kg, pH remained constant at 9.7, the effect of jet loop mixing did not improve the performance based on pH. After a further 10 min (up to 120 min) of stirring and jet loop mixing, the pH remained constant at pH 9.7. For mixtures containing 1.0 kg and 1.5 kg of lime, the pH increased to 11.4 and 11.9 respective after the first 10 min (up to 100 min on stream) of stirring and jet loop mixing. A further 10 min (up to 110 min on stream) of stirring and jet loop mixing resulted in pH slightly increasing for the mixture containing 1.0 kg lime, to pH 11.5 and slightly decreasing for the mixture containing 1.5 kg of lime to pH 11.8. After a further 10 min (up to 120 min on stream) of stirring and mixing in jet loop, the pH of both mixtures remained constant at 11.5 (Figure 4.12b) and 11.8 (Figure 4.12c) respectively. During treatment of EAMD (1000 L) with KFA (167 kg) and lime (0.5 kg), the EC was fluctuating as shown in Figure 4.12a. For the mixtures containing 1.0 kg or 1.5 kg, the EC decreased slightly then remained almost constant for about 90 min then started to decrease gradually as illustrated in Figures 4.12b and 4.12c respectively.

When EAMD (1000 L) was treated with 167 kg of KFA, 1.0 kg or 1.5 kg of lime, this resulted in the product water having a higher pH. The pH was reduced by sparging CO_2 into the water. After 10 min (up to 130 min on stream) of carbonation using CO_2, the pH of the waters was brought down to 8.6 and 9.2 for the mixture containing 1.0 kg (Figure 4.12b) and 1.5 kg (Figure 4.12c) of lime respectively. Before carbonation the water was first separated from the SR.

For analysis purpose, samples were collected every 10 to 30 min during the treatment of EAMD (1000 L) with 167 kg of KFA and lime (0.5 kg, 1.0 kg or 1.5 kg). The samples were filtered using a 0.45 µm membrane filter paper prior to analysis using IC and ICP-OES. The results obtained after analysis are depicted in Figure 4.13.

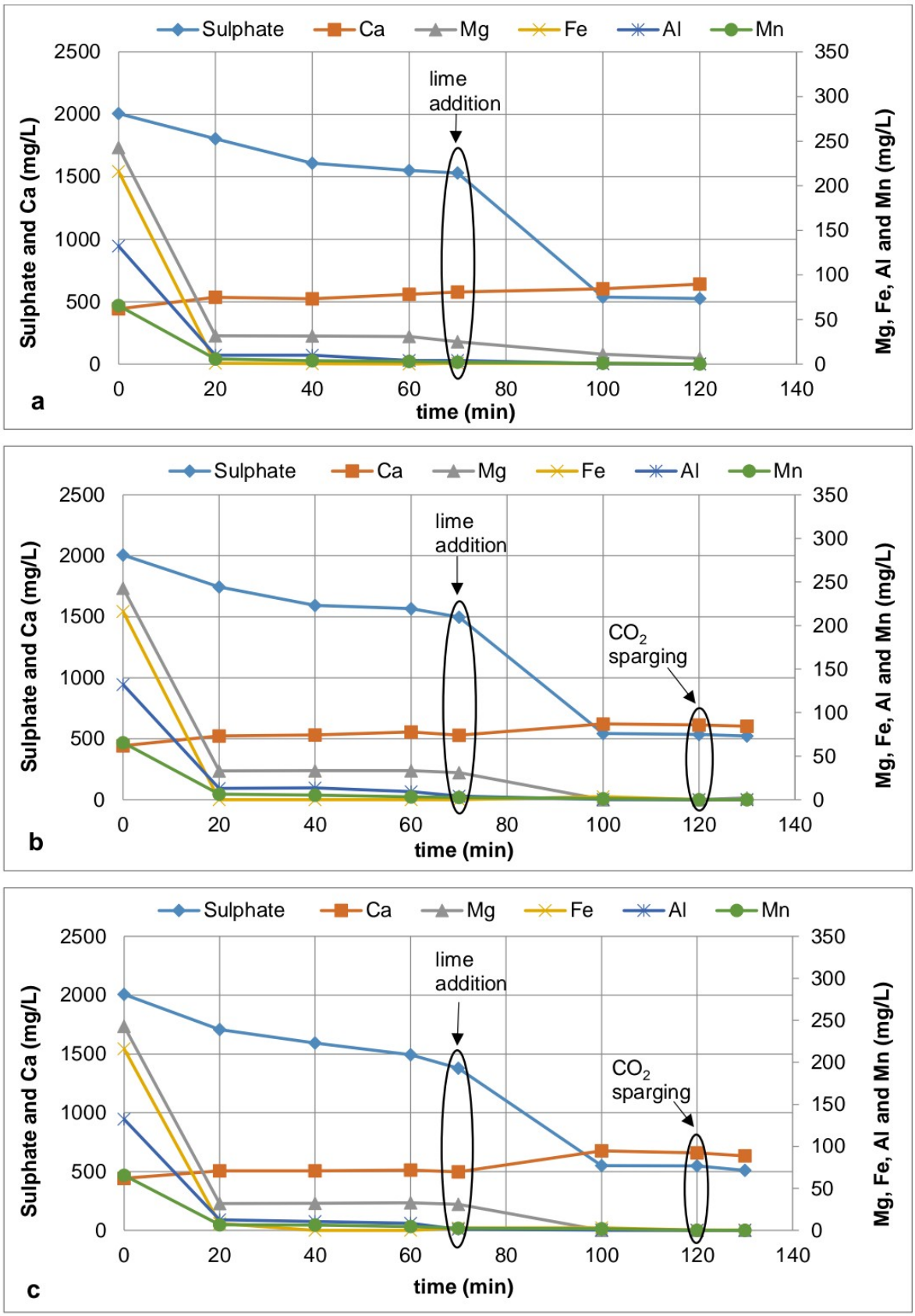

Figure 4.13: Sulphate, Ca, Mg Fe, Al and Mn concentration during the treatment of 1000 L of Eyethu AMD with Kendal FA (167 kg), and 0.5 kg (a), 1.0 kg (b) or 1.5 kg (c) of lime.

Treatment of EAMD with KFA (167 kg) for about 70 min resulted in SO_4^{2-} concentration decreasing from 2006.28 mg/L to 1530.58 mg/L (Figure 4.13a). After 70 min, 0.5 kg of lime was added to the mixture of EAMD and KFA (Figure 4.13a), and stirred for about 20 min (up to 90 min on stream) for homogeneous mixing and then circulated through the JLRs for about 10 min (up to 100 on stream); resulting in SO_4^{2-} concentration decreasing from 1530.58 mg/L to 536.78 mg/L. After a further 20 min (up to 120 min on stream) of stirring and jet loop mixing, SO_4^{2-} concentration decreased to 525.21 mg/L (Figure 4.13a). When Eyethu mine water was treated with 167 kg of KFA, the concentration of Ca increased from 442.75 mg/L to 576.78 mg/L after the first 70 min from starting time. The dissolution of CaO present in KFA was responsible for the initial increase in Ca ions concentration. The addition of 0.5 kg of lime (at 70 min on stream) resulted in Ca ions concentration increasing to 640.52 mg/L up to 120 min as more lime was added to the mixture of EAMD and KFA (Figure 4.13a), thus, making more CaO available for dissolution. This also resulted in the pH of the water increasing due to more CaO dissolving into the mine water. As water pH was increasing, SO_4^{2-} concentration was decreasing, thus, making SO_4^{2-} removal pH dependent.

During neutralisation of 1000 L of EAMD with 167 kg of KFA for the first 70 min, the concentration of Ca ions increased from 442.75 mg/L to 529.81 mg/L, while SO_4^{2-} concentration decreased from 2006.28 mg/L to 1496.62 mg/L as depicted in Figure 4.13b. The reduction in SO_4^{2-} concentration is usually credited to the formation of gypsum at lower pH and or ettringite at elevated pH values (Madzivire, 2012a). After adding 1.0 kg of lime (at 70 min on stream), the concentration of Ca increased to 621.87 mg/L and that of SO_4^{2-} decreased to 543.59 mg/L (Figure 4.13b) up to 100 min. After a further mixing of the solution for about 20 min (up to 120 min on stream), the concentrations of Ca ions and SO_4^{2-} further decreased to 612.38 mg/L and 535.99 mg/L respectively (Figure 4.13b). Increasing the amount of lime to 1.5 kg, resulted in SO_4^{2-} concentration decreasing from 1378.58 mg/L to about 551.25 mg/L (Figure 4.13c). The concentration of SO_4^{2-} decreased from 2006.28 mg/L to 1378.58 mg/L in the first 70 min of neutralising Eyethu mine water with KFA (167 kg) prior to lime (1.5 kg) addition. Before adding lime, the concentration of Ca increased from 442.75 mg/L to 497.73 mg/L, this further increased to 676.16 mg/L (up to 100 min) after the addition of 1.5 kg of lime (at 70 min) as shown in Figure 4.13c. After 10 min (up to 130 min) of carbonation using CO_2 for pH reduction, this process resulted in the concentration of SO_4^{2-} slightly decreasing to 522.14 mg/L and 510.01 mg/L, and the concentration of Ca also slightly decreased to 603.55 mg/L and 634.18 mg/L for the mixtures containing 1.0 kg (Figure 4.13b) and 1.5 kg (Figure 4.13c) of lime respectively. It was observed that, during the treatment of EAMD with KFA for about 70 min, the concentration of SO_4^{2-} was varying for the same amount of FA used, and SO_4^{2-} concentration was in the range of 1350 mg/L to 1550 mg/L (Figure

4.13). This showed that although the amount FA was kept constant, the concentration of SO_4^{2-} was varying after about 70 min of reacting Eyethu mine water with KFA, the same thing was observed during the treatment of Eyethu mine water with LFA (section 4.3.1.2; Figure 4.5).

Neutralisation of EAMD with KFA and different amounts of lime showed that Mg, Fe, Al and Mn concentrations were significantly reduced, with some of these elements being removed by almost 100% (Figure 4.13). Several authors (Gitari et al., 2006; 2008b; Madzivire, 2012a) reported that heavy metals removal was dependent on pH. As the pH of the mine water increased, the removal rate of heavy metals also increased. Elements such as Mg, Mn and Fe total removal occurred only when the pH of minimal solubility of their respective hydroxides was attained, $Mg(OH)_2$ around pH 10, $Mn(OH)_2$ at pH 9 and $Fe(OH)_3$ at around pH 6 respectively (Gitari et al., 2006; Madzivire, 2012a). During the treatment of EAMD with KFA and 0.5 kg of lime after 120 min, Mg concentration decreased from 243.99 mg/L to 6.52 mg/L at pH 9.7. While Fe, Al and Mn concentration decreased from 216.07 mg/L, 132.25 mg/L and 65.59 mg/L to 0.18 mg/L, 0.13 mg/L and 0.09 mg/L respectively (Figure 4.13a) after 120 min of mixing. As more lime was added, this resulted in Mg concentration further decreasing. In the case of neutralisation of EAMD (1000 L) with KFA (167 kg) and 1.0 kg or 1.5 kg of lime, the concentration of Mg decreased to 0.05 mg/L (Figure 4.13b) and 0.01 mg/L (Figure 4.13c) respectively after 120 min of mixing as the pH of the solution was above 10. After 10 min (up to 130 min) of carbonation using CO_2, the concentration of Mg, Fe, Al and Mn was 2.02 mg/L, 0.12 mg/L, 0.20 mg/L and 0.13 mg/L for the mixture containing 1.0 kg of lime. For the mixture containing 1.5 kg of lime, the concentration of Mg, Fe, Al and Mn was 0.09 mg/L, 0.22 mg/L, 0.18 mg/L and 0.09 mg/L respectively. In term of Mg, Fe, Al and Mn removal, all 3 mixtures met the TWQR required for domestic water use. Although, there was slight increase in the concentration of elements such as Mg, Fe, Al and Mn after carbonation, the concentrations of these elements were still within the TWQR for domestic water for the mixtures containing 1.0 kg (Figure 4.13b) or 1.5 kg (Figure 4.13c) of lime respectively. Treatment of EAMD (1000 L) with KFA (167 kg) and different amount lime (0.5 kg, 1.0 kg or 1.5 kg) did not decrease SO_4^{2-} concentration to within the TWQR required for domestic water use. The product water quality can be improved by polishing-up the water using ion exchange or other processes. After treatment of EAMD with KFA (167 kg) and different amounts lime (0.5 kg, 1.0 kg or 1.5 kg); 1.0 kg of lime was selected as the optimum amount lime, so as lime amount could be kept at a minimum. Water of good quality was recovered when EAMD (1000 L) was neutralised with KFA (167 kg) and lime (1.0 kg).

After treatment of 1000 L of EAMD with 167 kg of KFA and 1.0 kg of lime, a sample of the solid residue recovered after neutralisation was collected, dried and analysed using XRD. The XRD spectra of the solid residue is shown in Figure 4.14.

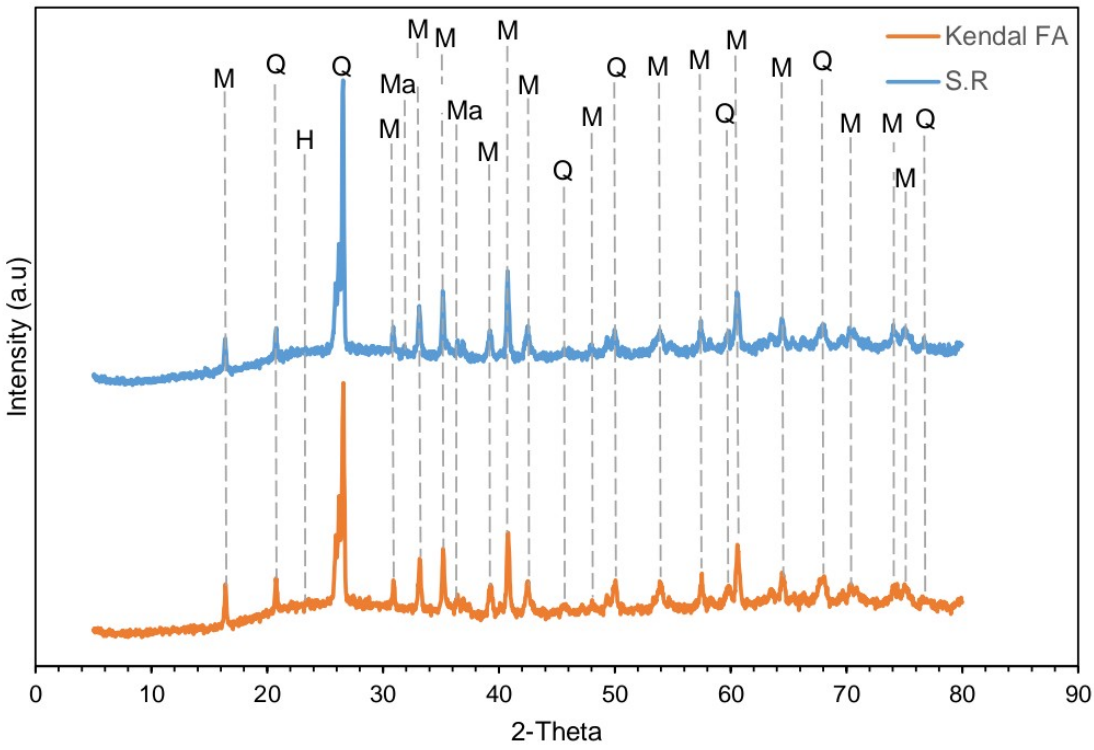

Figure 4.14: Comparison of XRD spectra of Kendal FA to that of the solid residue generated after treatment of 1000 L of Eyethu AMD with 167 kg of Kendal FA and 1.0 kg lime (M-mullite; Q-quartz; H-hematite; Ma-maghemite).

The SR's XRD spectra showed no ettringite or gypsum peaks. It was difficult to assume that the decrease in SO_4^{2-} concentration observed during the treatment of EAMD (1000 L) with KFA (167 kg) and lime (1.0 kg) was due to gypsum precipitation without evidence. The peaks of M, Q, H and Ma present in the fresh KFA were also observed in the SR as shown in Figure 4.14, therefore, no new mineral phase was formed.

After treatment of EAMD (1000 L) with 167 kg of KFA and 1.0 kg of lime, a sample of the solid residue produced was collected and analysed using XRF. The results obtained are presented in Table 4.6.

Table 4.6: Elemental composition of KFA and solid residue generated after treatment of EAMD (1000 L) with KFA (167 kg) and lime (1.0 kg)

	Major oxide	
% w/w	**KFA**	**S.R**
SiO_2	53.06	51.25
Al_2O_3	30.53	30.42
CaO	5.75	5.13
Fe_2O_3	4.77	4.90
TiO_2	1.63	1.62
MgO	1.55	1.73
K_2O	0.69	0.67
Na_2O	0.16	0.00
P_2O_5	0.48	0.55
MnO	0.04	0.08
Cr_2O_3	0.03	0.03
V2O5	0.01	0.02
LOI	1.33	2.75
Total	**100.05**	**99.14**

KFA stands for Kendal fly ash and SR for solid residues.

Based on the results obtained after XRF analysis, it was observed that the oxides of Fe, Mg, and Mn slightly increased in the solid SR. The amount of Ca, Si and Al oxides in the SR was lower compared to fresh KFA. The increase for oxides of Fe, Mg and Mn in the SR was attributed to the precipitation of these elements out of EAMD. The oxide of P also increased in the SR, but that of K and Ti decreased in the solid residue compared to fresh KFA. Cr_2O_3 content remained constant. Only a small amount of CaO was available for dissolution from the one entrapped in the matrix. These results show that KFA still has it binding properties to be used in geopolymer or zeolite synthesis.

4.3.2.3. Effect of adding $Al(OH)_3$ to the mixture of EAMD, KFA and lime

At this stage a combination of KFA, lime and $Al(OH)_3$ was investigated in order to reduce the concentration of SO_4^{2-} to within the TWQR for potable water. EAMD was reacted with 167 kg of KFA, 1.0 Kg of lime and 0.31 kg of $Al(OH)_3$. EAMD was first treated with KFA for about 90 min, and then lime was added to the mixture of EAMD and KFA after 90 min and the new solution was mixed up to 130 min, after 130 min $Al(OH)_3$ was added to the mixture of EAMD, KFA and lime, and mixed up to 180 min. The pH and EC were recorded every 10 min. The results obtained are shown in Figure 4.15.

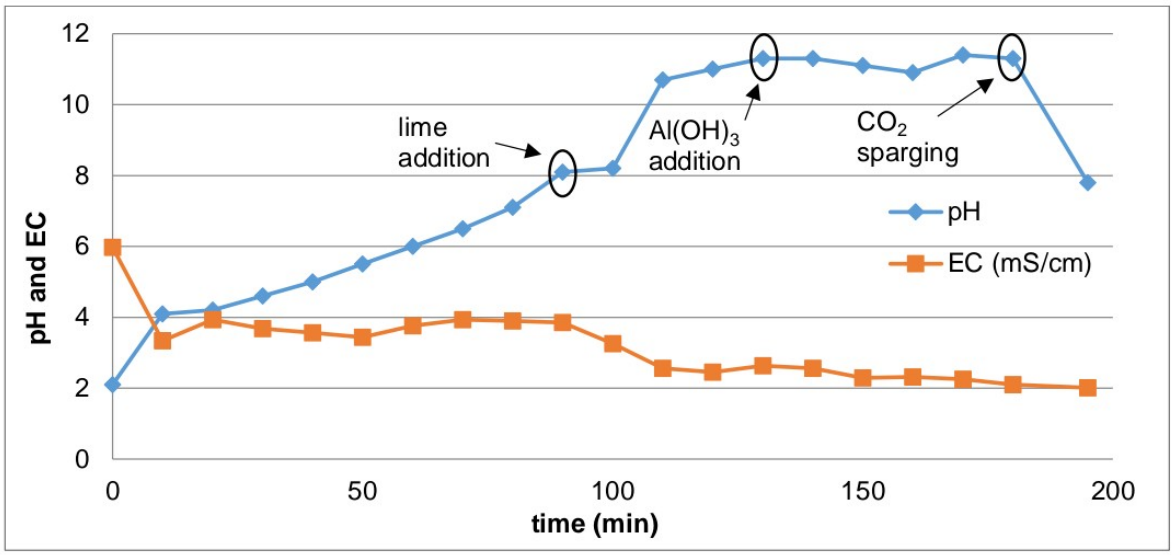

Figure 4.15: pH and EC during treatment of 1000 L of EAMD with 167 kg of KFA, 1.0 kg of lime and 0.31 kg of $Al(OH)_3$.

Treatment of EAMD with 167 kg of KFA for about 90 min resulted in the pH of the water increasing from 2.1 to 8.1. After the first 90 min, 1.0 kg of lime was added to the mixture. Figure 4.15 shows that addition of lime resulted in the pH of the mixture increasing to 10.7 after 20 min (up to 110 min) of stirring and the pH slightly increased to 11.3 after a further 20 min of stirring and jet loop mixing (up to 130 min on stream). At 130 min, 0.31 kg of $Al(OH)_3$ was added to the mixture. Addition of 0.31 kg of $Al(OH)_3$ (at 130 min) resulted in the pH of the water slightly decreasing to 11.1 after 20 min (up to 150 min) of stirring for homogeneous mixing. When EAMD, KFA, lime and $Al(OH)_3$ mixture was stirred and circulated through the jet loop reactors for about 20 min (up to 170 min), it resulted in the pH of the water slightly decreasing to 10.9 for the first 10 min (up to 160 min) and then increased to 11.4 after 10 more min of mixing (up to 170 min), a further 10 min of reaction resulted in a slight decrease in the pH at 11.3 (up to 180 min). To reduce the pH of the water to within the TWQR limits required for potable water, CO_2 was used. Before carbonation took place, the water was first separated from the SR. Therefore, CO_2 was sparged only into the water recovered not the mixture. After 15 min of carbonation using CO_2, the pH of the water decreased from 11.3 to 7.8 (Figure 4.15). CO_2 was sparged for a duration of 1 min and 30 sec. Treatment of EAMD (1000 L) with KFA (167 kg), lime (1.0 kg) and 0.31 kg of $Al(OH)_3$, resulted in the EC of the water decreasing from 5.97 mS/cm to 2.01 mS/cm (Figure 4.15).

During treatment of EAMD with 167 kg of KFA, 1.0 kg of lime and 0.31 kg of $Al(OH)_3$, samples were collected after every 20 min and filtered through a 0.45 µm membrane filter paper and the filtrate was analysed for determination of elemental content. The results obtained are shown in Figure 4.16.

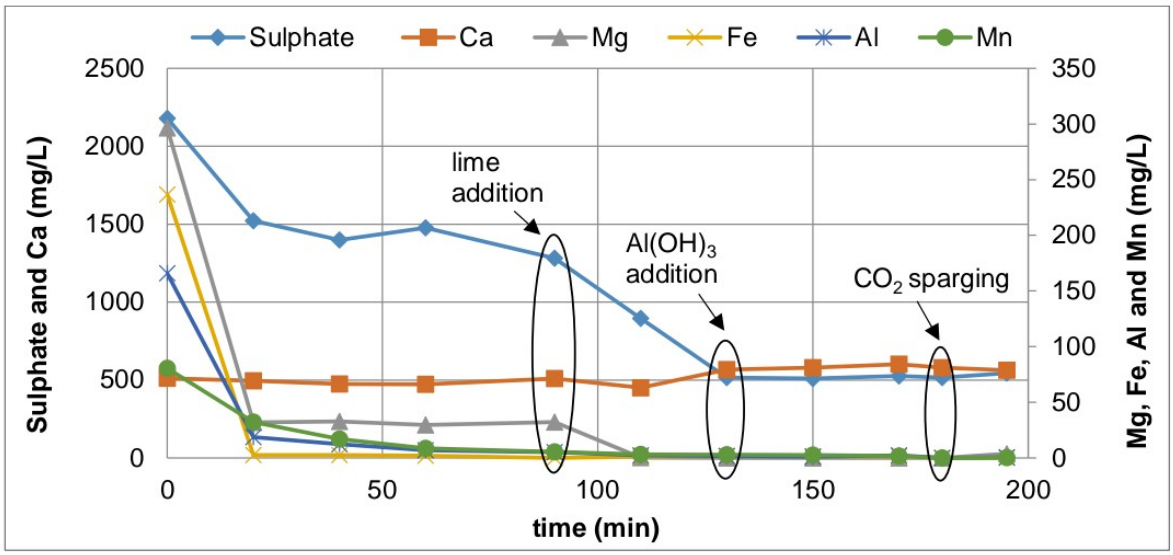

Figure 4.16: Sulphate, Ca, Mg, Fe, Al and Mn concentration during treatment of EAMD (1000 L) with 167 kg of KFA, 1.0 kg of lime and 0.31 kg of $Al(OH)_3$.

Treatment of 1000 L of EAMD with 167 kg of KFA for about 90 min resulted in the decrease of SO_4^{2-} content in EAMD from 2179.61 mg/L to 1282.00 mg/L and the concentration of Ca slightly decreased from 512.26 mg/L to 509.30 mg/L. After adding 1.0 kg of lime to the mixture of EAMD and KFA (after the first 90 min) and stirred for about 20 min (up to 110 min), resulted in the decrease of SO_4^{2-} concentration to 894.80 mg/L and that of Ca further decreased to 450.90 mg/L as illustrated in Figure 4.16. The mixture of EAMD, KFA and lime was further stirred, and jet loop mixed for a further 20 min (up to 130 min on stream), which resulted in SO_4^{2-} concentration decreasing to 516.57 mg/L and Ca concentration increased to 566.50 mg/L (Figure 4.16). After 130 min of stirring and jet loop mixing of the mixture, 0.31 kg of $Al(OH)_3$ was added, which resulted in the SO_4^{2-} concentration slightly decreasing to 509.95 and Ca concentration increased to 580.00 mg/L after 20 min of stirring (up to 150 min on stream). After further stirring and jet loop mixing the mixture for about 20 min (up to 170 min), the concentration of SO_4^{2-} slightly increased to 526.93 mg/L and Ca concentration also increased to 601.50 mg/L. After a further 10 min (up to 180 min) of stirring and jet loop mixing, the concentrations of SO_4^{2-} and Ca decreased to 516.12 mg/L and 580.11 mg/L respectively. To reduce the pH of the processed water after separation from the solids, CO_2 was sparged; and this resulted in the concentration of SO_4^{2-} increasing to 544.7 mg/L and Ca concentration decreased to 562.4 mg/L after 15 min of carbonation (up to 195 min on stream).

During the treatment of 1000 L of EAMD with 167 kg KFA, 1.0 kg of lime and 0.31 kg of $Al(OH)_3$, heavy metals such as Mg, Fe, Al and Mn were significantly removed (Figure 4.16). For example, when EAMD was treated with Kendal FA for about 90 min, the concentration of elements such as Mg, Fe, Al and Mn decreased from 296.37 mg/L, 236.70 mg/L, 165.88 mg/L

and 80.56 mg/L to 32.31 mg/L, 0.00 mg/L, 5.26 mg/L and 5.50 mg/L respectively. Addition of 1.0 kg of lime after 90 min, resulted in the concentration of most of these elements further decreasing but that of Fe slightly increased. The concentration of Mg further decreased to 0.00 mg/L, Al to 1.69 mg/L, Mn decreased to 2.89 mg/L and Fe concentration increased to 1.86 mg/L up to 130 min. When 0.31 kg of $Al(OH)_3$ was added to the mixture after 130 min, the concentration of Mg remained constant at 0.00 mg/L, that of Fe slightly decreased to 1.41 mg/L, Al concentration slightly increased to 2.34 mg/L and that of Mn slightly decreased to 1.76 mg/L as shown in Figure 4.16 up to 170 min. After a further 10 min of stirring and jet loop mixing (up to 180 min), the concentration of Mg remained constant at 0.00 mg/L, that of Fe, Al and Mn decreased to 0.00 mg/L, 0.01 mg/L and 0.02 mg/L respectively, therefore, meeting the TWQR limits for domestic water use. After 15 min of carbonation using CO_2 (up to 195 min), the concentrations of Mg, Fe, Al and Mn increased to 3.84 mg/L, 0.01 mg/L, 0.69 mg/L and 0.27 mg/L respectively as shown in Figure 4.16. After treatment of EAMD (1000 L) with 167 kg of KFA, 1.0 kg of lime and 0.31 kg of $Al(OH)_3$, it was observed that, only Mg and Fe concentrations were within the TWQR required for potable, Al and Mn were not within the TWQR (Figure 4.16).

A sample of the SR recovered after 180 min of neutralisation of 1000 L of EAMD with 167 kg of KFA, 1.0 kg of lime and 0.31 kg of $Al(OH)_3$ was collected and analysed for mineralogy using XRD. The XRD results are shown in Figure 4.17.

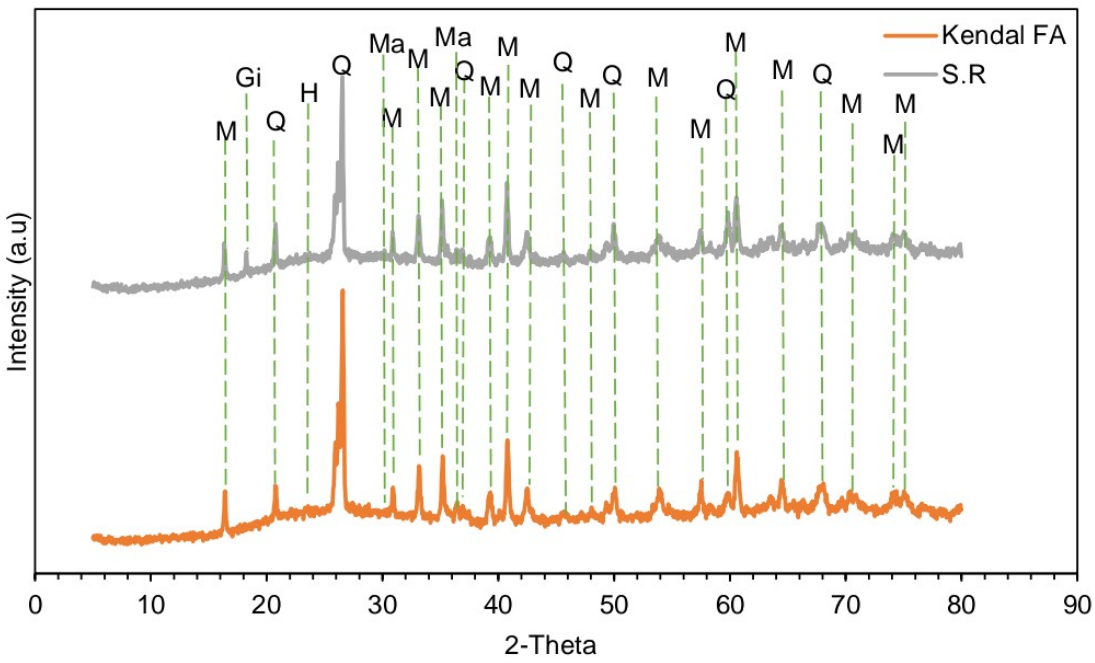

Figure 4.17: XRD spectra of the SR recovered after treatment of 1000 L of EAMD with 167 kg of KFA, 1.0 kg of lime and 0.31 kg of Al(OH)3 (Q-Quartz, M-Mullite, H-Hematite, Ma-Maghemite, Gi-Gibbsite).

The SR XRD spectra collected after 180 min of treating EAMD with KFA (167.0 kg), lime (1.0 kg) and 0.31 kg of $Al(OH)_3$ showed the appearance of a gibbsite peak at 18° 2θ being formed as a new mineral (Figure 4.17). No sign of gypsum or ettringite peaks appeared. Even after the addition of $Al(OH)_3$ ettringite precipitation did not occur. Ettringite is said to be stable in the pH range of 11.5 – 12.5, which was not reached during this experiment. The presence of gibbsite peak in the SR, proves that Al concentration was control by the formation of this mineral phase (Gitari et al., 2008b).

The XRF results of the SR recovered after treatment of EAMD (1000 L) with KFA (167 kg), lime (1.0 kg) and 0.31 kg of $Al(OH)_3$ were compared to that of the fresh KFA. The results obtained are tabulated in Table 4.7.

Table 4.7: Elemental composition of the solid residue generated after treating 1000 L of EAMD with 167 kg of KFA, 1.0 kg of lime and 0.31 kg of Al(OH)3 compared to fresh KFA

	Major oxide	
% w/w	**KFA**	**S.R**
SiO_2	53.06	50.67
Al_2O_3	30.53	28.65
CaO	5.75	4.83
Fe_2O_3	4.77	6.08
TiO_2	1.63	1.56
MgO	1.55	1.78
K_2O	0.69	0.63
Na_2O	0.16	0.08
P_2O_5	0.48	0.46
MnO	0.04	0.08
Cr_2O_3	0.03	0.03
V2O5	0.01	0.02
LOI	1.33	3.67
Total	**100.05**	**98.54**

The XRF results of the SR showed that major oxides of Fe, Mg and Mn increased in the solid residue. The increase in the amount of Fe, Mg and Mn oxides in the SR was due to the precipitation of these elements out of Eyethu AMD. CaO percentage decreased in the SR compared to fresh KFA. This decrease in CaO content was due to the dissolution of CaO in the water during treatment. The oxides of Al, Si, Ti, K, Na and P were less in the solid residue compared to fresh KFA. The decrease for SiO_2 content could be due to the leaching of Si from KFA into the water. It was observed that the SR when dried still has the properties to be used for the synthesis of geopolymeric or zeolitic materials.

4.4. COMPARISON BETWEEN LETHABO AND KENDAL FLY ASH BASED ON SO_4^{2-} REMOVAL FROM EAMD

Under this section the effectiveness of Lethabo FA on the removal of SO_4^{2-} from Eyethu AMD is compared to that of Kendal FA. SO_4^{2-} percentage removal and change in pH trends as a function of AMD: FA ratios for the final process waters are shown in Figure 4.18.

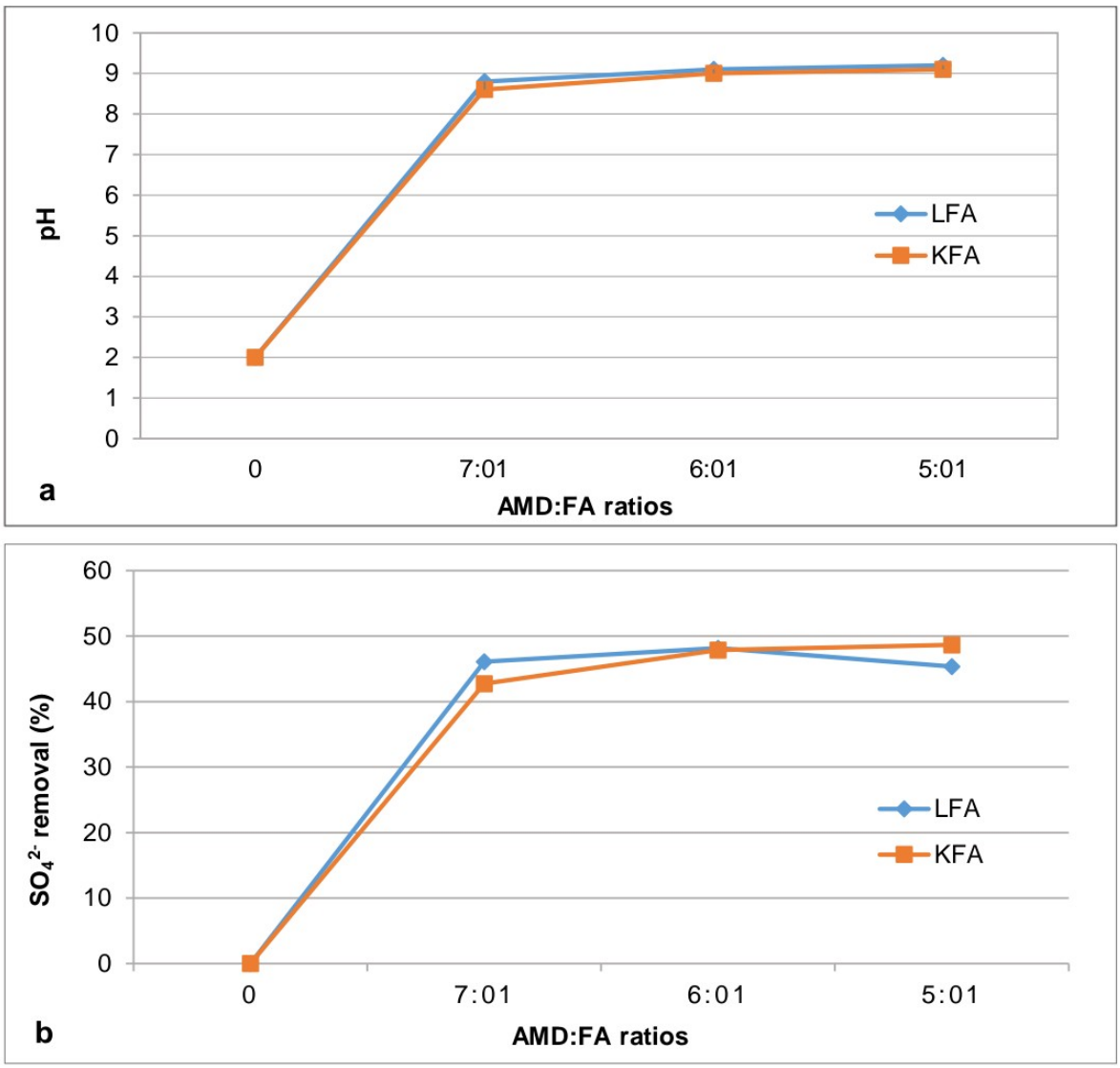

Figure 4.18: pH trends (a) and SO_4^{2-} percentage removal (b) for different AMD: FA ratios for the final process waters during treatment of EAMD with LFA or KFA.

Treatment of EAMD with different amount of LFA or KFA resulted in the pH of the mine water rising from acidic pH to alkaline pH. Figure 4.18a above shows the change in pH for the final process waters and Figure 4.18b shows the % removal of SO_4^{2-} for different AMD: FA ratios when EAMD was neutralised with LFA or KFA respectively. The contact time (70 min) of AMD and FA was the same for all the ratios investigated during treatment of EAMD with LFA (Figure

4.2) or KFA (Figure 4.10). It was observed that the breakthrough to alkaline pH for all the AMD: FA ratios investigated during treatment of EAMD with LFA was reached within 40 - 50 min (Figure 4.2). When EAMD was reacted with KFA, the breakthrough to alkaline pH was reached within 10 - 50 min as shown in Figure 4.10. When EAMD was neutralised with LFA, the final pH of the process waters for the ratios investigated varied from 8.8 – 9.2 while when EAMD was treated with KFA the final pH varied from 8.6 – 9.1 at different AMD: FA ratios as shown in Figure 4.18a. It was observed that the pH of the process waters was slightly higher for LFA when this was used to treat EAMD compared to KFA; for all the ratios investigated. Both LFA and KFA follow the same trend, as the amount of FA was increasing, the value of pH was also increasing, although the increase was marginal as shown in Figure 4.18a. Judging by the pH values, it was observed that the time required to attain a given circumneutral or alkaline pH value, was a bit longer during neutralisation of EAMD with LFA than with KFA (Figure 4.2 and 4.10). As previously reported (Gitari et al., 2006), CaO presents in FA is the main alkalinity provider and the delay observed with LFA could be due to a smaller free CaO content available for dissolution than in KFA (Table 4.1) as CaO content in KFA was a bit higher compares to LFA.

Treatment of EAMD with LFA resulted in a significant removal of SO_4^{2-} from Eyethu mine water. At higher and intermediate AMD: FA ratios of 7:1 and 6:1 respectively, SO_4^{2-} % removal was 46.11% and 48.16% respectively as shown in Figure 4.18b. As the AMD: FA ratio was lowered to 5:1, a decrease in SO_4^{2-} % removal was observed, as the amount of LFA was increased in the reaction mixture, resulting in 45.35% of SO_4^{2-} being removed (Figure 4.18b) at the contact time investigated (70 min). During treatment of EAMD with KFA, at AMD: FA ratios of 7:1, 6:1 and 5:1; SO_4^{2-} % removal was 42.74%, 47.87% and 48.66% respectively for the ratios investigated (Figure 4.18b). It was observed that at higher AMD: FA ratio, LFA % removal base on SO_4^{2-} was higher compared to KFA. At an intermediate ratio, only a slight difference was observed as the percentage removal was almost the same. At lower ratio, the % removal of SO_4^{2-} using KFA was superior to that of LFA as shown in Figure 4.18b. It was observed that both FA sources show the capacity to treat AMD, thus, significantly removing SO_4^{2-}.

4.5. SYNTHESIS OF THE GEOPOLYMER (BACKFILL MATERIAL) USING THE SOLID RESIDUES

Treatment of AMD with FA generates a significant amount of solid residues (SR) that required disposal. Under this section the parameters investigated during the synthesis of SR based

geopolymer (backfill material) are discussed, based on the strength developed by the synthesised geopolymer.

Treatment of EAMD with LFA or KFA and lime (Figures 4.5b and 4.13b) showed that SO_4^{2-} and different toxic metals were significantly removed. After the treatment process, samples of the solid residues recovered were collected and analysed for elemental composition using XRF analysis and results obtained are tabulated in Table 4.4 for LFA and Table 4.6 for KFA respectively. After XRF analysis, it was observed that both (LFA and KFA) were still possessing their pozzolanic properties to be used as binders in geopolymer synthesis. The parameters investigated are presented under section 3.7 (Table 3.6) and the results are presented in Table 4.8 and discussed below. The strength was calculated using Eq. (4.1).

Table 4.8: Compressive strength of the SR based geopolymer backfill material synthesised

	Block dimension (mm)				
Exp.	**Length**	**Width**	**Load (kN)**	**Age (days)**	**Strength (MPa)**
1	98.20	99.00	0.00	60.00	0.00
2	100.00	100.00	0.00	28.00	0.00
3	99.80	99.80	2.20	28.00	0.22
4	100.00	98.40	6.95	28.00	0.71
5	99.80	98.60	0.90	28.00	0.09
6	100.00	99.40	4.80	28.00	0.48
7	100.00	98.20	7.20	28.00	0.73
8	100.00	100.00	6.65	28.00	0.68
9	100.00	99.00	15.98	28.00	1.61
10	102.00	99.00	35.00	28.00	3.47
11	100.00	102.00	55.25	28.00	5.42
12	100.00	100.00	75.75	28.00	7.58

In order to assess the suitability of the SR to be used as backfill material a set of experiments was performed. During these experiments different parameters were investigated. Compressive strength (CS) testing was carried out for 28 days. Eq. (4.10) was used to calculate the CS of the geopolymer synthesised.

$$CS = \frac{F * 1000}{A} \quad (4.10)$$

Where, CS is the compressive strength in MPa, F is the force or load at point of failure in kN and A is the initial cross-sectional area in m^2.

4.5.1. Effect of FA on strength development

Experiment 1 – 4 in Table 3.6, investigated the effect of FA addition to the SR. The results obtained after adding FA to the SR are presented in Table 4.8 above. The first experiment as

shown in Table 3.6 was done without adding any binder or liquid activator to the SR recovered. When dried, this did not develop any strength after a prolonged curing time of 60 days as shown in Table 4.8. After adding FA (Exp. 2, Table 3.6) to the SR and a small amount of water, it was observed that the material (geopolymer) still did not develop any strength after 28 days. Addition of Na_2SiO_3 liquid (Exp. 3, Table 3.6) resulted in the material developing a strength of 0.22 MPa as shown in Table 4.8. Further strength enhancement was observed when a low amount of OPC was added (Exp. 4, Table 3.6), this resulted in the strength increasing by 69 %. Formation of calcium silicate hydrate (CSH) gel could be responsible of the increment in the strength of the material after OPC addition. It was observed that the material reached a strength of 0.71 MPa (Exp. 4, Table 4.8), which is a suitable strength for backfill.

4.5.2. Effect of NaOH and Na_2SiO_3 on strength development

Several studies have shown that NaOH and Na_2SiO_3 liquids or the mixture of these two solutions can be used as activators in the geopolymerisation process (Nyale et al., 2013; Kalombe et al., 2020b). Although, no report has been found in literature that addresses the addition of Na_2SiO_3 or NaOH liquids to the SR recovered after treatment of AMD with FA, thus, developing it into a geopolymer or backfill material. Therefore, this study will attempt to address the impact of liquid activator on the SR recovered after treatment of AMD with FA. The addition of NaOH and/or Na_2SiO_3 to the SR was done based on the formulation (best) developed by Kalombe et al. (2020b) for the synthesis of FA-based geopolymer. Reacting the SR with the mixture of NaOH and Na_2SiO_3 liquids as activator (Exp. 5, Table 3.6) did not result in the material developing sufficient strength. As shown in Table 4.8, the strength developed was only 0.09 MPa. It was observed that, although the XRF results show that the FA (SR) still possessed its pozzolanic properties after AMD treatment, it has lost its binding effect, due to the fact that it has been reacted for a long period during AMD treatment. Adding a low amount of binder (OPC) resulted in the strength of the material increasing by 81 % as shown in Table 4.8 (Exp. 6) compared to when the SR was reacted with the liquid activator only. Increasing the amount of OPC from 3 wt.% to 6 wt.% resulted in the strength of the material further increasing. During experiment 6 and 7 as shown in Table 3.6, when 3 wt.% and 6 wt.% of cement was added to the SR, the material developed a strength of 0.48 MPa and 0.73 MPa respectively as shown in the Table 4.8.

The previous study by Vadapalli et al. (2008) showed that when 3% of binder (OPC) was added to the SR, the material developed a strength of 0.11 MPa after 28 days. Increasing the curing time to 90 days, resulted in the material strength increasing to 0.23 MPa. It was observed that the material was gaining strength over time. As the curing time was further

increased to 410 days the strength developed was approximately 0.30 MPa. The authors reported that, addition of OPC as binder increased the strength of the material by 300% compared to the material without. For the current study, when 3% of binder was added the material developed a strength of 0.48 MPa after 28 days. The addition of liquid activators could be responsible for the early strength development. Strength developed after 6% of binder addition was within the range required for backfill material (0.7 – 2.0 MPa). It is necessary to stay within this range for enabling future excavation.

4.5.3. Effect of cement on strength development

Exp. 8 – 12 (Table 3.6) showed the effect of OPC on the compressive strength of the geopolymer backfill paste synthesised. The results obtained were presented in Table 4.8 (Exp. 8 – 12). To see what was the overall impact of the binder on the strength of the final product, this was increased up to 30% just for the investigation. It was observed that as the amount of the OPC binder was increasing, the compressive strength of the material was also increasing. It was observed that for material in which the binder was higher than 6%, the strength reached within the backfill strength range. When 6% of binder was added to the SR (Exp. 8, Table 3.6) with minimum amount of municipal water, the strength developed by the material was closer to the strength required for backfill, this was 0.68 MPa. It was believed that this strength will increase over time as was reported by Vadapalli et al. (2008). Further increases of the binder to 10% (Exp. 9, Table 3.6), resulted in the material developing a strength of 1.61 MPa after 28 days (Exp. 9, Table 4.8). Replacing water with Na_2SiO_3 liquid (Exp. 10, Table 3.6), resulted in the material strength increasing by 53.6% to 3.47 MPa. According to Vadapalli et al. (2008) the strength development of the SR relies on both the type of binder and the chemistry of the water used. When the amount of binder was increased to 15% (Exp. 11) and 30% (Exp. 12, Table 3.6), the material developed a strength of 5.52 MPa (Exp. 11) and 7.58 MPa (Exp. 12, Table 4.8) respectively, which is too high for backfill but allows other products to be made.

The SR has been observed to be less reactive than fresh FA when using liquid activators. However, it was observed that addition of binder resulted in the SR gaining sufficient strength. It has to be noted that the standard used for testing the material was that of concrete, since it was one aim to develop the SR into geopolymer as a construction material, for example paving bricks. The procedure followed was that of geopolymer synthesis. Unconfined compressive test, also known as uniaxial compressive strength (UCS), is a parameter commonly used in geotechnical design. The strength of backfill material is determined using uniaxial compression test. UCS refers to the maximum axial compressive stress that a specimen can resist when there is no restricting tension. Cemented paste backfill (CPB) is commonly used

as backfill material. CPB consists of mine tailings as the main component, which account for about 80 Wt.%, to which binder and water are added to achieve the desired rheological and strength characteristics (Benzaazoua et al., 2002). However, mine tailings are reported to be the cause of acid mine water generation when exposed to the impact of water and oxygen. The main disadvantage of mine tailings in backfill is the possibility of the backfill losing strength during curing time due to a chemical weathering (Benzaazoua et al., 2002).

A good backfill material is not only a material that will give support to pillars and walls, avoid subsidence or decrease the volume of voids in underground mining of coal. But this must also be able to stop AMD formation at source and the usage of SR recovered from AMD-FA treatment can provide this characteristic. The study by Gitari et al. (2008a) had shown how the SR that was recovered from AMD treatment with FA could be used to neutralise AMD in a passive treatment method. The authors reported that the SR successfully generated alkalinity over a prolonged period of time. It is common knowledge that most metals concentrations attenuation from AMD are pH dependent. The current investigation on AMD treatment with FA at pilot plant industrial capacity has shown that the SR recovered can be suitable as backfill material based on the strength developed by the material when a low amount of binder (OPC) was added to the SR.

CHAPTER 5

ENGINEERING TECHNIQUES AND PROJECT COSTING

5.1. INTRODUCTION

The engineering techniques such as the overall mass balance around the pilot plant and the energy balance around the major equipment (main pump: P1, Figure 3.7; section 3.5.3.1.) of the pilot plant are presented in this chapter. This chapter will also present the project costing.

5.2. ENGINEERING TECHNIQUES AROUND THE PILOT PLANT

Engineering techniques such as material and energy balances around the pilot plant are presented under this section.

5.2.1. Material balance

The effect of different parameters such as the amount of LFA or KFA, lime and addition of $Al(OH)_3$ were investigated during the neutralisation of EAMD at 1000 L pilot plant capacity. Based on the findings, it was revealed that LFA or KFA could be used to treat EAMD with minimum amount of lime, thus meeting the TWQR for potable water with respect to some elements at a large scale. The material balance was done in order to determine the input (raw material) and the output (product). This is none other than the law of conservation of mass application, according to which mass cannot be created or destroyed (Felder and Rousseau, 2005). The first thing done was to define the process boundary as shown in Figure 5.1 before any calculation.

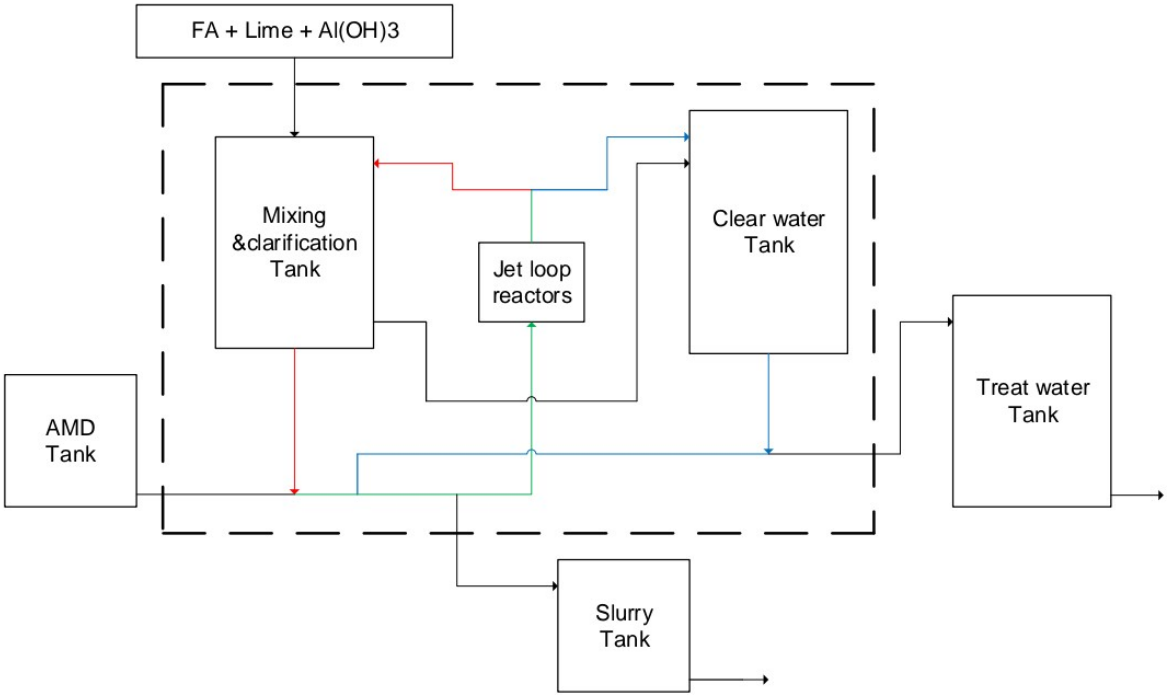

Figure 5.1: Process boundary determination for overall material balance.

All calculations were resolved around the general conservation equation (Eq. 5.1):

Material in - Material out + Generation - Consumption = Accumulation (5.1)

After defining the process boundary, different assumptions were made to simplify the general equation:

- It was assumed that the system is at steady state: the accumulation term was set to zero.
- The balanced quantity is total mass: the generation and consumption terms were set to zero. After making these assumptions, the general equation reduces to:

Material in (input) = Material out (output) (5.2)

5.2.1.1. Results and discussions

The bulk density of the AMD was measure, and this was found to be:

$$\rho_{AMD} = 996.81 \text{ kg/m}^3$$

The volume of AMD was constant throughout the experiment:

$$V_{AMD} = 1000 \text{ L} = 1 \text{ m}^3$$

Since the density and the volume of AMD are known, the mass can easily be determined using Eq. (5.3):

$$\rho = \frac{M}{V} \tag{5.3}$$

Making M subject of formula resulted in:

$$M = \rho \times V \tag{5.4}$$

$M = 996.81 \times 1 = 996.81$ kg

The mass of AMD was calculated using the density and the volume and this was found to be 996.81 kg. Figure 5.2 illustrates the system as a whole showing the streams that coming in and going out of the system boundary. The composition of the feed (input) streams, the known variables, are tabulated in Table 5.1.

Table 5.1: Composition of feed streams

Element	Stream	Mass (kg)
AMD	1	996.81
Fly Ash	2	167.00
Lime		1.00
Total mass input		1164.81

Flowrate is most given in mass flowrate than mole flowrate, because the former is more easily measured in practice than the latter.

5.2.1.2. Component balance

This consisted of determining the concentration as mass fraction of each component in the feed streams. Eq. (5.5) was used:

$$X_A = \frac{M_A}{M_T} \tag{5.5}$$

Where;

X_A: stands for mass fraction of component A

M_A: stands for mass of component A

M_T: stands for total mass of all components in a particular stream entering or leaving a system.

The mass fraction of fly ash (X_{FA}) was determined using data in Table 5.1 as follows:

$$X_{FA} = \frac{167.0}{168.0} = 0.994$$

The mass fraction of the other components such as lime and AMD are presented in Figure 5.2.

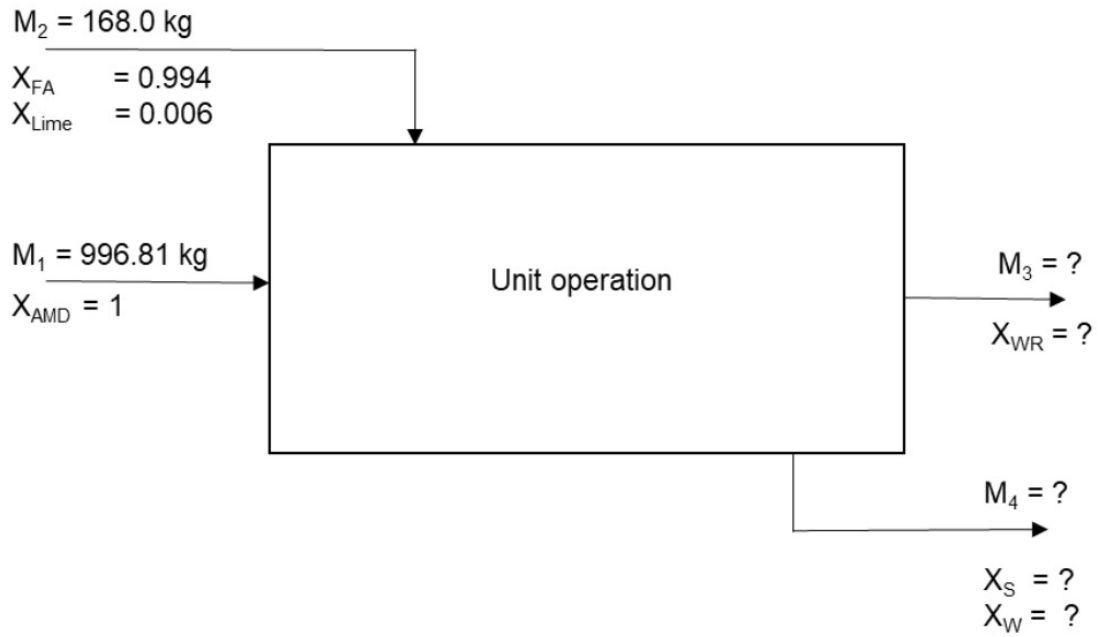

Figure 5.2: Initial overall mass balance block flow diagram (BFD).

Figure 5.2 shows the initial mass balance BFD around the pilot plant for AMD treatment process. Where;

M_1: mass of AMD fed

M_2: total mass of FA and lime fed

M_3: mass of water recovered

M_4: mass of sludge generated (solid residues) from the process

From Figure 5.2 it is necessary to observe what the known and unknown variables are. The unknowns are M_3, M_4, X_{WR} (mass fraction of the water recovered) and (X_S and X_W) are the mass fractions of solid and water in the generated solid residues respectively. After 130 min of neutralisation and carbonation, 0.695 m^3 of water was recovered which is about 692.78 kg. The percentage of water recovered was calculated using Eq. (5.6) below:

Percentage of water recovered (W_R) $= \left(\frac{M_3}{M_1}\right)$ x 100 (5.6)

$$W_R\ (\%) = \left[\left(\frac{692.78}{996.81}\right) \times 100\right] = 69.5\ \%$$

Since M_1, M_2, and M_3 are known, M_4 was calculated using Eq. (5.2) as shown below:

$M_1 + M_2 = M_3 + M_4 \rightarrow M_4 = M_1 + M_2 - M_3 = 996.81 + 168.0 – 692.78 = 472.03$ kg

The purpose of this study was not only to treat AMD with FA, by adding minimum amount of chemical reagents but also to recover as much water as possible using this treatment technique, while investigating the pilot plant performance in term of SO_4^{2-} removal, energy consumption etc. From the 1000 L of AMD that was fed, 695 L of water was recovered which represents about 69.5% of the mine water fed to the process. Since the total mass of the sludge is known, the mass of solid and water can easily be determined. It was observed that 30.5% of water was retained in the sludge produced. To determine the amount of water and solid in the sludge, the moisture content of this was first determined.

5.2.1.3. Moisture content determination

Three samples of equivalent masses of the sludge were collected and dried in the oven at a temperature of 105 ˚C for 24 hours. After cooling, the dry samples were weighed, and their masses recorded as given in Table 5.2.

Table 5.2: Moisture content of Lethabo FA

Sample	Wet mass A (g)	Dry mass B (g)	Moisture W (%)
1	250.13	89.02	64.41
2	250.12	88.97	64.43
3	250.11	89.06	64.39
		Average W	64.41

W stands for moisture.

The moisture content was determined using the following formula (Eq. 5.7):

$$W = \left(\frac{A-B}{A}\right) \times 100 \quad (5.7)$$

Where;

W: Moisture in the sample (%),

A: Mass of wet sample (g), and

B: Mass of dry sample (g).

Using Eq. (5.7), the moisture content of the sludge was calculated as follows (sample 1, Table 5.2):

$$W_1 = \left(\frac{A - B}{A}\right) \times 100 = \frac{250.13 - 89.02}{250.13} \times 100 = 64.41\%$$

The average moisture content of the generated sludge was found to be 64.41% (Table 5.2). The amount of water retained in sludge was found using the moisture and the total mass of sludge as shown below (Eq. 5.8):

Amount of H_2O in sludge = Av moisture content of sludge * mass of sludge (5.8)

Amount of H_2O in sludge = 0.6441 * 472.03 = 304.03 kg

The mass of water in the sludge was found to be 304.03 kg (0.305 m^3). 90 - 95% of this water can be recovered by installing a dewatering unit operation (sludge separator), thus improving the process. This unit operation will enable the solid to be separated from the water.

Since the total mass of the sludge and water are known, the mass of solid in sludge was calculated using Eq. (5.9):

Mass of sludge = mass of water + mass of solid (5.9)

472.03 kg = 304.03 kg + mass of solid (kg), therefore;

Mass of solid = 472.03 – 304.03 = 168.0 kg

Figure 5.3 represent the final overall mass balance BFD of the pilot plant for the neutralisation of AMD using FA and lime. All the unknown components were determined, and the results depicted below. Where the following represents:

M_1: total mass of AMD
M_2: total mass of FA and lime
M_3: total mass of the water recovered
M_4: total mass of the sludge (solid residues) produced after treatment of AMD
X_{AMD}: mass fraction of AMD
X_{FA}: mass fraction of FA
X_{Lime}: mass fraction of lime
X_{WR}: mass fraction of water recovered

X_S: mass fraction of solids in the sludge (solid residues)

X_W: mass fraction of water in the sludge

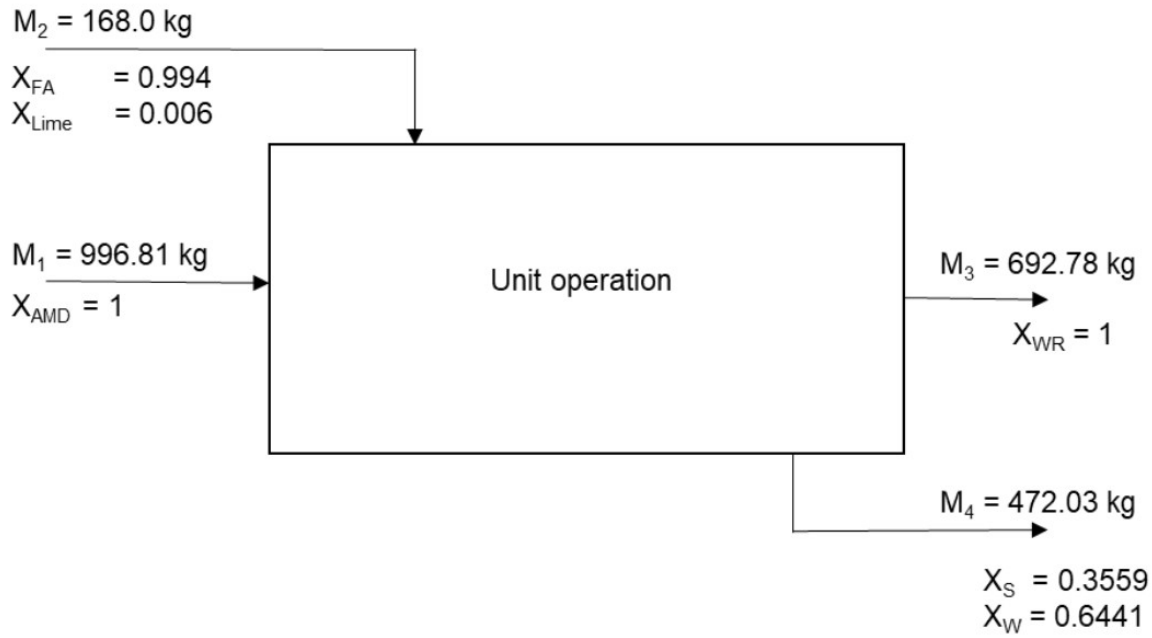

Figure 5.3: Final overall mass balance BFD of the pilot plant.

From the overall material balance as shown in Figure 5.3, 996.81 kg (1 m^3) of AMD was fed into the process, out of which 692.78 kg (0.695 m^3) was recovered as product water after the neutralisation process and the remaining water (0.305 m^3) was retained in the sludge. The total mass of the sludge generated was 472.03 kg, out of which 304.03 kg (0.305 m^3) was water and 168.0 kg solid. It was observed that the mass of solid recovered was the same as the mass of FA + lime that was fed before treatment took place. From the assumptions made, it was observed that the material fed into the system was equal to the material out of the system. Thus, mass was conserved as stated by the law of conservation of mass. If a dewatering unit operation is added to this system, 90 - 95% of clean water can be recovered using this treatment process. The water recovered during this investigation was found to be good for irrigation purposes as shown by the results obtained after various analyses, such as IC and ICP-OES (Chapter 4).

5.2.2. Energy balance

This fluid system was designed to transport a mixture of AMD, FA, lime, and $Al(OH)_3$ from one-unit operation to another while maintaining a specific flow rate, velocity, and elevation difference. The system can consume mechanical energy in the centrifugal pump during the

treatment process. In addition to mass balance, another significant quantity to consider in fluid flow calculation is energy balance or conservation of energy, as indicated in Eq. (5.10).

Accumulation = energy in – energy out + generation – consumption (5.10)

This pilot plant was designed and constructed to use less expensive chemical reagents, equipment, and lower operating cost by minimising the amount of energy consumption. The first law of thermodynamics stated that energy is conserved as shown by Eq. (5.10). As a result, energy, like mass and momentum, cannot be generated or destroyed, but it can travel across the boundaries of a system. Energy can exist in many forms: work, potential energy, kinetic energy, heat, internal energy, electrical energy, and the one that is conserved is the total energy (Sinnott, 2005).

The pilot plant under investigation consisted of three pumps as shown in the PI&D (Figure 3.7; section 3.5.3.1). The energy balance (conservation of energy) was done only on the main pump (P1); since P1 was mainly used throughout the treatment process compared to P2 and P3. It can be said that P1 is the heart of this pilot plant.

The simplest and easiest way to use the relationship between velocity, pressure and elevation in a moving fluid is by applying the Bernoulli's principle in order to determine the energy imparted by the pump to the fluid. Eq. (5.11) below shows the Bernoulli equation:

$$P_{in} + \rho\frac{v_{in}^2}{2} + \rho g z_{in} = P_{out} + \rho\frac{v_{out}^2}{2} + \rho g z_{out} \quad (5.11)$$

In Eq. (5.11), the suffixes in and out describe the input and output positions, respectively. where;

P: stands for pressure (N/m^2 or Pa)

V: stands for fluid velocity (m/s)

ρ: stands for fluid density (m^3/kg)

g: stands for gravitational acceleration (m/s^2)

z: stands for the elevation head of the cross-sectional centre in relation to a datum (m)

Energy per unit volume before equals energy per unit volume after, according to Eq. (5.11). Eq. (5.11) can be modified when gains and losses of head are taken into account. This is mostly referred to as the Extended Bernoulli equation, and this is a very useful equation in

solving most fluid flow problems. The Extended or Head form of Bernoulli equation is obtained by dividing the energy form throughout by the magnitude of the gravitational acceleration (g) and the fluid density (ρ) as shown by Eq. (5.12):

$$\frac{P_1}{\rho g} + \frac{v_1^2}{2g} + z_1 + H_P = \frac{P_2}{\rho g} + \frac{v_2^2}{2g} + z_2 + h_f + h_V \quad (5.12)$$

Where,

H_P: denotes the head developed by the pump or pumping head, or system head in meter (m)

h_f: denotes the head due to friction in pipe in meter (m)

h_V: denotes the head due to velocity or velocity head loss cause by fittings or valves etc. in meter (m)

For every equation that will be introduced a brief description will be given, then followed by calculation and discussion of the result obtained.

5.2.2.1. Methodology

The treatment (neutralisation) process was carried out for 120 minutes using the up-scaled pilot plant (1000 L) newly implemented. This pilot plant is equipped with devices which required energy for them to do work, which are, the agitator and pumps (P1, P2 and P3). The agitator was used throughout the neutralisation cycle. P2 and P3 each with a capacity of 1.5 and 0.75 kW respectively, were only used to transfer the treated water after settling from unit E-5 to unit E-7 and the product water after carbonation, was transferred from unit E-7 to unit E-8 respectively (see Figure 3.7; section 3.5.3.1). The energy consumed by these two pumps was assumed to be negligible. P1 has a capacity of 15 kW and was used throughout the experiment that is why in this investigation the conservation of energy calculation was only evaluated around P1. The results are presented and discussed below.

5.2.2.2. Results and discussions

For a quick reminder, for a smooth and easy operation the experiment was run on cycles. Such as feed cycle, this is when the AMD was fed into the system to fill up the mixing tank, neutralisation (treatment) cycle, carbonation cycle and slurry cycle to name just a few. All these cycles are described in Chapter 3 (section 3.5.3.1). The total energy consumed during the treatment process will amount to all the cycles (from AMD feeding to slurry discharging), where P1 was used. However, the energy balance calculation will be shown only for the

neutralisation cycle, since this is the main cycle of this treatment process. The information needed to perform the energy balance around P1 is given in Table 5.3.

Table 5.3: Parameters to be used for energy balance

Parameters	Units	Value
Pipe diameter	m	0.05
Pipe length	m	5.80
Viscosity	Pa.s	0.004
Density	kg/m^3	1419.45
Flowrate	m^3/s	0.0068

The diameter is the inner diameter (ID) of the pipe, the length (L) is the total length of the pipe, the viscosity (μ) is that of the slurry, the density (ρ), and the volumetric flowrate donated by Q. Table 5.4 below gives the total number of fittings and valves around the neutralisation cycle.

Table 5.4: Type of fittings and valves (neutralisation cycle)

Valves and fittings	No. of fittings	Diameter (m)	K values (K_L)	K_T values
90˚ elb standard	6	0.05	0.75	4.50
Valves (ball)	9	0.05	0.05	0.45
Tee branch flow	3	0.05	2.00	6.00
Tee inline flow	1	0.05	0.90	0.90
Union	9	0.05	0.08	0.72
Strainer	1	-	5.50	5.50
Exit (pipe)	1	0.05	1.00	1.00
Entry (pipe)	1	0.05	0.50	0.50
			Total	19.57

The K_L denotes the loss coefficient; it is a dimensionless number to calculate the velocity head loss. And K_T denotes for the sum of K_L of a particular component (fitting). This will further be described when discussing minor losses in pipes. The loss coefficients are given in textbooks (Perry et al., 1997; Coulson et al., 1999; Cengel and Cimbala, 2006)

A. Pipe cross-sectional area

Since the pipe diameter (Table 5.3) was known, the cross-sectional area (A) of the pipe was determined using the following Eq. (5.13):

$$A = \frac{\pi D^2}{4} \tag{5.13}$$

Therefore,

$$A = \frac{\pi(0.05)^2}{4} = 1.963 \times 10^{-3}\ m^2$$

The cross-sectional area of the pipe was found to be 1.963 x10^{-3} m^2.

B. Velocity of fluid in pipe

Velocity is one of the three parameters, including volumetric flowrate and mass flow rate used as measures of fluid flow rate for either open channel or pipe flow. The velocity parameter mostly used is the average velocity since velocity is never constant over the cross-sectional area of flow in pipe, duct or open channel. The average velocity was calculated using Eq. (5.14):

$$V = \frac{Q}{A} \qquad (5.14)$$

Where:
V: fluid velocity in pipe
Q: volumetric flowrate of fluid
A: pipe cross sectional area

From Eq. (5.14) the velocity was calculated by using the area found from Eq. (5.13) and the volumetric flow rate in Table 5.3. Eq. (5.14) demonstrates that the flow velocity is inversely proportional to the pipe's cross-sectional area; this is an illustration of the principle of mass conservation when applied to fluid flow. Therefore:

$$V = \frac{0.0068}{1.963 \times 10^{-3}} = 3.464\ m/s$$

The fluid was flowing in a 0.05 m pipe diameter at 3.464 m/s. If the pipe diameter is reduced, the velocity of the fluid will increase, and will decrease by increasing the diameter of the pipe.

C. Reynolds number determination

In order to determine the friction factor, the Reynolds number is needed. The Reynolds number is used to characterise the regimes of flow (Geankoplis, 1993). Studies by Reynolds show that transition from laminar to turbulent flow in tubes is a function of different factors: the diameter of the tube and the viscosity, density, and the average velocity of the fluid (liquid) (McCabe et al., 1993; Geankoplis, 1993). When grouping these four quantities the Reynolds number was obtained, which is dimensionless as shown by Eq. (5.15).

$$\mathrm{Re} = \frac{\rho V D}{\mu} \quad (5.15)$$

Where,

Re: stands for Reynolds number

μ: stands for viscosity of fluid (Pa.s)

$$\mathrm{Re} = \frac{1419.45 \text{ x } 3.464 \text{ x } 0.05}{0.004} = 61462.19$$

According to McCabe et al. (1993), flow is always laminar at a Reynolds number below 2100 and turbulent at a Reynolds number above 4000. Between values of 2100 and 4000 a transition region is found, meaning that the flow can be laminar or turbulent, depending upon the conditions at the tube entrance and the distance from the entrance. From the obtained result, it was observed that the flow in the pipe was turbulent based on the Reynolds number value of 61462.19 obtained.

D. Friction factor determination

The friction factor is dependant of the Reynolds number and the pipe roughness. The friction factor is a critical variable in determining the head loss in the pipe due to friction. The material of construction (pipe) was stainless steel with an absolute pipe roughness of 1.5 x10^{-3}. This was divided by the pipe diameter to determine the relative pipe roughness as shown in Eq. (5.16):

$$e = \frac{\varepsilon}{d} \quad (5.16)$$

Where:

e: stands for relative pipe roughness (dimensionless)

Ɛ: stands for absolute pipe roughness in metre (m)

d: pipe diameter (inside) in metre (m)

Therefore,

$$e = \frac{1.5 \times 10^{-3}}{0.05} = 0.03$$

With a Reynolds number of 61462.185 and a relative pipe roughness of 0.03, the Darcy friction factor was determined using the Moody Chart (Figure A.4, Appendix A), and this was found to be 0.059 as shown in Figure A.4.

E. Friction losses

Friction losses, also known as friction head. The viscosity of fluid and surface (inside) of pipe offer resistance to the flow of fluid through a pipe, and the energy of the moving fluid is lost in the process of overcoming it. Frictional head loss refers to the loss of energy per unit weight of fluid. This can be determined by the Darcy-Weisbach equation (White, 2003):

$$h_f = f_D \times \frac{L}{D} \times \frac{v^2}{2g} \quad (5.17)$$

Where:
h_f: denotes friction head loss (m)
f_D: denotes Darcy friction factor
L: pipe total length (m)
D: pipe diameter (inside) (m)
V: velocity (average) (m/s)
g: acceleration due to gravity (m/s^2)

Fanning friction (f_F) is equal to one quarter of the Darcy factor; therefore, the Fanning friction was calculated by dividing the Darcy factor by four, and the Fanning friction was found to be 0.01475. Replacing f_D with f_F in Eq. (5.17) the friction head was calculated as follow:

$$h_f = f_D \times \frac{L}{D} \times \frac{v^2}{2g} = 0.01475 \times \frac{5.8}{0.05} \times \frac{(3.464)^2}{2 \times 9.81} = 1.046 \text{ m}$$

Because the Fanning friction factor is more often used by chemical engineers, it was substituted for the Darcy friction factor in Eq. 5.17. The head loss due to friction in pipe was found to be 1.046 m.

F. Shock losses

Piping system consists of different components such as fittings, valves, bends, elbows, tees, pipe inlet and exit, enlargements and constructions etc. Because of the flow separation and mixing, these components disrupt the smooth flow of fluid, resulting in extra losses. Fittings experience shock losses. The type of fitting determines the magnitude of the pressure loss.

This magnitude is quantified by a constant known as the K-factor or loss coefficient (White, 2003). Eq. (5.18) is used to determine the pressure drop.

$$h_v = \sum K \frac{V^2}{2g} \quad (5.18)$$

Where:

h_v: stands for shock losses or head loss due to fittings (m)

Σ: stands for sum

K: stands for loss coefficient

Using information in Table 5.4 and Eq. (5.18), the head loss due to different components was determined as shown below. It has to be noted that the K-factor is different for each component and in most cases, the manufacturer or generic table gives it (see Figure A.5, Appendix A).

$$h_v = 19.57 \text{ x} \frac{(3.464)^2}{2 \text{ x } 9.81} = 11.969 \text{ m}$$

The head loss due to fittings was found to be 11.969 m. To minimise this loss, the number of fittings need to be kept at a minimum.

G. Pumping head

A system's total head is made up of static head, friction head, and head loss due to fittings. This can be calculated using the following formula (Eq. 5.19):

$$H_P = (z_{out} - z_{in}) + f\frac{LV_2^2}{2gD} + \Sigma K \frac{V_2^2}{2g} \quad (5.19)$$

The first term on the right-hand side in Eq. (5.19) represent the static head, the second term represent the friction head, and the last one stands for head loss due to fittings (shock losses). In a close loop circulating system, the static head is not exhibited (which is the case in the current system); therefore, the pumping head is the sum of the friction head and head loss due to fittings as shown below.

$H_P = h_f + h_v = 1.046 + 11.969 = 13.015$ m

The pump developed a total head of 13.015 m. The power to overcome this head loss was determined as shown below.

H. Fluid power determination

The fluid power, also known as the hydraulic power, is the power gained by the fluid from the pump, to increase its velocity and pressure. The following Eq. (5.20) was used to determine it:

(5.20)

$$\text{Power}_{\text{Fluid}} = \text{Q} \times \rho \times \text{H}_{\text{P}} \times \text{g}$$

Therefore,

$$\text{Power}_{\text{Fluid}} = 0.0068 \times 1419.45 \times 13.015 \times 9.81 = 1232.373\ \text{W} \approx 1.232\ \text{kW}$$

The energy imparted by the pump to the fluid was found to be 1.232 kW.

I. Shaft power

This is the mechanical power transmitted to the pump by the shaft. It is obtained by using the following Eq. (5.21):

$$\text{Power}_{\text{Shaft}} = \frac{\text{Power}_{\text{Fluid}}}{\eta_{\text{Pump}}} \quad (5.21)$$

Where,

η_{Pump}: stands for pump efficiency (%)

The Shaft power is generally determined by dividing the hydraulic power by the efficiency of the pump. With a pump efficiency of 29%. Therefore, the shaft power was calculated as follow:

$$\text{Power}_{\text{Shalt}} = \frac{1.232}{0.29} = 4.248\ \text{kW}$$

The power supplied by the motor to the pump shaft was 4.248 kW.

J. Motor power

This is the amount of energy required by the pump motor to rotate the pump shaft. It can also be referred to as the electrical power. It is calculated using the following Eq. (5.22):

$$\text{Power}_{\text{Motor}} = \frac{\text{Power}_{\text{ Shaft}}}{\eta_{\text{Motor}}} \quad (5.22)$$

Where,

η_{Motor}: represents motor efficiency (%)

The motor power is calculated by dividing the shaft power to the efficiency of the motor. The motor had an efficiency of 89.5%, thus the motor power was calculated as shown below.

$$\text{Power}_{\text{Motor}} = \frac{4.248}{0.895} = 4.746 \text{ kW}$$

With an efficiency of 89.5%, the pump motor needed a power of 4.746 kW to turn the pump shaft.

K. Energy consumption calculation

This is the energy consumed to neutralise 1000 L of AMD using FA (167 kg) and lime (1.0 kg). It is expressed by the following Eq. (5.23):

$$E = \frac{P_M * t}{3600} \quad (5.23)$$

Where,

E: stands for energy (kWh),

P_M: stands for motor power (kW), and

t: stands for time (hour)

The neutralisation of 1000 L of AMD took about 7200 s (about 2 hours). Therefore,

$$E = \frac{4.746 * 7200}{3600} = 9.492 \text{ kWh}$$

The energy consumed by the pump after 7200 s of neutralisation was found to be 9.492 kWh, which is equivalent to 34.171.2 kJ of energy consumed.

The type of pump used for this operation was a centrifugal pump with a power capacity of 15 kW, with a pump and motor efficiencies of 29% and 89.5% respectively. To minimise the loss of energy the pipe diameter was kept constant. The slurry (AMD+FA+lime) with a density and viscosity of 1419.45 kg/m^3 and 0.004 Pa.s respectively, was flowing in a pipe length of 5.80 m with a pipe diameter of 0.05 m at an average velocity of 3.464 m/s. The pump developed a head of 13.015 m, in term of pressure drop across the pump this was 181.231 kPa. The pilot plant was designed in order to use as little energy as possible during treatment of AMD and

recovering the water of a quality that meets TWQR standard in South Africa for a purpose such as domestic, irrigation or industrial application. The energy balance calculation was done specifically for the slurry centrifugal pump (P1). The power required to treat 1000 L of acid mine drainage with 167 kg of coal fly ash and 1.0 kg of lime, using a jet loop reactor pilot plant at a flow rate of 0.0068 m^3/s was found to be 4.746 kW. The energy consumed by the pump after 7200 s, which is equivalent to 120 min (2 hrs) was found to be 9.492 kWh. Comparing the actual value to the theoretical value, which was 15 kW. It was observed that the theoretical value was 68.36 % bigger than the actual value. This brought the conclusion that, the pump was oversized.

The treatment consists of different cycles to simplify the operability. The total energy consumed from feeding the AMD to the slurry discharge is given in Table 5.5.

Table 5.5: Total energy consumed during the treatment of EAMD (1000 L) with FA (167 kg) and lime (1.0 kg)

		Cycle			
Parameters	**Unit**	**Feeding**	**Neutralisation**	**Carbonation**	**Sludge**
Time	min	4.000	120.00	10.00	4.000
Fluid power	kW	0.381	1.232	0.037	0.222
Shaft power	kW	1.315	4.248	0.129	0.766
Motor power	kW	1.470	4.746	0.144	0.856
Energy consumed	kWh	0.098	9.492	0.024	0.057

The results in Table 5.5 show the power that was supplied by the pump to the fluid and the energy consumed by the pump during different cycles of the treatment process of EAMD with FA and lime. A total power of 7.216 kW was needed to treat EAMD with LFA or KFA and lime. The total energy consumed from feeding the AMD to the solid residue (sludge) discharge was found to be 9.671 kWh after 138 min (2.30 hrs) of treatment.

5.3. PROJECT COSTING

The current study consists of treating mine water with FA in combination with chemical reagents including lime CaO and $Al(OH)_3$. The mine water to be treated can be either circumneutral or acidic. The costing is done on the existing pilot plant; therefore, determining the production cost at the current plant condition (investigation study). The investment on the plant construction was obtained from the manufacture invoices based on different equipment consisting of the plant. Chemical plants are constructed to make profit, thus estimating the required investment and the cost of production is critical before determining the project's

profitability. (Sinnott, 2005). The plan is to scale up the current plant and make it a continuous process. This section presents the costing and project evaluation.

5.3.1. Treated water using optimum conditions

Different technologies for treating mine water exist, the main obstacle encountered by these technologies is the high cost associated with the treatment of the mine water. These technologies include lime neutralisation, limestone neutralisation, biological sulphate removal, biological metal removal etc. (Gitari et al., 2006). Many studies have been done on the treatment of mine water, and alternative liming agents are being sought to decrease the cost of treatment. Previous studies have shown that it is possible to neutralise mine water using FA as liming agent (Petrik et al., 2003; Gitari et al., 2006; 2008b; Vadapalli et al., 2008; Madzivire et al., 2015; Kalombe et al., 2020a). FA is being generated in huge amounts at electricity generating companies by burning coal at high temperatures. In SA, for example only 5% of the FA produced is utilised with the rest being dispose as landfill (Vadapalli et al., 2008).

In this study, the water recovered during the treatment of EAMD with FA and lime was found to be suitable for irrigation purposes. The optimum ratio during treatment of EAMD with different amounts of FA (LFA or KFA) was obtained at a L/S (AMD/FA) of 6:1 as discussed in sections 4.3.1.1 and 4.3.2.1**,** and the optimum amount (w/v %) of lime was 0.1 % (w/v %) (sections 4.3.1.2 and 4.3.2.2). The removal of SO_4^{2-} and other elements such as Fe, Mg, Al and Mn was successful with some of these elements meeting the TWQR limits for domestic water set by the DWAF.

5.3.2. Production of clean water from AMD treated with FA and lime

Under this section, different costs associated to the production cost are presented and discussed. These costs include: the capital investment cost, operating cost, working capital cost etc.

5.3.2.1. Capital investment cost

Several methods for estimating capital investment cost are available. The choice to be made depend upon the details and the amount of data available, as well as the level of accuracy desired (Peters and Timmerhaus, 1991). These methods include preliminary (approximate) estimates with an accuracy of ± 30%, authorisation (budgeting) estimates with an accuracy of ±10 - 15% and detailed (quotation) estimates with an accuracy of about ±5 - 10%. Preliminary estimates are usually considered in the initial phases of a design project due to limited cost

data and design detail, authorisation estimates are used to obtain funding to progress with the design to the stage where an accurate and more detailed estimate can be developed, whereas detailed estimates are used for project control and estimates for fixed price contracts (Sinnott, 2005).

For this study, the costs of the equipment purchased were obtained directly from the plant contractor (IMVUSA Stainless) or vendors of different parts consisting of the plant. Detailed estimates were used to evaluate the unit production cost of the current project. According to Sinnott (2005), detailed estimates are based on a finished (or almost finished) process design, firm quotations for equipment, and a comprehensive analysis and estimation of cost of construction.

Any process's total investment comprises of fixed-capital investment (FCI) for physical equipment and plant facilities, as well as working capital, which must be accessible to pay salaries, keep raw materials and products on hand, and manage other items necessitating a direct cash expenditure. As a result, while performing a costing analysis for any industrial process, capital investment costs, manufacturing costs, and expenditures, including income taxes, must all be considered (Peters and Timmerhaus, 1991). The FCI is the capital required to supply the essential production and plant facilities, whereas working capital is the capital required to operate the facility. Fixed capital is the money paid to contractors; it is a one-time expense that is not recouped at the conclusion of the project's life, except for scrap value, whereas working capital is mostly recouped at the end. A project's total capital investment is the sum of its fixed and working capital (Peters and Timmerhaus, 1991; Sinnott, 2005). Working capital is a variable cost that can range from 5% of fixed capital for a basic, single-product process with little or no completed product storage to 30% for a multi-product process generating a wide variety of product grades for a sophisticated market, for example synthetic fibres (Sinnott, 2005).

Concerning this project, the fixed capital investment was obtained from the contractor (IMVUSA Stainless Pty Ltd). This cost includes the cost of: (a) design and other engineering and construction management; (b) all equipment and their installation; (c) all piping, instrumentation and control systems. This did not include the cost of: (1) buildings and structures; (2) auxiliary facilities, such as utilities, land and civil engineering work because the current project still at an investigative stage.

Table 5.6 shows some of the equipment (major) and the installed cost of the particular equipment consisting of the pilot plant.

Table 5.6: Major equipment of the jet loop reactor pilot plant with a capacity of 1000 L

Equipment	Material of construction	Char. Size	Cost (Rand)
Mixing tank	Stainless Steel (SS)	1.5 m^3	69 832.00
Jet loop rectors	Cast Iron	-	-
Slurry pump (P1)	Cast Iron	15 kW	11 720.00
Jib crane (hoist)	Steel	250 kg	47 338.04
Clean water tank	PVC	5 m^3	11 690.00
Water recovered tank	PVC	5 m^3	18 250.00
AMD storage tank	PVC	10 m^3	36 500.00
		Total	**195 330.04**

Table 5.6 shows only the cost of major equipment; however, the fixed capital investment of this project was about R1 294 223.05, this is the money that was invested for the construction of the pilot plant with a capacity of 1000 L as shown on the P&ID in Figure 3.6 (section 3.5.4). The cost of raw materials was estimated as shown in the following section.

5.3.2.2. Estimation of operating costs

A. Raw material cost

The raw material cost consisted of the cost of lime only since the AMD and FA were free on board, these were supplied by Eskom. The transportation cost to deliver the AMD and FA on site could have been considered but these were not taken into consideration for the current study. The estimation cost of lime was based on the overall material (mass) balance of the process as shown in Figure 5.3 (section 5.2.1.3). 167 kg of FA and 1.0 kg of lime were the amount of reactants needed to neutralise 996.81 kg (1 m^3) of EAMD with 692.78 kg (0.695 m^3) of water recovered per batch. The rate of production of water recovered for the current study was 2078.34 kg (2.085 m^3) of water recovered per day. The total number of working days in one year was assumed 264 days per year, which is equivalent to 22 working days per month. Based on the water recovered as shown in Figure 5.3 (overall material balance), the plant has the capacity to produce 546 681.76 kg H_2O (equivalent to 550 440 L) per annum, which is equivalent to 550.44 m^3 per annum. The cost of raw material was estimated using a basis of 1000 kg (1 tonne) of lime for R2 852.72 (source: https://m.alibaba.com/High-Quality-Calcium-Oxide-with-Good-price/CAS:1305-78-8, Accessed on 02 November 2021). Table 5.7 shows the cost of raw material used in this study.

Table 5.7: Cost of raw materials used for a plant producing 548 681.76 kg H_2O per year

Raw materials	Ton/day	Ton/year	Rand/year
Lime	0.003	0.792	2 259.35

The results in Table 5.7 show that the amount of lime required to produce 546 681.76 kg of water per year is 0.792 tonne. The cost of lime at the market at the beginning of the year 2021 was R2 852.72. As a result, the cost of lime was R2 259.35 to produce 546 681.76 kg (550.44 m^3) of water per annum. It must be noted that the cost of raw material accounts for only 0.14% of the annual production costs as shown in Table 5.10.

B. Utilities and operating labour costs

The cost of utilities (C_{UT}) on the current study consisted of the cost of electricity only. This was estimated through the energy balance, which is presented under section (5.2.2.2). The total energy consumed per 692.78 kg of water produced was 9.671 kWh. The rate of energy consumed per day during the treatment process was 29.013 kWh for a daily production rate of 2078.34 kg (2.085 m^3) of water. The cost of electricity in SA is 209 cents per kWh (R2.09) (source: https://businesstech.co.za/news/energy/306592/south-africas-petrol-and-electricity-pricesvstheworld/#:~:text=With%20the%20RCA%20included%2C%20the,to%20106.8%20cents%20per%20kWh, Accessed on the 5th of October 2021). The estimation cost of the utilities is shown in Table 5.8.

Table 5.8: The cost of utilities used for a plant capacity of 548 681.76 kg per year of water

Equipment	kWh/day	kWh/year	Rand/year
Slurry pump (P1)	29.013	7 659.432	16 008.213

The estimated utilities cost for the slurry pump (P1) to produce 548 681.76 kg of water was found to be R16 008.213 per year as shown in Table 5.8.

The operating labour cost was based on 4 operators working on the pilot plant for a daily production of 2078.34 kg (2.085 m^3) of water. The working hours per day were 8 hours, which makes a total of 32 hours. The operating labour cost is depicted in Table 5.9.

Table 5.9: Operating labour cost for 4 operators running the pilot plant

	hour/day	Hour/year	ZAR/Hr.	Operator	ZAR/year
Operating labour cost	8	2112	73.82	4	623 631.36

The results in Table 5.9 show that a plant producing 548 681.76 kg of water per year required 4 operators and an average cost of R155 907.84 per year per operator at a rate of R73.82 per hour (Source: https://www.Salaryexpert.com/salary/job/water-plant-operator/south-africa, Accessed on 7th October 2021). The operating labour cost was R623 631.36 per year. It has to be noted that the current rate of production is not the final rate, the project still at an

investigative stage. The operating labour cost account for 38.90% of total production cost, which is very higher.

The total production cost and unit production cost summary is shown in Table 5.10. The calculation was inspired from work done by Apostolakou et al. (2009) and from Sinnott (2005).

Table 5. 10: summary of operating cost calculation for a plant capacity of 548 681.76 kg/year

Cost item	Calculations	Million Rand (ZAR)	%
1. Raw materials	From material balances	0.0022594	0.14
2. Miscellaneous materials	1 % of FCI	0.0129422	0.81
3. Utilities	From material balances	0.0160082	1.00
(A). Variable costs	(1) + (2) + (3)	0.0312098	
4. Maintenance	10 % of FCI	0.1294223	8.07
5. Operating labour	Manning estimates	0.6236314	38.90
6. Lab costs	20 % of (5)	0.1247263	7.78
7. supervision	20 % of (5)	0.1247263	7.78
8. Plant overheads	50 % of (5)	0.3118157	19.45
9. Capital charges	10 % of FCI	0.1294223	8.07
10. Insurance, local taxes, royalties	4 % of FCI	0.0517689	3.23
(B). Fixed costs	(4) + (5) + … + (10)	1.4955131	
(C). Direct production costs	(A) + (B)	1.5267229	
11. General overheads + R&D	5 % of (C)	0.0763361	4.76
(D). Annual production costs	(1) + (2) + … + (11)	1.6030591	100.00
Production cost R/kg	$\frac{\text{Annual production costs}}{\text{Plant Capacity}} = \frac{1.6030591\ \text{x}10^{6}}{548681.76} = \text{R}2.92/\text{kg}$		

Note: FCI stands for fixed capital investment

The total annual production cost for a jet loop reactor pilot plant for water neutralisation was estimated to be R1.603 million while the unit production cost was estimated to be R2.92 per kg (equivalent to R2.91/L) of water produced as shown in Table 5.10. With a daily production rate of 2078.34 kg (2085 L or 2.085 m^3), which was projected to a plant capacity of 548 681.76 kg per year (264 working days/year), this resulted in the cost of production being quite expensive compared to the price of water on the market. The average cost of potable reticulated water is R0.02448/L. Water in South Africa is tariffed based on the service rendered as well as water consumption. For example, water which is used primarily for domestic purposes and supplied to a single residential property is tariffed at R19.80 per kilo litre (kl) for water consumption of 0 to ≤ 6 kl. For industrial use, potable water is tariffed at R40.40/kl. Water reclamation – bulk tariff is R5.47/kl (this is the tariff related to the selling of water reclaimed from the Wastewater Treatment Plants and used by bulk water branch). Non-potable water for irrigation, commercial, industrial and domestic usage (user infrastructure) is

tariffed at R2.78/kl (source: https://resource.capetown.gov.za/documentcentre/Documents/Financial%20documents/Ann62021-22WaterandSanitation-Water-NoRestriction.pdf, Access on 7th November 2021). The higher cost in production is because the process was performed at a low daily production rate. Increasing the daily production rate will decrease the cost of production per litre of water produced.

The operating labour cost amounted to about 38.90% of the annual production costs. It must be noted that 548 681.76 kg (550 440 L) per year of water produced is not the final installed capacity, since the project is still at an investigative stage. The daily production rate can be increased by decreasing the contact time during the treatment of AMD with FA and lime. Thus, keeping this at a minimum. For the current study, the contact time parameter was not investigated. At the current production rate, the cost per unit production is quite high. The profitability of a chemical process plant is determined using different methods including the net present value (NPV), the return on investment (ROI), the payback period (PBP) and the discounted cash flow rate of return (DCFR). At this stage of the study none of these methods were performed as the process is quite expensive based of the unit production rate calculated (Table 5.10) compared to cost of water on the market. The profitability of this process can be can determined after the process is fully optimised.

It must be noted that the current study is performed on a semi-batch process with the aim to scale it up and make it a continuous process (next stage of the current study) based on the findings obtain during this investigation. Therefore, more investigation needs to be done to increase the daily production rate. The results shown in Chapter 4 are the first data to ever been generated for this pilot plant. Although, the treatment of mine water at a larger pilot plant capacity (1000 L) was successful; however, more data are required to validate the technology at an industrial scale.

CHAPTER 6

CONCLUSIONS AND RECOMMENDATIONS

6.1. INTRODUCTION

The present study consists of treating acid mine water from Eyethu coalmine with CFA from Lethabo and Kendal power plants. The conclusions to the research as well as the recommendations and suggestions are presented in this chapter. Answers to research questions (chapter 1, section 1.4) will also be provided in this chapter based on the general findings.

6.2. CONCLUSIONS

The main aim of this study was to evaluate the performance of a jet loop reactor pilot plant with a capacity to treat 1000 L of mine water using FA from 2 different power stations (Lethabo and Kendal) with a view to optimise the process. Treatment of mine water with FA is not new. However, this has only been done at laboratory scale, this is the first time that it is done at an industrial (pilot) scale. Previous studies at beaker and large (80 L jet loop) laboratory scale (Petrik et al., 2003; Gitari et al., 2006; Vadapalli et al., 2008; Surender, 2009; Madzivire, 2012a; Madzivire et al., 2015) showed that when mine water (AMD) was co-disposed with FA, this resulted in the pH of the water rising from acidic to circumneutral or alkaline pH. Therefore, attenuation of different toxic elements as well as SO_4^{2-}, from the mine water occurred.

In this study, the raw materials (LFA, KFA and EAMD) were characterised using different analytical methods such as XRD, XRF, ICP-OES and IC. XRD analysis showed that both LFA and KFA were predominantly made up of quartz and mullite mineral phases. Characterisation of LFA and KFA by XFR revealed that major oxides in LFA were SiO_2 (56.71%) and Al_2O_3 (29.22%), and in KFA these were SiO_2 (53.06%) and Al_2O_3 (30.53%). LFA and KFA were classified as Class F FA based on the classification by ASTM standards due to the percentage sum of Si, Al and Fe oxides which was greater than 70%. The use of FA to treat mine water takes advantage of the CaO found in the FA; in LFA and KFA this was 4.59 and 5.75% respectively. Eyethu mine water was found to be acidic. The pH value of EAMD was around pH 2.0. IC analysis for anions determination showed that SO_4^{2-} concentration in EAMD was high; with major elements including Mg, Al, Fe, Ca, and Mn; after ICP-OES analysis, the concentration of these elements was high and above the limits set by DWAF for domestic water. Based on different characterisation done, EAMD was deemed unsuitable for any purpose (domestic, industrial or irrigation).

Based on the results obtained when treating EAMD with LFA or KFA, the process was optimised at AMD:FA ratio of 6:1 using LFA or KFA, thus, increasing the water pH from acidic region to alkaline region. SO_4^{2-} percentage removal at this ratio was 48.16% and 47.87% when EAMD was neutralised with LFA or KFA respectively after 70 min of contact time. At this time a maximum pH of 9 was achieved. Treatment of EAMD with LFA or KFA at AMD: FA of 6:1 resulted in the success removal of all major elements such as Mg, Fe, Al and Mn. The percentage removal of these elements was 91.99, 99.94, 96.76 and 98.28% when using LFA, and 90.55, 99.93, 97.98 and 99.54% when using KFA.

Addition of 0.5, 1.0 and 1.5 kg of lime to the reaction mixture of EAMD and LFA resulted in the pH of the mine water reaching a value of 10.60, 11.80 and 12.20 respectively after 120 min; with SO_4^{2-} being removed by 74.63, 73.54 and 74.64% respectively. All major elements (Mg, Fe, Al and Mn) were successfully removed to within the TWQR limits required by the DWAF for domestic water for all the mixtures. In the case of EAMD treatment with KFA, the water reached a pH of 9.7, 11.50 and 11.80 after adding 0.5, 1.0 and 1.5 kg of lime respectively to the mixture of EAMD and KFA. SO_4^{2-} percentage removal was 73.82% for the mixture containing 0.5 kg of lime, 73.97 and 74.58% for the mixtures containing 1.0 and 1.5 kg of lime respectively. Major elements such Mg, Fe, Al and Mn were successfully removed to below the DWAF limits required for domestic water for all mixtures. The results obtained revealed that only a small amount of lime was needed to elevate the water pH to greater than 11. Therefore, 1.0 kg of lime was selected as the optimum amount of lime during this investigation so as to keep the chemical reagent (lime) at a minimum.

$Al(OH)_3$ addition to EAMD that have been treated to pH greater than 11 by LFA or KFA and lime did not improve the performance in cleaning up of the water with respect to SO_4^{2-} removal as the concentration of this was still above 500 mg/L. therefore, $Al(OH)_3$ addition to the process was deemed an unnecessary expense as it did not provide any additional benefit to the process. SO_4^{2-} percentage removal was found to be 74.41 and 75.01% for the mixture containing LFA or KFA respectively after $Al(OH)_3$ addition.

It was observed that when the water pH reached 11 or greater, optimum removal of Mg was achieved, this precipitates out as $Mg(OH)_2$. Fe and Al were observed to significantly being removed at pH 5 - 9 while Mn was observed to significantly being removed around pH 9 and above. Thus, the removal of these elements was found to be pH dependent. When a pH value of 11 or greater was reached, the optimum removal of all major elements within Eyethu mine water was achieved. With SO_4^{2-} being removed to within the limits set for Class II (400 – 600 mg/L) domestic water guidelines. The precipitation of gypsum at lower pH as well as ettringite

formation at higher pH, are two of the many mechanisms that controlled SO_4^{2-} concentration. Three factors were found to influence the ultimate pH of the solution and the rate of reaction during the neutralisation process, which are the AMD: FA ratio, extra lime added and contact time.

The optimum condition when treating EAMD with LFA or KFA and lime was obtained at AMD: FA ratio of 6:1 and 1.0 kg of lime to achieve a pH above 11, thus, removing SO_4^{2-} from EAMD by approximately 74%. These findings demonstrated that the treatment of mine water with FA and minimum amount of lime can be scaled up from 80 L pilot plant laboratory scale to 1000 L pilot plant industrial capacity using jet loop reactors. However, these studies (from previous investigations to the current stage) has shown that treatment of mine water using FA is site specific, therefore, the effectiveness and efficiency of the neutralisation process will depend on the mineralogy of FA as well as the chemistry of mine water as the deferential or limiting factors. The change in AMD and FA composition could slow the efficiency of neutralisation, and therefore affecting SO_4^{2-} and heavy metals removal. This factor makes it difficult to standardise the process for different qualities of FA to be used for the treatment of AMD, thus making this treatment process a flexible process with respect to FA and AMD compositions. The amount of FA and lime will be adjustable base on the quality of the AMD to be treated as well as the composition of the FA itself.

The findings after the treatment of EAMD (1000L) to a AMD:FA ratio of 6:1 using LFA or KFA and 1.0 kg of lime revealed that the process water recovered is fit for irrigation and industrial applications. Although most of the elements investigated were within the TWQR required for domestic water, this will require some polishing by ion exchange resins or zeolite adsorption to be suitable for domestic application.

The results obtained showed that it is possible to achieve a zero effluent process. The SR was found to be less reactive than FA as this could only develop a very low strength of 0.09 MPa when liquid activators (NaOH and/or Na_2SiO_3) was used. However, strength within backfill material range was achieved when low amount of OPC was added as binder. The backfill material synthesised during this study containing a mixture of SR, OPC (6%) binder and small quantity of water developed a strength of 0.68 MPa; and this material was found to be suitable to seal mine voids, as a result, air entrance can be prevented. This would stop the production of acidic mine water in abandoned mines, providing a cradle-to-cradle solution for post mining.

The amount of process water recovered after treatment of 1000 L of EAMD with 167 kg of LFA or KFA and 1.0 kg of lime after about 130 min (neutralisation and carbonation cycles) was 695 L (692.78 kg); which is about 69.5% of the water fed was recovered. The remaining water was

in the sludge. The energy balance revealed that the neutralisation cycle was the most energy consuming cycle since this was the main cycle of this treatment process. The total power required to neutralise 1000 L of EAMD with LFA or KFA (167 kg) and lime (1.0 kg) was found to be 7.216 kW. Therefore, the total energy consumed (from the feed cycle to the sludge discharge cycle) was 9.671 kWh. The findings from the energy balance revealed that the pump (P1) used during this treatment process was oversized, only 48.11% of the pump installed capacity (15 kW) was used after 138 min of the treatment (From AMD feeding cycle to sludge discharge cycle). The neutralisation cycle accounted for about 98.15% of the total energy consumed.

The information obtained from the pilot plant contractor revealed that the fixed capital investment was about R1 294 223.05, this was the money invested to build the pilot plant with a capacity to treat 1000 L of mine water. The annual production cost of a pilot plant producing 550 440 L of water per year was estimated to be R1 603 059.10 with a unit production cost estimated at R2.91/L. It has to be noted that the current production rate is not the actual production of the pilot plant, this was just estimated for the investigation at the current stage of the project. It was found that the labour operation cost accounted for about 38.90% of the annual production cost while the cost of raw material accounted only for about 0.14%. Only lime was accounted for raw material cost.

During this study, a special emphasis was given to the removal of SO_4^{2-} from mine water. The reduction of SO_4^{2-} content was used to evaluate the jet loop reactors pilot plant's performance. FA amount used and final pH achieved were found to be influenced by a variety of factors, including the mineralogy of FA and the composition or quality of the mine water to be treated. These parameters are crucial for the validation of AMD-FA treatment technology as well as its effectiveness. At a 1000 L jet loop reactor scale, AMD treatment with FA and a small amount of lime has demonstrated to be an effective process method for improving mine water quality at a larger scale. The water recovered during this study was suitable for irrigation and industrial use, meeting the TWQR established by the DWAF standard criteria for irrigation and industrial category 4. However, more data are needed to validate the technique, allowing it to produce high-quality water for domestic purposes.

6.3. RECOMMENDATIONS AND SUGGESTIONS

This study has shown that mine water from Eyethu coalmine can be successfully treated with fly ash from Lethabo and Kendal power stations, thus, significantly reducing SO_4^{2-} content and removing heavy metals from the mine water. In order to enhance the performance in cleaning

up of the water as well as increase the yield, different recommendations and suggestions are provided for future studies, these include:

- A large database is needed to validate the technology at an industrial scale by performing more experiments using fly ash from various power stations.
- Simultaneously adding fly ash and lime to the mine water so as these two reactants can react together for an extended time. An automatic data logging system will be needed to identify the optimal contact times and related in pH variations.
- Installation of a dewatering unit system (sludge separator) is recommended to increase the yield of the treated water. This can take place using either filters or deep thickeners to a solid concentration of 65 – 90% by weight. It is very important that settling trials are conducted in order to determine the thickening requirements should the process be scaled up for backfill processes.
- To investigate the effectiveness and efficiency of CO_2 to reduce Ca ions concentration from the product water.
- Installation of flow meters on different streams is recommended so that the flowrate on those streams can be measured.
- To investigate the effectiveness of $Al(OH)_3$ on SO_4^{2-} removal as ettringite precipitate.
- To assess the probability of traces elements from FA leaching into the mine water.
- To perform a full economic analysis by scaling up the process so that the process profitability can be determined.

REFERENCES

Adriano, D.C., Page, A.L., Elseewi, A.A., Chang, A.C. and Straughan, I. 1980. Utilization and Disposal of Fly Ash and Other Coal Residues in Terrestrial Ecosystems: A Review 1. *Journal of Environmental Quality*, *9*(3): 333-344.

Ahmaruzzaman, M. 2010. "A review on the utilization of fly ash", Progress in Energy and Combustion Science; 36: 327 - 363.

Akcil, A. and Koldas, S. 2006. Acid Mine Drainage (AMD): causes, treatment and case studies. *Journal of Cleaner Production*, *14*(12-13): 1139-1145.

Akinyemi, S.A., Akinlua, A., Gitari, W.M., Akinyeye, R.O. and Petrik, L.F. 2011. The leachability of major elements at different stages of weathering in dry disposed coal fly ash. *Coal Combustion and Gasification Products*, *3*(2): 28-40.

Aksu, Z. and Yener, J. 1999. The usage of dried activated sludge and fly ash wastes in phenol biosorption/adsorption: comparison with granular activated carbon. *Journal of Environmental Science & Health Part A*, *34*(9): 1777-1796.

Al Bakri, A.M., Kamarudin, H., Bnhussain, M., Nizar, I.K., Rafiza, A.R. and Zarina, Y. 2012. The processing, characterization, and properties of fly ash based geopolymer concrete. *Review on Advance Material Science*, *30*: 90-97.

Alasali, M.M. and Malhotra, V.M. 1991. Role of concrete incorporating high volumes of fly ash in controlling expansion due to alkali-aggregate reaction. *Materials Journal*, *88*(2): 159-163.

Alhamed, M. 2016. 'Passive and Active Treatment of Coal Mine Water', (15 January).

Alinnor, I.J. 2007. Adsorption of heavy metal ions from aqueous solution by fly ash. *Fuel*, *86*(5-6): 853-857.

Allison, R.P., 2005. Electrodialysis treatment of surface and waste waters. *Technical Papers. Ground Engineering*, 1-6.

American Society for Testing and Materials (ASTM). 2005 Committee C-9 on Concrete and Concrete Aggregates. *Standard specification for coal fly ash and raw or calcined natural pozzolan for use in concrete*. ASTM International.

Annandale, J.G., Jovanovic, N.Z., Hodgson, F.D.I., Usher, B.H., Aken, M.E., Van der Westhuizen, A.M., Bristow, K.L. and Steyn, J.M. 2006. Prediction of the environmental impact and sustainability of large-scale irrigation with gypsiferous mine-water on groundwater resources. *Water SA*, *32*(1): 21-28.

Apostolakou, A.A., Kookos, I.K., Marazioti, C. and Angelopoulos, K.C. 2009. Techno-economic analysis of a biodiesel production process from vegetable oils. *Fuel Processing Technology*, *90*(7-8): 1023-1031.

ASTM C-618-12. 1993. Standard Specification for Coal Fly Ash and Raw or Calcined Natural Pozzolana for Use in Concrete. West Conshohocken, PA: American Society for Testing and Materials.

Ayanda, O. S., Fatoki, O. S., Adekola, F. A. and Ximba, B. J. 2012. 'Characterization of fly ash generated from Matla power station in Mpumalanga, South Africa'. *E-Journal of Chemistry*, 9(4): 1788–1795.

Barbosa, V.F. and MacKenzie, K.J. 2003. Synthesis and thermal behaviour of potassium sialate geopolymers. *Materials Letters*, *57*(9-10): 1477-1482.

Basu, M., Pande, M., Bhadoria, P.B.S. and Mahapatra, S.C. 2009. Potential fly-ash utilization in agriculture: a global review. *Progress in Natural Science*, *19*(10): 1173-1186.

Beavon, K. 2004. Johannesburg: the making and shaping of the city. Leiden, Koninklijke Brill.

Benzaazoua, M., Belem, T. and Bussiere, B. 2002. Chemical factors that influence the performance of mine sulphidic paste backfill. *Cement and Concrete Research*, *32*(7): 1133-1144.

Berland, J.M. and Juery, C. 2002. Les procédés membranaires pour le traitement de l'eau. *Document technique FNDAE*, (14): 1-71.

Bilodeau, A. and Malhotral, V.M. 1992. Concretes Incorporating High Volumes of ASTM Class F Fly Ashes: Mechanical Properties and Resistance to De-icing Salt Scaling and to Chloride-Ion Penetration. *Special Publication*, 132: 319-350.

Bilodeau, A., Sivasundaram, V., Painter, K.E. and Malhotra, V.M. 1994. Durability of concrete incorporating high volumes of fly ash from sources in the USA. *Materials Journal*, *91*(1): 3-12.

Blissett, R.S. and Rowson, N.A. 2012. A review of the multi-component utilisation of coal fly ash. *Fuel*, *97*: 1-23.

Blowes, D.W., Ptacek, C.J., Jambor, J.L. and Weisener, C.G. 2003. The geochemistry of acid mine drainage. *Treatise on geochemistry*, *9*: 612.

Bobbins, K. 2015. Acid mine drainage and its governance in the Gauteng City-Region.

Bosman, D.J. 1983. Lime treatment of acid mine water and associated solids/liquid separation. *Water Science and Technology*, *15*(2): 71-84.

Bosman, D.J., Clayton, J.A., Maree, J.P. and Adlem, C.J.L. 1990. Removal of sulphate from mine water with barium sulphide. *International Journal of Mine Water*, *9*(1-4): 149-163.

Bowell, R.J., Dill, S., Cowan, J. and Wood, A. 2004. A review of sulfate removal options for mine waters. *Proceedings of mine water*, 75-88.

Brahammaji, G.S.V., and Muthyalu, P.V. 2015. A Study on Performance of Fly Ash Based Geopolymer Concrete. *International Journal of Advances in Engineering and Technology*, 8(4): 574-586.

Breck, D.W., 1984. *Zeolite molecular sieves: structure, chemistry and use*. Krieger.

California Mining Association. 1991. Mine Waste Management. *Edited and Authored by Ian Hutchison and Richard D. Ellison. Sponsored by the California Mining Association, Sacramento, CA*.

Campaner, V.P., Luiz-Silva, W. and Machado, W. 2014. Geochemistry of acid mine drainage from a coal mining area and processes controlling metal attenuation in stream waters, southern Brazil. *Anais da Academia Brasileira de Ciências*, *86*(2): 539-554.

Campbell, A.E. 1999. *Chemical, physical and mineralogical properties associated with the hardening of some South African fly ashes* (Doctoral dissertation, University of Cape Town).

Cengel, Y. A. and Cimbala, J.M. 2006. Fluid Mechanics Fundamentals and Applications. New York: McGraw-Hill.

Chindaprasirt, P. and Rattanasak, U. 2010. Utilization of blended fluidized bed combustion (FBC) ash and pulverized coal combustion (PCC) fly ash in geopolymer. *Waste Management*, *30*(4): 667-672.

Cho, H., Oh, D. and Kim, K. 2005. A study on removal characteristics of heavy metals from aqueous solution by fly ash. *Journal of Hazardous Materials*, *127*(1-3): 187-195.

Coetzee, H., Hobbs, P.J., Burgess, J.E., Thomas, A. and Keet, M. 2010. *Report to the Inter-ministerial committee on acid mine drainage: Mine water management in the* 272 *Witwatersrand gold fields with special emphasis on acid mine drainage.* South Africa: Council for Geoscience.

Coetzee, H., Van Tonder, D., Wade, P., Esterhuyse, S., Van Wyk, N., Ndengu, S., Venter, J. and Kotoane, M. 2007. Acid mine drainage in the Witwatersrand: Department of Minerals and Energy, Pretoria, Council for Geoscience Report No 2007-0260: 81.

Coetzee, H., Wade, P. and Winde, F. 2006. An assessment of sources, pathways, mechanisms and risks of current and future pollution of water and sediments in the Wonderfontein Spruit Catchment, Water Research Commission, WRC Report No. 1214/1/06, Pretoria: 202.

Cole-Parmer. 2021. pH-measurement. 5 March. (Online) Available at: https://www.coleparmer.com/tech-article/ph-measurement-faqs. (Access on 10 May 2021).

Corbett, E.A., Anderson, R.C. and Rodgers, C.S. 1996. Prairie revegetation of a strip mine in Illinois: fifteen years after establishment. *Restoration Ecology*, 4(4): 346-354.

Coulson, J.M., Richardson, J.F., Backhurst, J.R., and Harker, J.H. 1999. Chemical Engineering: Fluid Flow, Heat and Mass Transfer. Volume 1, 6th Ed. Lincoln: Butterworth-Heinemann.

Coulton, R., Bullen, C. and Hallett, C. 2003. The design and optimisation of active mine water treatment plants. *Land Contamination and Reclamation*, *11*(2): 273-280.

Cravotta III, C.A. 2008. Dissolved metals and associated constituents in abandoned coal-mine discharges, Pennsylvania, USA. Part 1: Constituent quantities and correlations. *Applied Geochemistry*, *23*(2): 166-202.

Cravotta III, C.A., Brady, K.B., Rose, A.W. and Douds, J.B., 1999, March. Frequency distribution of the pH of coal-mine drainage in Pennsylvania. In *US Geological Survey Toxic Substances Hydrology Program–Proceedings of the Technical Meeting: US Geological Survey Water-Resources Investigations Report*, 99: 313-324.

Davidovits, J. 1991. Geopolymers. Journal of thermal analysis, 37(8): 1633-1656

Davidovits, J. 1994, October. Properties of geopolymer cements. In *First international conference on alkaline cements and concretes* (1: 131-149). Scientific Research Institute on Binders and Materials Kiev, Ukraine.

Davidovits, J., 1999, June. Chemistry of geopolymeric systems, terminology. In *Geopolymer*, 99(292): 9-39). sn.

Davidovits, J., 2008. *Geopolymer chemistry and applications*. Geopolymer Institute.

Department of Water Affairs and Forestry. 1993. South African Water Quality, Guidelines: 4. DWAF, SA.

Department of Water Affairs and Forestry. 1996a. "South African Water Quality, Guidelines: 2nd ed. 1*: Domestic Use*". Pretoria, South Africa: CSIR Environmental Services.

Department of Water Affairs and Forestry. 1996b. "South African Water Quality Guidelines: 2nd ed. 3: *Industrial Use*". Pretoria, South Africa: CSIR Environmental Services.

Department of Water Affairs and Forestry. 1996c. "South African Water Quality, Guidelines: 2nd ed. 4: *Agricultural Use: Irrigation*". Pretoria, South Africa: CSIR Environmental Services.

Duarte, R.A. and Ladeira, A.C. 2011. Study of manganese removal from mining effluent. *Mine Water-Managing the Challenges (IMWA 2011, Aachen, Germany)*, 297-300.

Engineering ToolBox. 2004. Pipe and Tube System Components – Minor (Dynamic) Loss Coefficients. (online) Available at: https://www.engineeringtollbox.com/minor-loss-coeffients-pipes-d_626.html, (Access on October 15, 2021)

Environmental Protection Agency (EPA). 2009. "Frequently Asked Questions Regarding the Disposal of Coal Ash at the Perry County Arrowhead Landfill Uniontown, Alabama", U. S. Environmental Protection Agency Superfund Division.

Eskom. 2016. Ash management, February 20. Available at: http://www.eskom.co.za/news/Pages/Feb20.aspx. (Accessed 25 June 2021).

Fatoba, O.O. 2008. Chemical compositions and leaching behaviour of some South African fly ashes, MSc thesis, Chemistry Department, University of the Western Cape, Cape Town.

Felder, R.M. and Rousseau, R.W. 2005. Elementary principles of chemical processes*, 3rd ed*. John Wiley.

Ferguson, K.D. and Erickson, P.M. 1988. Pre-mine prediction of acid mine drainage. In *Environmental Management of Solid Waste* (24-43). Springer, Berlin, Heidelberg.

Feris, L. and Kotze, L. 2015. The regulation of acid mine drainage in South Africa: law and governance perspectives. Potchefstroom Electronic Law Journal.17: 2104-2163.

Ferone, C., Colangelo, F., Cioffi, R., Montagnaro, F. and Santoro, L. 2011. Mechanical performances of weathered coal fly ash based geopolymer bricks. *Procedia Engineering*, *21*: 745-752.

Fester, V.G., Slatter, P.T., Vadapalli, V.R.K. and Petrik, L., 2008. Use of Fly Ash to Treat Acid Mine Drainage Before Use in Backfill Operations. Paste 2008, International Seminar on Paste and Thickened Tailings, Kasane.

Ford, K.L. 2003. Passive treatment systems for acid mine drainage.

Fripp, J., Ziemkiewicz, P.F. and Charkavorki, H. 2000. *Acid mine drainage treatment*. ARMY ENGINEER WATERWAYS EXPERIMENT STATION VICKSBURG MS.

Gaikwad, R.W., Sapkal, R.S. and Sapkal, V.S. 2010. Removal of copper ions from acid mine drainage wastewater using ion exchange technique: factorial design analysis. *Journal of Water Resource and Protection*, *2*(11): 984-989.

Gazea, B., Adam, K. and Kontopoulos, A. 1996. A review of passive systems for the treatment of acid mine drainage. *Minerals Engineering*, *9*(1): 23-42.

Geankoplis, C.J. 1993. *Transport processes and separation process principles, 3rd ed.* New Jersey: Prentice-Hall.

Geldenhuys, A.J., Maree, J.P., de Beer, M. and Hlabela, P. 2003. An integrated limestone/lime process for partial sulphate removal. *Journal of the Southern African Institute of Mining and Metallurgy*, *103*(6): 345-353.

Germishuizen, C., Franzsen, S., Grobler, H., Simate, G.S. and Sheridan, C.M. 2018. Case study modelling for an ettringite treatment process. *Water SA*, *44*(1): 86-92.

Ghosal, S. and Self, S.A. 1995. Particle size-density relation and cenosphere content of coal

fly ash. *Fuel*, *74*(4): 522-529.

Giannopoulou, I. and Panias, D. 2007. Structure, design and applications of geopolymeric materials. In *Proceedings of the 3rd International Conference on Deformation Processing and Structure of Materials*, 20-22.

Gilbert, N. 2015. Acid Mine Drainage, what are the dangers? Pennsylvania State. November 3

Gitari, M.W., Petrik, L.F., Etchebers, O., Key, D.L., Iwuoha, E. and Okujeni, C. 2006. Treatment of acid mine drainage with fly ash: removal of major contaminants and trace elements. *Journal of Environmental Science and Health Part A*, *41*(8): 1729-1747.

Gitari, W.M., Petrik, L.F., Etchebers, O., Key, D.L. and Okujeni, C. 2008b. Utilization of fly ash for treatment of coal mines wastewater: Solubility controls on major inorganic contaminants. *Fuel*, *87*(12): 2450-2462.

Gitari, W.M., Petrik, L.F., Etchebers, O., Key, D.L., Iwuoha, E. and Okujeni, C. 2008a. Passive neutralisation of acid mine drainage by fly ash and its derivatives: A column leaching study. *Fuel*, *87*(8-9): 1637-1650.

Gitari, W.M., Petrik, L.F., Key, D.L. and Okujeni, C. 2010. Partitioning of major and trace inorganic contaminants in fly ash acid mine drainage derived solid residues. *International Journal of Environmental Science & Technology*, *7*(3): 519-534.

Gitari, W.M., Petrik, L.F., Key, D.L. and Okujeni, C. 2013. Inorganic contaminants attenuation in acid mine drainage by fly ash and its derivatives: column experiments. *International Journal of Environment and Pollution*, *51*(1-2): 32-56.

Gitari, W.M., Somerset, V.S., Petrik, L.F., Key, D., Iwuoha, E. and Okujeni, C. 2003. Treatment of Acid Mine Drainage with Fly Ash: Removal of Major, Minor Elements, SO_4 and Utilization of the Solid Residues for Wastewater Treatment. In *International Ash Utilization Symposium, Centre for Applied Energy Research, University of Kentucky,* 1-23.

Golden Software. 2018. What is a piper plot (trilinear diagram)? 19 September. (Online) Available at: https://support.goldensoftware.com/hc/en-us/articles/115003101648-What-is-a-piper-plot-trilinear-diagram-. (Access on 2 February 2021).

González, A., Navia, R. and Moreno, N. 2009. Fly ashes from coal and petroleum coke

combustion: current and innovative potential applications. *Waste Management & Research*, *27*(10): 976-987.

Gray, N.F. 1998. Acid mine drainage composition and the implications for its impact on lotic systems. *Water Research*, *32*(7): 2122-2134.

Hanson, A. 1995. Natural Zeolites. Many merits, meagre markets. *Ind. Miner.*, *339*: 40-53.

Hardjito and Rangan. 2005c. Development and Properties of Low-Calcium Fly Ash-Based Geopolymer Concrete: Curtin University of Technology.

Hardjito, D. 2005b. Studies of fly ash-based geopolymer concrete (Doctoral dissertation, Curtin University).

Hardjito, D., Wallah, S.E., Sumajouw, D.M. and Rangan, B.V. 2005a. Fly ash-based geopolymer concrete. *Australian Journal of Structural Engineering*, *6*(1): 77-86.

Hedin, R.S. and Nairn, R.W. 1992. Designing and sizing passive mine drainage treatment systems. *US Bureau of Mines, Pittsburgh Research Centre, Pittsburgh, USA*.

Hedin, R.S. and Watzlaf, G.R. 1994b. The effects of anoxic limestone drains on mine water chemistry. *USBM SP A*, *6*: 185-194.

Hedin, R.S., Watzlaf, G.R. and Nairn, R.W. 1994a. Passive treatment of acid mine drainage with limestone. *Journal of Environmental Quality*, *23*(6): 1338-1345.

Höller, H. and Wirsching, U. 1985. Zeolite formation from fly ash. *Fortschritte der Mineralogie*, *63*(1): 21-43.

Hollman, G.G., Steenbruggen, G. and Janssen-Jurkovičová, M. 1999. A two-step process for the synthesis of zeolites from coal fly ash. *Fuel*, *78*(10): 1225-1230.

https://businesstech.co.za/news/energy/306592/south-africas-petrol-and-electricity-prices-vstheworld/#:~:text=With%20the%20RCA%20included%2C%20the,to%20106.8%20cents%20per%20kWh. (Accessed on the 5th of October 2021)

https://emis.vito.be/en/bat/tools-overview/wass/techniques. (Access on 25 March 2021).

https://m.alibaba.com/High-Quality-Calcium-Oxide-with-Good-price/CAS:1305-78-8. (Accessed on 02 November 2021).

https://resource.capetown.gov.za/documentcentre/Documents/Financial%20documents/Ann62021-22WaterandSanitation-Water-NoRestriction.pdf. (Access on 7th November 2021).

https://www.carbonbrief.org/mapped-worlds-coal-power-plants. (Access on 15 February 2021).

https://www.Salaryexpert.com/salary/job/water-plant-operator/south-africa. (Accessed on 7 October 2021).

Hu, M., Zhu, X. and Long, F. 2009. Alkali-activated fly ash-based geopolymers with zeolite or bentonite as additives. *Cement and Concrete Composites*, *31*(10): 762-768.

Huggins, F.E. 2002. Overview of analytical methods for inorganic constituents in coal. *International Journal of Coal Geology*, *50*(1-4): 169-214.

International Atomic Energy Agency. 2002. Application of Ion Exchange Processes for the Treatment of Radioactive Waste and Management of Spent Ion Exchangers. Vienna

Itskos, G., Koukouzas, N., Vasilatos, C., Megremi, I. and Moutsatsou, A. 2010. Comparative uptake study of toxic elements from aqueous media by the different particle-size-fractions of fly ash. *Journal of Hazardous Materials*, *183*(1-3): 787-792.

Iyer, R.S. and Scott, J.A. 2001. Power station fly ash—a review of value-added utilization outside of the construction industry. *Resources, Conservation and Recycling*, *31*(3): 217-228.

Izquierdo, M., Querol, X., Davidovits, J., Antenucci, D., Nugteren, H. and Fernández-Pereira, C. 2009. Coal fly ash-slag-based geopolymers: microstructure and metal leaching. *Journal of Hazardous Materials*, *166*(1): 561-566.

Jennings, S.R., Blicker, P.S. and Neuman, D.R. 2008. Acid mine drainage and effects on fish health and ecology: *A Review*. Reclamation Research Group.

Johnson, D.B. and Hallberg, K.B. 2005. Acid mine drainage remediation options: a review. *Science of the Total Environment*, *338*(1-2): 3-14.

Kalin, M., Fyson, A. and Wheeler, W.N. 2006. The chemistry of conventional and alternative treatment systems for the neutralization of acid mine drainage. *Science of the Total Environment*, *366*(2-3): 395-408.

Kalombe, R.M., Ojumu, T.V., Katambwe, V.N., Nzadi, M., Bent, D., Nieuwouldt, G., Madzivire, G., Kevern, J. and Petrik, L.F. 2020a. Treatment of acid mine drainage with coal fly ash in a jet loop reactor pilot plant. *Minerals Engineering*, *159*, 106611.

Kalombe, R.M., Ojumu, V.T., Eze, C.P., Nyale, S.M., Kevern, J. and Petrik, L.F. 2020b. Fly ash based Geopolymer building materials for green and sustainable development. *Materials*, *13*(24): 5699.

Kefeni, K.K., Msagati, T.A. and Mamba, B.B. 2017. Acid mine drainage: prevention, treatment options, and resource recovery: a review. *Journal of Cleaner Production*, *151*: 475-493.

Kentish, S.E. and Stevens, G.W. 2001. Innovations in separations technology for the recycling and re-use of liquid waste streams. *Chemical Engineering Journal*, *84*(2): 149-159.

Kim, S.J., Lim, K.H., Joo, K.H., Lee, M.J., Kil, S.G. and Cho, S.Y. 2002. Removal of heavy metal-cyanide complexes by ion exchange. *Korean Journal of Chemical Engineering*, *19*(6): 1078-1084.

Kleinmann, R.L.P., Hedin, R.S. and Nairn, R.W. 1998. Treatment of mine drainage by anoxic limestone drains and constructed wetlands. In *Acidic Mining Lakes* (303-319). Springer, Berlin, Heidelberg.

Klink, M.J. 2003, The potential use of South African coal fly ash as a neutralization treatment option for acid mine drainage, MSc thesis, University of the Western Cape, Cape Town.

Kong, D.L. and Sanjayan, J.G. 2008. Damage behavior of geopolymer composites exposed to elevated temperatures. *Cement and Concrete Composites*, *30*(10): 986-991.

Koukouzas, N., Hämäläinen, J., Papanikolaou, D., Tourunen, A. and Jäntti, T. 2007. Mineralogical and elemental composition of fly ash from pilot scale fluidised bed combustion of lignite, bituminous coal, wood chips and their blends. *Fuel*, *86*(14): 2186-2193.

Kruger, R.A. 1997. Fly ash beneficiation in South Africa: creating new opportunities in the marketplace. *Fuel*, *76*(8): 777-779.

Kruger, R.A. and Krueger, J.E. 2005. Historical development of coal ash utilization in South Africa. *WOCA Lexington April,* 11-15.

Kumari, S., Udayabhanu, G. and Prasad, B. 2010. Studies on environmental impact of acid mine drainage generation and its treatment: an appraisal. *Indian Journal of Environmental Protection*, *30*(11): 953-967.

Kumari, S., Udayabhanu, G. and Prasad, B. 2010. Studies on environmental impact of acid mine drainage generation and its treatment: an appraisal. *Indian Journal of Environmental Protection*, *30*(11): 953-967.

Kumpiene, J., Lagerkvist, A. and Maurice, C. 2007. Stabilization of Pb- and Cu-contaminated soil using coal fly ash and peat. *Environmental pollution*, *145*(1): 365-373.

Kuyucak, N. 2002. Acid mine drainage prevention and control options. *CIM bulletin*: 96-102.

Lai, K.C., Chen, J.W., Chen, W.T., Wan, T.J., Wen, J.C. and Shu, C.M. 2014. Applications of the Taguchi Method for Key Parameter Screening in Electrodialysis Reversal Used for High Salinity Wastewater. *CLEAN–Soil, Air, Water*, *42*(12): 1751-1758.

Langley, W.S., Carette, G.G. and Malhotra, V.M. 1989. Structural concrete incorporating high volumes of ASTM class fly ash. *Materials Journal*, *86*(5): 507-514.

Larsen, D. and Mann, R. 2005. Origin of high manganese concentrations in coal mine drainage, eastern Tennessee. *Journal of Geochemical Exploration*, *86*(3): 143-163.

Li, Y. and Lin, Y. 2002. *Compacting solid waste materials generated in Missouri to form new products: final technical report*. Capsule Pipeline Research Center, College of Engineering, University of Missouri-Columbia.

Lingling, X., Wei, G., Tao, W. and Nanru, Y. 2005. Study on fired bricks with replacing clay by fly ash in high volume ratio. *Construction and building materials*, *19*(3): 243-247.

Lokeshappa, B. and Dikshit, A.K. 2011. Disposal and management of fly ash. *International Conference on Life Science and Technology IPCBEE*, 3: 11-14.

Lottermoser, B.G., 2010. Mine Wastes: Characterization, Treatment, Environmental Impacts. 3rd Ed. Berlin: Springer-Verlag Berlin Heidelberg.

Luis, F. O., Marcos, L. S., Rubens, M., Claudete, G., James, C., Silva, L. F. O., Oliveira, M. L. S., Kautzmann, R. M., Ramos, C. G., Izquierdo, M., Dai, S., Wilcox, J., Hoffman, J. and Hower, J. C. 2014. 'Suggested Citation format for this article : Geochemistry and Mineralogy of Coal-

Fired Circulating Fluidized Bed Combustion Fly Ashes'.

Lukacs, H. and Ortolano, L. 2015. West Virginia has not directed sufficient resources to treat acid mine drainage effectively. *The Extractive Industries and Society*, *2*(2): 194-197.

Madzivire, G. 2010a. *Removal of sulphates from South African mine water using coal fly ash,* MSc thesis, Chemistry Department, University of the Western Cape.

Madzivire, G. 2012a. "Chemistry and speciation of potentially toxic and radioactive elements during mine water treatment" (Doctoral dissertation, University of the Western Cape).

Madzivire, G., Gitari, W.M., Vadapalli, V.R.K. and Petrik, L.F. 2015. Jet loop reactor application for mine water treatment using fly ash, lime and aluminium hydroxide. *International Journal of Environmental Science and Technology*, *12*(1): 173-182.

Madzivire, G., Gitari, W.M., Vadapalli, V.R.K., Ojumu, T.V. and Petrik, L.F. 2011. Fate of sulphate removed during the treatment of circumneutral mine water and acid mine drainage with coal fly ash: Modelling and experimental approach. *Minerals Engineering*, *24*(13): 1467-1477.

Madzivire, G., Gitari, W.M., Viswanath, R.K., Vadapalli, V.R.K. and Petrik, L.F. 2012b. Application of a jet loop reactor to enhance removal of sulphates from mine water using coal fly ash, lime and aluminium hydroxide. *International Mine Water Association:* Annual conference.

Madzivire, G., Maleka, P.P., Vadapalli, V.R., Gitari, W.M., Lindsay, R. and Petrik, L.F. 2014. Fate of the naturally occurring radioactive materials during treatment of acid mine drainage with coal fly ash and aluminium hydroxide. *Journal of Environmental Management*, *133*: 12-17.

Madzivire, G., Petrik, L.F., Gitari, W.M., Balfour, G., Vadapalli, V.R.K. and Ojumu, T.V. 2009. Role of PH on sulphate removal from circumneutral mine water using coal fly ash.

Madzivire, G., Petrik, L.F., Gitari, W.M., Ojumu, T.V. and Balfour, G. 2010b. Application of coal fly ash to circumneutral mine waters for the removal of sulphates as gypsum and ettringite. *Minerals Engineering*, *23*(3): 252-257.

Maest, A.S., Nordstrom, D.K. and LoVetere, S.H. 2004. Questa baseline and pre-mining ground-water quality investigation 4. Historical surface-water quality for the Red River Valley, New Mexico, 1965 to 2001. *US Geological Survey Scientific Investigations Report*, *5063*: 150.

Malhotra, V.M. 1990. Durability of concrete incorporating high-volume of low-calcium (ASTM Class F) fly ash. *Cement and Concrete Composites*, *12*(4): 271-277.

Malhotra, V.M. 2002. High-Performance High-Volume Fly Ash Concrete, ACI Concrete International, 24(7): 1-5.

Malhotra, V.M. and Ramezanianpour, A.A., 1994. Fly ash in Concrete. 2nd edition. *CANMET, Ontario*, 21-25.

Manoharan, V., Yunusa, I.A.M., Loganathan, P., Lawrie, R., Skilbeck, C.G., Burchett, M.D., Murray, B.R. and Eamus, D. 2010. Assessments of Class F fly ashes for amelioration of soil acidity and their influence on growth and uptake of Mo and Se by canola. *Fuel*, *89*(11): 3498-3504.

Maslehuddin, M., Al-Mana, A.I., Shamim, M. and Saricimen, H. 1989. Effect of Sand Replacement on the Early-Age Strength Gain and Long-Term Corrosion-Resisting Characteristics of Fly Ash Concrete. *Materials Journal*, *86*(1): 58-62.

Mattigod, S.V., Rai, D., Eary, L.E. and Ainsworth, C.C. 1990. Geochemical factors controlling the mobilization of inorganic constituents from fossil fuel combustion residues: I. Review of the major elements. *Journal of Environmental Quality*, *19*(2): 188-201.

McCabe, W.L., Smith, J.C. and Harriott, P. 1993. Unit operations of chemical engineering, 5th ed. New York: McGraw-Hill.

McCarthy, T.S. 2011. The impact of acid mine drainage in South Africa. *South African Journal of Science*, *107*(5-6): 1-7.

Misheer, N., Madzivire, G., Gitari, W. M., Ojumu, T. V., Balfour, G. and Petrik, L. F (2010). Removal of sulphates from South African mine water using coal fly ash. – In: Wolkersdorfter, Ch. & Freund, A. Mine Water & Innovative Thinking, 151 – 155. Sydney, Nova Scotia (CBU Press).

Missengue-Na-Moutoula, R. 2016. Synthesis of ZSM-5 zeolite from South African fly ash and its application as solid catalyst, Doctoral dissertation, Chemistry Department, University of the Western Cape.

Mohan, S. and Gandhimathi, R. 2009. Removal of heavy metal ions from municipal solid waste leachate using coal fly ash as an adsorbent. *Journal of Hazardous Materials*, *169*(1-3): 351-359.

Moncur, M.C., Ptacek, C.J., Blowes, D.W. and Jambor, J.L. 2005. Release, transport and attenuation of metals from an old tailings impoundment. *Applied Geochemistry*, *20*(3): 639-659.

Moreno, N., Querol, X., Ayora, C., Pereira, C.F. and Janssen-Jurkovicová, M. 2001. Utilization of zeolites synthesized from coal fly ash for the purification of acid mine waters. *Environmental Science and Technology*, *35*(17): 3526-3534.

Morin, K.A. and Hutt, N.M. 2001. Environmental geochemistry of mine site drainage*: Practical theory and case studies, Digital Edition*. MDAG Publishing (www. mdag. com), Surrey, British Columbia.

Moriyama, R., Takeda, S., Onozaki, M., Katayama, Y., Shiota, K., Fukuda, T., Sugihara, H. and Tani, Y. 2005. Large-scale synthesis of artificial zeolite from coal fly ash with a small charge of alkaline solution. *Fuel*, *84*(12-13): 1455-1461.

Munnik, V., Hochmann, G., Hlabane, M. and Law, S. 2010. The social and environmental consequences of coal mining in South Africa. *A CASE STUDY. Environmental Monitoring Group*.

Murayama, N., Yamamoto, H. and Shibata, J. 2002. Mechanism of zeolite synthesis from coal fly ash by alkali hydrothermal reaction. *International Journal of Mineral Processing*, *64*(1): 1-17.

Muriithi, G.N., Petrik, L.F. and Doucet, F.J. 2014. Remediation of industrial brine using coal-combustion fly ash and CO_2. *Desalination*, *353*, 30-38.

Musyoka, N.M., Missengue, R., Kusisakana, M. and Petrik, L.F. 2014. Conversion of South African clays into high quality zeolites. *Applied Clay Science*, *97*: 182-186.

Musyoka, N.M., Petrik, L.F. and Hums, E., 2012b. Synthesis of zeolite A, X and P from a South African coal fly ash. In *Advanced Materials Research,* 512: 1757-1762. Trans Tech Publications Ltd.

Musyoka, N.M., Petrik, L.F., Balfour, G., Ndungu, P., Gitari, W.M. and Hums, E. 2012a. Synthesis of zeolites from coal fly ash: Application of a statistical experimental design. *Research on Chemical Intermediates*, *38*(2): 471-486.

Musyoka, N.M., Petrik, L.F., Fatoba, O.O. and Hums, E. 2013. Synthesis of zeolites from coal fly ash using mine waters. *Minerals Engineering*, *53*: 9-15.

Myneni, S.C., Traina, S.J. and Logan, T.J. 1998. Ettringite solubility and geochemistry of the Ca (OH) 2–Al2 (SO4) 3–H2O system at 1 atm pressure and 298 K. *Chemical Geology*, *148*(1-2), 1-19.

Nairn, R.W. and Mercer, M.N. 2000. Alkalinity generation and metals retention in a successive alkalinity producing system. *Mine Water and the Environment*, *19*(2), 124-133.

Neculita, C.M., Zagury, G.J. and Bussière, B. 2007. Passive treatment of acid mine drainage in bioreactors using sulphate-reducing bacteria. *Journal of Environmental Quality*, *36*(1): 1-16.

Nkongolo, E.B. 2020. *Passive treatment of acid mine drainage using South African coal fly ash in a column reactor*, MEng thesis, Chemical Engineering Department, Cape Peninsula University of Technology.

Nollet, H., Roels, M., Lutgen, P., Van der Meeren, P. and Verstraete, W. 2003. Removal of PCBs from wastewater using fly ash. *Chemosphere*, *53*(6): 655-665.

Nyale, S.M. 2014. Geopolymers from South African Fly Ash: Synthesis and Characteristics. Doctoral dissertation, Chemistry Department, University of the Western Cape.

Nyale, S.M., Babajide, O.O., Birch, G.D., Böke, N. and Petrik, L.F. 2013. Synthesis and characterization of coal fly ash-based foamed geopolymer. *Procedia Environmental Sciences*, *18*: 722-730.

Olds, W.E., Tsang, D.C., Weber, P.A. and Weisener, C.G. 2013. Nickel and zinc removal from acid mine drainage: roles of sludge surface area and neutralising agents. *Journal of Mining*, *2013*.

Oztekin, E. and Altin, S. 2016. Wastewater treatment by electrodialysis system and fouling problems. *TOJSAT*, *6*(1): 91-99.

Palomo, A., Grutzeck, M.W. and Blanco, M.T. 1999. Alkali-activated fly ashes: a cement for the future. *Cement and Concrete Research*, *29*(8): 1323-1329.

Pandey, V.C. and Singh, N. 2010. Impact of fly ash incorporation in soil systems. *Agriculture, Ecosystems and Environment*, *136*(1-2): 16-27.

Perry, R. H., Green, D. W., and Maloney, J. O. 1997. Perry's Chemical Engineer's Handbook, 7th Ed. New York: McGraw-Hill.

Peters, M.S. and Timmerhaus, K.D. 1991. Plant design and economics for chemical engineers, 4th ed. New York: McGraw-Hill.

Petrik, L., White, R., Klink, M., Somerset, V., Key, D.L., Iwuoha, E., Burgers, C. and Fey, M.V., 2005. Utilization of fly ash for acid mine drainage remediation. *Water Research Commission Report*, (1242/1): 05.

Petrik, L.F., White, R.A., Klink, M.J., Somerset, V.S., Burgers, C.L. and Fey, M.V. 2003. Utilization of South African fly ash to treat acid coal mine drainage, and production of high quality zeolites from the residual solids. In *Proceedings of the Ash Utilization Symposium, Lexington, KY, USA* (Vol. 2022), October.

Pierre Louis, A.M., Yu, H., Shumlas, S.L., Van Aken, B., Schoonen, M.A. and Strongin, D.R. 2015. Effect of phospholipid on pyrite oxidation and microbial communities under simulated acid mine drainage (AMD) conditions. *Environmental Science and Technology*, *49*(13): 7701-7708.

Potgieter-Vermaak, S.S., Potgieter, J.H., Monama, P. and Van Grieken, R. 2006. Comparison of limestone, dolomite and fly ash as pre-treatment agents for acid mine drainage. *Minerals Engineering*, *19*(5): 454-462.

Querol, X., Umaña, J.C., Plana, F., Alastuey, A., Lopez-Soler, A., Medinaceli, A., Valero, A., Domingo, M.J. and Garcia-Rojo, E. 2001. Synthesis of zeolites from fly ash at pilot plant scale. Examples of potential applications. *Fuel*, *80*(6): 857-865.

Ram, L.C., Masto, R.E. 2010. "An appraisal of the potential use of fly ash for reclaiming coal mine spoil", Journal of Environmental Management; 91: 603 - 617.

Rose, A.W. 2004. April. Vertical flow systems—effects of time and acidity relations. In *Proceeding annual meeting of the american sociecty of mining and reclamation and the 25th West Virginia Surface Mine Drainage Task Force, Morgantown WV, USA* (1595-1616).

Saadat, A.H.M., Islam, M.S., Islam, M.S., Parvin, F. and Sultana, A., 2018. Desalination Technologies for Developing Countries: A Review. *Journal of Scientific Research*, *10*(1): 77-97.

Saikia, N., Kato, S. and Kojima, T. 2006. Behavior of B, Cr, Se, As, Pb, Cd, and Mo present in waste leachates generated from combustion residues during the formation of ettringite. *Environmental Toxicology and Chemistry: An International Journal*, *25*(7): 1710-1719.

Sakorafa, V., Michailidis, K. and Burragato, F. 1996. Mineralogy, geochemistry and physical properties of fly ash from the Megalopolis lignite fields, Peloponnese, Southern Greece. *Fuel*, *75*(4): 419-423.

Salomons, W. and Förstner, U. eds. 2012. *Environmental management of solid waste: Dredged material and mine tailings*. Berlin: Springer Science & Business Media.

Scheetz, B.E. and Earle, R. 1998. Utilization of fly ash. *Current Opinion in Solid State and Materials Science*, *3*(5): 510-520.

Scott, R. 1995. Flooding of Central and East Rand Gold Mines: *An Investigation into Controls Over the Inflow Rate, Water Quality and the Predicted Impacts of Flooded Mines: Report*. WRC.

Seervi, V., Yadav, H.L., Srivastav, S.K. and Jamal, A. 2017. Overview of active and passive systems for treating acid mine drainage. *IARJSET*, *4*(5): 131-137.

Sheoran, A.S. and Sheoran, V. 2006. Heavy metal removal mechanism of acid mine drainage in wetlands: a critical review. *Minerals engineering*, *19*(2): 105-116.

Shon, H.K., Vigneswaran, S., Kandasamy, J. and Cho, J. 2002. Membrane technology for organic removal in wastewater.

Simate, G.S. and Ndlovu, S. 2014. Acid mine drainage: Challenges and opportunities. *Journal of Environmental Chemical Engineering*, *2*(3): 1785-1803.

Singh, G. 1987. Mine water quality deterioration due to acid mine drainage. *International journal of mine water*, *6*(1): 49-61.

Sinnott, R., 2005. Coulson and Richardson Chemical Engineering*: Chemical Engineering Design,* Vol. 6, 4th ed. Oxford: Elsevier Buttreworth-Heinmann.

Skousen, J.G. 2002. A brief overview of control and treatment technologies for acid mine drainage. *American Society of Mining and Reclamation*, 879-899.

Skousen, J.G. and Ziemkiewicz, P.F. 2005. Performance of 116 passive treatment systems for acid mine drainage. *Proceedings, American Society of Mining and Reclamation, Breckenridge, CO*, 1100-1133.

Skousen, J.G., Rose, A., Geidel, G., Foreman, J., Evans, R. and Hellier, W. 1998. Handbook of technologies for avoidance and remediation of acid mine drainage. *National Mine Land Reclamation Center, Morgantown*, *131*.

Skousen, J.G., Sexstone, A. and Ziemkiewicz, P.F. 2000. Acid mine drainage control and treatment. American Society of Agronomy and American Society for Surface Mining and Reclamation. *Agronomy*, *41*(6): 1-42.

Skousen, J.G., Simmons, J., McDonald, L.M. and Ziemkiewicz, P.F. 2002. Acid–base accounting to predict post-mining drainage quality on surface mines. *Journal of Environmental Quality*, *31*(6): 2034-2044.

Skousen, J.G., Zipper, C.E., Rose, A., Ziemkiewicz, P.F., Nairn, R., McDonald, L.M. and Kleinmann, R.L. 2017. Review of passive systems for acid mine drainage treatment. *Mine Water and the Environment*, *36*(1): 133-153.

Smit, J.P. and Pretorius, L.E. 2000. The treatment of polluted mine water. *Journal of African Earth Sciences*, *31*(1): 72-72.

Somerset, V., Petrik, L. and Iwuoha, E. 2008. Alkaline hydrothermal conversion of fly ash precipitates into zeolites 3: the removal of mercury and lead ions from wastewater. *Journal of Environmental Management*, *87*(1): 125-131.

Song, J. and Choi, Y. 2015. Design of photovoltaic systems to power aerators for natural purification of acid mine drainage. *Renewable Energy*, *83*: 759-766.

Srinivasan, R. and Manoj, D. 2017. Flexural Behavior of Reinforced Geopolymer Concrete under Day-Light Curing. *International Journal of Engineering Science and Computing*.

Steenari, B.M., Schelander, S. and Lindqvist, O. 1999. Chemical and leaching characteristics of ash from combustion of coal, peat and wood in a 12 MW CFB–a comparative study. *Fuel*, *78*(2): 249-258.

Stevens, G. and Dunn, D. 2004. Fly ash as a liming material for cotton. *Journal of Environmental Quality*, *33*(1): 343-348.

Surender, D. 2009. *Active neutralization and amelioration of acid mine drainage with fly ash*, MSc thesis, University of the Western Cape.

Takeda, H., Hashimoto, S., Honda, S. and Iwamoto, Y. 2010. In-situ formation of novel geopolymer–zeolite hybrid bulk materials from coal fly ash powder. *Journal of the Ceramic Society of Japan*, *118*(1380): 771-774.

Taylor, J., Pape, S. and Murphy, N. 2005, August. A summary of passive and active treatment technologies for acid and metalliferous drainage (AMD). In *Proceedings of the in Fifth Australian workshop on Acid Mine Drainage*.

Temuujin, J., Williams, R.P., Riessen, A. 2009. "Effect of mechanical activation of fly ash on the properties of geopolymer cured at ambient temperature". *Journal of Materials Processing Technology;* 209, 5276 - 5280.

Tkaczewska, E., Mróz, R. and Łój, G. 2012. Coal–biomass fly ashes for cement production of CEM II/AV 42.5 R. *Construction and Building Materials*, *28*(1): 633-639.

Tolonen, E.T., Sarpola, A., Hu, T., Rämö, J. and Lassi, U. 2014. Acid mine drainage treatment using by-products from quicklime manufacturing as neutralization chemicals. *Chemosphere*, *117*: 419-424.

Trumm, D. 2010. Selection of active and passive treatment systems for AMD—flow charts for New Zealand conditions. *New Zealand journal of geology and geophysics*, *53*(2-3): 195-210.

Trussell-technologies. 2021. The Process and Water Quality Specialists: *Desalination*. (Online) Available at: http://www.trusselltech.com/technologies/desalination/classes-of-pressure-driven-membranes. (Access on 25 March 2021).

Tutu, H., McCarthy, T.S. and Cukrowska, E. 2008. The chemical characteristics of acid mine drainage with particular reference to sources, distribution and remediation: The Witwatersrand Basin, South Africa as a case study. *Applied Geochemistry*, *23*(12): 3666-3684.

US EPA. 1994 Acid Mine Drainage Prediction. Technical Document. U.S. Environmental Protection Agency, Office of Solid Waste Special Waste Branch, EPA530-R-94-036, NTIS PB94-201829.

Vadapalli, V.R.K., Fester, V., Petrik, F.L. and Slatter, P. 2014. Effect of fly ash size fraction on the potential to neutralise acid mine draining and rheological properties of sludge. *Desalination and Water Treatment*, 52(37-39): 6947-6955.

Vadapalli, V.R.K., Gitari, M.W., Petrik, L.F., Etchebers, O. and Ellendt, A. 2012. Integrated acid mine drainage management using fly ash. *Journal of Environmental Science and Health, Part A*, *47*(1): 60-69.

Vadapalli, V.R.K., Klink, M.J., Etchebers, O., Petrik, L.F., Gitari, W., White, R.A., Key, D. and Iwuoha, E., 2008. Neutralization of acid mine drainage using fly ash, and strength development of the resulting solid residues. *South African Journal of Science*, *104*(7-8): 317-322.

Van Dam, T. J. 2010. Geopolymer concrete (No. FHWA-HIF-10-014).

Van Jaarsveld, J.G.S., Van Deventer, J.S.J. and Lorenzen, L. 1997. The potential use of geopolymeric materials to immobilise toxic metals: Part I. Theory and applications. *Minerals Engineering*, *10*(7): 659-669.

Vano Engineering. 2012. Head Loss Coefficients. (Online) Available at: https://vanoengineering.wordpress.com/2012/12/30/head-loss-coefficients. (Access on 15 October 2021).

Vassilev, S.V. and Vassileva, C.G. 2007. A new approach for the classification of coal fly ashes based on their origin, composition, properties, and behaviour. *Fuel*, *86*(10-11): 1490-1512.

Wade, P.W., Woodborne, S., Morris, W.M., Vos, P. and Jarvis, N.V. 2002. Tier 1 risk assessment of selected radionuclides in sediments of the Mooi River Catchment. *WRC Project*, (K5/1095).

Wałek, T.T., Saito, F. and Zhang, Q. 2008. The effect of low solid/liquid ratio on hydrothermal synthesis of zeolites from fly ash. *Fuel*, *87*(15-16): 3194-3199.

Wang, S. and Wu, H. 2006. Environmental-benign utilisation of fly ash as low-cost adsorbents. *Journal of Hazardous Materials*, *136*(3): 482-501.

Warren, C.J. and Dudas, M.J. 1984. Weathering Processes in Relation to Leachate Properties of Alkaline Fly Ash 1. *Journal of Environmental Quality*, *13*(4): 530-538.

Weitkamp, J. 2000. Zeolites and catalysis. *Solid State Ionics*, *131*(1-2): 175-188.

White, F. M. 2003. Fluid Mechanics, 5th Ed. New York: McGraw-Hill.

White, S. 2003. Wetland Use in Acid Mine Drainage Remediation.

Winde, F. and Wade, P.W. 2006. *An Assessment of Sources, Pathways, Mechanisms and Risks of Current and Potential Future Pollution of Water and Sediments in Gold-mining Areas of the Wonderfonteinspruit Catchment: Report to the Water Research Commission*. Water Research Commission.

Woolard, C. ., Strong, J. and Erasmus, C. 2002. 'Evaluation of the use of modified coal ash as a potential sorbent for organic waste streams.' *Applied Geochemistry*, 17: 1159–1164.

World Energy Council (WEC). 2016. World energy resources, 24th ed, 13 October 2016. (Online). Available at: https://www.worldenergy.org/publications/2016/world-energy-resources-2016/. (Access 25 April 2021).

World Health Organization. 1993. *Guidelines for drinking-water quality*. World Health Organization.

World Health Organization. 2011. *Guidelines for drinking-water quality, 3th ed, incorporating first and second addenda Volume 1 - Recommendations.* Geneva: WHO Press.

Xu, H. and Van Deventer, J.S.J. 2000. The geopolymerisation of alumino-silicate minerals. *International Journal of Mineral Processing*, *59*(3): 247-266.

Yadav, H.L. and Jamal, H.Y.A. 2015. Removal of heavy metals from acid mine drainage: a review. *International Journal of New Technology in Science and Engineering.*, *2*: 77-84.

Young, S.C. 1993. Physical and hydraulic properties of fly ash and other by-products from

coal combustion. Electric Power Research Institute.

Zagury, G.J., Neculita, C. and Bussiere, B. 2007. Passive treatment of acid mine drainage in bioreactors: short review, applications, and research needs. In *Proceedings of the 60th Canadian geotechnical conference and 8th joint CGS/IAH-CNC specialty groundwater conference, Ottawa, Canada* (1439-1446).

Zaluski, M., Foote, M., Manchester, K., Canty, M., Willis, M., Consort, J., Trudnowski, J., Johnson, M. and Harrington-Baker, M.A. 1999. Design and construction of bioreactors with sulfate-reducing bacteria for acid mine drainage control In Situ and On-Site Bioremediation. In *The Fifth International Symposium, San Diego, California*.

Ziemkiewicz, P.F., Skousen, J.G. and Simmons, J. 2003. Long-term performance of passive acid mine drainage treatment systems. *Mine Water and the Environment*, *22*(3): 118-129.

Zipper, C. and Skousen, J.G. 2014. Passive Treatment of Acid Mine Drainage. *Acid Mine Drainage, Rock Drainage, and Acid Sulphate Soils: Causes, Assessment, Prediction, Prevention, and Remediation*, 339-353.

Zipper, C.E., Skousen, J.G. and Jage, C.R. 2018. Passive treatment of acid-mine drainage.

APPENDIX

APPENDIX A

Under this section the spectra obtained from the XRD analysis are presented. The friction factor determination from the moody diagram is also presented.

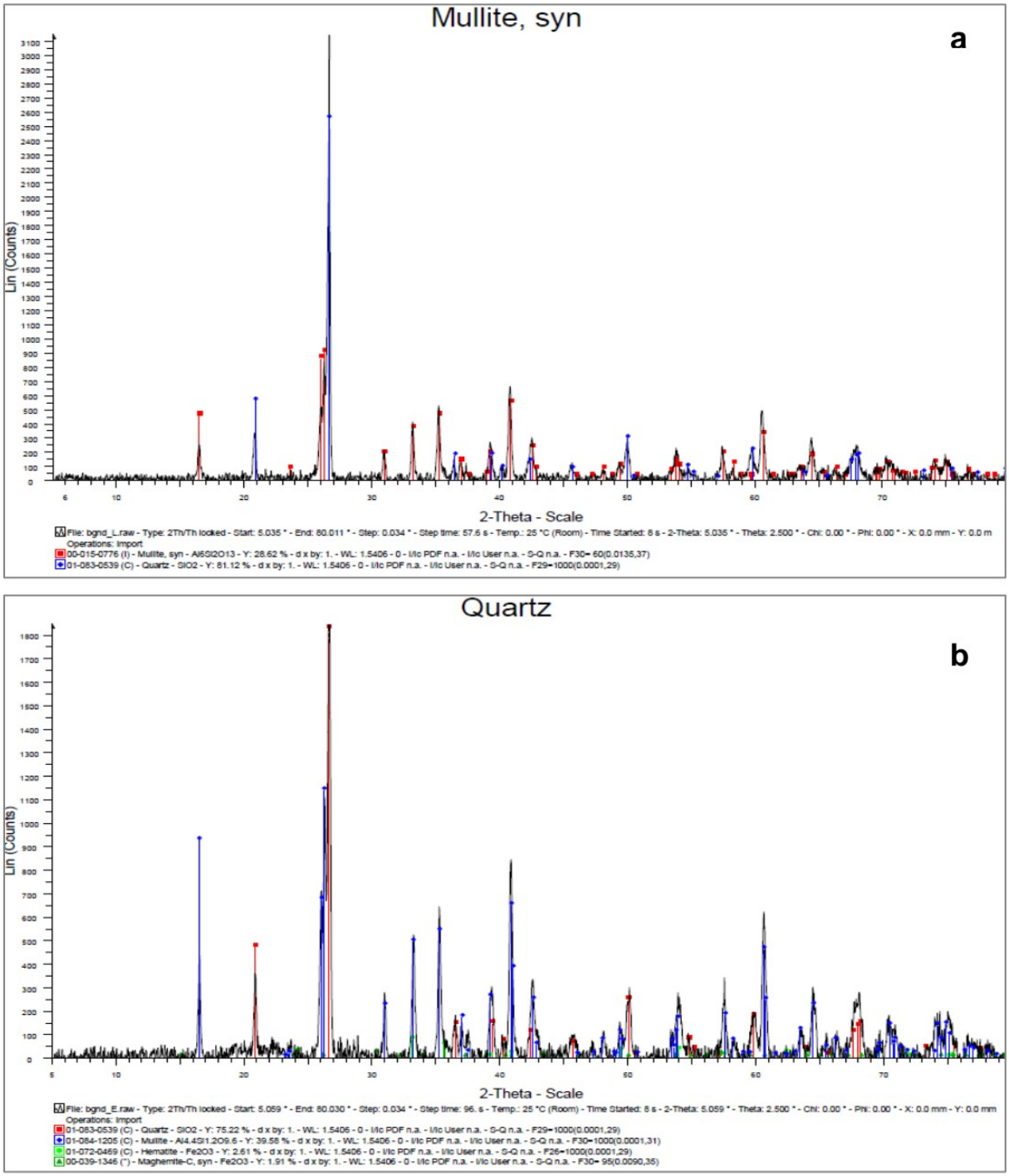

Figure A.1: Mineral phase identification responsible for the peaks on the raw LFA (a) and KFA (b) spectra.

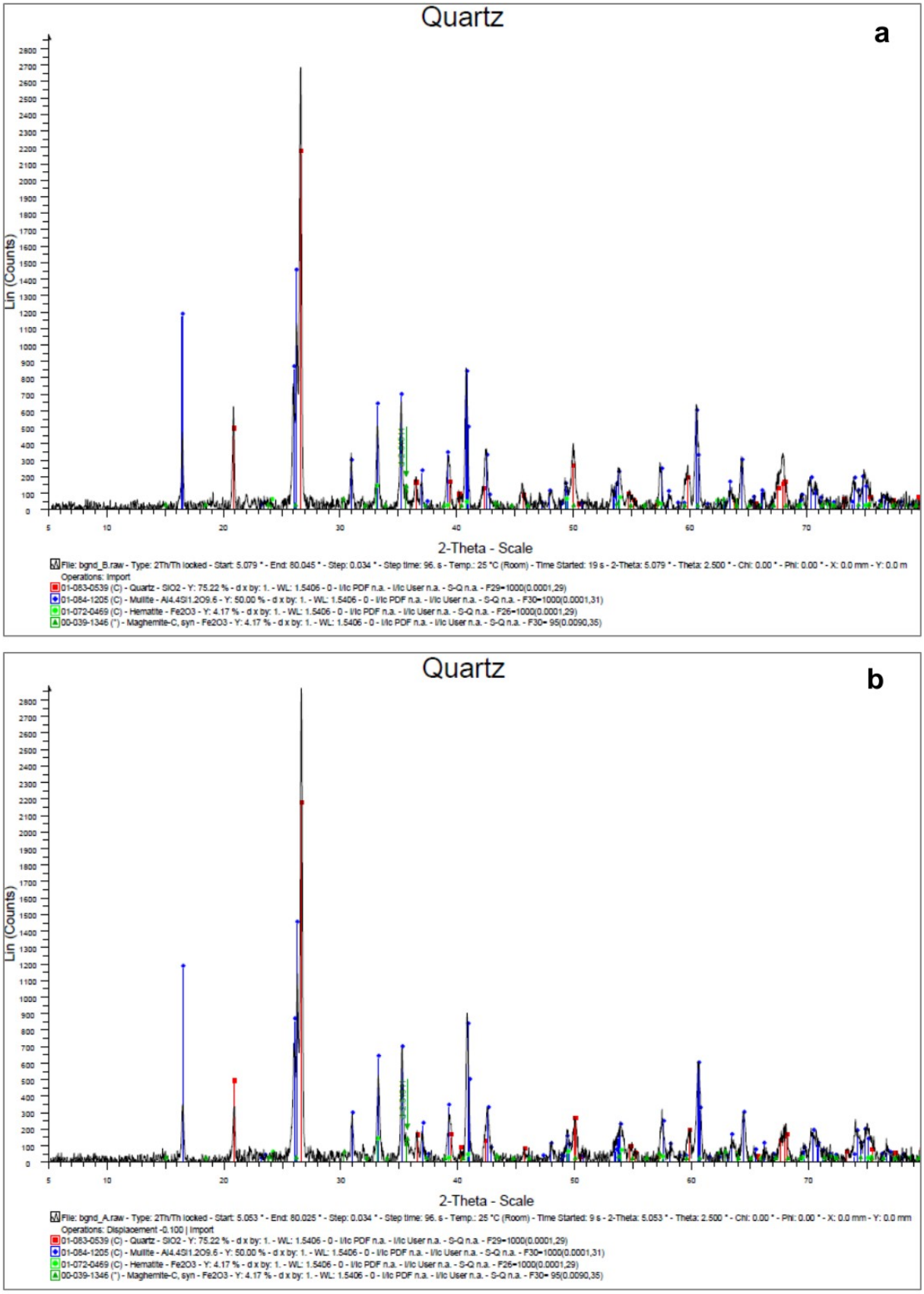

Figure A.2: Mineral phase identification responsible for the peaks on the SR spectra recovered after treatment of EAMD (1000 L) with 167 kg of LFA (a) or KFA (b) and 1.0 kg of lime.

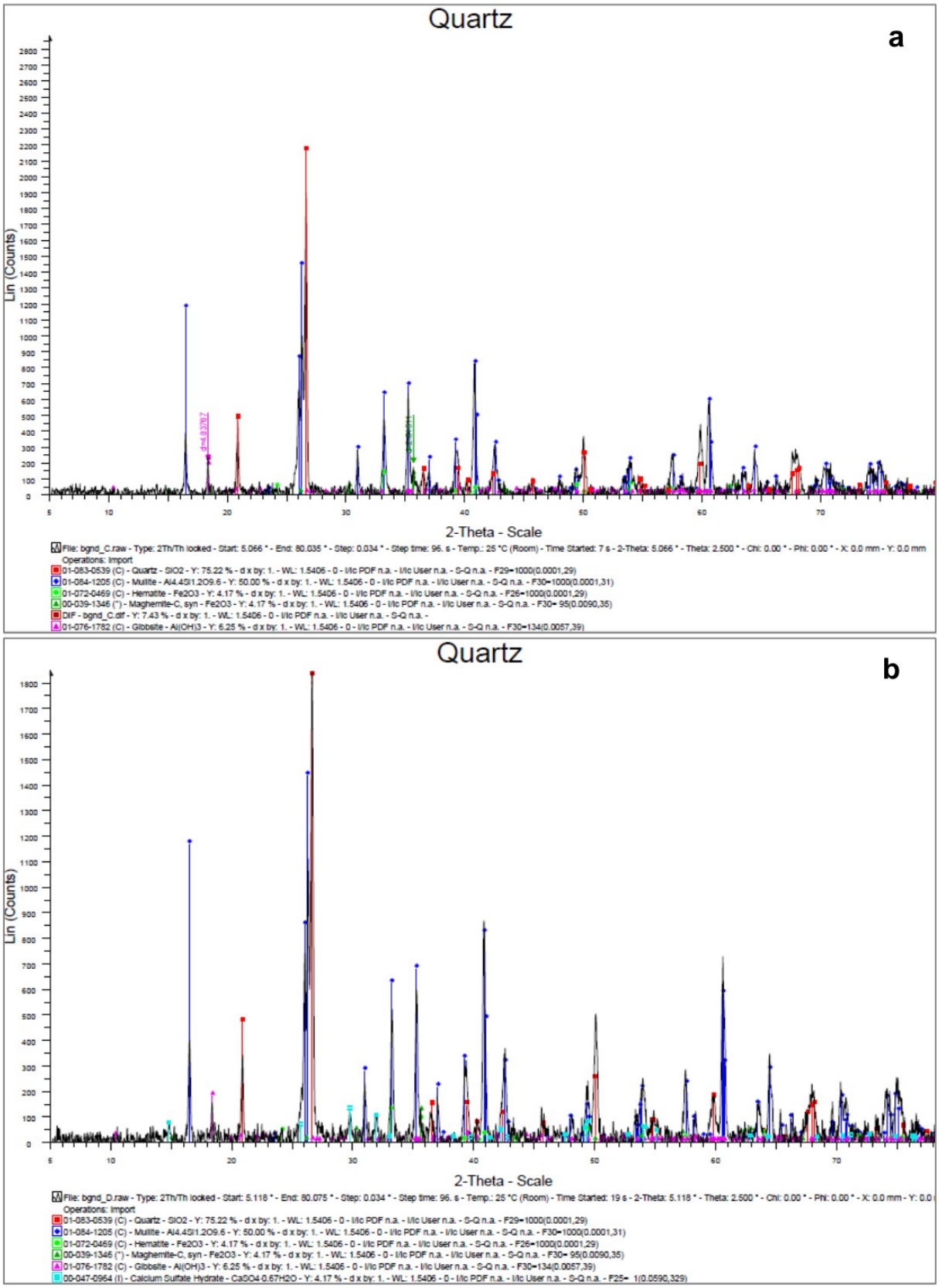

Figure A.3: Mineral phase identification responsible for the peaks on the SR spectra recovered after treatment of EAMD (1000 L) with 167 kg of KFA (a) or LFA (b), lime (1.0 kg) and 0.30 kg of $Al(OH)_3$.

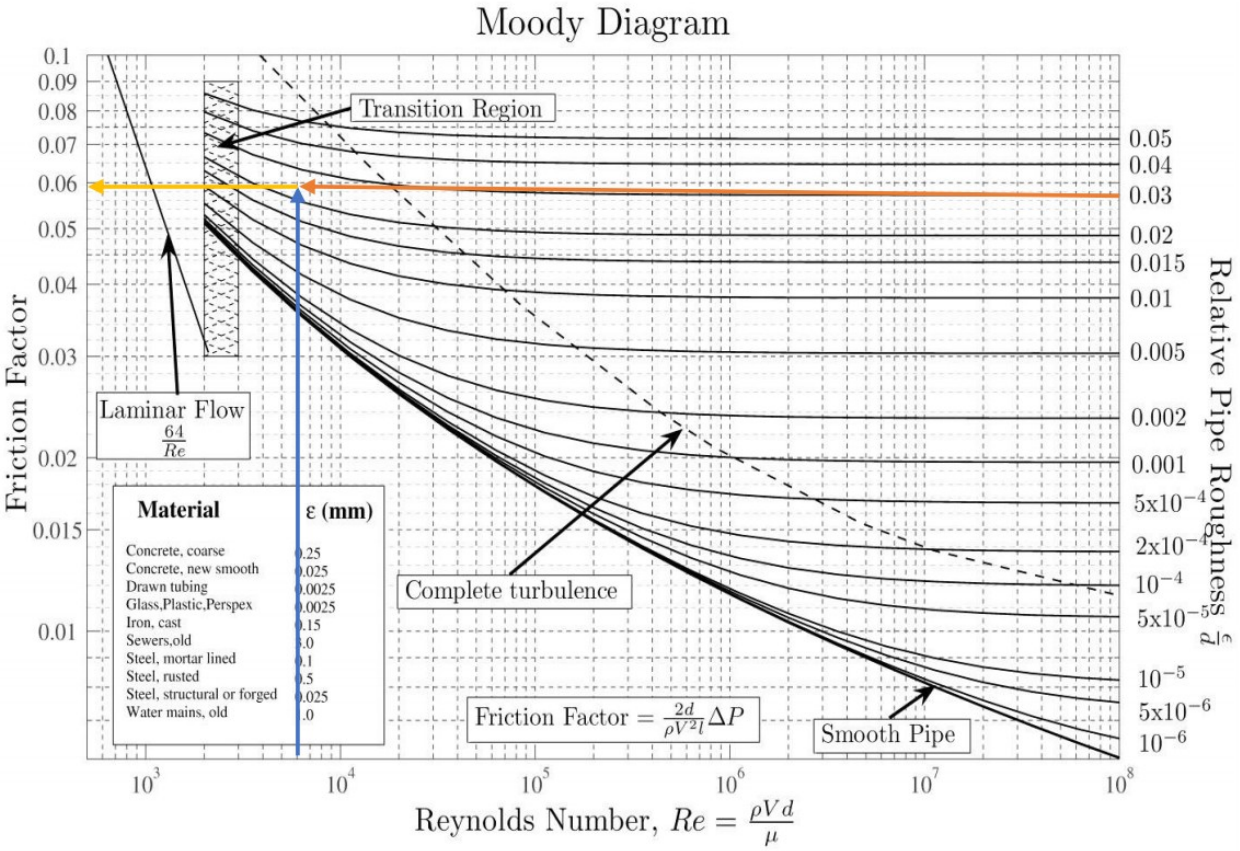

Figure A.4: Friction factor determination using Reynolds number and relative pipe roughness.

Kinetic Energy Factors	
Type of fitting or configuration	e_v
Elbow, 45°	0.35
Elbow, 90°	0.75
Tee	1
Return bend	1.5
Coupling	0.04
Union	0.04
Gate valve (wide open)	0.17
Gate valve (half open)	4.5
Glove valve (wide open)	6
Globe valve (half open)	9.5
Angle valve (wide open)	2
Check valve (ball)	70
Check valve (swing)	2
Water meter (disk)	7
Rounded entrance to pipe	0.05
Sudden contraction	0.45(1-B)*
Sudden expansion	$(1/B-1)^2$
Expansion into infinite reservoir	1**
Orifice	$2.7(1-B)(1-B^2)/B^2$

*B= (smaller cross-sectional area)/(larger cross-sectional area)
**for this case, use the upstream value of <v>

a. Elbows	
Regular 90°, flanged	0.3
Regular 90°, threaded	1.5
Long radius 90°, flanged	0.2
Long radius 90°, threaded	0.7
Long radius 45°, flanged	0.2
Regular 45°, threaded	0.4
b. 180° return bends	
180° return bend, flanged	0.2
180° return bend, threaded	1.5
c. Tees	
Line flow, flanged	0.2
Line flow, threaded	0.9
Branch flow, flanged	1.0
Branch flow, threaded	2.0
d. Union, threaded	0.08
e. Valves	
Globe, fully open	10
Angle, fully open	2
Gate, fully open	0.15
Gate, $\frac{1}{4}$ closed	0.26
Gate, $\frac{1}{2}$ closed	2.1
Gate, $\frac{3}{4}$ closed	17
Swing check, forward flow	2
Swing check, backward flow	∞
Ball valve, fully open	0.05
Ball valve, $\frac{1}{3}$ closed	5.5
Ball valve, $\frac{2}{3}$ closed	210

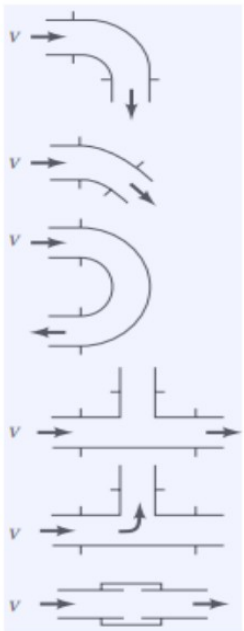

Figure A.5: Loss coefficients (K-factors) of different pipe components (Engineering ToolBox, 2004; Vano Engineering, 2012).

APPENDIX B

Under this section different elements consisting of Eyethu mine water are presented in various tables. This is EAMD composition before and after treatment with FA only and in combination with some chemical reagents.

Table B.1: Composition of EAMD before and after treatment with different amount of LFA (143 kg, 167 kg or 200kg)

	Raw AMD	Treated AMD											
		143 kg				167 kg				200 kg			
Parameter	0 min	20 min	40 min	60 min	70 min	20 min	40 min	60 min	70 min	20 min	40 min	60 min	70 min
pH	2.00	6.3	7.9	8.6	8.8	6.4	7.1	8.5	9.1	6.3	8.1	9.0	9.2
EC (mS/cm)	4.92	3.36	3.34	3.44	3.22	3.62	3.55	3.37	3.21	3.51	3.40	3.27	3.19
		Treated AMD											
		143 kg				167 kg				200 kg			
mg/L	0 min	20 min	40 min	60 min	70 min	20 min	40 min	60 min	70 min	20 min	40 min	60 min	70 min
Chloride	15.38	17.36	17.33	17.80	14.95	21.1	21.34	21.17	20.02	19.59	18.7	20.9	15.69
Sulphate	2680.00	1813.23	1601.25	1523.94	1444.18	1785.74	1518.48	1437.05	1389.22	1523.94	1514.92	1510.81	1464.54
Al	120.00	8.29	3.64	4.70	4.28	1.74	0.06	0.08	3.89	2.06	1.36	3.26	3.11
As	2.41	1.20	1.77	1.34	0.10	< -0.005	< -0.007	< -0.007	0.004	< 1.21	3.08	< 1.39	< 0.96
Ba	0.20	3.38	3.69	4.01	3.27	0.004	0.004	0.004	0.05	4.39	4.42	5.18	5.30
Ca	219.60	527.00	565.70	677.70	631.10	430.44	426.55	433.58	505.71	561.78	622.78	595.04	516.63
Cd	< 0.005	< 0.25	< -0.07	< -0.05	< -0.20	< -0.0004	< -0.0006	< -0.001	0.002	0.33	0.65	< -0.08	< -0.13
Co	1.62	1.35	4.08	6.88	1.47	0.26	0.24	0.04	0.09	2.22	5.08	< 0.46	< 0.21
Cr	< 0.005	1.93	7.03	1.06	1.14	0.01	0.02	0.05	0.11	1.35	3.86	3.61	4.26
Cu	0.05	10.79	7.34	6.66	7.67	0.008	0.005	0.004	0.002	< -0.21	< 0.38	< -.0.44	< -0.72
Fe	209.81	4.78	< 0.11	0.77	0.52	0.14	0.01	0.01	0.13	1.85	1.69	3.73	0.22
K	11.14	0.87	0.90	0.89	0.91	0.13	0.16	0.19	0.19	0.26	0.25	0.35	0.38
Mg	256.11	22.25	22.72	20.86	22.34	25.57	25.13	23.88	20.51	28.73	27.94	27.89	25.08
Mn	62.84	5.80	3.43	1.37	1.83	6.29	5.84	2.65	1.08	6.21	3.27	2.89	1.40
Mo	< 0.005	0.47	1.16	1.39	1.57	< -0.002	< 0.00122	0.02	0.12	0.78	2.08	1.18	1.91
Na	44.62	4.68	5.03	4.64	5.02	3.39	3.24	3.112	5.50	5.64	5.49	5.58	5.21

Table B.2: Composition of EAMD before and after treatment with different amount of KFA (143 kg, 167 kg or 200 kg)

	Raw AMD	Treated AMD											
		143 kg				167 kg				200 kg			
Parameter	0 min	20 min	40 min	60 min	70 min	20 min	40 min	60 min	70 min	20 min	40 min	60 min	70 min
pH	2.00	5.60	7.00	8.20	8.60	8.40	8.90	9.00	9.00	7.90	9.00	9.20	9.10
EC (uS/cm)	4.92	3.67	3.56	3.55	3.52	3.55	3.51	3.20	3.43	3.54	3.52	3.46	3.17
		Treated AMD											
		143 kg				167 kg				200 kg			
(mg/L)	0 min	20 min	40 min	60 min	70 min	20 min	40 min	60 min	70 min	20 min	40 min	60 min	70 min
Chloride	15.38	18.96	19.7	20.97	14.81	19.51	19.49	19.26	14.59	18.86	19.76	19.93	15.91
Sulphate	2680.00	1795.05	1539.21	1516.40	1534.62	1680.55	1552.99	1571.93	1397.00	1633.33	1624.25	1574.87	1375.83
Al	120.00	8.15	5.77	4.09	3.45	7.42	6.69	2.44	2.43	7.91	5.96	3.91	2.17
As	2.41	< 1.73	< 1.428	< 1.27	< 1.64	2.09	1.88	< 1.71	0.004	< 1.63	< 0.30	< 0.50	< 0.30
Ba	0.20	4.13	3.21	3.34	2.28	5.87	3.99	2.74	0.05	3.733	3.084	3.127	2.801
Ca	219.60	461.23	416.69	456.71	513.00	524.53	568.58	543.86	625.43	432.36	455.10	436.51	476.23
Cd	< 0.005	0.44	< -008	< -0.17	< -0.17	< -0.13	< -0.13	< -0.12	0.002	< -0.16	< -0.18	< -0.20	0.1836
Co	1.62	2.23	3.98	2.45	0.80	3.042	< 0.24	< 0.8809	0.01	37.98	< 0.364	< 0.1817	< 0.608
Cr	< 0.005	1.76	2.14	2.39	2.39	3.26	3.09	2.29	0.18	2.13	2.26	2.17	4.77
Cu	0.05	0.69	0.76	0.69	1.02	< -0.09	< -0.56	0.65	0.002	< -0.14	< 0.09	< 0.40	0.95
Fe	209.81	5.93	1.71	1.21	0.41	< -4.58	1.09	0.90	0.14	5.80	1.85	1.80	0.80
K	11.14	0.82	0.74	0.79	0.71	0.79	0.87	0.82	0.92	0.89	0.97	0.96	0.96
Mg	256.11	30.22	26.60	26.26	26.16	31.45	30.77	22.95	24.28	25.52	25.96	23.33	23.72
Mn	62.84	5.79	3.70	2.07	1.50	5.45	4.17	3.03	0.29	5.12	3.85	2.35	2.23
Mo	< 0.005	3.42	1.13	1.56	0.15	2.17	2.90	1.26	0.14	1.65	2.96	1.68	0.20
Na	44.62	4.47	4.10	4.16	4.11	5.5	6.13	3.99	5.87	4.18	4.38	4.25	4.37

Table B.3: Composition of EAMD before and after treatment with LFA (167 kg), and different amount of lime (0.5 kg or 1.0 kg)

	Raw AMD	Treated AMD													
		0.5 kg							1.0 kg						
Parameter	0 min	20 min	40 min	60 min	70 min	100 min	120 min	130 min	20 min	40 min	60 min	70 min	100 min	120 min	130 min
pH	2.00	7.60	9.00	9.40	9.40	10.70	10.60	8.50	6.80	8.40	8.90	9.10	11.80	11.80	8.70
EC (mS/cm)	4.94	3.30	2.68	2.79	2.85	2.46	2.10	2.08	2.37	2.99	2.61	2.42	2.26	2.52	2.16
		Treated AMD													
		0.5 kg							1.0 kg						
mg/L	0 min	20 min	40 min	60 min	70 min	100 min	120 min	130 min	20 min	40 min	60 min	70 min	100 min	120 min	130 min
Chloride	21.44	19.34	20.52	20.89	20.42	20.13	17.21	15.89	19.47	15.59	18.65	17.98	19.39	16.25	15.17
Sulphate	2006.28	1865.46	1621.43	1597.36	1581.48	564.45	528.95	508.96	1702.38	1641.24	1648.96	1521.74	587.97	525.21	530.82
Al	132.25	14.22	13.82	3.22	1.54	0.04	0.01	0.34	14.29	11.15	5.73	2.57	0.11	0.05	0.17
As	0.09	< - 0.006	< - 0.008	< - 0.007	< -0.008	< - 0.007	< - 0.006	< - 0.007	< - 0.007	< - 0.008	< - 0.006	< - 0.005	< - 0.007	< - 0.006	0.01
Ba	0.03	0.007	0.005	0.006	0.007	0.003	0.001	0.013	0.008	0.006	0.009	0.008	0.007	0.003	0.05
Ca	442.75	422.25	438.24	454.54	458.81	471.52	489.28	501.99	446.39	450.31	496.33	499.92	525.72	598.02	622.19
Cd	0.06	< - 0.001	< - 0.001	< - 0.001	< -0.001	< - 0.001	< - 0.001	< - 0.0012	< - 0.001	< - 0.001	< - 0.001	< - 0.001	< - 0.001	0.001	0.002
Co	2.67	0.065	0.002	0.002	0.001	< 0.00004	< 0.0005	0.0006	0.129	0.023	0.014	0.005	0.0002	0.004	0.01
Cr	0.03	0.006	0.013	0.016	0.017	0.017	0.01	0.02	0.005	0.012	0.016	0.013	0.016	0.011	0.013
Cu	0.03	0.003	0.004	0.008	0.0044	0.003	0.002	0.003	0.006	0.002	0.004	0.005	0.004	0.0001	0.004
Fe	216.07	0.08	0.02	0.03	0.05	0.01	0.00	0.09	0.13	0.03	0.01	0.28	0.02	0.01	0.12
K	12.65	2.11	2.04	1.84	1.67	1.53	1.52	1.51	0.55	0.44	0.72	0.79	0.92	0.52	0.37
Mg	242.99	18.29	18.15	18.09	17.58	0.56	0.09	1.17	21.19	16.36	21.77	21.00	0.19	0.03	3.18
Mn	65.59	2.78	2.48	1.42	1.36	0.01	0.01	0.07	4.02	1.69	1.03	0.82	0.01	0.01	0.10
Mo	< 0.019	0.008	0.014	0.013	0.016	0.017	0.014	0.018	0.007	0.012	0.009	0.007	0.015	0.01	0.01
Na	53.93	3.60	3.32	3.37	3.35	3.01	3.01	2.99	3.08	2.27	3.58	3.22	3.28	3.00	3.08

Table B.4: Composition of EAMD before and after treatment with LFA (167 kg), and lime (1.5 kg)

Parameter	Raw AMD	Treated AMD 1.5 kg						
	0 min	20 min	40 min	60 min	70 min	100 min	120 min	130 min
pH	2.00	6.40	8.00	8.80	9.00	12.30	12.20	9.10
EC (uS/cm)		2.94	2.95	2.49	3.10	2.28	2.37	2.47
		Treated AMD 1.5 kg						
(mg/L)	0 min	20 min	40 min	60 min	70 min	100 min	120 min	130 min
Chloride	21.44	20.32	19.59	17.70	20.19	19.45	16.11	14.37
Sulphate	2006.28	1619.79	1604.11	1597.36	1486.23	585.05	515.92	508.83
Al	132.25	14.878	13.60	7.298	1.07785	0.12276	0.02	0.21
As	0.09	< -0.007	< -0.007	< -0.007	< -0.007	< -0.007	< -0.007	< -0.007
Ba	0.03	0.009	0.012	0.004	0.004	0.007	0.01	0.011
Ca	442.75	427.07	465.16	467.23	478.94	494.56	505.30	485.86
Cd	0.06	< -0.001	< -0.001	< -0.001	< -0.001	< -0.001	< -0.001	< -0.001
Co	2.67	0.19	0.05	0.004	0.001	< -0.0001	< 0.0005	0.0002
Cr	0.03	0.005	0.016	0.017	0.02	0.018	0.003	0.02
Cu	0.03	0.007	0.013	0.003	0.004	0.003	0.003	0.003
Fe	216.07	0.108	0.106	0.018	0.016	0.023	0.001	0.06
K	12.65	0.54	0.64	0.78	0.80	0.77	1.56	0.71
Mg	242.99	22.88	22.91	18.74	21.569	0.25	0.01	0.91
Mn	65.59	4.634	2.876	1.184	0.576	0.008	0.010	0.02
Mo	< 0.019	0.0053	0.015	0.014	0.016	0.014	0.00	0.01
Na	53.93	3.29	3.47	2.57	3.42	3.07	2.89	2.78

Table B.5: Composition of EAMD before and after treatment with KFA (167 kg), and different amount of lime (0.5 kg, 1.0 kg or 1.5 kg)

		Treated AMD												
	Raw AMD	0.5 kg						1.0 kg						
Parameter	0 min	20 min	40 min	60 min	70 min	100 min	120 min	20 min	40 min	60 min	70 min	100 min	120 min	130 min
pH	2.00	6.30	7.70	8.20	8.4	9.70	9.70	6.50	7.60	8.00	8.40	11.40	11.50	8.60
EC (uS/cm)	4.94	3.26	3.33	3.58	2.93	2.85	2.45	3.74	3.66	3.56	3.59	3.39	2.22	2.12
		Treated AMD												
		0.5 kg						1.0 kg						
(mg/L)	0 min	20 min	40 min	60 min	70 min	100 min	120 min	20 min	40 min	60 min	70 min	100 min	120 min	130 min
Chloride	21.44	20.95	20.71	25.05	24.12	20.68	17.31	21.41	20.8	21.04	20.82	20.91	20.65	20.62
Sulphate	2006.28	1804.27	1608.30	1551.70	1530.58	536.78	525.21	1744.71	1594.36	1565.85	1496.62	543.59	535.99	535.99
Al	132.25	10.01	10.00	4.02	4.00	0.38	0.13	13.14	13.45	9.22	4.21	0.35	0.08	0.20
As	0.09	1.98	2.34	2.05	2.24	2.86	0.001	< 1.40	< 0.56	2.20	< 1.13	2.87	< 0.02	< 0.001
Ba	0.03	4.17	4.42	4.07	4.25	4.61	0.01	4.36	4.14	4.04	4.09	5.50	0.03	0.06
Ca	442.75	534.89	522.72	559.91	576.78	640.52	640.52	522.06	531.15	556.51	529.81	621.87	612.38	603.55
Cd	0.06	0.19	< -0.09	< 0.009	0.005	< -0.14	0.002	0.61	0.17	< 0.07	< -0.06	< -0.12	< -0.001	0.002
Co	2.67	3.97	3.14	1.68	0.86	< 0.20	< -0.001	2.21	1.33	0.46	0.28	< 0.19	0.001	0.004
Cr	0.03	2.51	3.05	3.35	2.84	2.76	0.003	9.37	1.078	1.146	1.077	0.772	0.041	0.07
Cu	0.03	< 0.20	< -0.08	< -0.75	< -0.26	< -0.11	< -0.01	< -0.32	< -0.26	< -0.55	< -0.60	< -0.59	< -0.001	< 0.000
Fe	216.07	0.98	0.37	0.31	0.97	0.40	0.18	< -6.99	< -5.36	< -0.85	< -3.30	3.40	0.01	0.122
K	12.65	0.77	0.74	0.82	0.84	0.85	0.35	0.74	0.67	0.69	0.67	0.63	0.28	0.39
Mg	242.99	31.83	31.62	31.03	25.12	11.24	6.52	33.20	33.49	33.21	30.98	0.17	0.05	2.017
Mn	65.59	5.72	3.74	3.14	2.25	1.13	0.09	6.47	5.17	3.26	2.58	1.20	0.10	0.13
Mo	< 0.019	10.71	1.91	2.26	2.06	2.43	0.11	5.83	1.19	1.59	1.73	1.46	0.06	0.13
Na	53.93	5.59	5.57	5.66	5.77	5.83	4.62	5.75	5.74	5.75	5.48	5.49	4.89	5.24

Table B.6: Composition of EAMD before and after treatment with KFA (167 kg), and lime (1.5 kg)

	Raw AMD	Treated AMD						
		1.5 kg						
Parameter	0 min	20 min	40 min	60 min	70 min	100 min	120 min	130 min
pH	2.0	5.90	6.30	7.00	7.50	11.90	11.80	9.20
EC (uS/cm)	4.94	3.76	3.74	3.70	3.65	3.44	2.72	2.46
		Treated AMD						
		1.5 kg						
(mg/L)	0 min	20 min	40 min	60 min	70 min	100 min	120 min	130 min
Chloride	21.44	19.96	20.7	20.44	21.02	20.82	19.52	21.13
Sulphate	2006.28	1707.42	1593.78	1493.12	1378.58	551.25	549.22	549.22
Al	132.25	12.67	10.46	8.44	1.40	0.36	0.20	0.18
As	0.09	2.96	2.85	< 0.79	< 1.40	2.49	0.02	0.01
Ba	0.03	5.39	5.05	6.05	6.75	4.44	0.01	0.002
Ca	442.75	505.41	505.88	512.79	497.73	676.16	658.97	634.18
Cd	0.06	0.64	0.57	0.22	< -0.09	< -0.11	< -0.09	< -0.13
Co	2.67	2.06	2.77	2.48	0.79	< 0.39	0.001	< -0.25
Cr	0.03	0.99	0.56	0.92	1.74	2.33	0.09	0.06
Cu	0.03	8.54	< -0.25	< -0.51	< -0.63	< -0.71	< 0.65	< -0.85
Fe	216.07	8.2	1.46	< -1.13	2.86	3.04	0.30	0.09
K	12.65	0.49	0.49	0.48	0.48	0.49	0.50	0.51
Mg	242.99	31.89	32.32	32.71	30.97	0.14	0.01	0.09
Mn	65.59	6.73	6.31	4.56	2.35	1.96	0.09	0.09
Mo	< 0.019	< -0.20	1.11	3.54	0.786	0.794	0.15	0.648
Na	53.93	5.29	5.54	5.38	5.17	5.15	5.00	5.16

Table B.7: Composition of EAMD before and after treatment with LFA (167 kg), lime (1.0 kg) and 0.31 kg of $Al(OH)_3$

	Raw AMD	Treated AMD									
Parameter	**0 min**	**20 min**	**40 min**	**60 min**	**90 min**	**110 min**	**130 min**	**150 min**	**170 min**	**180 min**	**195 min**
pH	2.10	5.20	5.80	6.50	8.00	10.80	11.10	11.00	11.30	10.80	8.60
EC (mS/cm)	5.97	3.73	3.74	3.72	3.64	2.53	2.49	2.52	2.32	2.21	2.03
	Raw AMD	**Treated AMD**									
(mg/L)	**0 min**	**20 min**	**40 min**	**60 min**	**90 min**	**110 min**	**130 min**	**150 min**	**170 min**	**180 min**	**195 min**
Chloride	16.90	18.73	19.03	17.32	17.29	19.26	19.60	18.77	20.21	18.21	17.23
Sulphate	2179.61	1423.50	1360.81	1317.40	1269.23	515.33	519.17	509.64	528.60	517.72	557.87
Al	165.88	16.35	9.10	4.62	2.48	0.31	0.17	0.15	0.12	0.20	0.71
As	0.02	3.06	2.76	2.11	2.21	2.09	2.75	1.48	1.11	0.009	0.005
Ba	0.05	2.77	3.08	2.88	3.63	7.55	4.19	3.59	6.69	0.02	0.06
Ca	512.26	479.63	481.92	471.61	514.68	570.54	663.07	593.79	668.87	608.24	580.69
Cd	0.01	0.83	7.73	< 0.44	< -0.18	< -0.08	< 0.11	< 0.31	< 0.07	0.0001	0.002
Co	3.31	2.53	2.31	2.04	5.87	< 0.14	< 0.39	< 0.56	< 0.03	< 0.02	0.01
Cr	0.32	1.51	8.58	9.89	1.74	1.57	2.09	2.28	1.98	0.05	0.15
Cu	0.83	1.65	0.75	3.79	0.12	0.78	0.62	0.47	0.10	0.01	0.003
Fe	236.70	1.31	0.44	0.20	0.15	0.94	< -6.98	< -1.507	0.84	0.10	0.41
K	13.87	0.69	0.71	0.69	0.70	0.66	0.70	0.69	0.79	0.41	0.30
Mg	296.37	30.53	28.81	28.68	30.31	0.82	0.29	0.13	0.01	0.01	3.80
Mn	80.56	16.76	8.89	5.67	5.87	3.23	1.66	0.92	0.27	0.10	0.38
Mo	< -0.002	1.19	5.54	1.18	2.42	2.14	2.44	2.32	2.49	< -0.01	0.19
Na	68.65	5.14	5.25	5.02	5.46	4.77	5.38	5.02	5.44	4.00	3.81

Table B.8: Composition of EAMD before and after treatment with KFA (167 kg), lime (1.0 kg) and 0.31 kg of $Al(OH)_3$

	Raw AMD	Treated AMD									
Parameter	**0 min**	**20 min**	**40 min**	**60 min**	**90 min**	**110 min**	**130 min**	**150 min**	**170 min**	**180 min**	**195 min**
pH	2.10	4.20	5.00	6.00	8.10	10.70	11.30	11.10	11.40	11.30	7.80
EC (mS/cm)	5.97	3.93	3.56	3.76	3.85	2.56	2.63	2.29	2.26	2.10	2.01
	Raw AMD	**Treated AMD**									
(mg/L)	**0 min**	**20 min**	**40 min**	**60 min**	**70 min**	**110 min**	**130 min**	**150 min**	**170 min**	**180 min**	**195 min**
Chloride	20.04	19.04	18.79	19.12	19.37	18.53	18.99	18.28	19.09	17.21	16.63
Sulphate	2179.61	1521.04	1398.91	1476.06	1476.38	894.8	516.57	509.95	526.93	516.12	544.66
Al	165.88	18.69	12.29	6.863	5.26	2.34	1.69	1.05	2.34	0.01	0.69
As	0.02	2.42	2.26	0.89	0.59	1.90	1.83	1.80	1.10	0.001	0.005
Ba	0.05	3.44	2.98	4.23	2.42	2.29	2.49	2.56	2.69	0.01	0.05
Ca	512.26	496.00	475.40	472.70	509.30	450.90	566.50	580.00	601.5	580.11	562.41
Cd	0.01	0.87	0.69	0.49	< -0.13	< -0.15	< 0.09	< 0.09	< -0.06	< -0.07	0.002
Co	3.31	2.52	2.39	2.10	3.79	< 0.37	< 0.21	< 0.26	< 0.000013	0.002	0.01
Cr	0.32	3.70	1.04	1.05	2.65	3.15	5.08	5.78	3.81	0.01	0.03
Cu	0.83	5.00	1.85	1.00	0.64	0.76	0.71	0.68	0.88	0.002	0.002
Fe	236.70	2.64	2.55	1.98	< 0.55	1.05	1.86	1.59	1.41	0.00	0.01
K	13.87	0.7	0.69	0.64	0.76	0.75	0.75	0.81	0.83	0.28	0.36
Mg	296.37	32.04	32.74	29.53	32.31	0.18	< -0.002	< -0.01	< -0.01	< -0.01	3.84
Mn	80.56	32.36	16.94	8.56	5.50	3.17	2.89	2.50	1.76	0.02	0.27
Mo	< -0.002	< 0.01	< -0.19	1.71	1.07	6.63	7.57	5.88	5.96	0.03	0.07
Na	68.65	5.61	5.31	4.97	5.79	5.29	5.38	5.47	5.00	3.85	4.14